TEXTURAL DIFFERENTIATION IN AUSTRALIAN SOILS

by

David J. Chittleborough, B. Agr. Sc. (Adel.), M. Agr. Sc. (Adel.)

Thesis submitted in total fulfillment of the requirements for the Degree of Doctor of Philosophy in the Department of Soil Science, University of Adelaide.

February, 1982

CONTENTS

		Page
LIST OF FIGURES		(iv)
LIST OF TABLES		(xviii)
ABSTRACT		(xxi)
STATEMENT		(xxiv)
ACKNOWLEDGEMENTS		(xxv)
CHAPTER 1	INTRODUCTION	1
CHAPTER 2	THE DEVELOPMENT OF THE URRBRAE LOAM	6
CHAPTER 3	SAMPLING AND DESCRIPTION OF SOILS	7
3.1	Selection	7
3.2	Methods	8
3.2.1	Field sampling	8
3.2.2	Analytical methods	10
3.3	Morphology and chemistry of soils	10
3.3.1	Gooromon Ponds sequence	10
3.3.2	Shinglehouse Creek sequence	20
3.3.3	Nowra Creek sequence	26
3.3.4	Hawkesbury River sequence	34
CHAPTER 4	PARTICLE-SIZE DISTRIBUTIONS	43
4.1	Introduction	43
4.2	Analytical methods	46
4.2.1	Method of dispersion	46
4.2.2	Determination of fine clay:total clay ratio	48
4.2.3	Detailed particle-size analysis	48
4.2.4	Calculation of the CPSD index	49
4.2.5	Weathering index	49
4.3	Results and discussion	49
4.3.1	Method of dispersion	49

Page

4.3.2 Fine clay:total clay ratios 57

4.3.3 Detailed particle-size analyses 62

4.3.4 Cumulative particle-size distribution index 71

4.3.5 Weathering index 77

4.4 Conclusions 79

CHAPTER 5 PHYSICAL WEATHERING AND SOIL DEVELOPMENT 80

5.1 Introduction 80

5.2 Methods and materials 82

5.2.1 Measurement of quartz 82

5.2.2 Measurement of proportion of rock fragments 83

5.3 Results and discussion 83

5.3.1 Particle-size distribution of gravel 83

5.3.2 Quartz content of the soil separates 86

5.3.3 Breakdown of rock fragments 93

5.4 Conclusion 95

CHAPTER 6 MICROMORPHOLOGY 97

6.1 Introduction 97

6.2 Sampling 98

6.3 Method of description and terminology 99

6.4 Micromorphology of the Gooromon Ponds sequence 99

6.4.1 Description 99

6.4.2 Discussion 101

6.5 Micromorphology of the Shinglehouse Creek sequence 106

6.5.1 Description 106

6.5.2 Discussion 110

6.6 Micromorphology of the Nowra Creek sequence 111

6.6.1 Description 111

6.6.2 Discussion 113

Page

6.7 Micromorphology of the Hawkesbury River sequence 116

6.7.1 Description 116

6.7.2 Discussion 122

6.8 General discussion 124

6.9 Conclusions 126

CHAPTER 7 ELEMENTAL CHEMISTRY 128

7.1 Introduction 128

7.2 Methods 130

7.2.1 Bulk density 130

7.2.2 Acid residue 131

7.2.3 Heavy minerals 131

7.2.4 Clay separations 132

7.2.5 Chemical analysis 133

7.2.6 Calculation of losses and gains of constituents 133

7.3 Results and discussion 137

7.3.1 Parent material uniformity 137

7.3.2 Weathering 152

7.3.3 Loss and gain of constituents 153

7.4 Conclusions 169

REFERENCES 170

LIST OF FIGURES

Figure		Page
1	Distribution of Australian texture contrast soils.	2
2	Types of chronosequences (after Vreeken, 1975).	4
3	Location of soil profiles and sequences: 1 Urrbrae fine sandy loam; 2 Gooromon Ponds; 3 Shinglehouse Creek; 4 Nowra Creek; 5 Hawkesbury River.	9
4	Location of soils of the Gooromon Ponds sequence.	11
5	Geology of the Gooromon Ponds sequence.	12
6.1	Land form of the Gooromon Ponds site: from 1:10,000 scale topographic maps.	13
6.2	Land form of the Gooromon Ponds site: from 1:2,500 scale topographic maps.	14
7	G1 profile.	18
8	G2 profile.	18
9	G3 profile.	18

Figure		Page
10	G4 profile.	18
11	G5 profile	18
12	Location of soils of the Shinglehouse Creek sequence.	21
13	Geology of the Shinglehouse Creek sequence.	22
14	Land form of the Shinglehouse Creek site: from 1:25,000 topographic maps.	23
15	S1 profile.	25
16	S2 profile.	25
17	S3 profile.	25
18	Location of soils of the Nowra Creek sequence.	27
19	Geology of the Nowra Creek sequence.	28
20	Land form of the Nowra Creek site: from 1:25,000 scale topographic maps.	29
21	N1 profile.	33
23	N3 profile.	33

Figure		Page
24	N4 profile.	33
25	Location of soils of the Hawkesbury River sequence.	35
26	Geology of the Hawkesbury River sequence.	36
27	Land form of the Hawkesbury River sequence.	37
28	H1 profile.	42
29	H2 profile.	42
30	H3 profile.	42
31	H4 profile.	42
32	H5 profile.	42
33	Effect of time of shaking of a soil of fine sandy loam texture on the yield of total clay and fine clay, and on the coarse clay: fine clay ratio.	51
34	Effect of time of shaking of a soil of medium clay texture on the yield of total clay and fine clay and on the coarse clay: fine clay ratio.	51

Figure		Page
35	Yield of clay, silt and sand after various shaking times (a) soil of sandy loam texture (b) soil of clay texture.	52
36	SiO_2:Al_2O_3 ratio for clay, silt and sand fractions as a result of shaking for various times; 10^2, 10^3 and 10^4 seconds (a) soil of sandy loam texture (b) soil of clay texture.	54
37	Electron micrographs of clay sized particles following shaking of a soil of sandy loam texture for various times. a) 0s b) 0s c) 1s d) 10s e) 100s f) 10,000s The line on the photograph represents 0.5 µm.	55
38	Electron micrographs of clay sized particles following shaking of a soil of clay texture for various times. a) 0s b) 1s c) 10s d) 100s The line on the photograph represents 0.5 µm.	56

Figure		Page
39	Depth functions of fine clay: total clay ratios for soils of the Gooromon Ponds sequence.	58
40	Depth functions of fine clay: total clay ratios for soils of the Shinglehouse Creek sequence.	59
41	Depth functions of fine clay: total clay ratios for soils of the Nowra Creek sequence.	60
42	Depth functions of fine clay: total clay ratios for soils of the Hawkesbury River sequence.	61
43.1	Particle-size distributions of A horizons of soils of the Gooromon Ponds sequence.	63
43.2	Particle-size distributions of B horizons of soils of the Gooromon Ponds sequence.	64
44.1	Particle-size distributions of A horizons of soils of the Shinglehouse Creek sequence.	65
44.2	Particle-size distributions of B horizons of soils of the Shinglehouse Creek sequence.	66
45.1	Particle-size distributions of A horizons of soils of the Nowra Creek sequence.	69

Figure		Page
45.2	Particle-size distributions of B horizons of soils of the Nowra Creek sequence.	68
46.1	Particle-size distributions of A horizons of soils of the Hawkesbury River sequence.	69
46.2	Particle-size distributions of B horizons of soils of the Hawkesbury River sequence.	70
71	Gravel content of soils of the Gooromon Ponds sequence.	84
72	Gravel content of soils of the Shinglehouse Creek sequence.	84
73	Gravel content of soils of the Nowra Creek sequence.	85
74	Gravel content of soils of the Hawkebury River sequence.	85
75	Particle-size distribution of quartz within the major horizons of the soils of the Gooromon Ponds sequence.	89
76	Particle-size distributions of quartz within the major horizons of the soils of the Shinglehouse Creek sequence.	90

Figure		Page
77	Particle-size distributions of quartz within the major horizons of the soils of the Nowra Creek sequence.	91
78	Particle-size distributions of quartz within the major horizons of the soils of the Hawkesbury sequence.	92
79.1	Profile G1 Granular fabric with some grains showing evidence of pre-weathering.	102
79.2	Profile G1 Rock fragment breaking up.	102
79.3	Profile G3, 14 cm. Mammillated orthovughs.	102
79.4	Profile G3, 48 cm. Fine grained rock fragment with iron halo.	102
79.5	Profile G3. Weak vosepic fabric with diffuse sesquioxide glaebule.	102
79.6	Profile G3, 74 cm. Rock fragment with sesquioxide halo.	102
79.7	Profile G3, 85 cm. Compound void ferri-argillan.	102
79.8	Profile G3, 98 cm. Quartz fragment breaking up along fractures.	102

Figure		Page
80.1	Profile G3, 98 cm. Voskelsepic fabric.	103
80.2	Profile G4, 42 cm. Vosepic fabric.	103
80.3	Profile G4, 60 cm. Void ferri-argillaus.	103
80.4	Profile G4, 80 cm. Mavosepic fabric.	103
80.5	Profile G5, 64 cm. Strong vomasepic fabric.	103
80.6	Profile G5, 73 cm. Silasepic fabric with fine laminated void argillaus.	103
81.1	Profile G3, 7 cm. Isotubules.	104
81.2	Profile G5, 44 cm. Discrete sesquioxide glaebule with undifferentiated fabric and thin ferri-argillaceous halo.	104
82.1	Profile S1, 4 cm. Sedimentary laminae.	108
82.2	Profile S1, 34 cm. Clay coatings around skeleton grains.	108
82.3	Profile S1, 40 cm. Granular fabric with sedimentary banding.	108

Figure		Page
82.4	Profile S1, 40 cm. Granular fabric showing inherited papules.	108
82.5	Profile S2, 39 cm. Argillaceous porphyroskelic fabric with mammillated orthovughs.	108
82.6	Profile S2, 39 cm. Argillaceous porphyroskelic fabric with fine sedimentary laminae.	108
82.7	Profile S2, 54 cm. Argillaceous porphyroskelic fabric with irregular sesquioxidic nodules.	108
82.8	Profile S2, 61 cm. Argillaceous porphyroskelic fabric with granular patches and void cutans.	108
83.1	Profile S2, 79 cm. Void argillans.	109
83.2	Profile S3, 0 cm. Break up of rock fragment.	109
83.3	Profile S3, 23 cm. Masepic fabric, with granic fabric along channel.	109
83.4	Profile S3, 23 cm. Distinct sepic and granic fabrics.	109
83.5	Profile S3, 32 cm. Papule (embedded void argillan)	109

Figure		Page
83.6	Profile S3, 32 cm. Lattisepic fabric.	109
83.7	Profile S3, 63 cm. Undifferentiated sesquioxide glaebule.	109
83.8	Profile S3, 74 cm. Ferri-argillaceous papule	109
84.1	Profile N1. Distinct granular and argillasepic fabrics.	114
84.2	Profile N1. Sedimentary banding.	114
84.3	Profile N1. Sesquioxide concentration around void (sesquan).	114
84.4	Profile N1. Argillasepic porphyroskelic fabric with sesquioxide concentration enclosing part of the matrix.	114
84.5	Profile N1. Chitonic fabric.	114
84.6	Profile N2, 11 cm. Mammillated vugh.	114
84.7	Profile N2, 27 cm. Fractured fine-grained rock fragment (siltstone) with sesquioxide concentrations along fractures.	114
84.8	Profile N2, 42 cm. Fractured rock fragment.	114

Figure		Page
85.1	Profile N2, 48 cm. Argillasepic prophyroskelic fabric with intertextic patches.	115
85.2	Profile N3, 15 cm. Undifferentiated sesquioxide nodule.	115
85.3	Profile N3, 30 cm. Mavosepic fabric.	115
85.4	Profile N2, 15 cm. Skelvosepic fabric.	115
85.5	Profile N4, 15 cm. Thick papule with iron banding.	115
85.6	Profile N4, 28 cm. Masepic fabric.	115
85.7	Profile N4, 58 cm. Void argillan.	115
85.8	Profile N4, 122 cm. Skelvosepic fabric with sesquans.	115
86.1	Profile H1, 44 cm. Granular fabric.	119
86.2	Profile H2, 16 cm. Sedimentary banding.	119
86.3	Profile H2, 33 cm. Void ferri-argillans and undifferentiated sesquioxide nodule.	119
86.4	Profile H2, 120 cm. Voskelsepic fabric.	119

Figure		Page
86.5	Profile H3, 2 cm. Argillasepic porphyroskelic fabric.	119
86.6	Profile H3, 51 cm. Thick papules with strong continuous orientation.	119
86.7	Profile H3, 43 cm. Void ferri-argillans and diffuse, irregular sesquioxide glaebules.	119
86.8	Profile H4, 73 cm. Granular fabric lining channel.	119
87.1	Profile H4, 73 cm. Thick, finely laminated void ferri-argillan.	120
87.2	Profile H4, 84 cm. Coarsely laminated void ferri-argillan with silt-size particles.	120
87.3	Profile H4, 84 cm. Void ferri-argillans and papules (embedded void ferri-argillans).	120
87.4	Profile H5, 61 cm. Mavosepic fabric.	120
87.5	Profile H5, 61 cm. Thick papules composed of kaolinite.	120
87.6	Profile H5, 61 cm. Void argillan with fine transverse fractures.	120

Figure		Page
87.7	Profile H5, 61 cm. Fabric of sesquioxide nodule.	120
87.8	Profile H5, 116 cm. Strong masepic fabric.	120
88.1	Profile H3, 73 cm. Sesquioxide glaebules with undifferentiated fabric.	121
88.2	Profile H4, 30 cm. Diffuse irregular sesquioxide nodules, strongly adhesive.	121
88.3	Profile H5, 51 cm. Two forms of sesquioxide nodules - 1) normal; equant, rounded, sharp external boundary. 2) irregular; diffuse external boundary, strongly adhesive. Iron staining along channels.	121
88.4	Profile H5, 120 cm. As for figure 88.3 except sesquioxide segregation more discrete.	121
89	Proportions of elements in the light and heavy fractions of the Gooromon Ponds sequence.	147
90	Proportion of elements in the light and heavy fractions of the Shinglehouse Creek sequence.	148

Figure		Page
91	Proportion of elements in the light and heavy fractions of the Nowra Creek sequence.	149
92	Proportion of elements in the light and heavy mineral fractions of the Hawkesbury River sequence.	150
93	Depth functions of the ratios $CaO:ZrO_2$, $Na_2O:ZrO_2$, $Fe_2O_3:ZrO_2$ for soils of the Gooromon Ponds sequence.	154
94	Depth functions of the ratios $CaO:ZrO_2$, $Na_2O:ZrO_2$, $Fe_2O_3:ZrO_2$ for soils of the Shinglehouse Creek sequence.	155
95	Depth functions of the ratios $CaO:ZrO_2$, $Na_2O:ZrO_2$, and $Fe_2O_3:ZrO_2$ for soils of the Nowra Creek sequence.	156
96.1	Depth functions of the ratio $CaO:ZrO_2$ for soils of the Hawkesbury River sequence.	157
96.2	Depth functions of the ratio $Na_2O:ZrO_2$ for soils of the Hawkesbury River sequence.	158
96.3	Depth functions of the ratio $Fe_2O_3:ZrO_2$ for soils of the Hawkesbury River sequence.	159

LIST OF TABLES

Table

1 Age, degree of textural differentiation and classification of soils of the Gooromon Ponds sequence.

2 Chemical data for soils of the Gooromon Ponds sequence.

3 Age, degree of textural differentiation and classification of soils of the Shinglehouse Creek sequence.

4 Chemical data for soils of Shinglehouse Creek sequence.

5 Age, degree of textural differentiation and classification of soils of the Nowra Creek sequence.

6 Chemical data for soils of the Nowra Creek sequence.

7 Age, degree of textural differentiation and classification of soils of the Hawkesbury River sequence.

8 Chemical data for soils of the Hawkesbury River sequence.

9 Effect of chemical pretreatments on the coarse clay: fine clay ratio for two soils.

10 Cumulative particle-size distribution index of sand fractions for selected horizons of the soils of the Gooromon Ponds sequence.

Table

11 Cumulative particle-size distribution index of sand fractions for selected horizons of the soils of the Shinglehouse Creek sequence.

12 Cumulative particle-size distribution index of sand fractions for selected horizons of the Nowra Creek sequence.

13 Cumulative particle-size distribution index of sand fractions for selected horizons of the Hawkesbury River sequence.

14 Ratios of fine silt: total silt (2-5 um:2-20 um) of selected horizons for soils of four terrace sequences.

15 Quartz content of separates from selected horizons of the soils of the terrace sequences.

16 Proportion of rock fragments in sand fractions of soils from four terrace sequences.

17 COLE values for various horizons of four terrace soils.

18 Ratios of oxides from various size and density fractions of soils from Gooromon Ponds.

19 Ratios of oxides from various size and density fractions of soils from Shinglehouse Creek.

20 Ratios of oxides from various size and density fractions of soils from Nowra Creek.

Table

21 Ratios of oxides from various size and density fractions of soils from Hawkesbury River.

22 Means and relative standard deviations of the oxide ratios of various fractions from the soils of four terrace sequences.

23 Losses and gains in volume and weight for selected horizons of three soils of the Gooromon Ponds sequence.

24 Losses and gains in volume and weight for selected horizons of two soils of the Shinglehouse Creek sequence.

25 Losses and gains of volume and weight for selected horizons of three soils of the Nowra Creek sequence.

26 Losses and gains of volume and weight for selected horizons of four soils of the Hawkesbury River sequence.

27 Losses and gains of oxides due to clay formation and clay migration as a result of soil formation.

TEXTURAL DIFFERENTIATION IN AUSTRALIAN SOILS

ABSTRACT

Three hypotheses; sedimentary layering, clay formation in situ and clay illuviation were proposed to account for the widespread distribution of Australian texture contrast soils. A review of the literature showed that the first two have been favoured but a critique of several studies on one texture contrast profile, the Urrbrae loam (a rhodoxeralf), indicated that clay illuvation was more likely. Further data, and the application of additional criteria, substantiated this hypothesis.

The processes involved in textural differentiation as a function of time were further investigated in four post-incisive sequences in eastern Australia. In each sequence there was a progressive increase in the degree of texture contrast, from uniform on the youngest terrace (sandy loam), through gradational on intermediate terraces of age 2000-5000 years, to strong (sand over heavy clay) on the oldest. Parent materials of the latter were >29 000 years old and in one sequence at Richmond on the Hawkesbury River, probably >100 000 years.

Detailed particle-size, distributions, from <0.6 um to 2 000 um at $\frac{1}{4}$ ϕ intervals and depth functions of the ratio fine clay (<0.2 um): coarse clay (0.2 - 2 um) provided evidence that considerable translocation of clay had taken place especially in the older soils. From the similarity of the cumulative particle-size indices, it was concluded that lithological discontinuities were not responsible for the presence of high clay B horizons. Nor was chemical weathering as judged on the basis of change in the depth functions of fine silt (2 - 5 um): total silt (2 - 20 um) ratios.

There was strong evidence for clay movement from micromorphological examination of thin sections. In all sequences there were fine sedimentary laminae in the youngest soils on the floodplains. These were seen to be disrupted in the next oldest soils by extreme faunal turbation which not only

obliterated evidence of colluvial and alluvial stratification but produced a profile uniform in texture and high in organic matter. Occasional iron segregations in the form of diffuse nodules and void cutans were visible but were prominent in the older soils which had gradational texture profiles i.e. with profiles of weak to moderate texture contrast. In these profiles clay maxima in the upper B horizon coincided with the maximum concentration of void cutans and papules. However, in the oldest soils; those with the highest clay in the B horizon, the coincidence between the total clay and illuviated clay was highest in the B_3 horizon. Coefficient of linear extensibility measurements correlate with the concentration of fine clay which is at a maximum in the B_2. There is a strong vomasepic fabric in the B_2 of the oldest profiles. Sesquans in the B horizon of the oldest Hawkesbury profile indicate that weathering in situ is significant only in the mature stage of profile development.

A fourth hypothesis was proposed for the development of the B horizon, viz physical breakdown of fine grained lithorelicts of gravel and sand size to quartz and alumino-silicate minerals of clay size. Changes in the particle-size distribution of quartz and changes in the proportion of gravel with depth indicate the main contribution of physical weathering is to the fine sand and silt fractions.

Proportions of resistant heavy minerals in the >2.96 g cm^{-3} fraction were estimated by X-ray fluorescent spectroscopy of elements zirconium, titanium, yttrium and phosphorus, which were assumed to be present only in zircon, rutile and ilmenite, xenotime and monazite respectively. Ratios of these elements in various fractions showed statistically insignificant changes with depth, thus ruling out the sedimentary layering hypothesis. Formation of clay by more intense chemical weathering of coarse minerals in the B horizon was discounted on the basis of constant ratios of $Fe_2O_3:ZrO_2$, $Na_2O:ZrO_2$, $CaO:ZrO_2$ in the silt fraction. In the oldest members of several sequences there was

evidence of chemical weathering but strong texture contrast was already apparent in younger profiles. Calculations of losses and gains on the basis of the tri-acid resistant fraction of the whole soil provided further strong evidence for the predominant role played by clay translocation and the minor contribution to the clay fraction of clay formation in place except in the oldest soils.

It was concluded that clay illuviation was the main mechanism responsible for textural differentiation with weathering in situ playing a minor, albeit with time, an increasingly important role.

STATEMENT

This thesis contains no material which has been accepted for the award of any other degree or diploma in any university, and this thesis contains no material published previously or written by any other person, except where due reference is made in the text of the thesis.

Any assistance received in preparing this thesis, and all sources used, have been acknowledged.

David J. Chittleborough
FEBRUARY 1982

ACKNOWLEDGEMENTS

I wish to thank my supervisor, Professor J.M. Oades for his interest and guidance throughout the project. I also wish to thank other members of the staff of the Waite Agricultural Research Institute and the staff of the Division of Soils, CSIRO, for their advice and assistance.

In particular I thank:
Dr. P. Walker for his help in locating the sampling sites in eastern New South Wales and numerous discussions; Mr. J. Hutka for carrying out the particle-size distribution analyses; Mr. T.W. Sherwin and Miss S. Potter for technical assistance; Mr. J. Cent for preparing the thin sections; Dr. K. Norrish and Mr. K. Northcote for many helpful discussions; Mr. B. Palk for preparing some of the photographs for publication; Mr. G. Rinder for line-work of the drawings; Mr J. Beattie for chemical analyses of the terrace soils.

Finally I thank the South Australian Department of Agriculture for allowing me to make this study.

Chapter 1

Introduction

Soils with markedly contrasting texture between surface and sub-surface horizons are an ubiquitous feature of the Australian landscape and a map of the distribution of these soils shows that they are very widespread, geographically and climatically, and are formed in igneous, metamorphic and sedimentary parent materials (Figure 1). 1/4 of the Australian continent is covered with such soils. No other comparable land mass has such a diverse and widespread array. 'The factual key for the recognition of Australian Soils' (Northcote 1968), has used the degree of texture contrast as the sole criterion for separating soils of the first level of subdivision. The population of Australian soils has been divided into three categories, uniform, gradational and duplex. Duplex, or texture contrast, soils are defined as those soils which have a texture contrast of at least 1 1/2 texture groups (e.g. loam to silty clay loam or greater, clay loam to light clay or greater) between A and B horizons. Horizon boundaries are clear to sharp.

Of the soil forming factors influencing development, time appears to be the most important. The Australian landscape is comparatively old and the parent materials from which soils have formed have, in many cases, been subject to a number of cycles of transport, deposition and weathering. This is in contrast to much of the northern hemisphere where glaciation during the Pleistocene 'swept' the landscape 'clean', exposing fresh parent material. Soil development over large areas is < 100 000 years old.

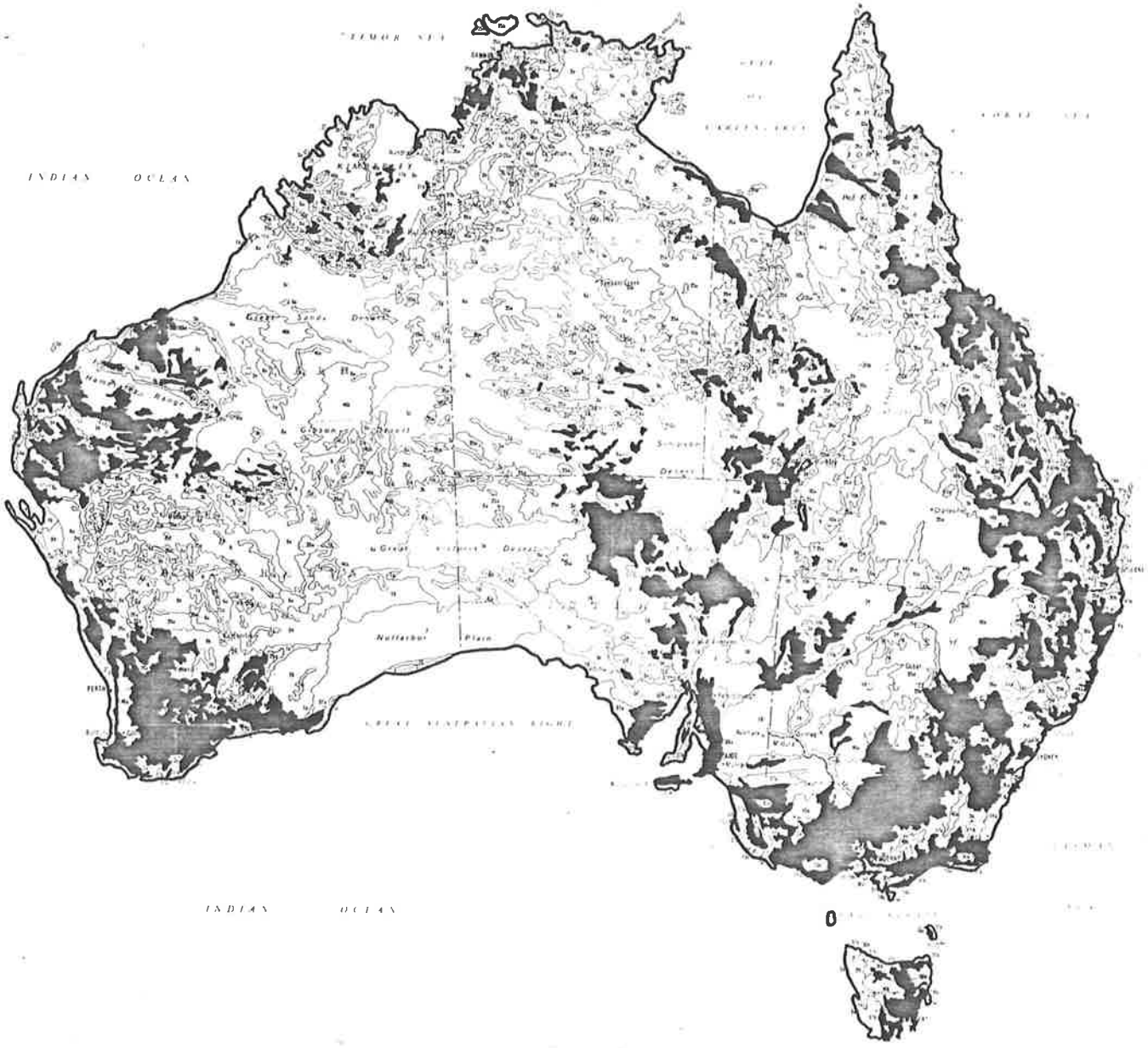

Figure 1 Distribution of Australian texture contrast soils

Studies in depositional landscapes of the Riverine Plain (Butler 1958, 1959), where a comparative ground-surface age can be deduced for soil sequences, show that the older members have the most pronounced texture contrast. Sequences of soil with progressively stronger texture contrast have been defined by Walker (1962a), Walker and Coventry (1976), Brewer and Walker (1969) in river valleys of eastern Australia. Young soils are uniform in texture down the profile, the oldest strongly duplex. These soils form chronosequences which are post-incisive according to the definition of Vreeken (1975) i.e. the sedimentary parent material of each soil was exposed at different intervals leading up to the present (Figure 2). Because radio carbon dating was available for the parent materials of many profiles, the sequences of Walker, Coventry and Brewer were considered excellent prospects for elucidating the processes involved in textural differentiation.

However, despite the widespread occurrence of duplex soils, there has been little systematic study (although much speculation) of their origin and development. Hypotheses regarding their formation, and criteria to test them, have not been clearly enunciated.

The processes which have been proposed to account for textural contrast fall into three main categories.

1. Sedimentary layering. The differences in particle size distribution are the result of an initially non-uniform parent material.
2. Formation of clay in position by differential weathering. Under this mechanism, there has been no clay movement.
3. Downward translocation of clay within an initially homogeneous material.

The relative importance of these three processes in the formation of Australian texture contrast soils is the subject of this thesis.

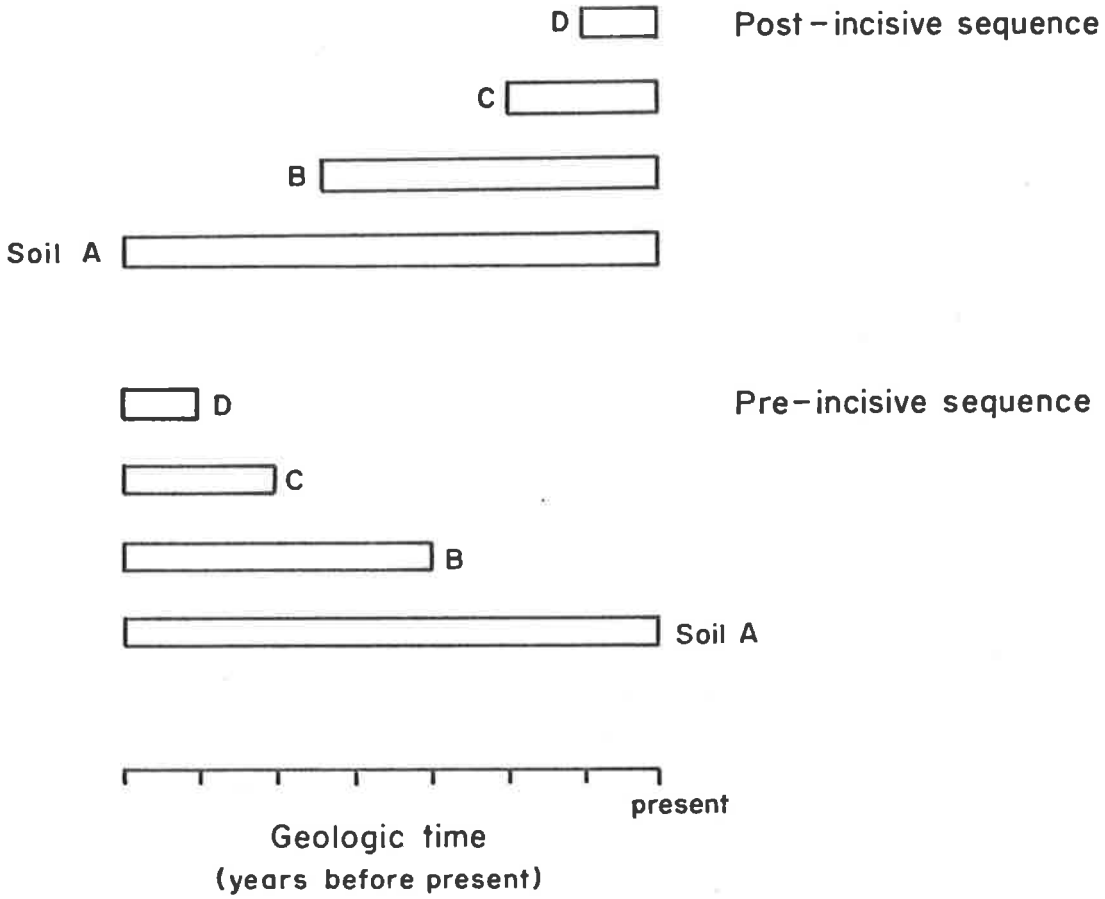

Figure 2 Types of chronosequences (after Vreeken, 1975)

The first part of the study of texture contrast soils involved the formulation of criteria to test the three hypotheses. Because of the divergent opinion about the origin of the Urrbrae loam, a strongly duplex soil (calcic rhodoxeralf) and the large amount of data available from previous studies, testing the hypothesis and evaluation of criteria were first carried out on this soil prior to more extensive work on the chronosequences in eastern Australia.

The work on the Urrbrae loam is reported in Chapter 2 and Chapters 3 to 7 report the investigation on soils of the river terraces in eastern Australia.

Chapter 2

The development of the Urrbrae loam

The work in this chapter is presented in the form of three published papers. The first (Chittleborough and Oades 1979) is a critique of previous studies on this soil and an evaluation of the criteria. Papers 2 and 3 (Chittleborough and Oades 1980 II and III) report the testing of the three hypotheses proposed in Chapter 1, using additional criteria.

It was concluded that clay illuviation was likely to have played a predominant role in the formation of the textural contrast of the Urrbrae loam. Furthermore, the criteria used to test the hypotheses were found to be workable: they could be measured with reasonable precision and accuracy: and consistent: similar conclusions were arrived at by different criteria.

Chittleborough, D. J. & Oades, J. M. (1979). The development of a red-brown earth. I A reinterpretation of published data. *Australian Journal of Soil Research, 17*(3), 371-381.

Chittleborough, D. J. & Oades, J. M. (1980). The development of a red-brown earth. II Uniformity of the parent material. *Australian Journal of Soil Research, 18*(4), 375-382.

Chittleborough, D. J. & Oades, J. M. (1980). The development of a red-brown earth. III The degree of weathering and translocation of clay. *Australian Journal of Soil Research, 18*(4), 383-393.

Chapter 3

Sampling and description of soils

3.1 Selection

Numerous studies of the hillslope and alluvial landscapes of eastern Australia have revealed that soil development in many areas has followed a cyclic or episodic pattern (van Dijk 1959, Walker 1962a, Mulcahy and Churchward 1973). This has been sufficiently general in the Riverine Plain of south eastern Australia for Butler (1959) to propose three distinct periods of soil development.

The common observation is the presence of a series of buried or relict geomorphic surfaces characterized by soils showing successive stages of soil development. Invariably soils on the youngest geomorphic surfaces are texturally undifferentiated, those on the oldest show very strong textural contrast and intermediate surfaces have gradational textures. The soils have sufficient features in common for Butler (1967) to attempt to correlate their ground-surfaces. Walker and Coventry (1976) state that the soil profiles of these alluvial landscapes "have such generality that the same pedogenetic processes must have been operative over large areas of humid south eastern Australia during the past 30,000 years". Many of these soils have been dated by the radio carbon method.

It was deemed important for the study of textural differentiation that time should be the dominant factor in producing soil differences. Therefore, the criterion for the selection of sites was that the terrace or hillslope sequence be of more than local occurrence. Similarity of

soils in particular geomorphic positions over a wide area would indicate that the observed variations were not the result of peculiarities in local soil forming factors such as parent material or local vegetational influences. Sequences were therefore chosen on the basis of previous studies in which the distribution of soils and geomorphic relationships were known. Another criterion for selection of soils which was considered desirable was that the age of the parent material had been determined. In many of the sequences selected, radio carbon dates had been measured.

Four sequences were chosen: Gooromon Ponds, a developmental sequence of 5 profiles; Shinglehouse Creek (3), Nowra Creek (4) and Hawkesbury River at Richmond (5). Sequences at Gooromon Ponds, Shinglehouse Creek and Hawkesbury River were in alluvial terrace of slope <2%; the Nowra sequence was in colluvium and alluvium on hillslopes up to 5% slope. Location is shown in Figure 3.

3.2 Methods

3.2.1 Field Sampling

Sampling of soils was carried out from pits dug with a back-hoe usually to a depth of two to three metres. Macromorphological descriptions were made according to the Soil Survey Manual (Soil Survey Staff 1951). Soils were classified according to the Factual Key (Northcote 1979) and the Soil Taxonomy (Soil Conservation Service 1975). Two or three kilograms of soil were sampled from each horizon or within an horizon if it was greater than 20 cm in thickness. Careful note was made of variations around pit faces. Undisturbed samples for bulk density and shrink-swell measurements were taken as close as practicable to the section where bulk sampling was carried out (Chapter 6).

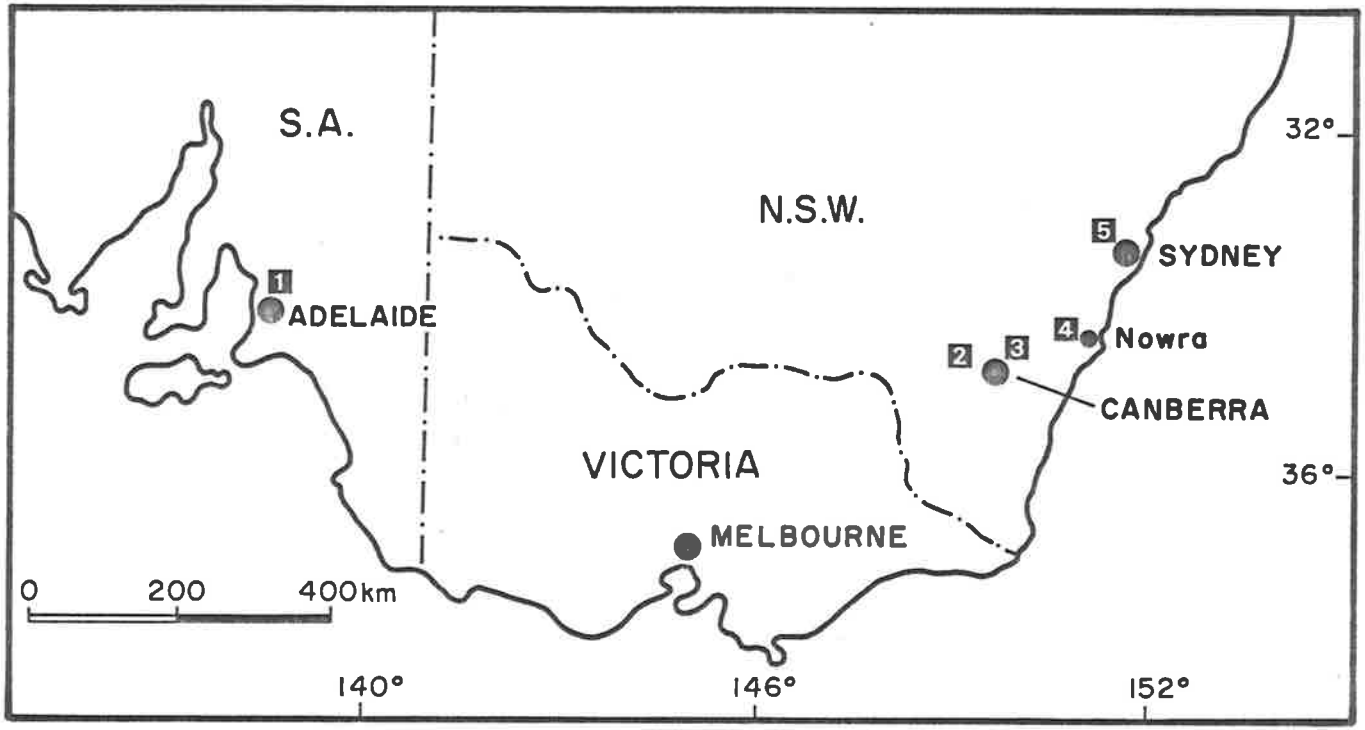

Figure 3 Location of soil profiles and sequences. 1. Urrbrae loam; 2. Gooromon Ponds; 3. Singlehouse Creek; 4. Nowra Creek; 5. Hawkesbury River

3.2.2 Analytical methods

Samples were air dried in a glasshouse, weighed and then ground lightly in a mortar with a pestle to pass through a 2 mm round-hole sieve.

The coarse fraction was washed to remove adhering fine particles, weighed and the proportion of gravel expressed as a percentage of the air dry soil. Extreme care had to be taken since many gravel fragments were highly fractured quartz conglomerates or fine grained siltstones which had a tendency to break readily into particles of sand or silt size.

The following analyses were made on the <2 mm fraction and results expressed on an oven-dry basis: pH, electrical conductivity and chloride by the triple electrode method (Loveday 1974); air dry water content; organic carbon (Tinsley 1950); exchangeable cations (Stace et al. 1968). Other analyses are described in the relevant chapters.

3.3 Morphology and chemistry of soils

3.3.1 Gooromon Ponds sequence

The Gooromon Ponds sequence is located 22km north of Canberra at an elevation of 610 m (Figure 4) and lies on a broad flood plain, 3 km wide, between Cow Flat Creek and Gooromon Ponds Creek. The creeks drain uplands which consist of fine and coarse grained Ordovician and Silurian sediments and Silurian acid volcanics (Figure 5; Canberra 1:50,000 geological map (Geological Survey of N.S.W., 1971)). Detailed stratigraphic descriptions have been published by Walker and Green (1976). A summary of the degree of textural development, classification and stratigraphic name for each of the five profiles is given in Table 1 and their relative geomorphic positions in Figures 6.1 and 6.2.

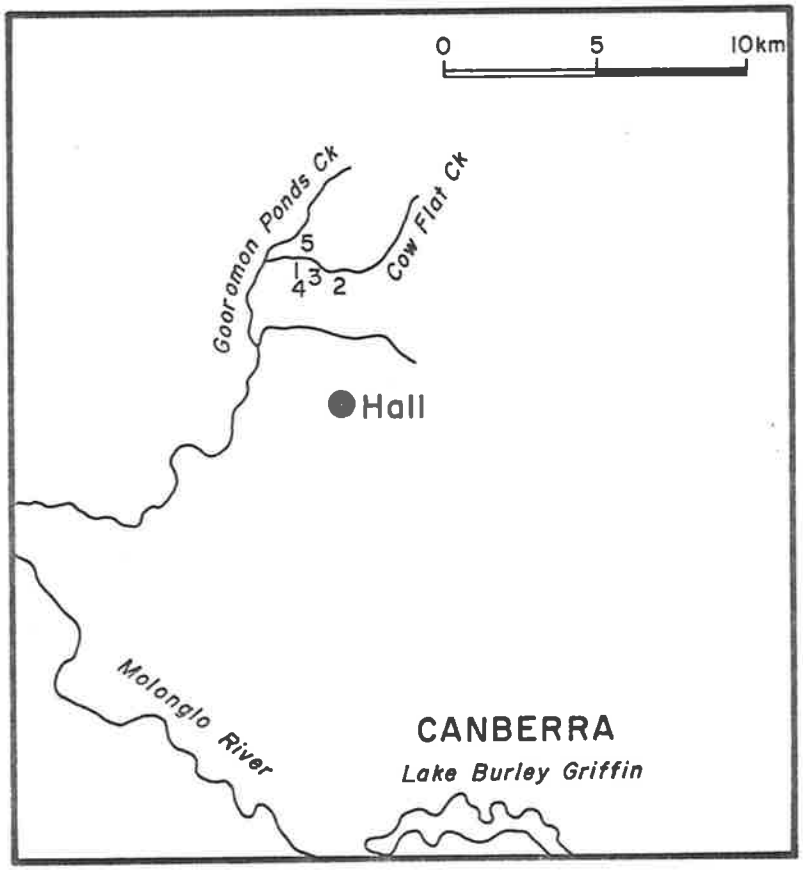

Figure 4 Location of soils of Gooromon Ponds sequence

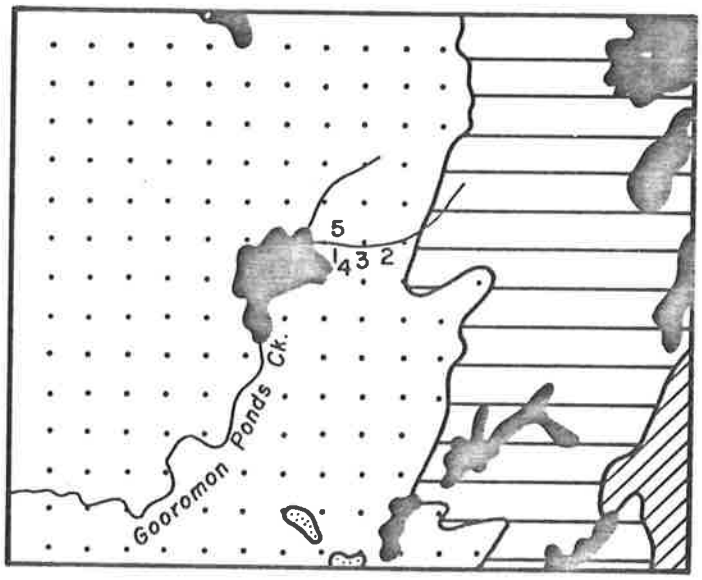


Quaternary alluvium - sands, clays


Devonian volcanics - rhyolite, dacite, tuff


Devonian granite - granite, adamellite, granodiorite


Silurian slate


Silurian volcanics - dacite, audesite, tuff

Figure 5 Geology of Gooromon Ponds sequence

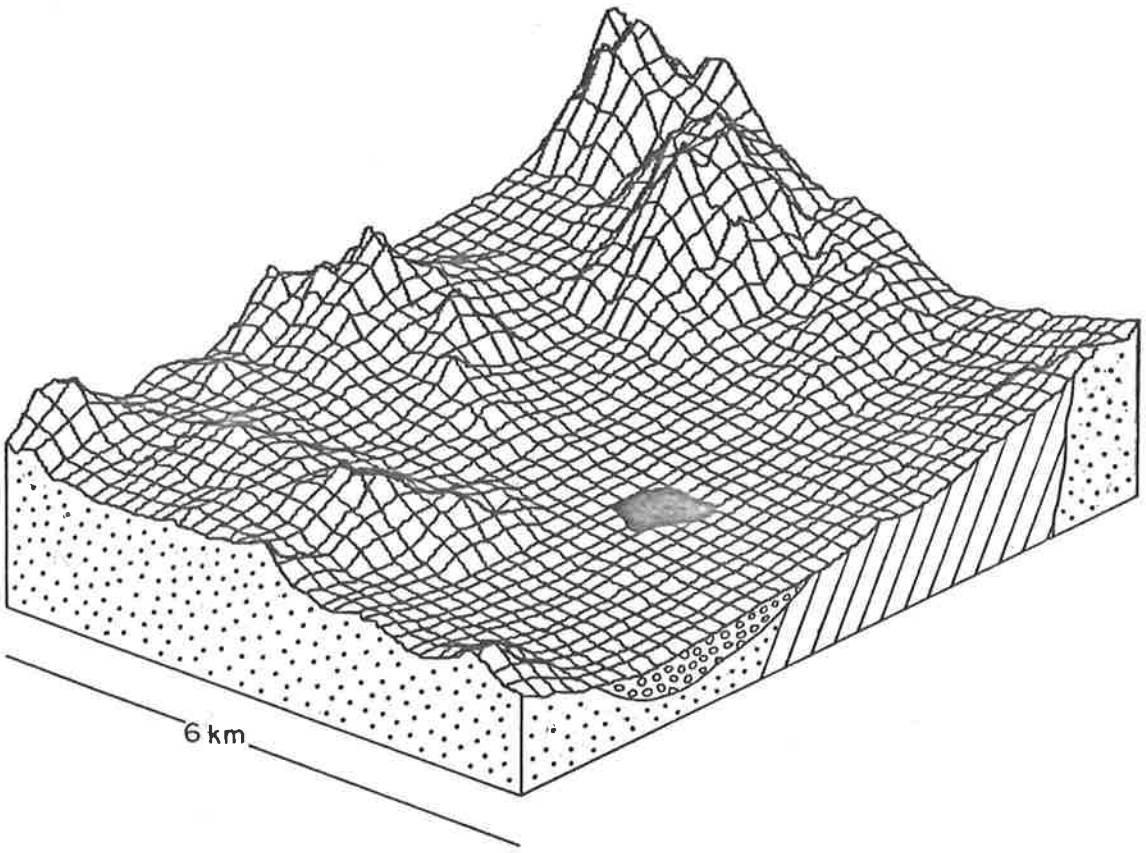

Figure 6.1 Land form of the Gooromon Ponds sequence (from 1:10,000 scale topographic maps)

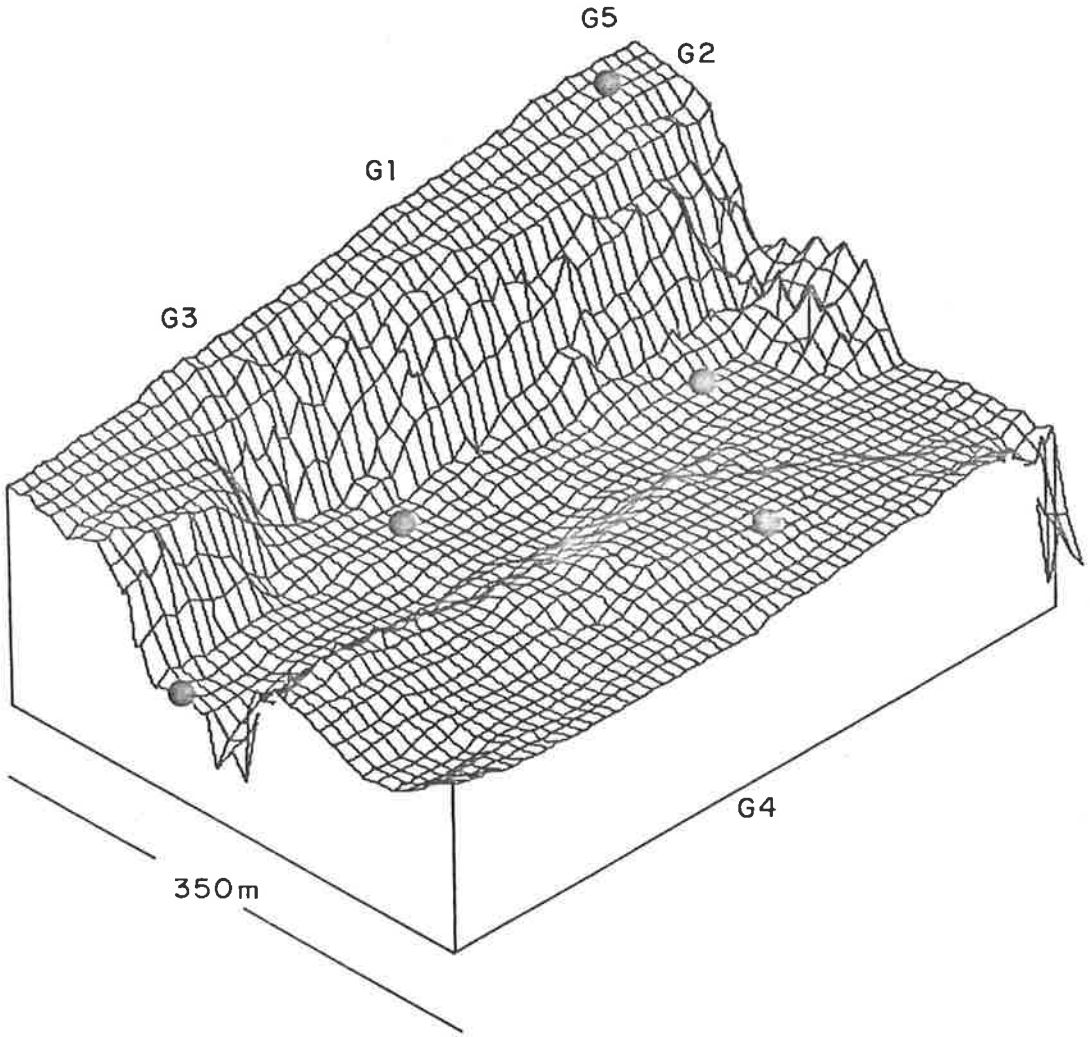

Figure 6.2 Land form of Gooromon Ponds sequence
(from 1:25,000 scale map)

Profile+ code	Stratigraphic* name and age (yrs BP)	Textural differentiation	Classification	
			Factual Key	Soil Taxonomy
G1	Cow Flat	Undifferentiated: Sedimentary layers evident throughout	Uc 1.21	Aquic Ustifluvent
G2	Glenesk 855	Undifferentiated: faunal turbation evident	Um 6.22	Fluventic Haplumbrept
G3	Bedulluck 3000	Slight: A1 and A2 horizon	Um 6.11	Fluventic Haplumbrept
G4	Spring	Moderate: A1, A2 and texture B	Dy 2.41	Ultic Haplustalf
G5	Tara	Strong: A1, A2 and pronounced B2	Dy 2.41	Ultic Haplustalf

* arranged in order of increasing age

\+ the profile code will be used throughout the thesis to identify the profile and facilitate the recognition of the age-relationship of the profile in the sequence: thus G5 is the oldest profile in the Gooromon Ponds sequence.

Table 1 Age, degree of textural differentiation and classification of soils of the Gooromon Ponds sequence.

G1 - Cow Flat unit (Figure 7)

depth (cm)	*horizon*	*description*
0	*A1*	*Dark greyish brown (10 YR 4/2) sandy loam, apedal, slightly hard; clear to*
18	*II C*	*10 YR 4/2 with strong brown (7.5 YR 5/8) mottles, sandy loam with gravel, apedal; gradational to*
32	*III C1*	*as above but loamy coarse sand with gravel, apedal; arbitrary to*
56	*III C2*	*dark yellowish brown (10 YR 4/6) with strong brown mottles, sandy loam, very friable at base; continuing to*
90		

G2 - Glenesk unit (Figure 8)

depth (cm)	*horizon*	*description*
0	*A1*	*Dark greyish brown (10 YR 4/2) loam, very hard, medium crumb; diffuse to*
20	*A12*	*Dark greyish brown (10 YR 4/2) loam, very hard, coarse sub angular blocky, arbitrary to*
40	*A13*	*As above; arbitrary to*
50	*A14*	*As above; continuing to*
70		

G3 - Bedulluck unit (Figure 9)

depth (cm)	*horizon*	*description*
0	*A11*	*Dark greyish brown (10 YR 4/2) loam, crumb, slightly hard; clear to*
12	*A12*	*Black (10 YR 2/1) loam, crumb, slightly hard; gradational to*
32	*B21*	*Black (10 YR 2/1) clay loam, crumb, slightly hard; diffuse to*
55	*II C1*	*Very dark grey (10 YR 3/1), occasional yellow mottles, gravelly clay loam, coarse granular, hard; clear to*
78	*II C2*	*Yellowish brown becoming greyish brown with depth with 10 YR 6/6 mottles, coarse sandy loam, apedal, very hard; clear to*
102	*II C3*	*As above but sandy light clay and brownish yellow mottles becoming more prominent with depth, abundant charcoal from 115 cm; continuing to*
160		

G4 - Spring unit (Figure 10)

depth (cm)	*horizon*	*description*
0	*A11*	*Very dark greyish brown (10 YR 3/2), sandy loam, crumb, soft; clear to*
6	*A12*	*As above but dark greyish brown (10 YR 4/2); gradational to*
13	*A21*	*Dark greyish brown (10 YR 4/2), gravelly sandy loam, crumb, slightly hard; gradational to*
21	*A22*	*Light yellowish brown (10 YR 6/4), gravelly sandy loam, apedal, slightly hard; clear to*
42	*B1*	*Brownish yellow (10 YR 6/6), clay loam, apedal, very hard; diffuse to*
57	*B2*	*Strong brown (7.5 YR 5/6), light clay sub angular blocky, very hard; diffuse to*
81	*C*	*Strong brown (7.5 YR 5/6), sandy clay loam, apedal, very hard; continuing to*
112		

G5 - Tara unit (Figure 11)

depth (cm)	*horizon*	*description*
0	*A1*	*Brown (7.5 YR 5/2), loam fine sandy, apedal, soft; clear to*
8	*A2*	*As above but light brown (7.5 YR 6/4); clear, wavy boundary to*
30	*B21*	*Red (2.5 YR 4/6) light clay, apedal, hard, some faunal mixing of A2 and B horizons; gradational to*
42	*B22*	*As above but weak sub angular blocky; diffuse to*
52	*B31*	*Yellowish red (5 YR 5/6), gravelly clay loam, weak sub angular blocky, very hard; diffuse to*
73	*C1*	*Yellowish brown (10 YR 5/4) with brownish yellow mottles (10 YR 6/6), sandy light clay, apedal, very hard; diffuse to*
100	*C2*	*As above but pale brown (10 YR 6/3) with a few brownish yellow mottles (10 YR 6/6); continuing to*
180		

Figure 7. G1 profile

Figure 8. G2 profile.

Figure 9. G3 profile.

Figure 10. G4 profile

Figure 11. G5 profile.

The most significant features of the chemical data (Table 2) are the change in depth functions of pH and organic carbon with time. Profiles G2 and G3

Profile	Horizon	depth (cm)	pH	EC (mS/cm)	Chloride (ppm)	Air dry moisture (%)	organic carbon (%)	exchangeable cations cec	Ca	Mg	K	Na	H
										(meq %)			
G1	A1	0-6	6.8	0.07	29	1.3	1.58	13.2	5.3	4.2	0.23	0.19	3.3
	IIC	18-32	7.1	0.05	24	1.3	0.67	11.1	4.4	3.7	0.10	0.42	2.5
	IIC1	42-56	7.4	0.17	122	1.1	0.23	7.6	3.8	3.8	0.10	0.72	0
G2	A11	0-20	6.1	0.05	22	1.8	2.05	16.8	6.4	3.9	0.52	0.14	5.8
	A12	20-40	6.6	0.03	<20	1.7	1.03	16.8	6.7	4.2	0.28	0.14	5.5
	A14	50-70	7.0	0.05	24	1.7	0.97	17.3	6.9	4.7	0.18	0.24	5.3
G3	A11	0-12	5.8	0.06	<20	2.1	2.79	24.0	6.4	3.4	0.31	0.11	13.8
	A12	24-32	6.5	0.03	<20	2.4	2.52	26.1	9.2	5.2	0.15	0.13	11.4
	A12	41-55	6.8	0.02	<20	1.6	1.22	16.8	7.0	4.0	0.13	0.11	5.6
	II C2	78-88	7.1	0.01	<20	0.8	0.23	7.1	2.7	2.0	0.09	0.09	2.2
	II C3	102-115	7.0	0.02	<20	1.7	0.27	13.7	4.6	5.5	0.16	0.26	3.2
G4	A11	0-6	5.7	0.07	<20	1.1	2.16	15.7	3.1	0.7	0.70	0.04	11.2
	A22	21-31	6.3	0.02	<20	0.8	0.25	6.0	3.6	0.4	0.20	0.05	1.7
	B2	57-69	6.7	0.02	<20	1.3	0.25	9.6	4.9	1.6	0.25	0.09	2.8
	C	81-96	6.9	0.01	<20	1.2	0.12	10.1	4.8	1.9	0.25	0.09	3.1
G5	A1	0-8	5.3	0.06	<20	0.8	1.78	10.1	1.6	0.4	0.39	0.03	7.7
	A2	8-18	5.1	0.05	<20	0.4	0.32	3.5	0.7	0.2	0.30	0.02	2.3
	B21	30-42	6.0	0.02	<20	1.4	0.28	12.2	4.1	1.1	0.41	0.04	6.6
	B31	65-73	6.9	0.02	<20	1.8	0.19	15.3	5.3	2.4	0.38	0.11	7.1

Table 2 Chemical data for Soils of the Gooromon Ponds sequence

have a much higher organic matter content throughout than either G1 or the older profiles. In the older profiles high organic carbon is restricted to the A1 horizon.

Both G2 and G3 show much evidence of bioturbation: they have a dark gray colouration and numerous fecal pellets, casts, burrows, tubules and organic fragments. The pH of the surface horizons becomes progressively more acid.

3.3.2 Shinglehouse Creek Sequence

This sequence is located 30 km north west of Canberra in a small etch basin (van Dijk and Woodyer 1961) of 4 km^2 (Figure 12). Few stratigraphic units have been defined (Coventry 1967) but only three were sampled (Figures 13, 14). The Doongalla unit (S3) is the most common soil in the area. The Shinglehouse unit (S2) occurs as a channel infilling in the Doongalla unit. The youngest profile Trawalla unit (S1) was sampled from a low terrace in a recent erosion gully of Shinglehouse Creek. A summary of the textural development, classification and stratigraphic names for each of the three profiles is given in Table 3. Ages are for radiocarbon dates of charcoal samples from the base of each profile. A range of age is given for S2 because dating of three samples from three different profiles gave different ages.

Profile code	Stratigraphic name and age (yrs BP)	Textural differentiation	Classification	
			Factual Key	Soil Taxonomy
S1	Trawalla 255	Undifferentiated: sedimentary laminae evident throughout	Uc 1.21	Aquic Ustifluvent
S2	Shinglehouse 1775-3065	Slight: A1 and A2 horizon	Um 6.11	Fluventic ~~Ust~~ Hapl umbrept
S3	Doongalla 6770	moderate: A1, A2, pedal B	Dy 2.21	Ultic Haplust~~alf~~ ult

Table 3. Age, degree of textural differentiation and classification of the soils of the Shinglehouse Creek sequence

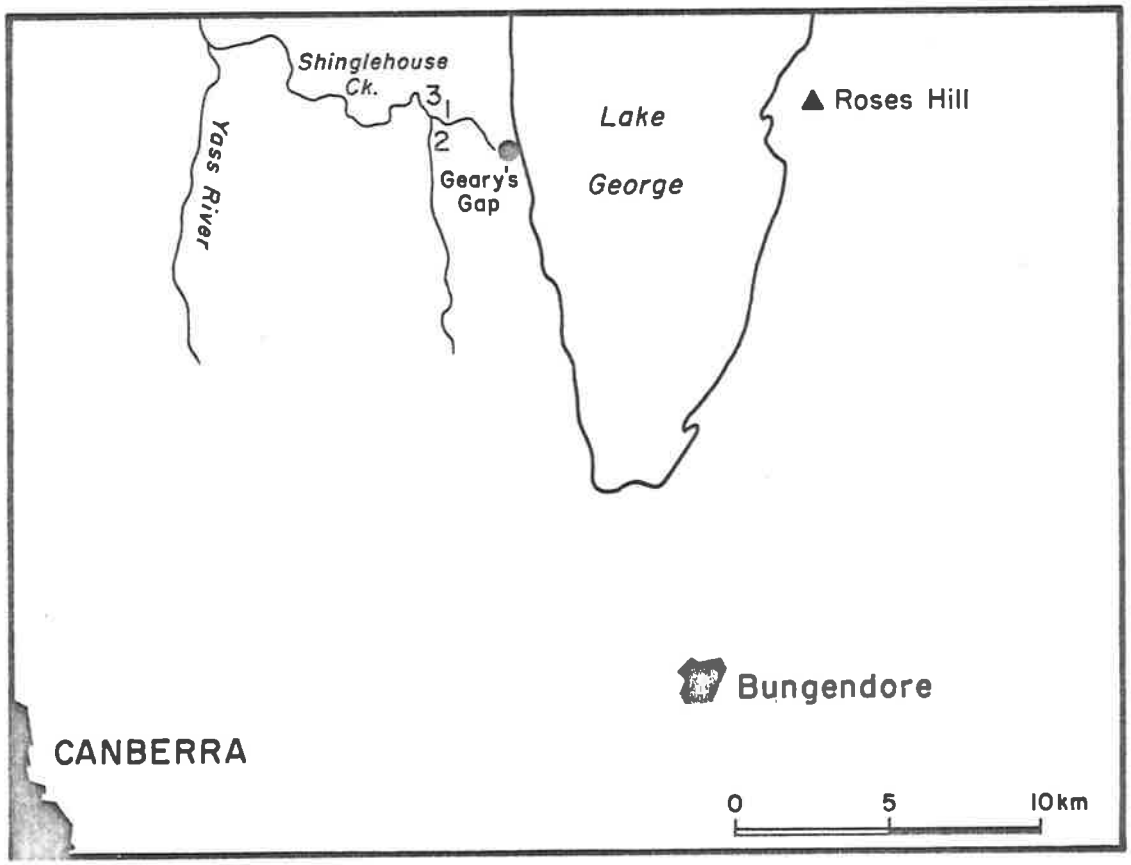

Figure 12 Location of soils of Shinglehouse Creek sequence

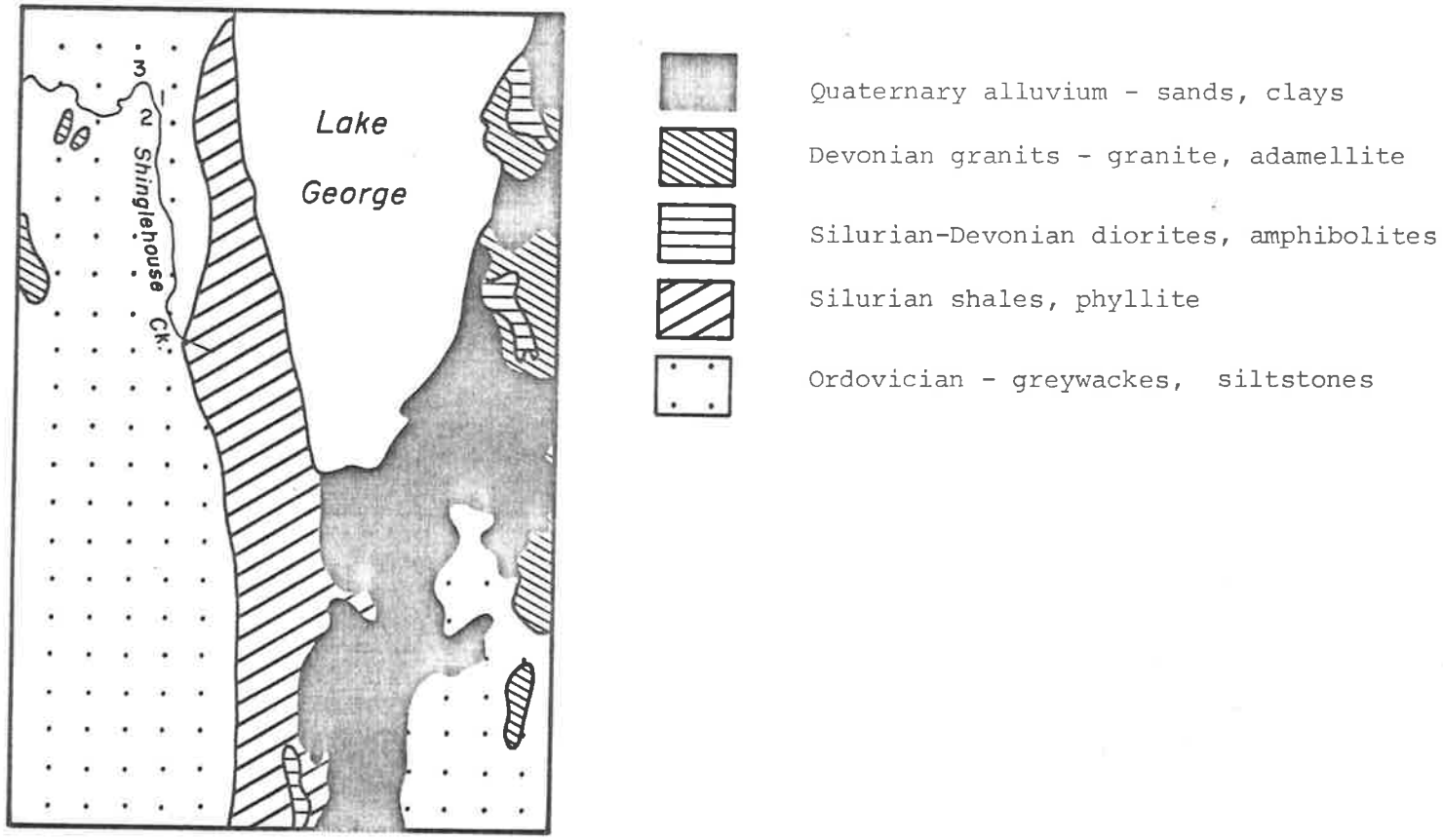

Figure 13 Geology of the Shinglehouse Creek sequence

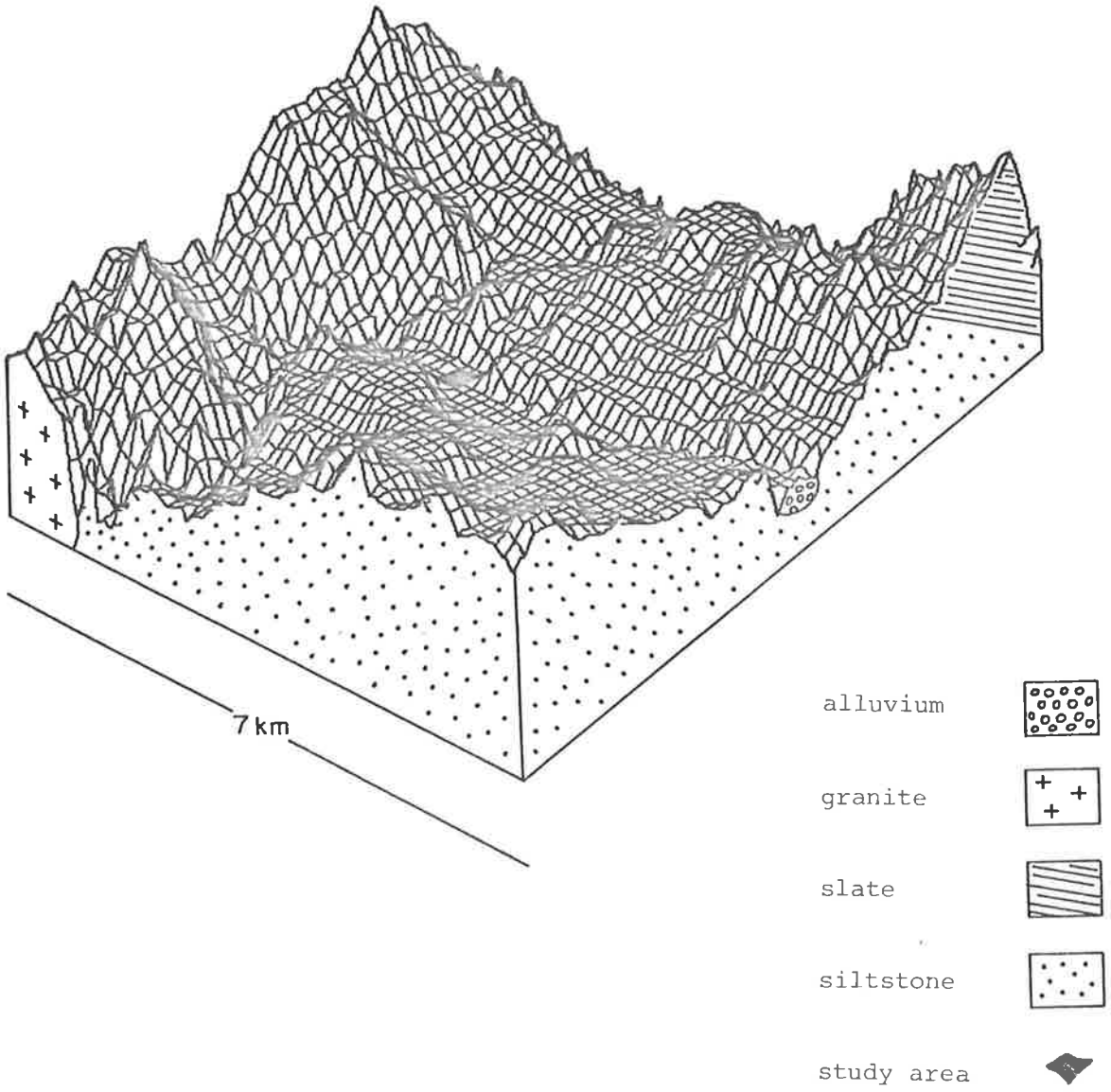

Figure 14 Land form of the Singlehouse Creek sequence (from 1:10,000 scale topographic maps)

S1 - Trawalla unit (Figure 15)

depth (cm)	*horizon*	*description*
0	*A1*	*Dark greyish brown (10 YR 4/2), loam fine sandy apedal, slightly hard; arbitrary to*
10	-	*As above but very hard consistence; arbitrary to*
20	-	*Brown (10 YR 4/3), fine sandy loam, apedal, very hard; arbitrary to*
30	-	*As above but yellowish brown (10 YR 5/4); diffuse to*
50	-	*Dark yellowish brown (10 YR 4/4), gravelly loam, apedal, very hard; continuing to*
110		

Numerous fine, cross-bedded laminae throughout

S2 - Shinglehouse unit (Figure 16)

depth (cm)	*horizon*	*description*
0	*A11*	*Very dark greyish brown (10 YR 3/2), loam, coarse crumb, slightly hard; clear to*
8	*A12*	*As above; arbitrary to*
20	*A13*	*As above; diffuse to*
30	*A3*	*Dark grey (10 YR 4/1.), light clay loam, weak sub angular blocky, slightly hard; diffuse to*
42	*B1*	*Greyish brown (10 YR 5/2), light clay loam, weak subangular blocky, slightly hard; clear to*
52	*B21*	*Greyish brown (10 YR 5/2), clay loam, weak subangular blocky, slightly hard; diffuse to*
60	*B22*	*As above but light clay and apedal; diffuse to*
70	*II C (?)*	*Dark grey (10 YR 4/1), light clay, apedal, very hard; continuing to*
110		

S3 - Doongalla unit (Figure 17)

depth (cm)	*horizon*	*description*
0	*A1*	*Brown (10 YR 4/3), fine sandy loam, apedal, slightly hard; clear to*
7	*A2*	*Bleached (dry), brown (10 YR 5/3), fine sandy loam, apedal, slightly hard; sharp to*
17	*B21*	*Strong brown (7.5 YR 5/6), clay loam, strong coarse subangular blocky, hard; gradational to*
28	*B22*	*As above but light clay; gradational to*
38	*B3*	*As for B22; diffuse to*
48	*B3C*	*As for B22 but apedal; diffuse to*
68	*C1*	*Brownish yellow (10 YR 6/6), light clay, apedal, very hard; continuing to*
108		

Figure 15. S1 profile

Figure 16. S2 profile.

Figure 17. S3 profile.

As in the Gooromon Ponds sequence, there is an initial increase in the organic matter with time: S2 has a high organic carbon content throughout and is equivalent in age and in landscape position to G2 and G3 which also have high organic carbon values (Table 4). However, unlike Gooromon Ponds, the pH is acid for all horizons in the sequence and varies from 5.4 to 6.9.

Profile	Horizon	depth (cm)	pH	EC (mS/cm)	Chloride (ppm)	Air dry moisture (%)	organic carbon (%)	exchangeable cations cec	Ca	Mg	K	Na	H
								(meq %)					
S1	A1	0-10	5.4	0.10	46	1.6	3.03	19.8	2.4	2.0	0.53	0.17	14.7
		20-30	5.6	0.04	<20	0.8	0.68	9.1	1.3	1.3	0.13	0.19	6.2
		50-70	6.2	0.04	27	1.1	0.45	10.6	1.3	1.7	0.09	0.50	7.0
S2	A11	0-8	5.6	0.05	<20	2.2	3.46	25.6	4.4	2.1	0.61	0.18	18.3
	A13	20-30	5.7	0.04	<20	2.0	1.31	21.9	3.0	2.3	0.14	0.21	16.2
	B1	42-52	6.3	0.03	<20	1.7	0.94	18.3	1.6	1.9	0.09	0.24	14.5
	II C(?)	70-90	6.9	0.07	<20	2.1	1.31	25.0	2.5	2.6	0.08	0.72	19.2
S2	A1	0-7	5.7	0.05	30	0.8	1.73	11.1	0.7	0.7	0.55	0.02	9.1
	B21	17-28	5.9	0.03	<20	0.9	0.60	10.1	1.6	1.6	0.38	0.11	6.4
	B3	38-48	6.0	0.02	<20	1.5	0.31	13.7	1.9	3.0	0.31	0.25	8.1
	C1	68-88	5.9	0.04	43	1.6	0.22	13.7	2.8	4.1	0.21	0.86	5.7

Table 4 Chemical data for soils of Shinglehouse Creek sequence

3.3.3 Nowra Creek sequence

The Nowra Sequence lies 8 km south of the Nowra township in a small creek draining an area which flows into the Shoalhaven River (Figure 18). The parent material of the soils is colluvium and alluvium of siltstone, shale and sandstone of Permian age (Figures 19 and 20). and profiles were sampled. These have been previously mapped and described by Walker (1962 a,b). The youngest soil, N1 (Tapitallee unit) is a valley fill in steeply sloping terrain and is frequently flooded. N2 (Minnamurra unit) was sampled in an erosion gully 1 km downstream from N1 in gently sloping terrain. This soil is subject

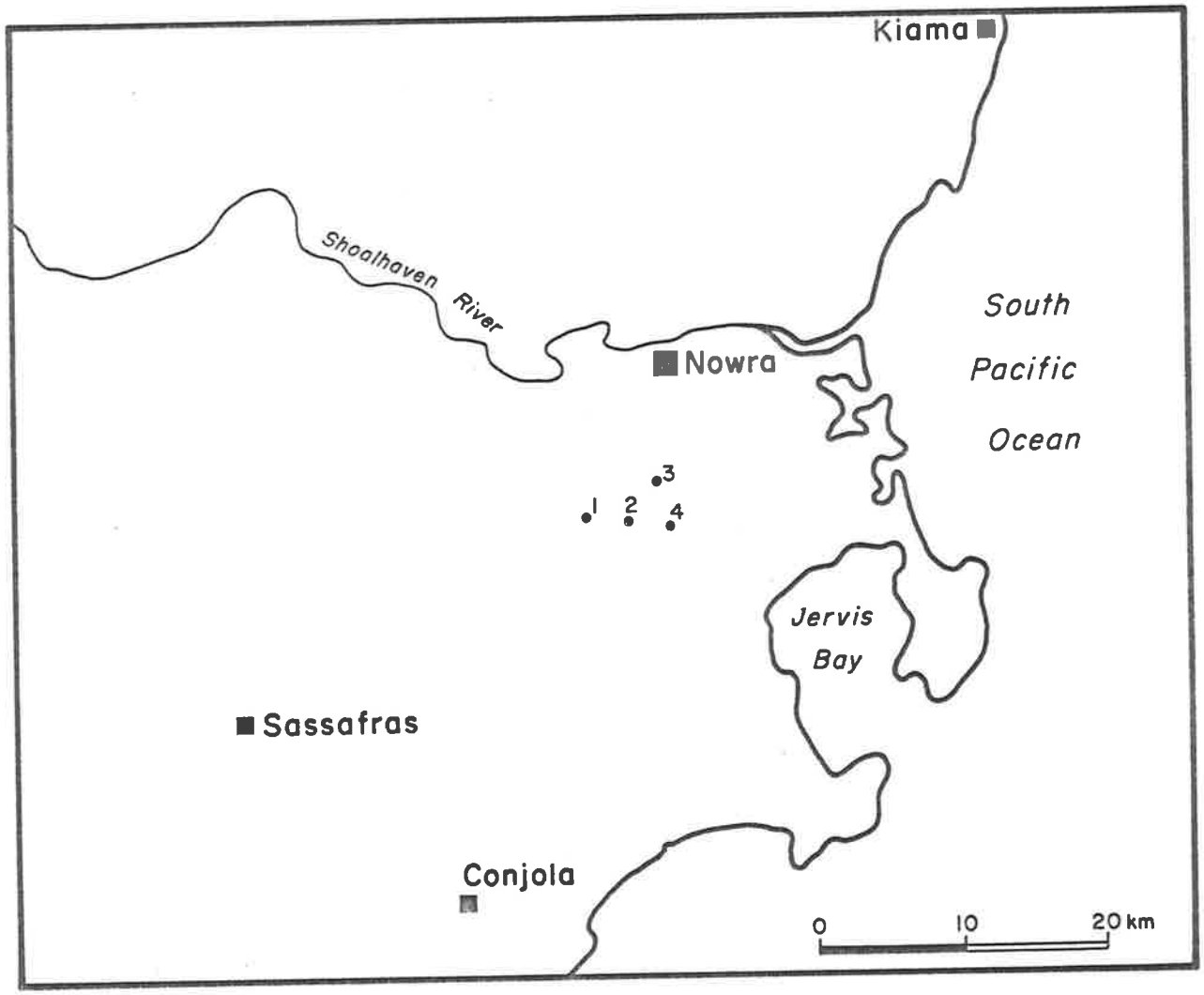

Figure 18 Location of soils of Nowra Creek sequence

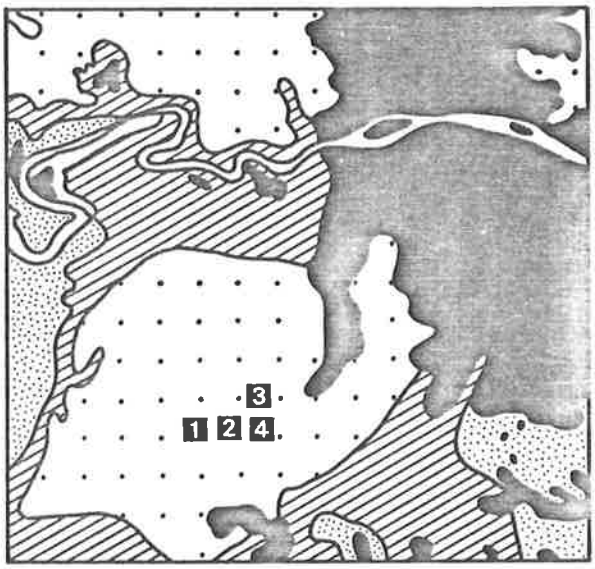


Quaternary alluvium - sands, clay


Permian sandstone


Permian siltstone


Permian siltstone - siltstone, shale

Figure 19 Geology of Nowra Creek sequence

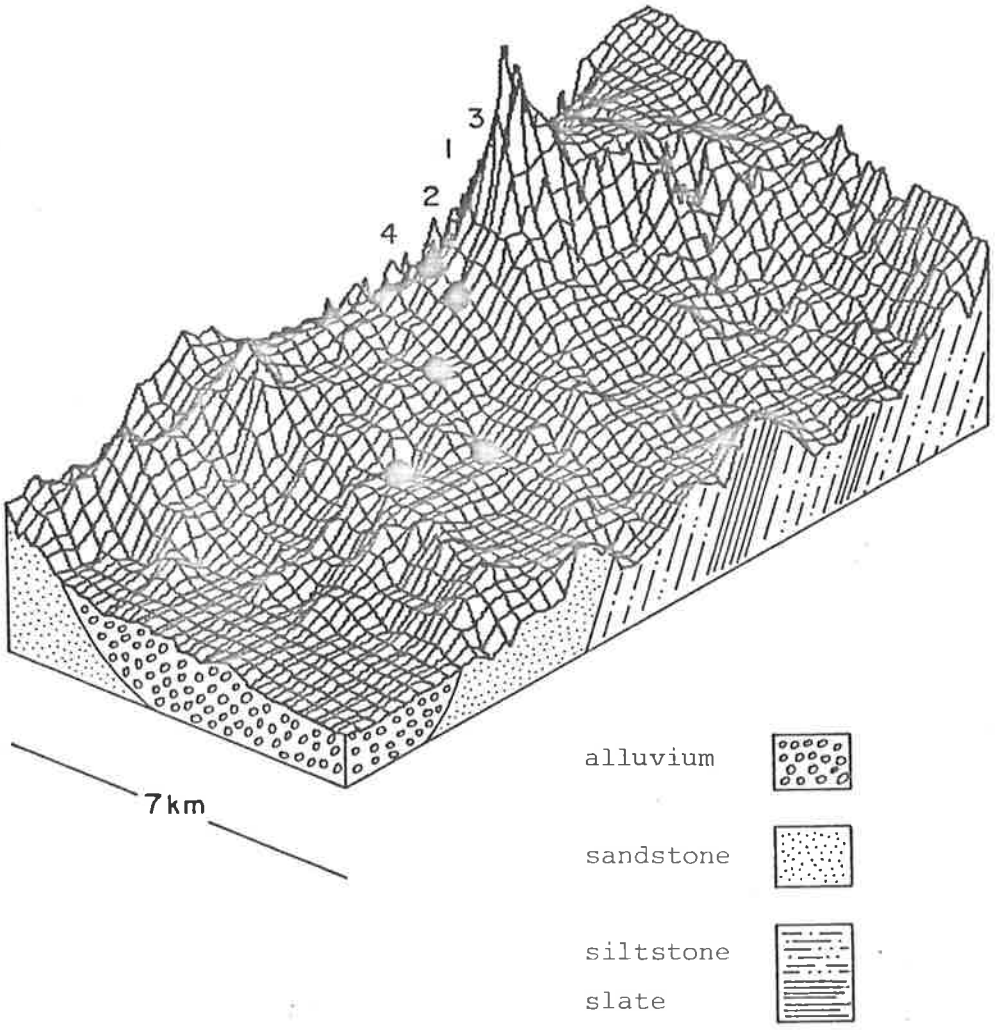

Figure 20 Land form of Nowra Creek sequence
(from 1:25,000 scale topographic maps)

to occasional brief, overbank flooding. N3 (Nowra Unit) and N4 (Wandandian unit) were sampled from creek banks. A summary of the textural development, classification and stratigraphic nomenclature for the profiles is given in Table 5.

Profile code	Stratigraphic name and age (years BP)	Textural differentiation	Classification	
			Factual Key	Soil Taxonomy
N1	Tapitallee 0-125	Undifferentiated: colluvial bands prominent	Um 1.41	Aquic Ustifluvent
N2	Minnamurra 390	weak: A and B	Um 6.21	Typic Fluvaquent
N3	Nowra 3740	moderate: A and B2	Gn 2.84	Aquic Haplustult
N4	Wandandian 29,000	Very strong: A1, bleached A2, B2	Dy 5.41	Aquic Haplustult

Table 5. Age, degree of textural differentiation and classification of the soils of the Nowra sequence

N1 - Tapitallee unit (Figure 21)

depth (cm)	*horizon*	*description*
0	*A1*	*Brown (10 YR 5/3) with yellowish brown (10 YR 5/6) mottles, fine sandy loam, apedal slightly hard; clear to*
5	*C1*	*As above; diffuse to*
18	*C2*	*As for A1 but find sandy loam and very hard consistence; clear to*
45	*II C*	*Minnamurra unit. Very dark greyish brown 10 YR 4/2) with strong brown (7.5 YR 5/6) mottles, clay loam, apedal, very hard; continuing to*
65		

N2 - Minnamurra unit

depth (cm)	*horizon*	*description*
0	*A11*	*Dark brown (7.5 YR 3/2), loam, coarse granular, hard; clear to*
7	*A12*	*As above but less organic matter; arbitrary to*
20	*B*	*Very dark grey with occasional dark yellowish brown (10 YR 4/6) mottles, clay loam, coarse granular, very hard; diffuse to*
41	*B*	*Es above but more mottles of 10 YR 4/6; clear to*
50	*C*	*As above but with soft weathering siltstone; clear to*
52	*II B*	*Very dark grey, heavy clay loam, coarse granular, very hard; continuing to*
70		

N3 - Nowra unit (Figure 23)

depth (cm)	*horizon*	*description*
0	*A1*	*Dark greyish brown (10 YR 4/2), loam, coarse granular, hard; clear to*
10	*B1*	*Dark greyish brown, clay loam, weak coarse granular, very hard; clear to*
25	*B21*	*Brown (10 YR 4/3), light clay, weak coarse granular, very hard; diffuse td*
35	*B22*	*Brown with yellowish brown (10 YR 5/4) mottles clay loam, weak coarse granular, very hard; diffuse to*
50	*B3*	*As above; diffuse to*
70	*C*	*As above but pedal; contibuing to*
110		

N4 - Wandandian unit (Figure 24)

depth (cm)	*horizon*	*description*
0	*A1*	*Very dark greyish brown (10 YR 3/2), fine sandy loam, weak granular, soft; clear to*
5	*A2*	*Bleached (dry), pale brown (10 YR 6/3), gravelly fine sandy loam, medium granular, hard; clear to*
17	*B1*	*Brown (10 YR 5/3) with faint pale brown (10 YR 6/3) mottles, light clay with gravel, medium granular, very hard; gradational to*
30	*B2*	*Grayish brown (10 YR 5/2) with faint pale brown mottles, heavy clay, medium granular, very hard; gradational to*
40	*B3*	*As above but weak coarse angular blocky; diffuse to*
60	*C1*	*Greyish brown (10 YR 5/2) with distinct pale brown (10 YR 6/3) mottles becoming faint with depth, heavy clay, weak coarse angular blocky, very hard; continuing to*
140		

The depth functions of organic carbon with time are similar to those of Gooromon Ponds and Nowra (Table 6). N2, the equivalent of G2 and S2, is high in organic carbon throughout, even when buried: the IIC horizon of N1 has an organic carbon content of 1.52%. As in the Gooromon Ponds sequence, profiles become more acid with age.

Profile	Horizon	depth (cm)	pH	EC (mS/cm)	Chloride (ppm)	Air dry moisture (%)	organic carbon (%)	exchangeable cations cec	Ca	Mg	K	Na	H
										(meq %)			
N1	C1	5-18	6.1	0.03	<20	2.0	0.86	15.8	3.0	3.4	0.20	0.70	8.5
	C2	32-45	6.3	0.03	<20	2.3	0.86	15.3	4.2	3.3	0.19	0.90	6.7
	IIC	45-55	6.4	0.03	<20	1.8	1.52	15.8	2.7	2.0	0.16	0.70	10.2
N2	A11	0-7	6.4	0.07	<20	2.3	3.26	20.5	7.8	4.0	0.48	0.25	8.0
	A12	7-20	6.3	0.06	<20	2.7	2.60	21.6	6.9	4.3	0.51	0.30	9.6
	B	30-41	6.8	0.05	<20	3.5	2.35	21.7	8.1	5.7	0.53	0.33	7.1
	C	50-60	7.0	0.07	38	2.0	1.58	17.9	6.4	5.3	0.28	0.84	5.1
N3	A1	0-10	5.8	0.03	<20	2.5	2.26	19.0	2.4	1.8	0.30	0.24	14.3
	B1	10-25	6.2	0.03	<20	1.7	0.92	15.3	2.2	2.4	0.15	0.55	10.0
	B21	25-35	5.9	0.04	22	1.9	0.63	17.3	1.5	2.8	0.15	0.81	12.1
	B22	35-50	5.9	0.06	61	1.7	0.66	15.8	1.0	2.7	0.16	1.00	10.9
	B3	50-70	6.2	0.13	193	1.5	0.52	13.2	1.3	3.8	0.14	1.70	6.3
N4	A1	0-5	5.8	0.03	<20	1.7	2.03	16.3	1.5	1.1	0.57	0.24	12.9
	A2	5-17	5.8	0.02	<20	1.5	0.92	13.2	0.70	0.7	0.39	0.10	11.3
	B1	17-30	5.7	0.03	<20	2.0	0.49	15.8	0.56	2.2	0.31	0.46	12.2
	B3	40-60	5.3	0.06	<20	3.4	0.30	23.3	0.36	3.4	0.26	1.10	18.2
	C3	120-140	5.1	0.17	205	2.5	0.30	22.6	0	4.8	0.19	2.40	15.2

Table 6 Chemical data for Soils of the Nowra Creek sequence

Figure 21. N1 profile.

Figure 23. N3 profile.

Figure 24. N4 profile.

3.3.4 Hawkesbury River sequence

This sequence is found on the Hawkesbury River terraces at Richmond, 30 km north west of Sydney (Figure 25). Soils have formed in alluvium derived from Triassic shales of the Wianamatta Group and quartzitic sandstones of the Hawkesbury sandstone (Figure 26). Five soil profiles were sampled, but it is not clear whether the oldest profile, the Londonderry soil unit (H5), forms part of the chronosequence.

The H1 profile (Lowlands unit) is on a level bank of the modern flood plain and is frequently flooded (Figure 27). H2 lies behind the level on the flood plain and is also subject to inundation. H3 and H4 are respectively on low and high terraces which are infrequently flooded. H5 is on a high terrace in an erosional landscape. It was not possible to inspect the parent material of this profile. No comparison could therefore be made of the nature of the parent material in relationship to other soils in the sequences, nor was any dating possible for this soil. It appears that there has been considerable erosion of the surface of H5.

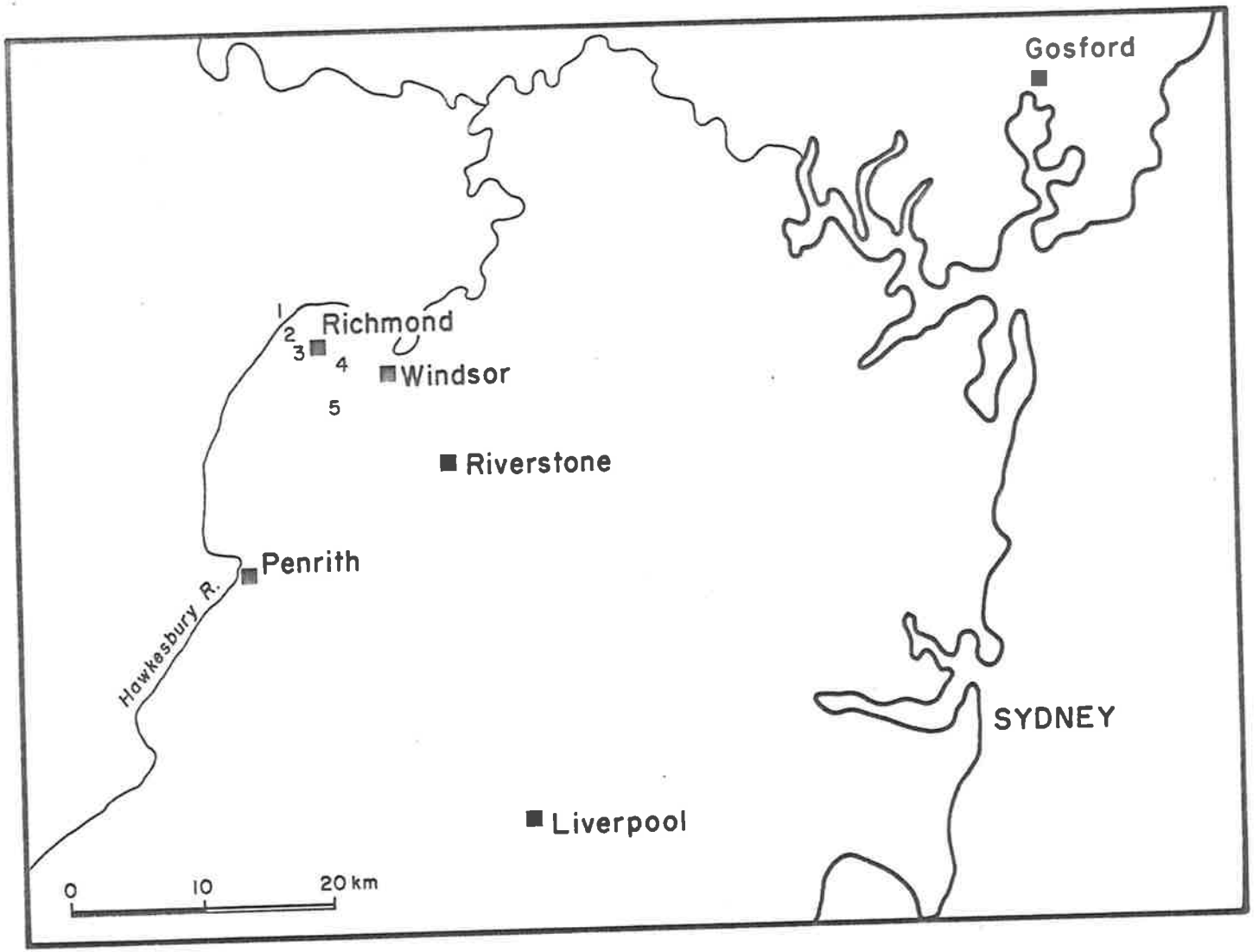

Figure 25 Location of soils of the Hawkesbury River sequence

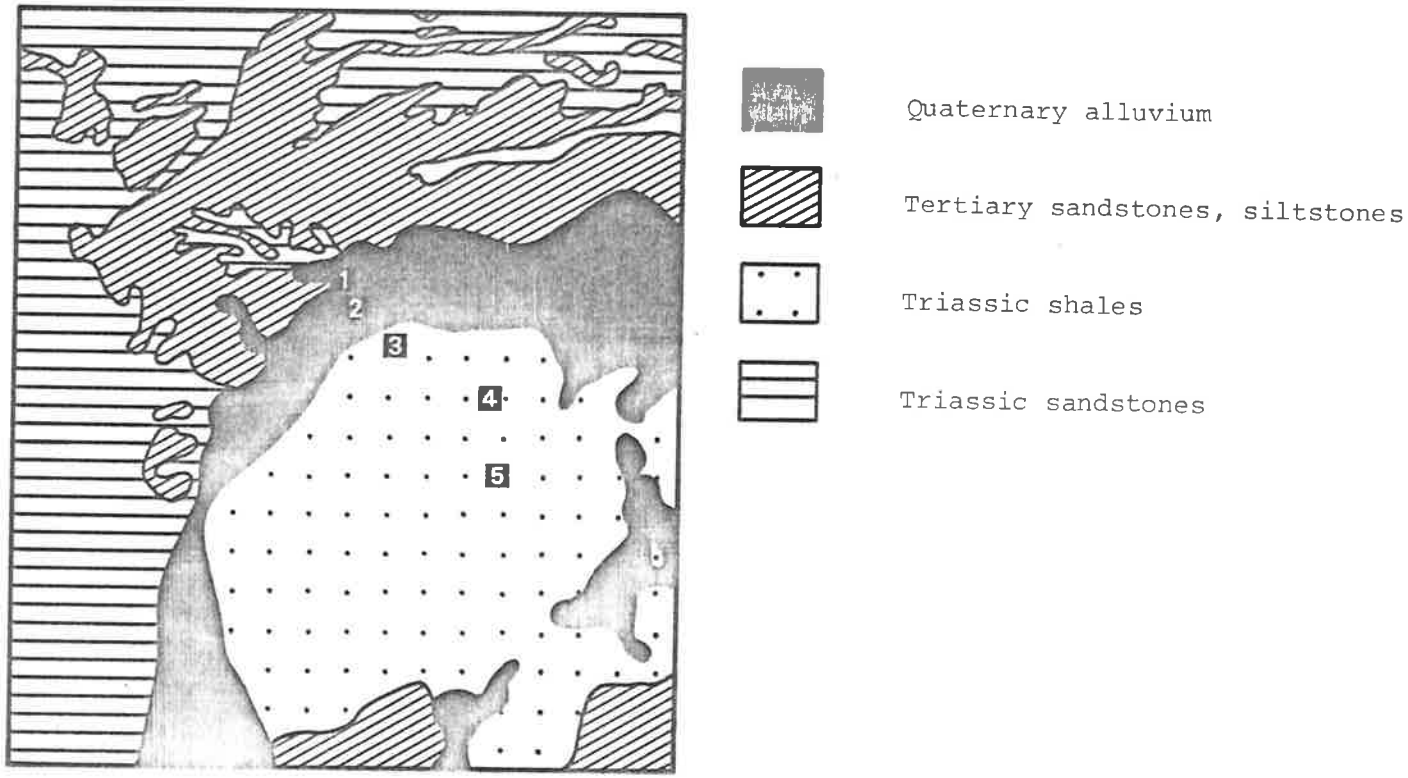

Figure 26 Geology of Hawkesbury River sequence

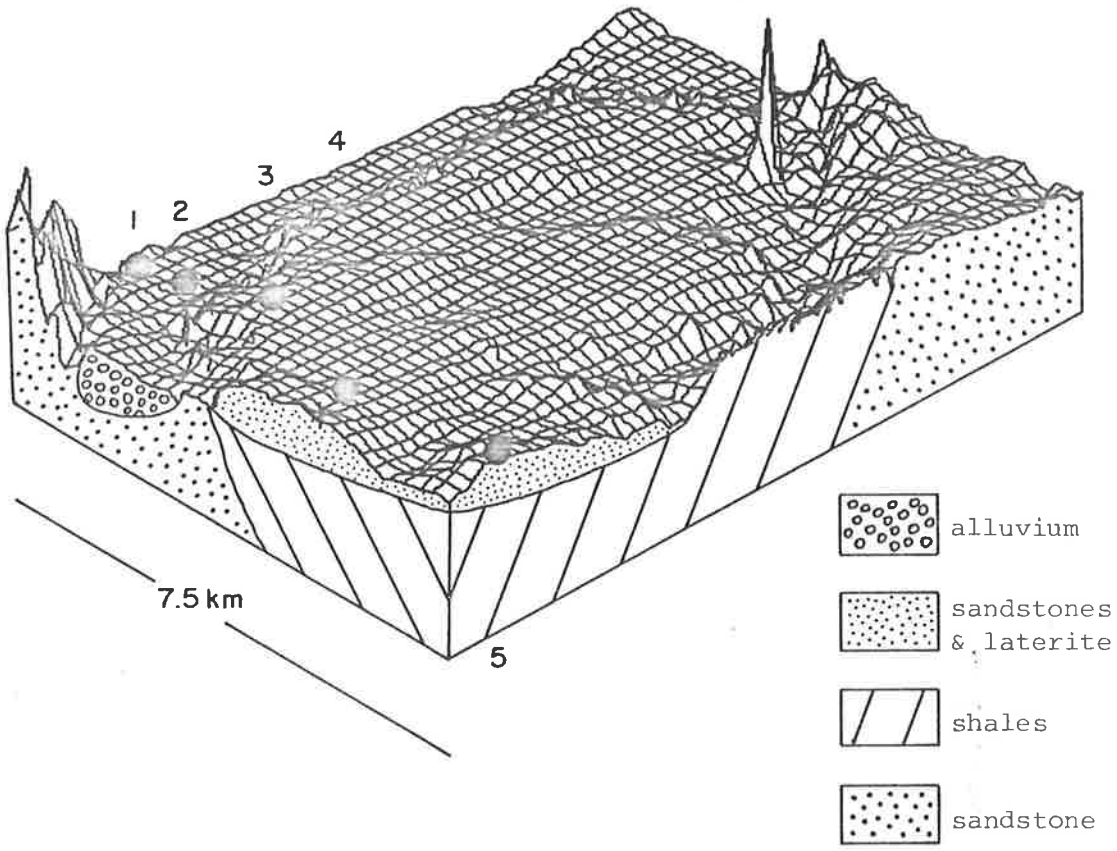

Figure 27 Land form of Hawkesbury River sequence (from 1:25,000 scale topographic maps)

Profile+ code	Stratigraphic* name and age (yrs BP)	Textural differentiation	Classification Factual Key	Classification Soil Taxonomy
H1	Lowlands undated	Undifferentiated:	Uc 1.24	Typic Quartzipsamment
H2	Unnamed undated	Weak: AB profile	Gn 2.1	Fluventic Haplumbrept
H3	Late Clarendon - Cranebrook 9220	moderate: AB profile	Gn 2.111	Typic Haplustalf
H4	Early Clarendon - Cranebrook 26700	strong: A1, thin bleached A2, B2 heavy clay	Dy 3.41	Typic Natr~~Pal~~eustalf
H5	Londonderry undated	very strong: A1, bleached A2, B2	Dy 3.81	Natrustalf ~~Paleustult~~

Table 7. Age, degree of textural differentiation and classification of the soils of the Hawkesbury River sequence

H1 - Lowlands unit (Figure 28)

depth (cm)	*horizon*	*description*
0	*A11*	*Dark brown (7.5 YR 3/2) loamy sand, apedal, loose, clear to*
15	*A12*	*As above but more dense; clear to*
40	*IIC*	*Dark reddish brown (5 YR 3/2), coarse loamy sand, apedal, very friable; continuing to*
150		

H2 - Unnamed (Figure 29)

depth (cm)	*horizon*	*description*
0	*A*	*Dark brown (7.5 YR 3/2), loamy sand, apedal, very friable, many roots; clear to*
15	*IIA*	*Dark reddish brown (5 YR 3/2), sandy loam, apedal, very friable; gradational to*
45	*IIB1*	*Dark reddish brown (5 YR 3/3), sandy loam, apedal, extremely firm; gradational to*
67	*IIB21*	*Reddish brown (5 YR 4/4), clay loam, apedal, extremely firm; gradational to*
88	*IIB22*	*As above except yellowish red (5 YR 4/6); diffuse to*
110	*IIB31*	*As for IIB22 but sandy loam; diffuse to*
150	*IIC1*	*Yellowish red (5 YR 4/6), coarse sandy loam, apedal, firm; continuing to*
170		

H3 - Lake Clarendon-Cranebrook unit (Figure 30)

depth (cm)	*horizon*	*description*
0	*A1*	*Reddish brown (5 YR 4/3), loamy sand, weak medium granular, very friable; gradational to*
18	*A3*	*As above but sandy loam; gradational to*
32	*B1*	*Dark reddish brown (2.5 YR 3/4), sandy clay loam, weak medium granular, extremely firm; gradational to*
48	*B21*	*As above but heavy sandy clay loam; diffuse to*
70	*B22*	*Dark red (2.5 YR 3/6), fine sandy light clay, weak medium granular, extremely firm, soft iron and manganese nodules; diffuse to*
90	*BC*	*As above; diffuse to*
120	*C*	*As above but apedal and becoming red (2.5 YR 4/6) with depth; continuing to*
170		

H4 - Early Clarendon-Cranebrook (Figure 31)

depth (cm)	*horizon*	*description*
0	*A1*	*Reddish brown, loamy sand, apedal, very friable; sharp to*
11	*B21*	*Reddish brown (5 YR 5/3) with red (2.5 YR 4/6) mottles, heavy clay, coarse columnar breaking to angular blocky, extremely firm; clear to*
23	*B22*	*Brown (10 YR 5/3) with red (2.5 YR 4/6) mottles, heavy clay, angular blocky, extremely firm; gradational to*
43	*B23*	*As above but weak angular blocky; gradational to*
70	*B3*	*Reddish brown (5 YR 4/4), clay, sub angular blocky, extremely firm; diffuse to*
100	*C*	*As above but apedal and becoming fine sandy clay with depth; continuing to*
160		

H5 - Londonderry Unit (Figure 32)

depth (cm)	*horizon*	*description*
0	*A1*	*Greyish brown (10 YR 5/2) loamy sand, apedal, very friable, many small roots, ironstone gravel; clear to*
10	*A21*	*As above but bleached (10 YR 7/2 dry); gradational to*
20	*A22*	*Light yellowish brown, loamy sand, apedal, very friable, many iron concretions; sharp, uneven boundary to*
35	*B21*	*Very pale brown (10 YR 7/3) codominant with strong brown (7.5 YR 5/6), clay, columnar with dark organic staining, extremely firm, iron concretions; diffuse to*
60	*B22*	*As above but no organic staining; diffuse to*
100	*BC*	*Light grey (10 YR 7/2), codominant with strong brown (7.5 YR 5/6), clay, apedal, extremely firm, iron concretions; continuing to*
160		

There is an increasing acidity with soil age (Table 8) but, unlike other sequences, there is no highly organic phase in the chronosequence. Another feature not in common with the other three sequences is the saline subsoil in the older members, H4 and H5. There is also a predominance of sodium and magnesium on the exchange of sites of these soils.

Profile	Horizon	depth (cm)	pH	EC (mS/cm)	Chloride (ppm)	Air dry moisture (%)	organic carbon (%)	exchangeable cations cec	Ca	Mg (meq %)	K	Na	H
H1	IIC1	40-58	6.8	0.04	<20	1.3	1.18	12.7	8.2	1.1	0.14	0.07	3.2
	IIC2	58-90	6.6	0.04	<20	1.4	1.54	13.2	7.4	2.0	0.10	0.10	3.6
	IIC3	90-120	6.4	0.04	<20	1.3	1.24	13.2	6.5	1.3	0.11	0.09	5.2
H2	IIA	15-30	6.2	0.02	<20	1.3	1.07	12.7	4.7	1.2	0.09	0	6.7
	IIB1	45-67	6.2	0.02	<20	1.4	0.62	10.1	4.4	1.3	0.10	0.07	4.2
	IIB21	67-88	6.2	0.02	<20	1.3	0.50	11.1	3.5	1.4	0.11	0.07	6.0
	IIB31	110-130	6.4	0.02	<20	1.1	0.21	7.6	2.7	1.6	0.10	0.04	3.2
	IIC1	150-170	6.5	0.02	<20	0.7	0.12	5.0	1.9	1.2	0.06	0	1.8
H3	A1	0-18	6.4	0.04	<20	0.6	0.82	6.5	1.5	0.6	0.52	0	3.9
	A3	18-32	6.2	0.04	<20	0.7	0.54	7.6	1.8	0.5	0.33	0	5.0
	B1	32-48	6.1	0.04	<20	0.8	0.34	3.0	1.9	0.3	0.35	0	0.4
	B21	48-70	6.1	0.04	<20	0.9	0.22	5.5	2.3	0.3	0.35	0	2.5
	BC2	90-120	6.1	0.03	<20	1.0	0.09	5.6	2.3	0.3	0.28	0.02	2.7
	C2	150-170	6.3	0.03	<20	1.3	0.08	7.1	3.1	0.7	0.31	0.05	2.9
H4	A1	0-11	5.4	0.02	<20	0.9	1.16	9.1	0.1	0.2	0.26	0.03	8.5
	B21	11-23	5.9	0.06	38	2.3	0.65	16.9	0.1	5.9	0.19	1.00	9.7
	B23	43-70	6.5	0.45	613	2.2	0.24	14.8	0	8.9	0.11	3.40	2.4
	C	100-130	7.4	0.62	885	1.7	0.09	11.7	0	7.4	0.13	2.80	1.4
H5	A1	0-10	5.5	0.02	<20	0.5	1.13	4.5	0	0.3	0.09	0.04	4.1
	A22	20-35	5.9	0.01	<20	0.6	0.14	3.0	0	0.2	0.06	0.06	2.7
	B21	35-60	6.3	0.06	60	2.6	0.27	15.9	0.2	4.3	0.07	1.10	10.3
	B22	80-100	7.2	0.27	391	2.9	0.20	17.0	0.1	6.8	0.05	3.00	7.0
	BC	130-160	6.6	0.44	636	2.6	0.06	15.4	0	6.5	0.07	3.60	5.2

Table 8 Chemical data for Soils of the Hawkesbury River sequence

Figure 28. H1 profile.

Figure 29. H2 profile.

Figure 30. H3 profile.

Figure 31. H4 profile.

Figure 32. H5 profile.

Chapter 4

Particle-size distributions

4.1 Introduction

Changes in particle-size with depth are almost ubiquitous features of soil profile development. Extensive use has been made of the particle-size distribution to characterize soils and most classification schemes have criteria based on textural variation within the profile and between soils. For example, in the new Soil Taxonomy, one criterion of an argillic horizon is that it normally should have a ratio of fine clay to total clay at least one third greater than in the overlying eluvial horizons or the underlying horizon (Soil Conservation Service 1975).

The particle-size distribution down a soil profile can provide evidence which helps to distinguish between three proposals to explain the origin of the high clay B horizon of texture-contrast soils viz. sedimentary layering, formation of clay in position by in situ chemical weathering and downward translocation of clay in an initially homogeneous material (Chittleborough and Oades 1979).

A number of physical and chemical criteria have been used to identify stratified sediment in soils. Thus Ruhe (1956) used the presence of stone lines to delineate surfaces of at least two different ages within interglacial materials in south-western Iowa. Foss and Rust (1968) used detailed particle-size distributions of the silt and sand fractions to study soil development in relation to loessial deposition and concluded that a palaeosol had developed on the Rockian till.

All methods involve the change in a particular criterion with depth. Methods for the statistical identification of such discontinuities in the depth function have been developed by Oertel and Giles (1966) and more fully by Raad and Protz (1971). On the basis of total sand : total silt ratios, Raad and Protz (1971) were able to set limits of significance for differences between populations of stratified sediments in soil profiles developed in fluvio-glacial terrain. Langohr et al (1975) have proposed a comparative particle-size distribution (CPSD) index to estimate the magnitude of discontinuities (or similarities) in parent materials. The index is based on the degree of correspondence between any two horizons of the particle-size distributions in the sand range. A value of 100 indicates two identical distributions, a value of 0 indicates that the distributions are completely different.

Little use has been made of particle-size properties of soils to assess the extent of chemical weathering, despite the fact that the process is likely to have a marked effect on the particle-size distribution. It is often inferred, from an increase in clay content, that there has been an increase in chemical weathering but there is invariably no evidence provided. Torrent and Nettleton (1979) have proposed a textural index for assessing chemical weathering in soils based on the change with depth of the fine silt to total silt. It can only be used in soil with texturally uniform parent materials and where there is little or no physical weathering.

An increase in the proportion of fine clay (<0.2 um) to coarse clay has been taken as an indication that clay has been illuviated. There appear to be two reasons for this inference. One is that a high ratio of fine to coarse clay is observed in horizons with higher total clay and which also show other signs that clay has moved e.g. the presence of void argillans (Smith and Buol 1968). Second, experimental evidence shows that

fine clay moves more readily than coarse (Dixit 1978). However, little use of the criterion has been made in pedogenic studies in Australia, despite the extent and diversity of texture-contrast soils compared to other continents. It should be pointed out that an increase in the ratio is not definitive evidence for clay illuviation. Other mechanisms may also be involved e.g. lateral transport of clay into the horizon and chemical weathering (Nikiforoff and Drosdoff 1943, Byers et al 1938). Where clay enrichment is due solely to mechanical transport, Rode (1964) uses the term lessivage to describe the process. The criterion for this mechanism is the simultaneous accumulation (as compared to the parent material) of clay and sesquioxides. Where there is a discrepancy, other processes such as in situ chemical weathering may be involved in the clay increase.

From the foregoing discussion, it is clear that, if particle-size data are to be used as pedogenic criteria, the methods used to obtain such data must be reliable and give consistent results. While there has been much investigation of the methods of obtaining distributions in the range >2 um and standard procedures established, there is a paucity of information on techniques in the sub-micron range.

Many soils with high clay contents are known to be difficult to disperse and have anomalously low clay contents when measured in relation to field assessment of texture (McIntyre 1976) and the cation exchange capacity (Stace et al 1968). Soils which exhibit this property to a marked extent have been termed sub-plastic (Butler 1976). Norrish and Tiller (1976) observed that the phenomenon is widespread. Reynders (1972) studied argillic horizons in Morrocco and noted, from discrepancies between cation exchange values of clays and the clay mineralogy, that dispersion of clay was very poor. This is despite the fact that the usual cementing agents such as organic matter, sesquioxides, silica or carbonates were not obvious. These somewhat random observations indicate that the standard

methods for sand, silt and clay determinations may be seriously in error for many clay-rich horizons. There are no data for the effect of dispersion on fine clay yield.

The purpose of this chapter will be two-fold. In the first part, an investigation will be made of the effect of dispersion on the fine clay and coarse clay yields. The second purpose will be to provide evidence for the mechanism(s) involved in textural differentiation using particle-size distribution data.

4.2 Analytical methods

4.2.1 Method of dispersion

Effect of the time of shaking on fine clay:coarse clay ratio

The experiment was carried out on two texturally different samples; a fine sandy loam and a medium clay, from the A and B horizons of the Urrbrae loam (a calcic rhodoxeralf, mixed, thermic). The soil had been air dried, lightly hand ground and passed through a 2 mm round-hole sieve.

Soil (1.6 g) was weighed into a 5 ml vial fitted with a press-seal plastic lid containing 1.2 ml distilled water, 0.4 ml sodium tripolyphosphate and 0.04 ml sodium hydroxide. Vials were shaken on a Spex Mixer Mill for 10^1, 10^2, 10^3, 10^4 and 5.08×10^4 seconds i.e. 10 seconds, 1 min 40 s, 16 min 40 s, 2 hours 46 min 40 s and 14 hours six minutes. Eight replicates of each soil for each shaking time were treated except for the longest shake where 4 replicates of each soil were used. Following shaking the total clay (<2 um) and fine clay (<0.2 um) were measured according to the method outlined in 4.2.2 below. Water contents of the soil samples were measured and results experessed on an oven-dry soil basis.

Effect of time of shaking on the elemental chemistry of the sand, silt and clay separates

The same soils used in the above experiment were prepared in an identical manner except that there were only three shaking times; 10^2, 10^3 and 10^4 seconds. Following dispersion, the clay was removed by repeated centrifugation and concentrated by rotary vaporation and freeze dried. Fine, medium and coarse silt (2-5, 5-10 and 10-20 um respectively), and fine and coarse sand (20-53, and 53-2000 um respectively) were separated by settling under gravity in tall-form beakers. The elemental chemistry of each fraction was determined by X-ray fluorescent spectroscopy according to the method of Norrish and Hutton (1969) as described in chapter 8.

Effect of chemical pretreatment on the coarse clay:fine clay ratio

Air dry soil (1.6 g) from the A and B horizon of the Urrbrae loam was weighed into a plastic vial and 1.6 ml distilled water added. Following physical disaggregation for 1 minute, either with an ultrasonic probe or a Spex Mixer Mill, the suspension was then subjected to a number of chemical treatments:

(1) saturation of the exchange complex with sodium or lithium ions by dialysis in IM NaCl or IM LiCl

(2) 30% H_2O_2 at 80°C until frothing subsided

(3) 2% NaOH for 30 minutes at 100°C

(4) IM sodium citrate (Tamura 1958).

Total clay and fine clay were measured as outlined earlier.

4.2.2 Determination of fine clay:total clay ratio

Initial determinations were made by separation of the clay fractions by continuous flow centrifugation (see chapter 8) but this proved extremely time consuming.

After experiments outlined in 3.2.1, the following procedure was adopted. 1.2 ml distilled water and 0.4 ml 10% Calgon were pipetted into a 5 ml plastic vial containing 1.6 g air dry soil. Following shaking in a Spex Mill for 1 minute, the suspension was washed into a 100 ml centrifuge tube, made up to 80 ml with distilled water and centrifuged for the appropriate time to permit settling of particles >2 um or >0.2 um. 5 ml aliquots were pipetted into a weighed container, oven dried and weighed.

From numerous replicates on samples with textures in the range loamy sand to medium clay it was calculated that the standard error was <5%. Careful calibration of the centrifuge for each speed was carried out by the method of Whitby (1955). This resulted in a significant adjustment to the time required for centrifugation as calculated from the integrated Stokes Law equation.

4.2.3 Detailed particle-size analysis

Particle-size was measured from 0.6 um to 2000 um at 0 intervals by centrifugation in the range 0.6-2 um (Steele and Bradfield 1934), by settling under gravity in the range 2-31 um (Day 1965) and by dry sieving for particles 31-2000 um diameter. Analyses were carried out on 5-50 g subsamples of the whole soil after air drying. Following physical disaggregation with an ultrasonic probe and treatment with H_2O_2 to remove organic matter, samples were placed on an end-over-end shaker for 12 hours. IM NaOH and 10% sodium tripolyphosphate were used as dispersing agents (Hutton 1955). The method is essentially that of Walker and Hutka (1977, 1979).

4.2.4 Calculation of the CPSD index

The CPSD was calculated for six sand fractions; limits 63, 88, 125, 250, 500 and 1000 um.

4.2.5 Weathering index

The weathering index was calculated in three steps for those soils in which detailed particle-size data were available. The procedure involved:

1. calculation of fine silt:total silt ratios at different depths down the profile
2. plotting the ratios down to the depth at which weathering was negligible
3. finding the slope of the regression line for the plot. This is the weathering index.

4.3 Results and discussion

4.3.1 Method of dispersion

Effect of time of shaking on the fine clay: coarse clay ratio

Results, expressed in the form of the graph of clay yield as a function of time (Figures 33, 34), show that time of shaking has a profound effect on the amount of clay extracted. Clay yields from the two soils were significantly different. In the fine sandy loam, both total clay and fine clay contents increased with time and the coarse clay:fine clay ratio dropped almost linearly from 1.9 at 10 to 0.7 at 14 hours. In the medium clay sample however, the total clay content reached a maximum after 100 s and thereafter remained practically constant. Fine clay content continued to rise, causing the coarse clay:fine clay ratio to drop by almost 1/3 of its value at 10 s.

The continued increase in yield of clay, either total or fine, could be due either to a breakdown of aggregates of clay of silt and fine sand size or a breakup of individual coarse grains by attrition. In the case of the medium clay, the source of the fine clay must be from the <2 um fraction and not coarser fractions. If coarser fractions were breaking down to yield clay, there would also be an increase in total clay yield. Plots of change in particle-size distributions of silt and sand size particles confirm this (Figure 35). But there is a significant contribution to the clay from the silt fraction of the fine sandy loam.

Effect of time of shaking on the elemental chemistry of the sand, silt and clay separates

If clay was being produced by attrition of coarse grains it would be expected that the mineralogy of the clay would not remain constant. Graphs of the silica:alumina (SiO_2:Al_2O_3) ratio show that there was an increase in SiO_2 in the clay fraction of the fine sandy loam (Figure 36). Increased time of shaking has caused the breakdown of quartz of sand and coarse silt size. However, in the medium clay sample, breakdown of quartz has only led to an enrichment of silt-size particles; the clay has been unaffected.

It appears that the degree of attrition depends on the proportion of coarse to fine particles in the soil sample. In the fine sandy loam there has been a significant contribution to the coarse clay fraction by mineral breakdown, in the medium clay sample attrition has only affected the silt fraction. Any shaking procedure must therefore be a compromise. It should proceed long enough to ensure breakup of aggregates but not so long that there is a significant contribution by attrition.

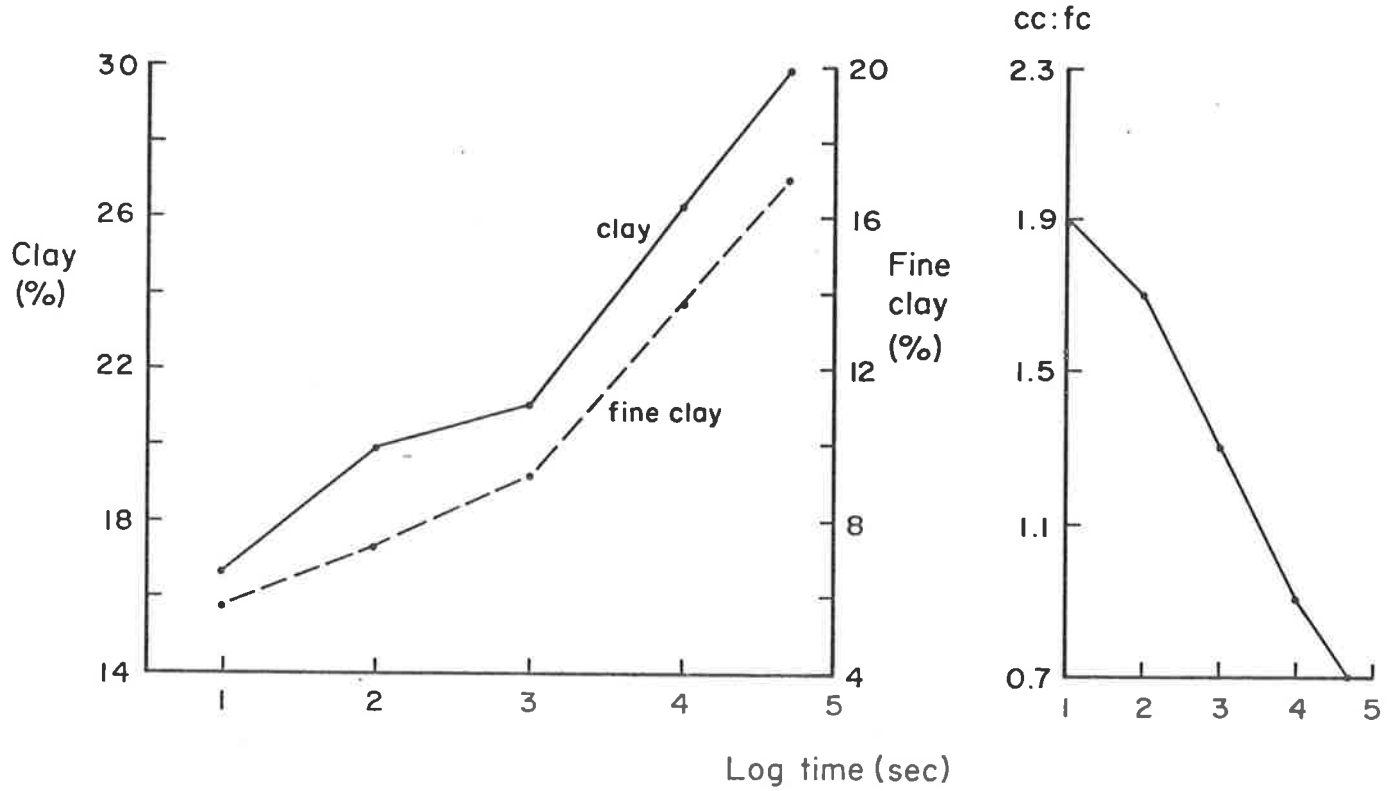

Figure 33 Effect of time of shaking of a fine sandy loam on the yield of total clay and fine clay, and on the coarse clay (cc): fine clay (fc) ratio

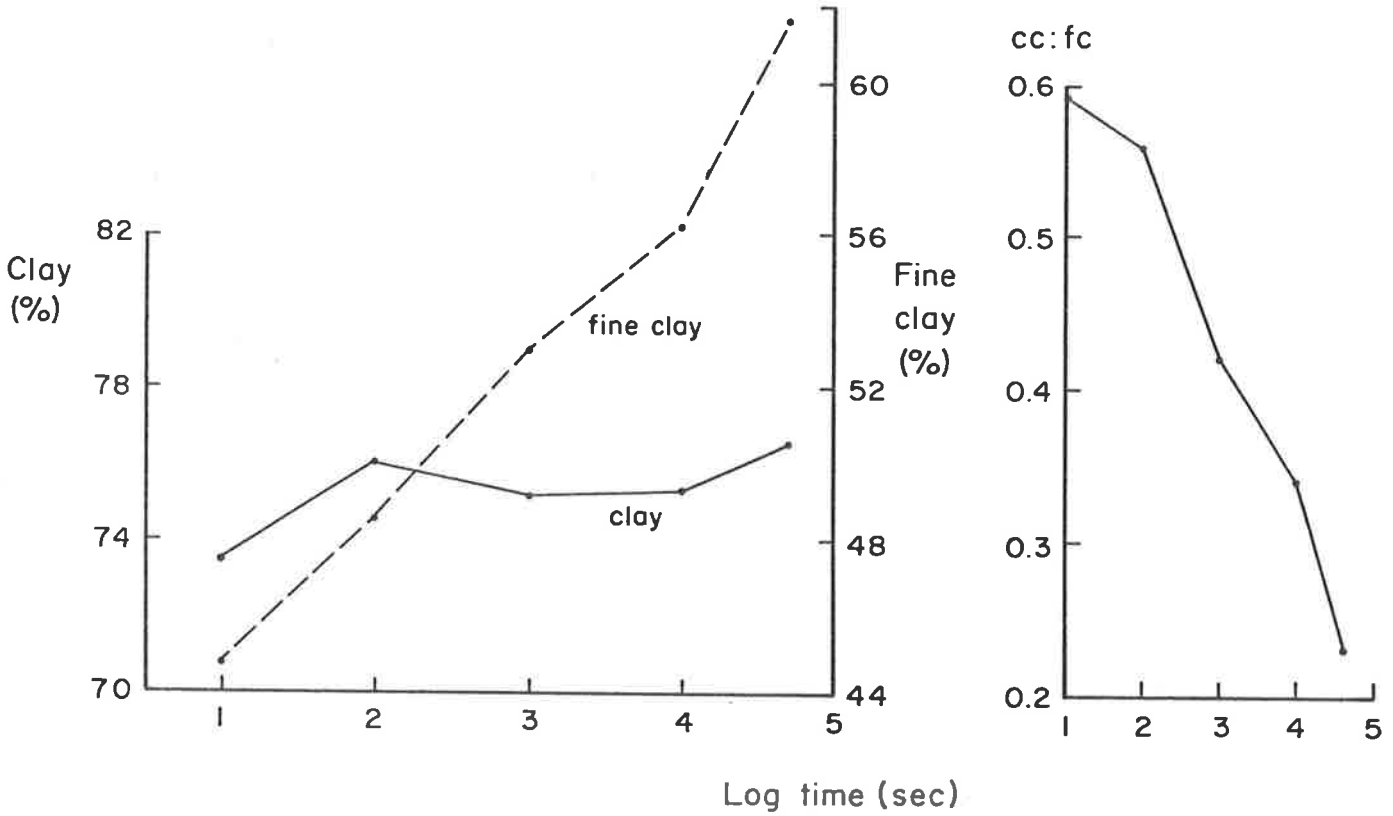

Figure 34 Effect of time of shaking of a clay on the yield of clay and fine clay, and on the coarse clay (cc): fine clay (fc) ratio

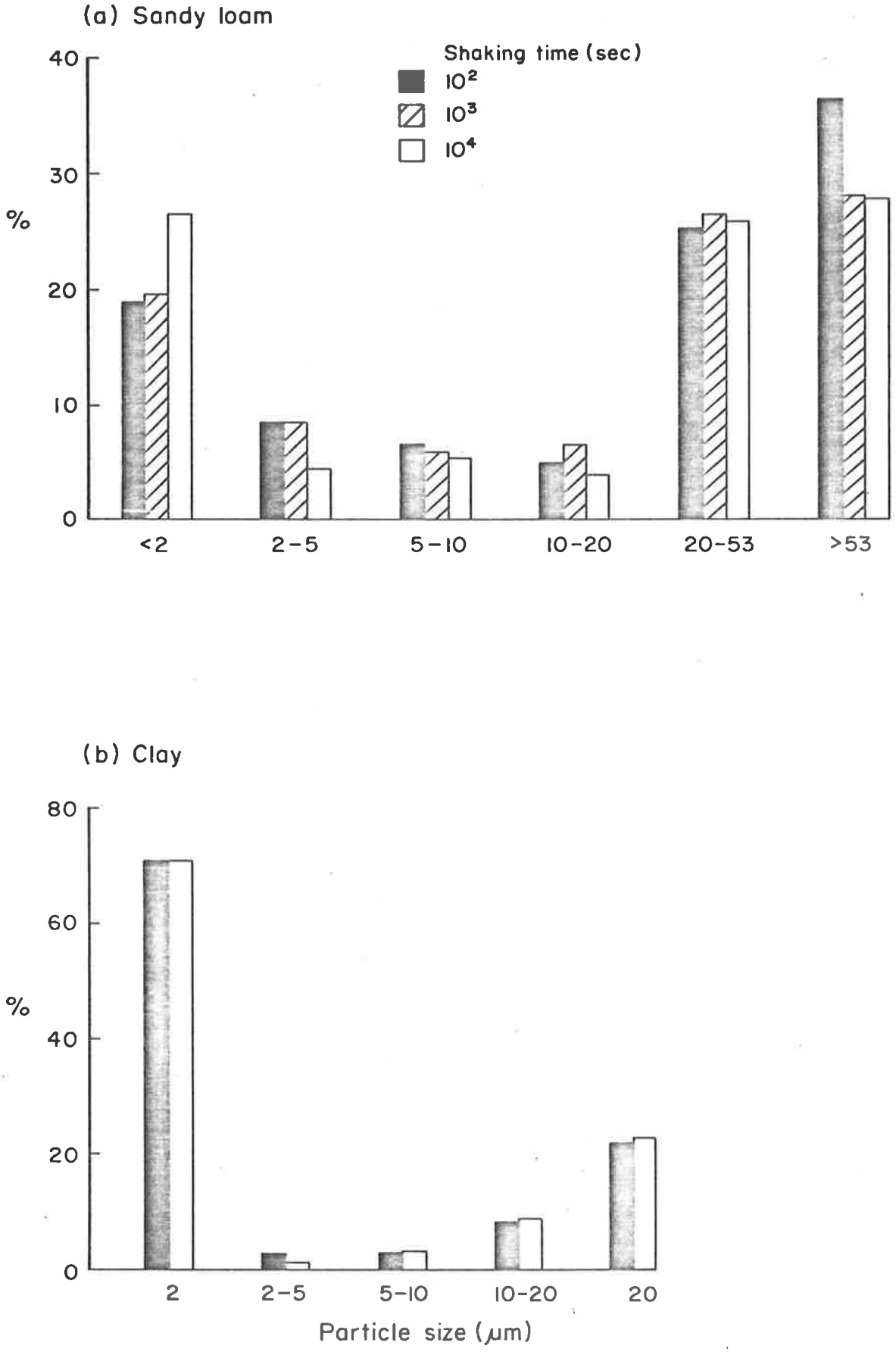

Figure 35 Yield of clay, silt and sand after various shaking times (a) sandy loam soil (b) clay (soil)

An attempt was made to determine the change in aggregation of particles with time by direct observation of the coarse clay fraction with a transmission electron microscope. Carbon replicas of the coarse clay separates from the soil samples after shaking for 10^0, 10^1, 10^2 and 10^3 seconds were prepared by the method of Greenland et al (1968).

Results were inconclusive. There were no obvious changes in aggregation with time (Figures 37, 38). However, the coarser grains of the fine sandy loam sample were observed to have coatings or incrustations of fine clay-size material (Figure 37). These incrustations were particularly obvious on grains shaken for 1 and 10 s but disappeared with time. Greenland and Wilkinson (1969) observed similar coatings and concluded that they were composed primarily of disordered silica and alumino-silicates rather than iron and aluminium oxides. Most was removed after shaking for 10^2 s although some still remained even after very long periods of shaking. The degree of adherance therefore varied considerably. It appears that these coatings may make a significant contribution to the fine clay fraction.

Effect of chemical pretreatment on the coarse clay:fine clay ratio

The chemical pretreatments were chosen to determine the effect of removal of free iron oxides (sodium citrate-dithionite), amorphous material (NaOH) and organic matter (H_2O_2). Lithium saturation was investigated because it had been shown to increase clay yield over sodium saturation in some sub-plastic soils of the Riverine Plain (Norrish and Tiller 1976).

Figure 37 Electron micrographs of clay sized particles following shaking of a soil of sandy loam texture for various times

a) 0 s

b) 0 s

c) 1 s

d) 10 s

e) 100 s

f) 10 000 s

This line on the photograph indicates 0.5 um

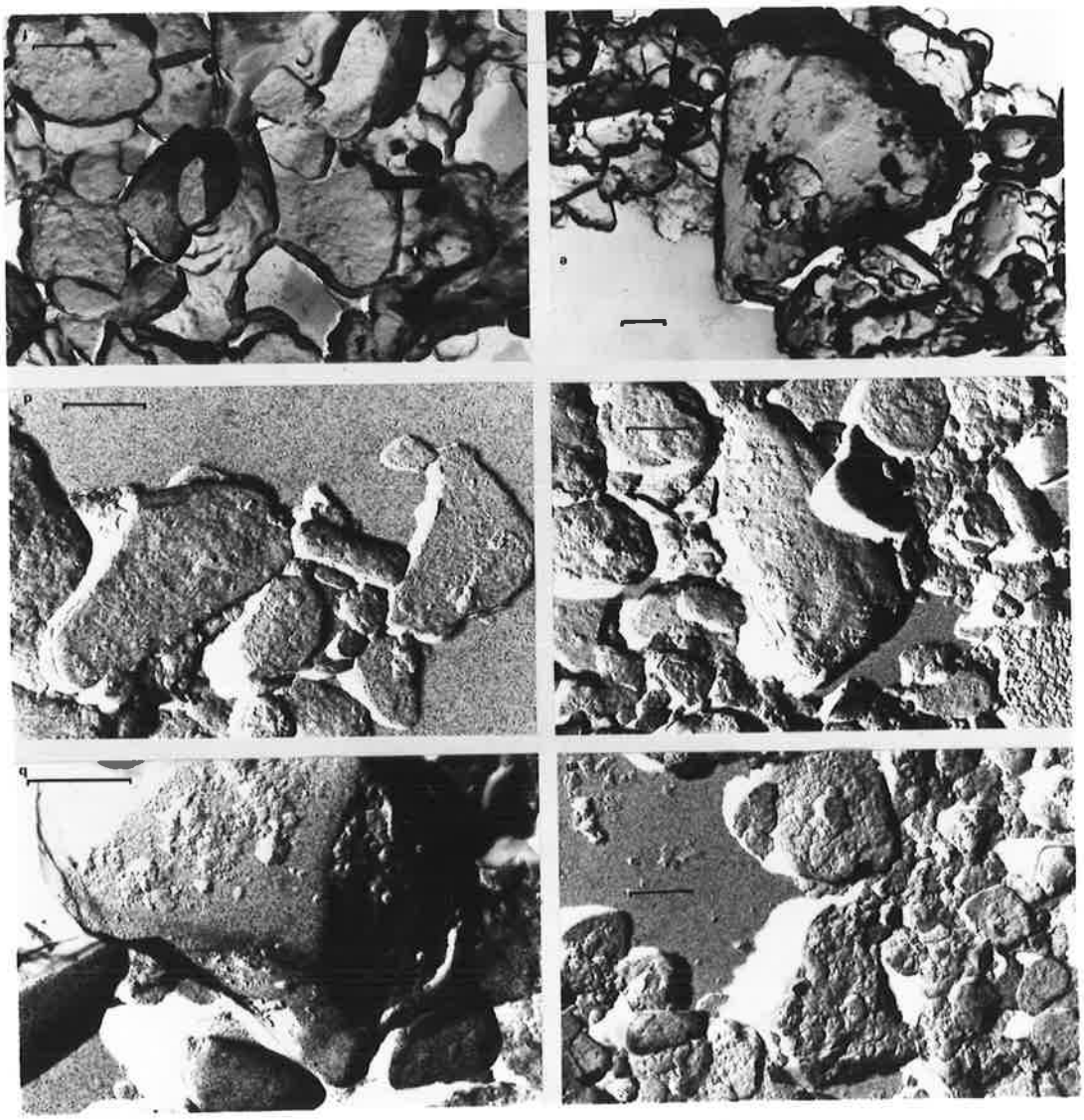

Figure 38 Electron micrographs of clay sized particles following shaking of a soil of clay texture for various times

a) 0 s

b) 1 s

c) 10 s

d) 100 s

This line on the photograph indicates 0.5 um

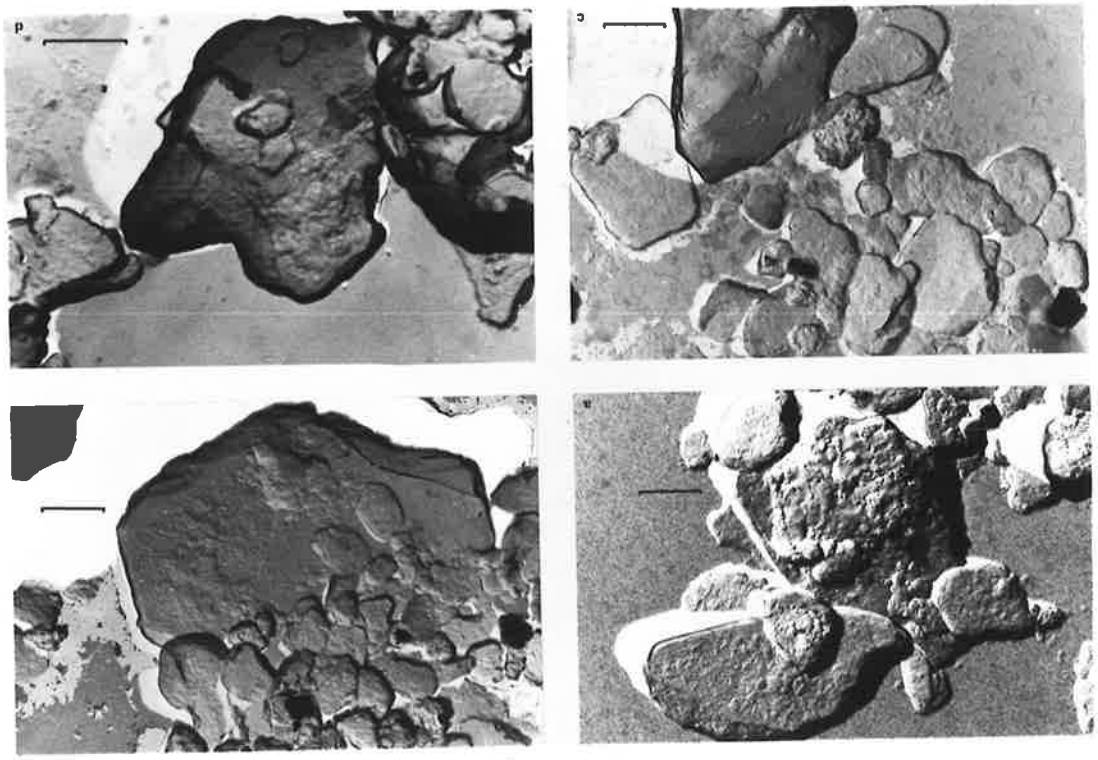

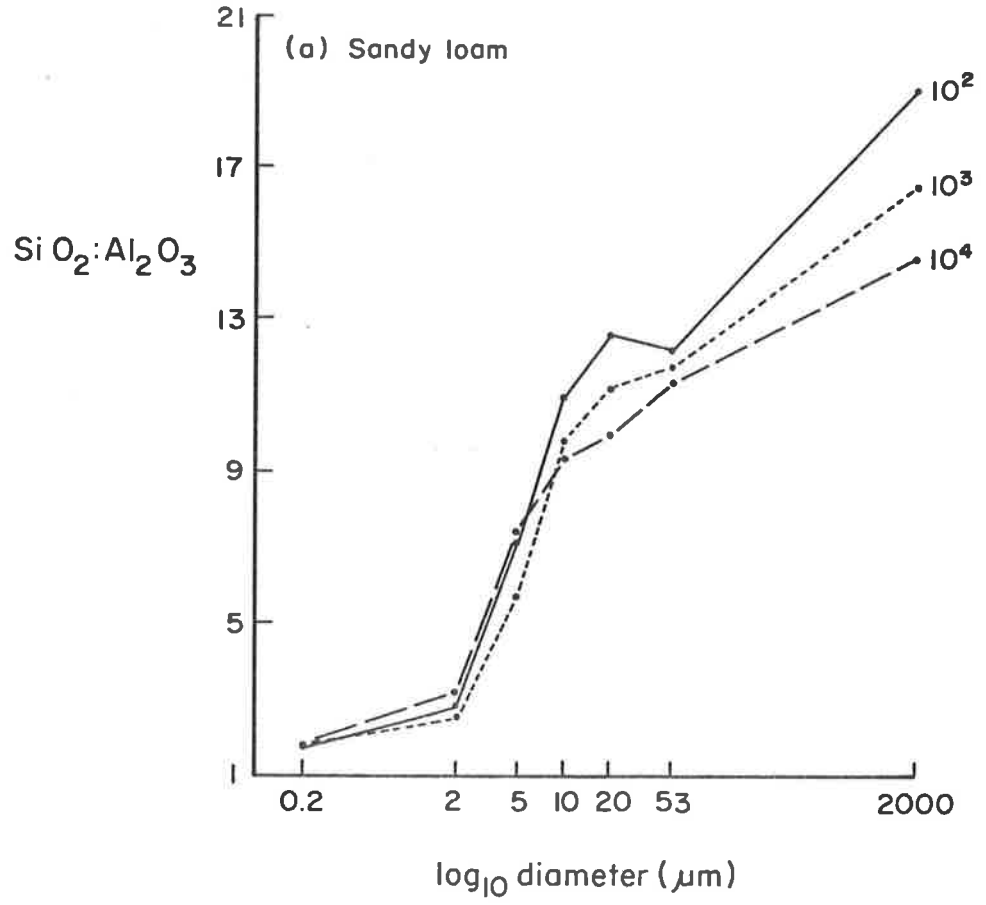

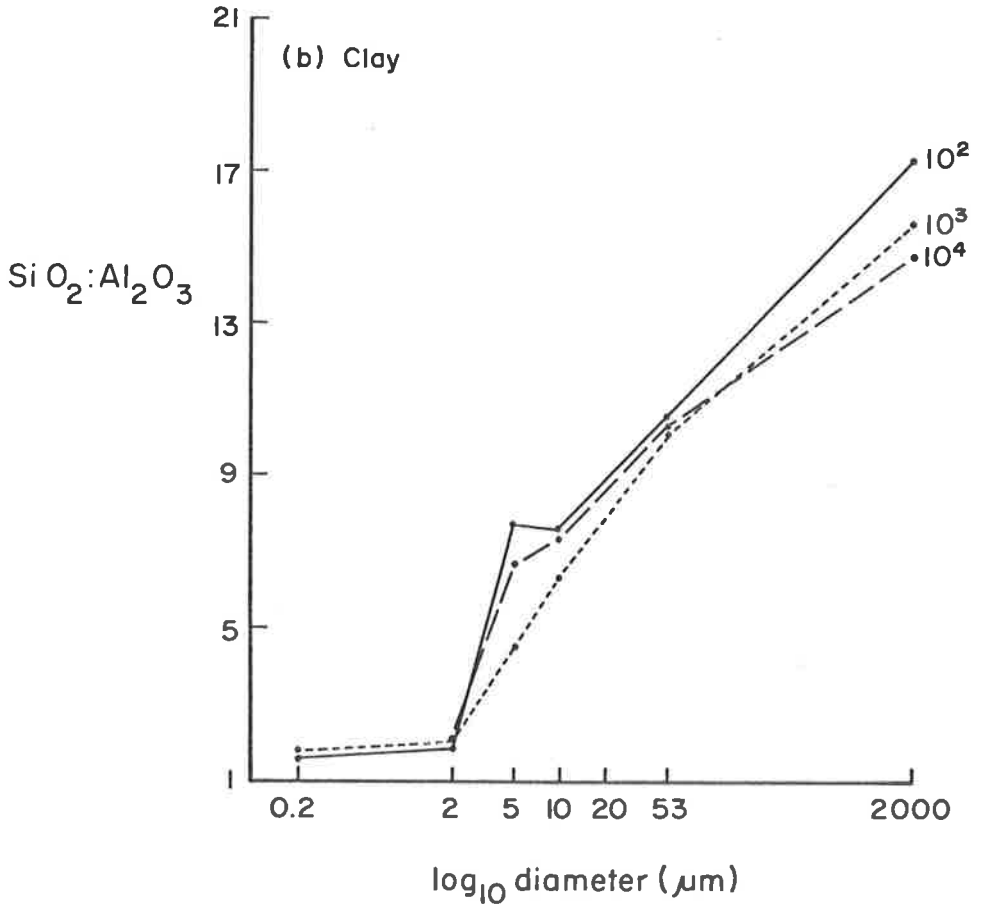

Figure 36 $SiO_2:Al_2O_3$ ratio for clay, silt and sand fractions as a result of shaking for 10^2, 10^3 and 10^4 seconds (a) sandy loam (b) clay

Results show that there was little effect on the coarse clay:fine clay ratio except for the sodium hydroxide treatment (Table 9). For both soils there was a significant increase in the ratio, presumeably because there is solubilization of the fine clay. Treatment with H_2O_2 reduced the ratio slightly for the fine sandy loam but not for the medium clay.

On the basis of the three experiments the procedure outlined in 4.2.2 was adopted. No chemical pretreatment was used. Disaggregation was only by shaking in a Spex Mill with a dispersing agent (Calgon).

treatment sequence	coarse clay:fine clay ratio	
	sandy loam	medium clay
Na^+	2.2	0.18
Li^+	2.2	-
H_2O_2; Na^+	1.3	0.17
H_2O_2; Li^+	1.8	-
H_2O_2: NaOH; Na^+	5.0	-
H_2O_2: NaOH; Li^+	7.4	-
NaOH; Na^+	-	∞
H_2O_2; Na^+	-	0.17
Na citrate; Na^+	-	0.22

Table 9. Effect of chemical pretreatments on the coarse clay:fine clay ratio for two soils.

4.3.2 Fine clay: total clay ratios

Plots of the depth functions of the fine clay to total clay ratios are given for the soils of each sequence in Figures 39

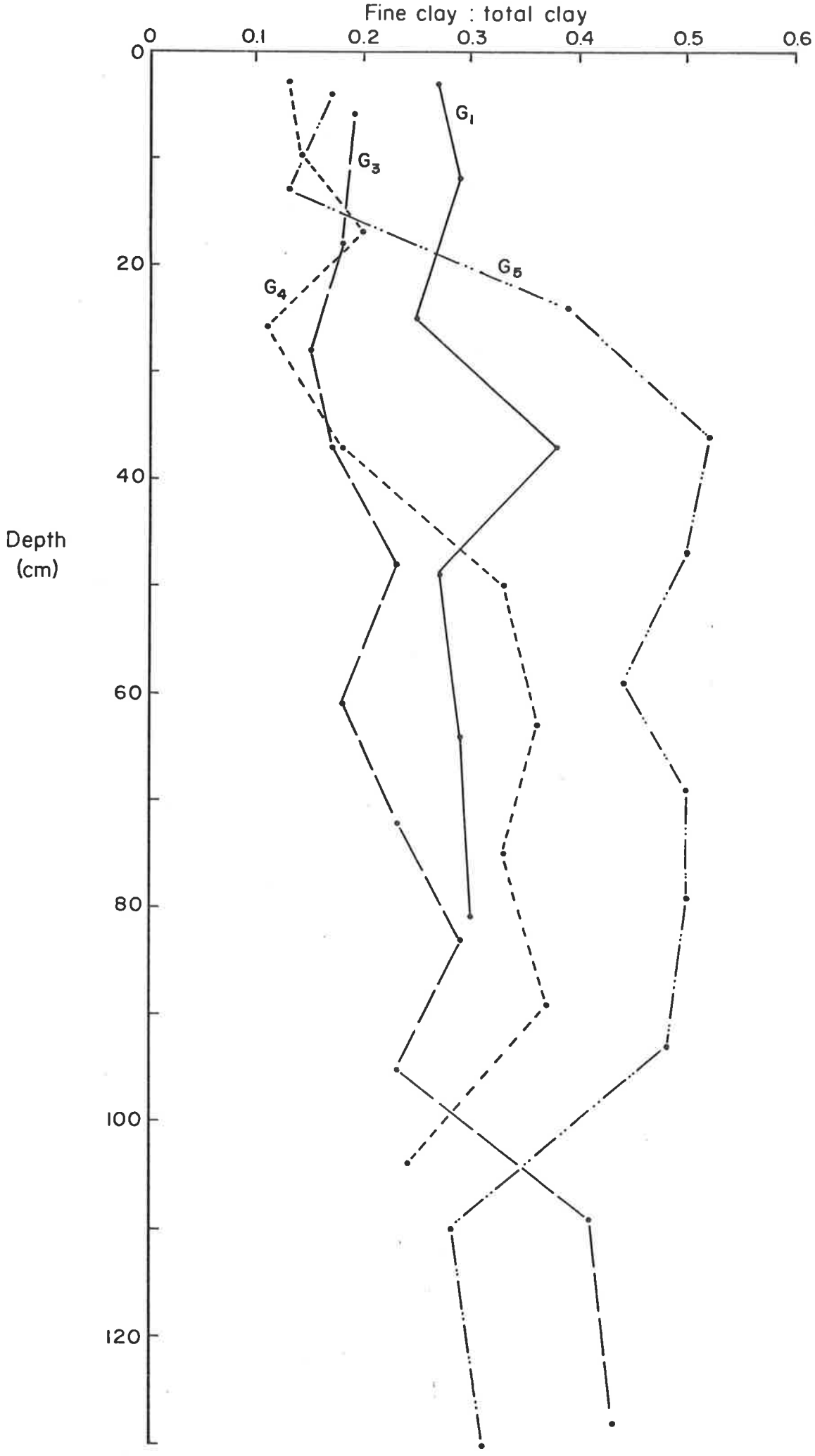

Figure 39 Depth functions of fine clay: total clay for soils of the Gooromon Ponds sequence

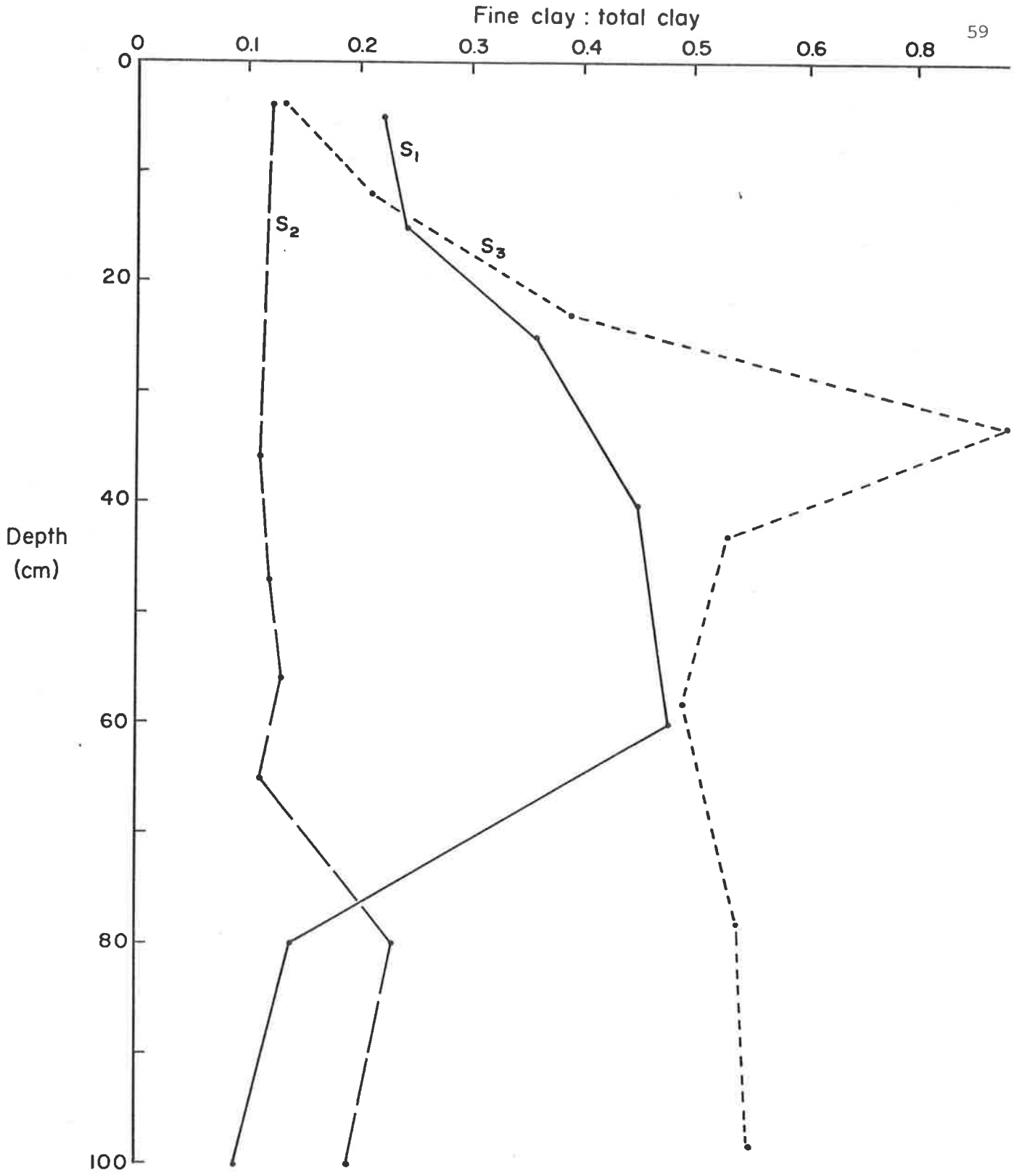

Figure 40 Depth functions of fine clay:total clay for soils of the Shinglehouse Creek sequence

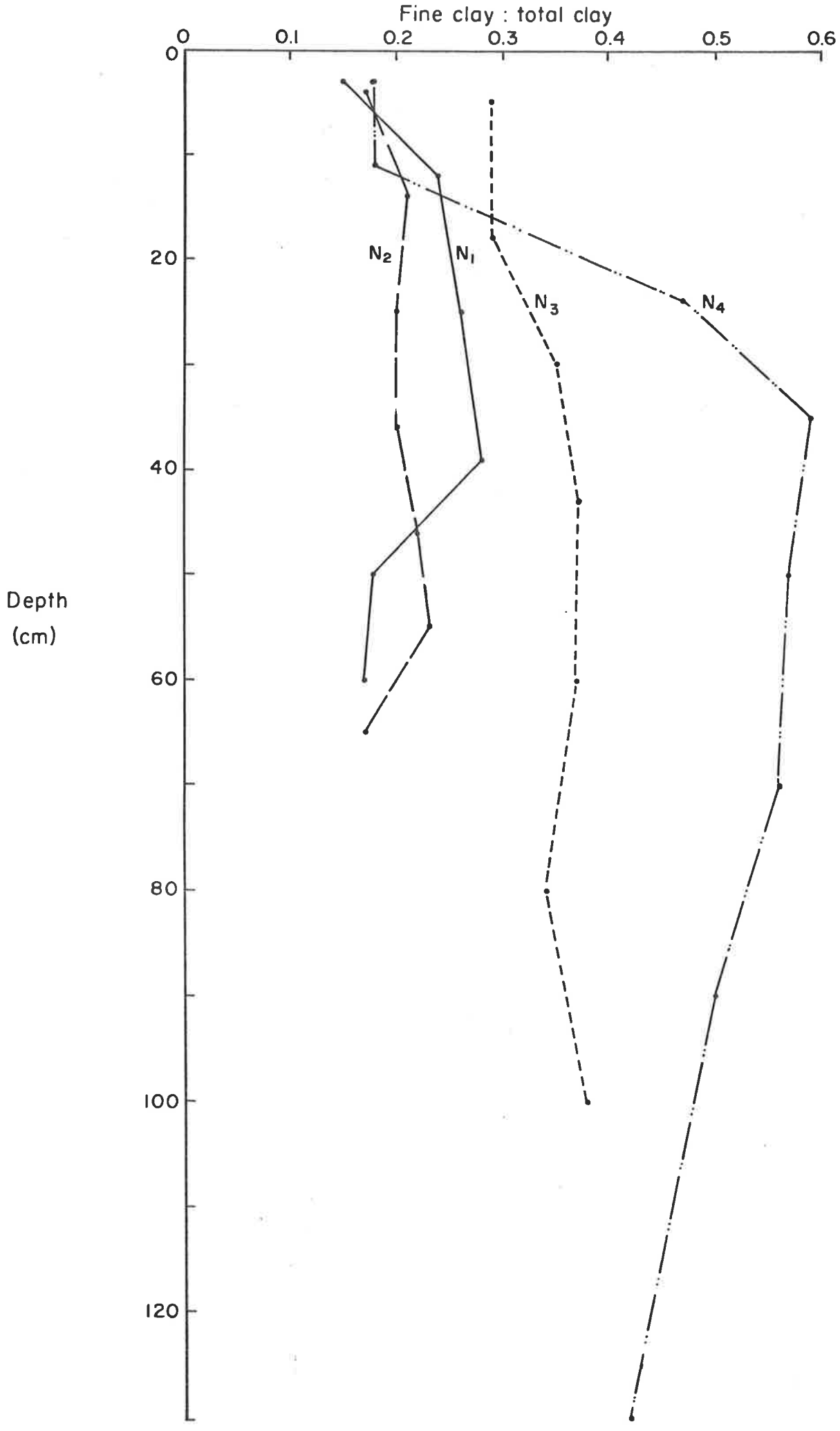

Figure 41 Depth functions of fine clay: total clay for soils of the Nowra Creek sequence

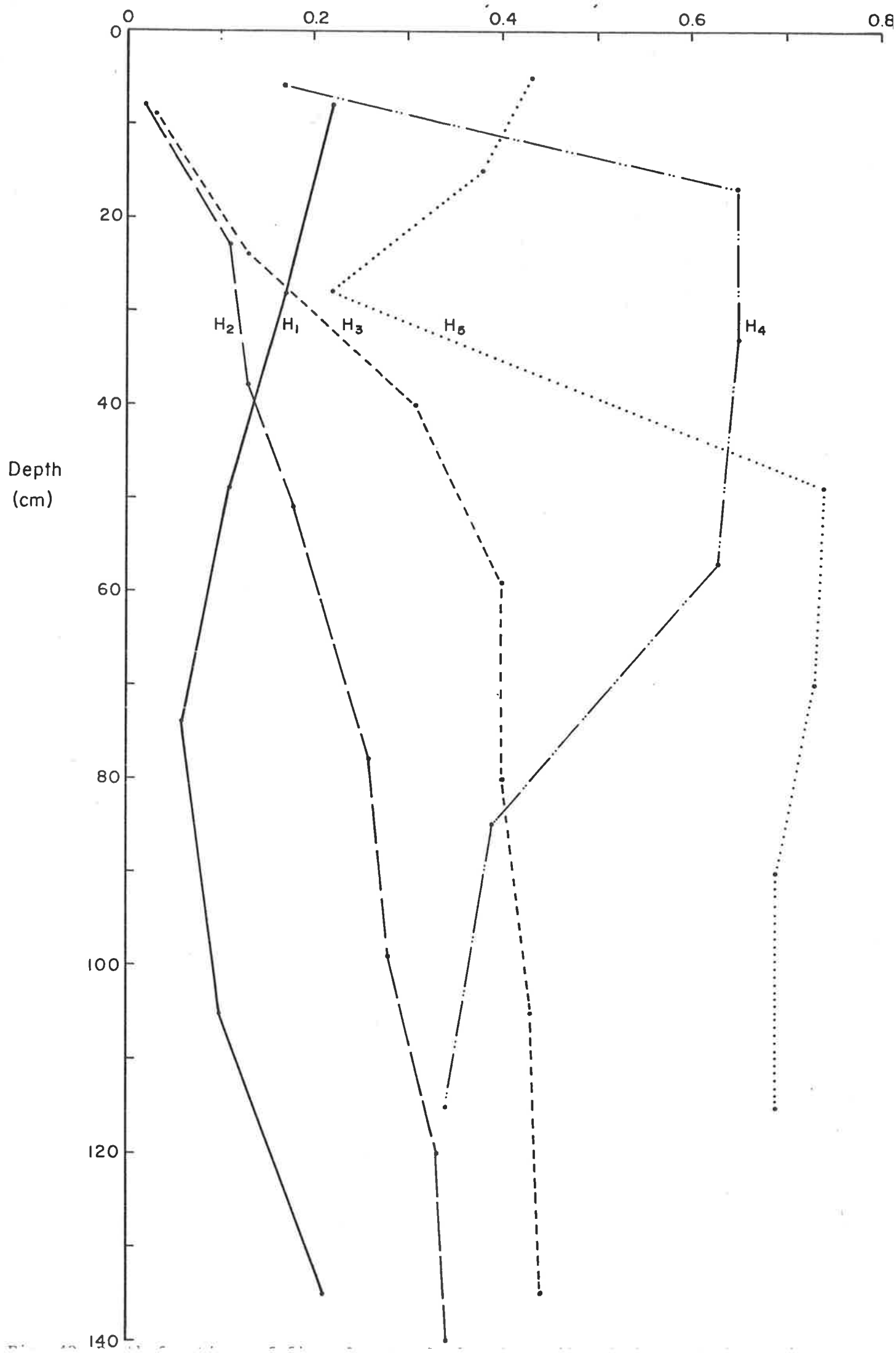
0
0.2
0.4
0.6
0.8
0
20
40
60
80
100
120
140
Depth
(cm)
H2
H1
H3
H5
H4

(Gooromon Ponds), 40 (Shinglehouse Creek), 41 (Nowra Creek), 42 (Hawkesbury River).

There is a similar change in the depth functions with time for all 4 sequences. From a relatively uniform ratio with depth in the youngest profiles, the ratio progressively becomes more skewed such that there is a marked reduction in the ratio in the A horizon and a marked increase in the B. S1 is probably of recent origin. There has been significant erosion in the area since settlement 130 years ago. New sediment may have been added which may account for the skewed distribution with depth.

The changes of the clay ratios with depth are consistent with an hypothesis of clay illuviation when one would expect that fine clay would move preferentially. This criterion has been adopted in the 'Soil Taxonomy' (Soil Conservation Service 1975) for the recognition of the argillic horizon. However, the evidence is not conclusive since it could be argued that fine clay may be generated by weathering of coarser grains in the B horizon and not in the A (differential weathering) or that there has been weathering throughout the profile with loss of fine clay products from the A horizon.

4.3.3 Detailed particle-size analyses

Results of the detailed particle-size analyses are presented as log probability plots for selected A and B horizons of each sequence (Figures 43 (Gooromon Ponds), 44 (Shinglehouse Creek), 45 (Nowra Creek), 46 (Hawkesbury River)). There is a similarity, in both the form of the plot and the manner in which this changes with time, between the four sequences.

Particle size distributions for the A horizons characteristically have a steep section in the sand size range and a much flatter

Figure 43.1 Particle-size distributions of A horizons of Gooromon Ponds soils

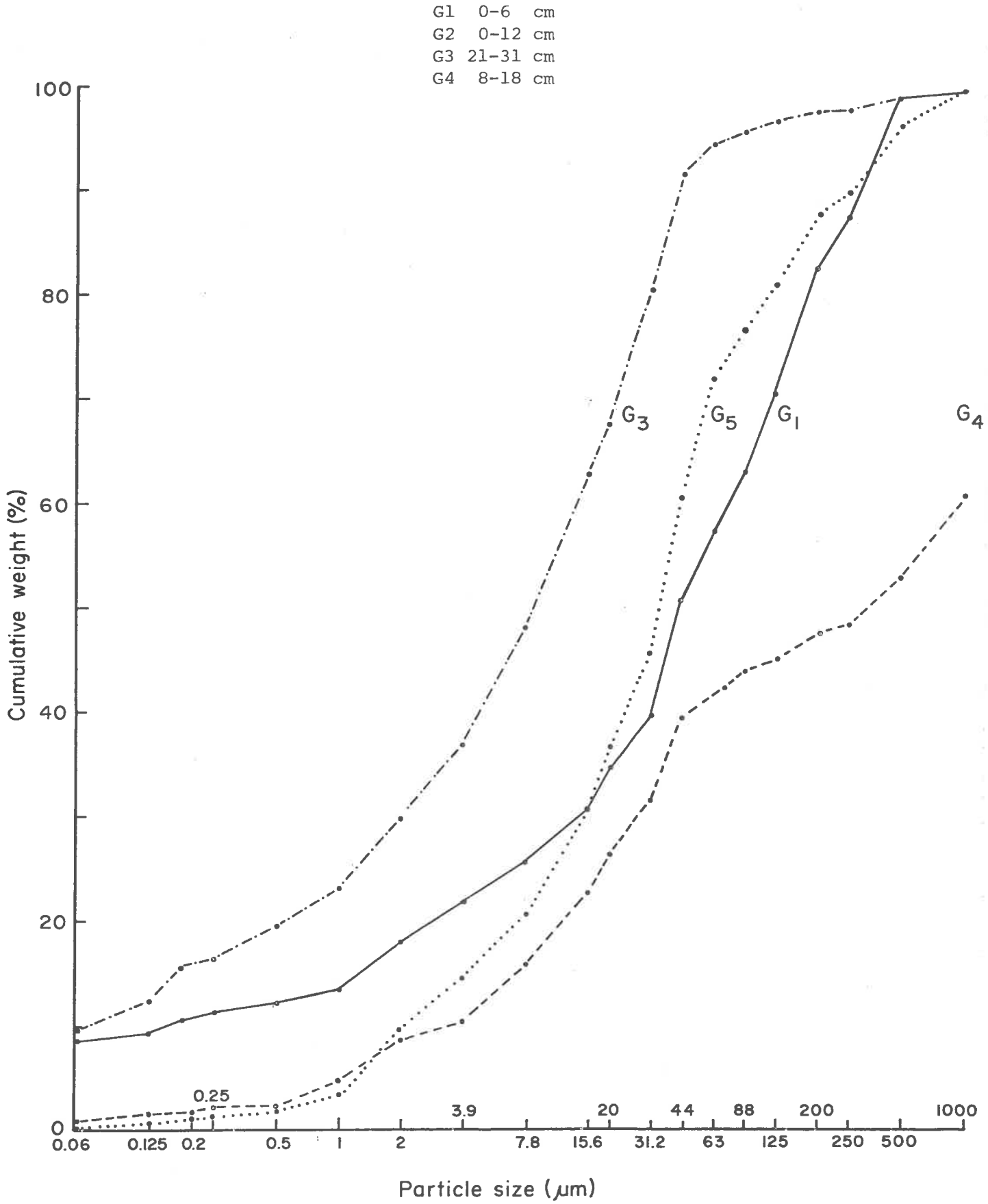

Figure 43.2 Particle-size distributions of B horizons of Gooromon Ponds soils

G3 41-55 cm
G4 57-69 cm
G5 42-52 cm

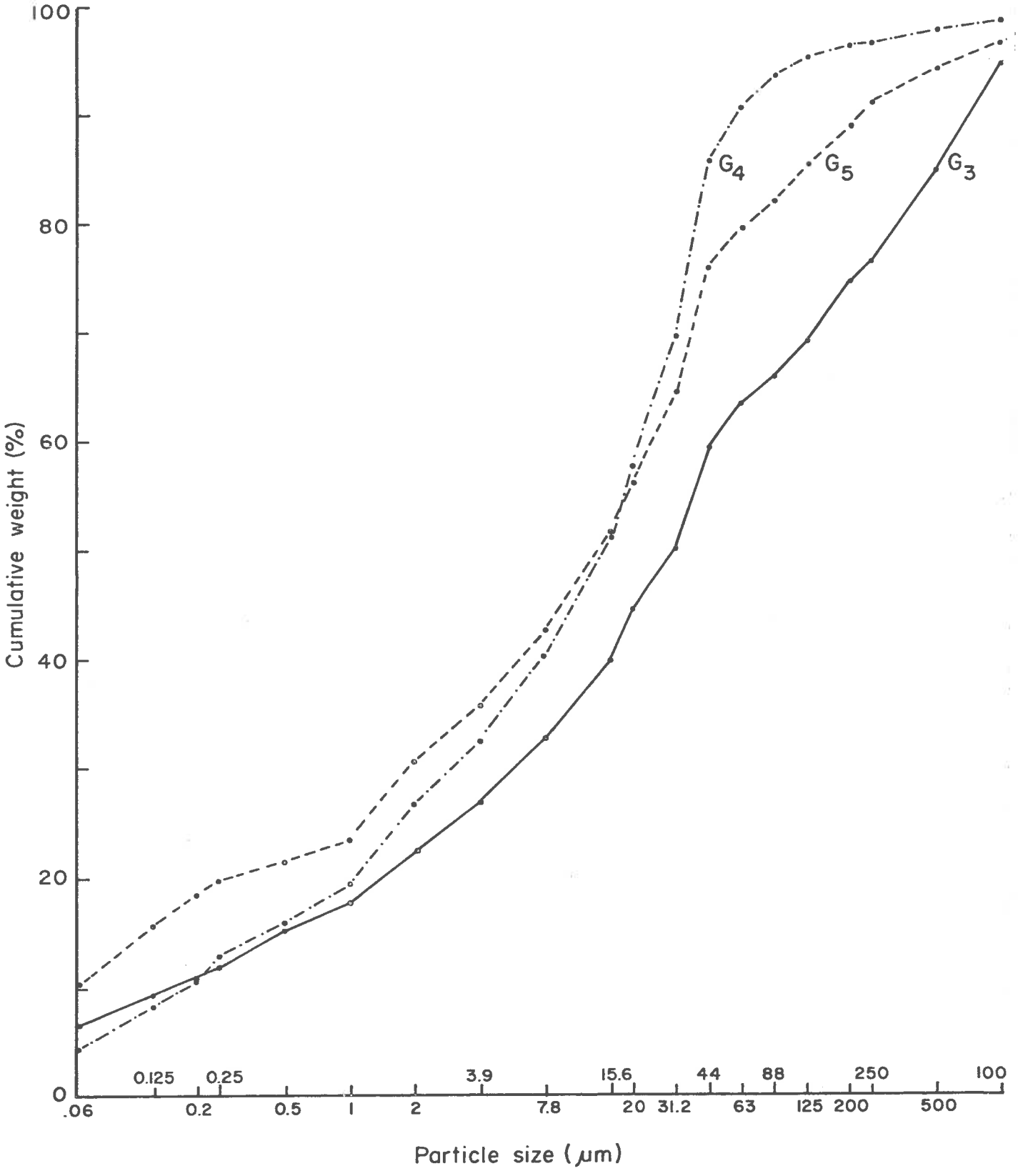

Figure 43.2 Particle-size distributions of B horizons of Gooromon Ponds soils

G3 41-55 cm
G4 57-69 cm
G5 42-52 cm

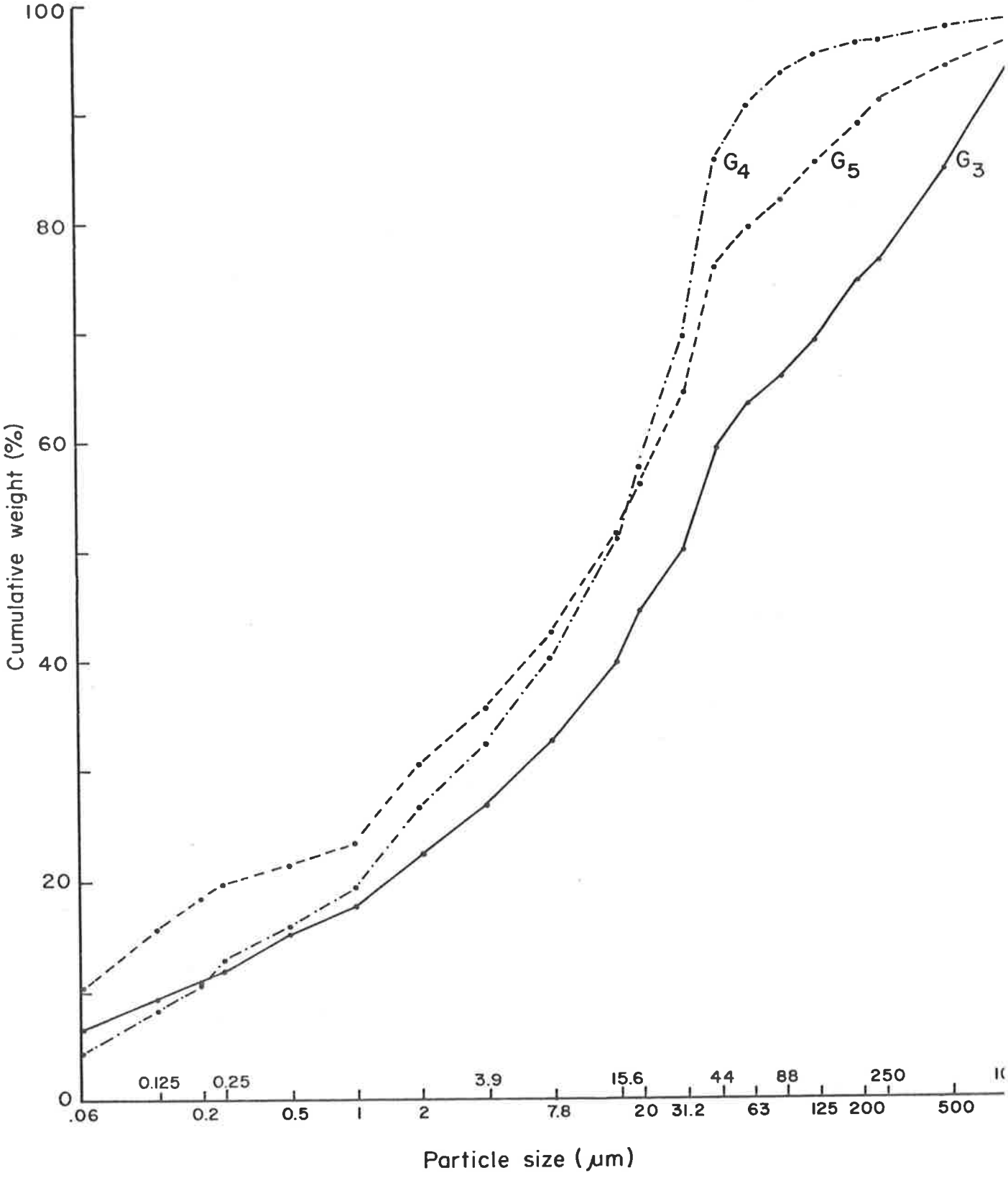

Figure 44.1 Particle-size distributions of A horizons of Shinglehouse Creek sequence

S1 20-30 cm
S2 20-30 cm
S3 38-48 cm

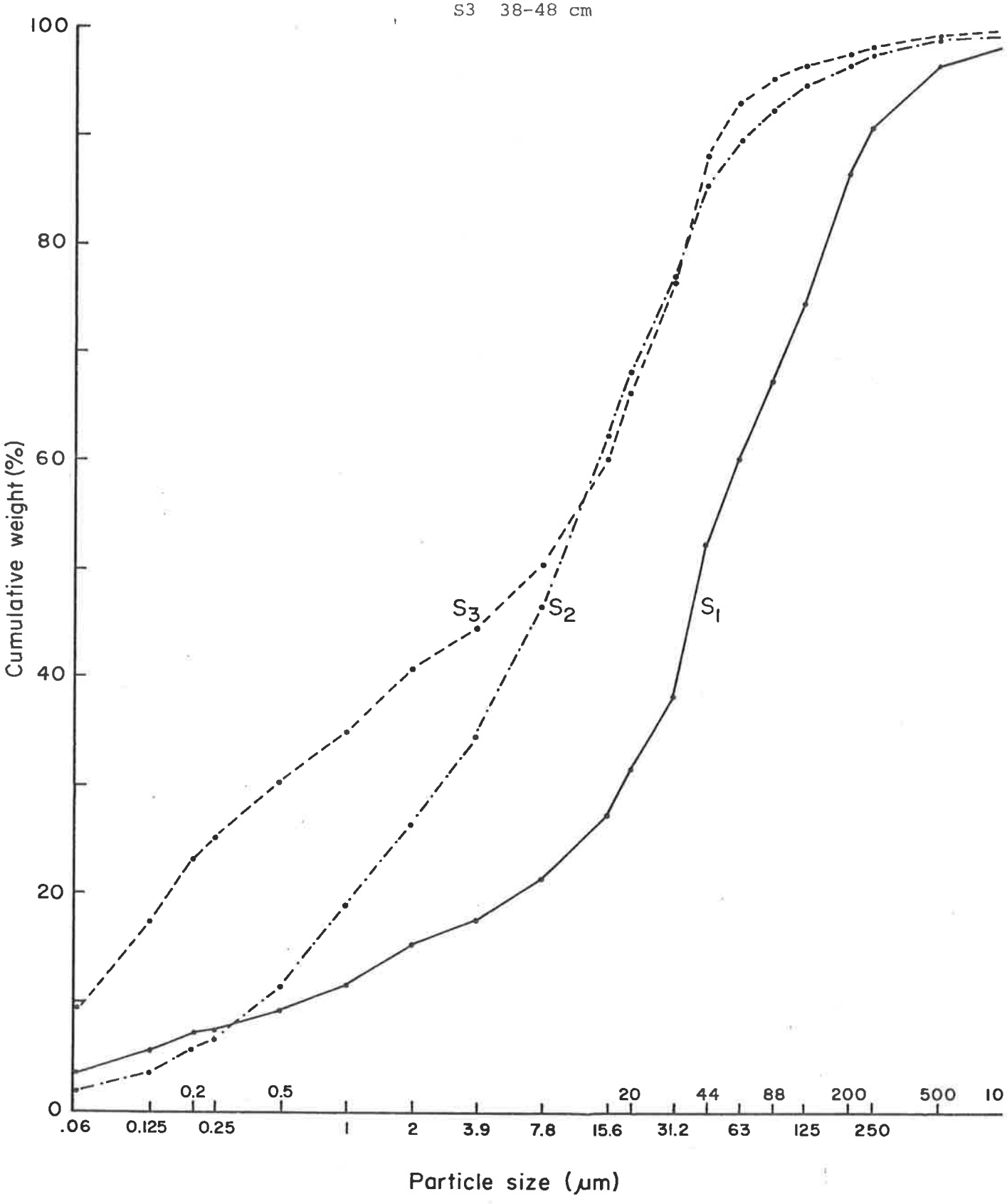

Figure 44.2 Particle-size distributions of B horizons of Shinglehouse Creek sequence

S2 42-52
S3 38-48

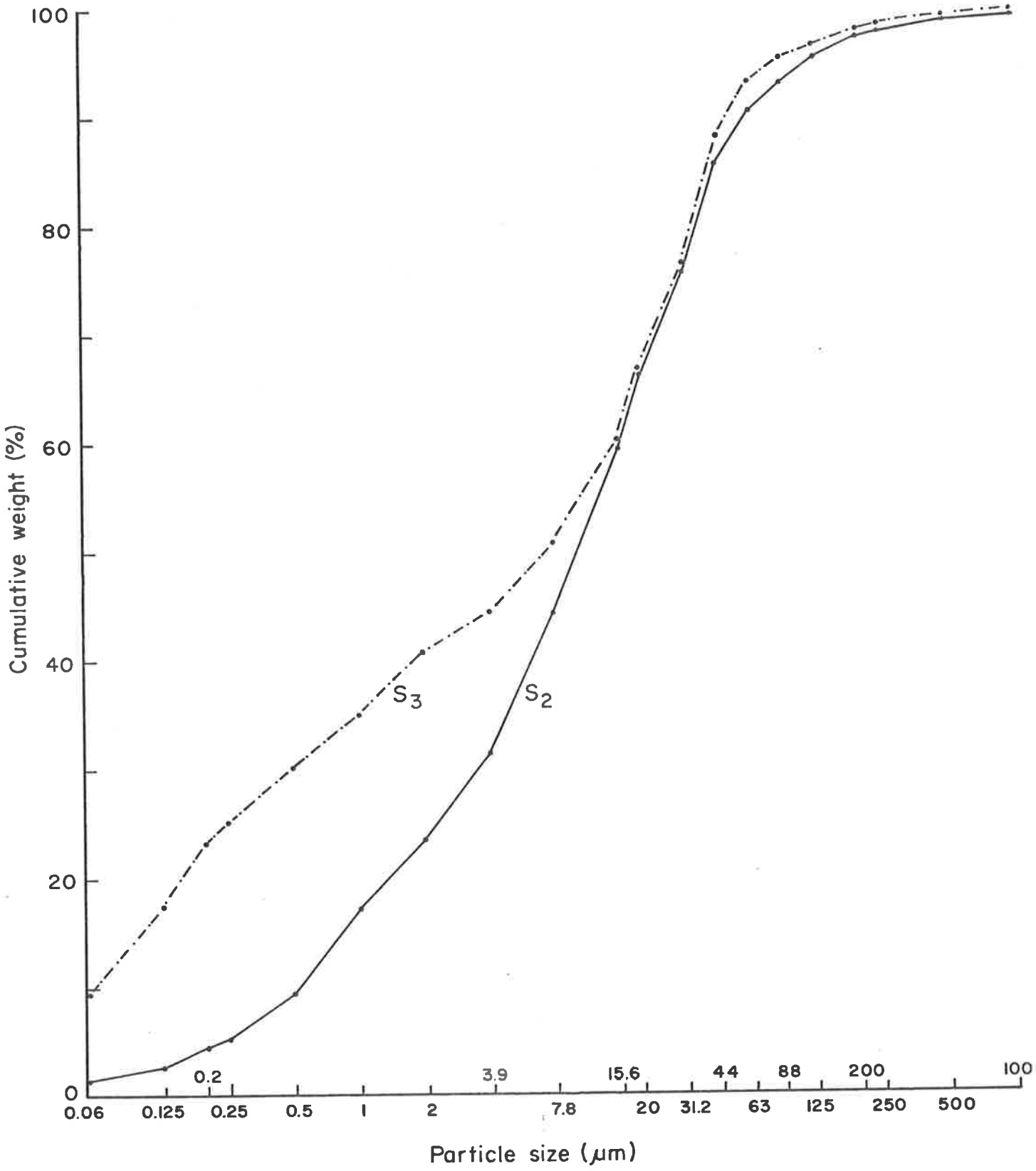

Figure 45.1 Particle-size distributions of A horizons of Nowra Creek sequence

N1 5-18 cm
N2 5-20 cm
N3 0-10 cm
N4 5-17 cm

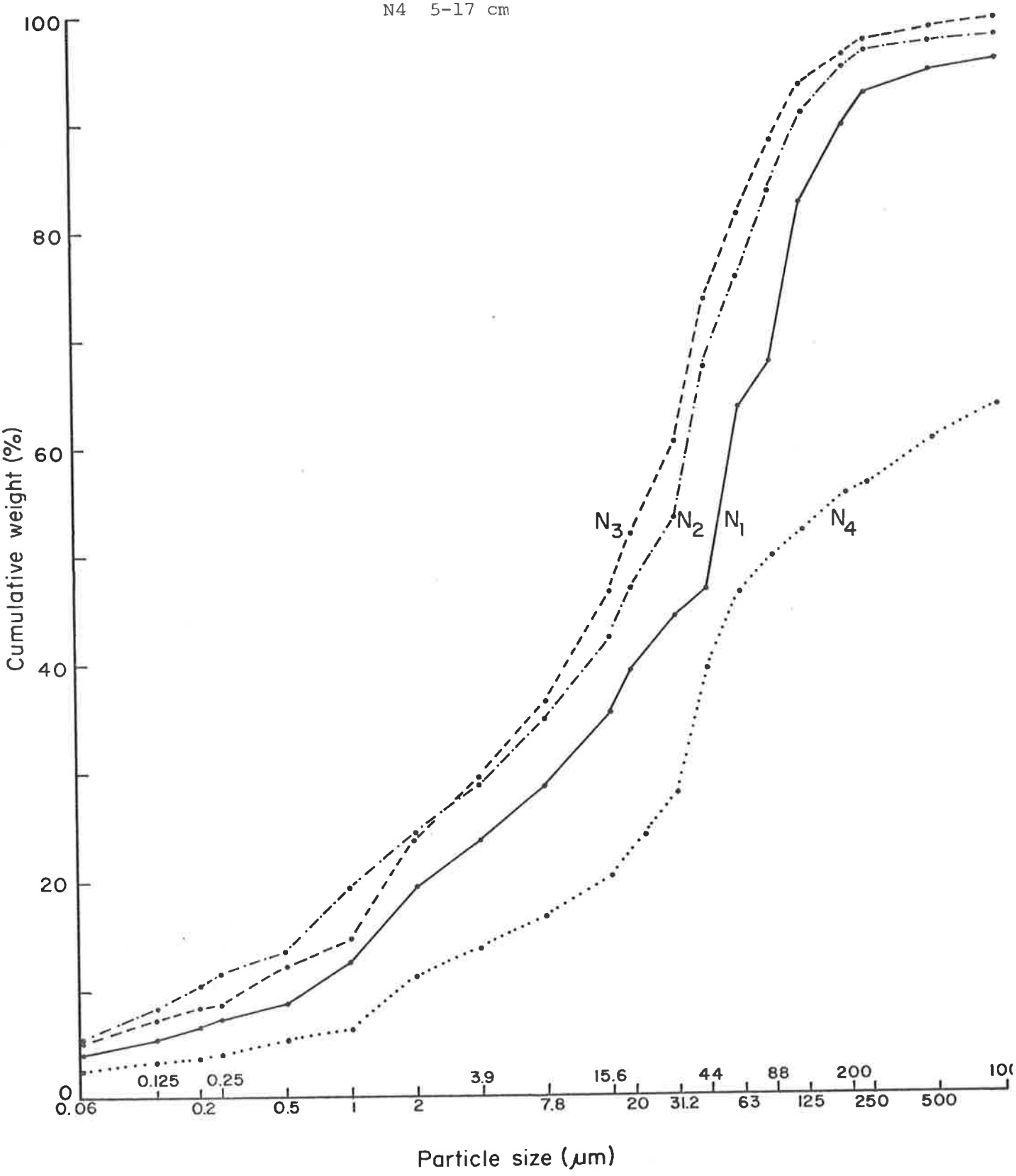

Figure 45.2 Particle-size distributions of B horizons of Nowra Creek sequence

N1 32-45 cm
N2 50-60 cm
N3 35-50 cm
N4 80-100cm

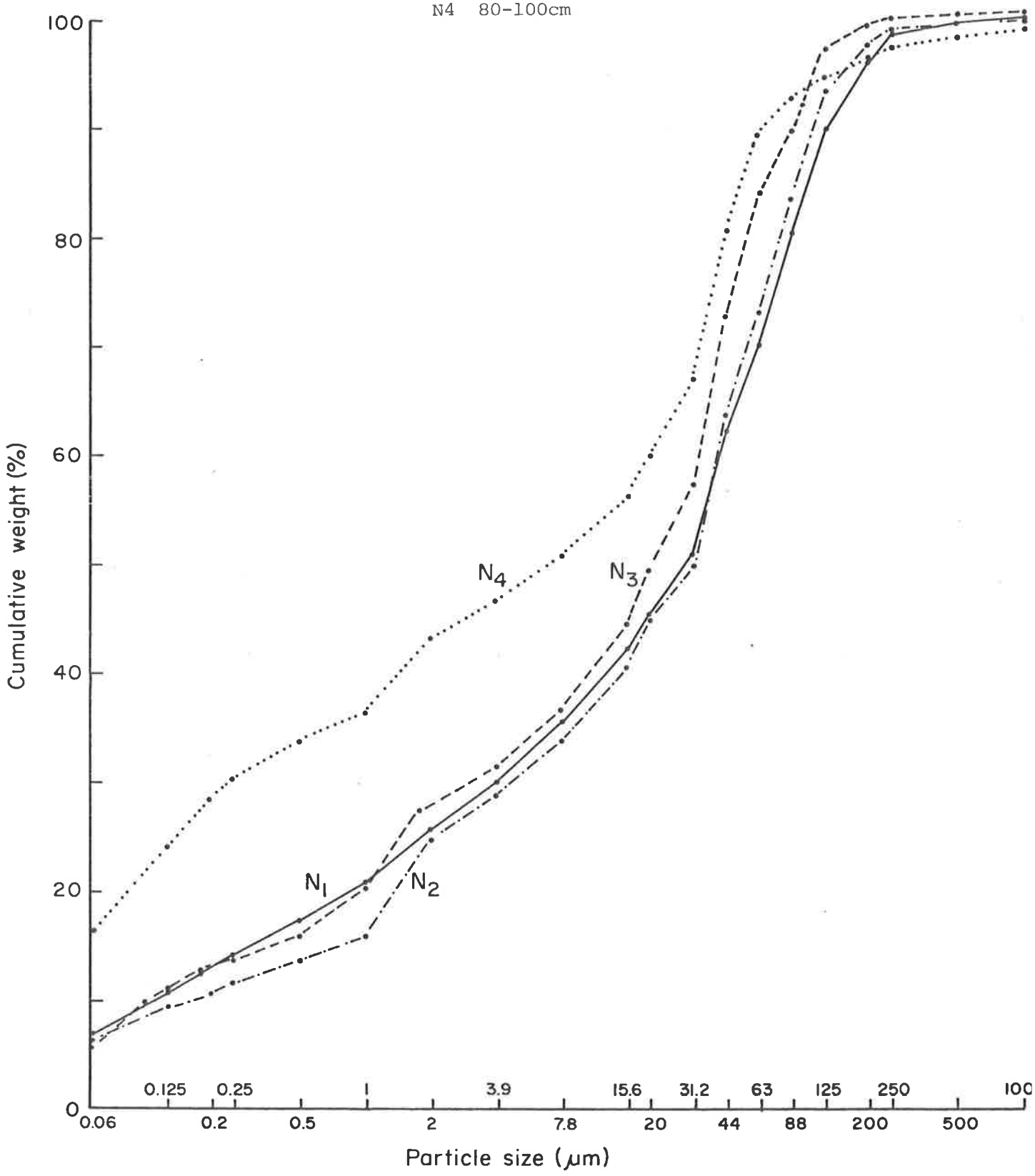

Figure 46.1 Particle-size distributions of A horizons of Hawkesbury sequence

H1 40-58 cm
H3 0-18 cm
H4 0-11 cm
H5 0-10 cm

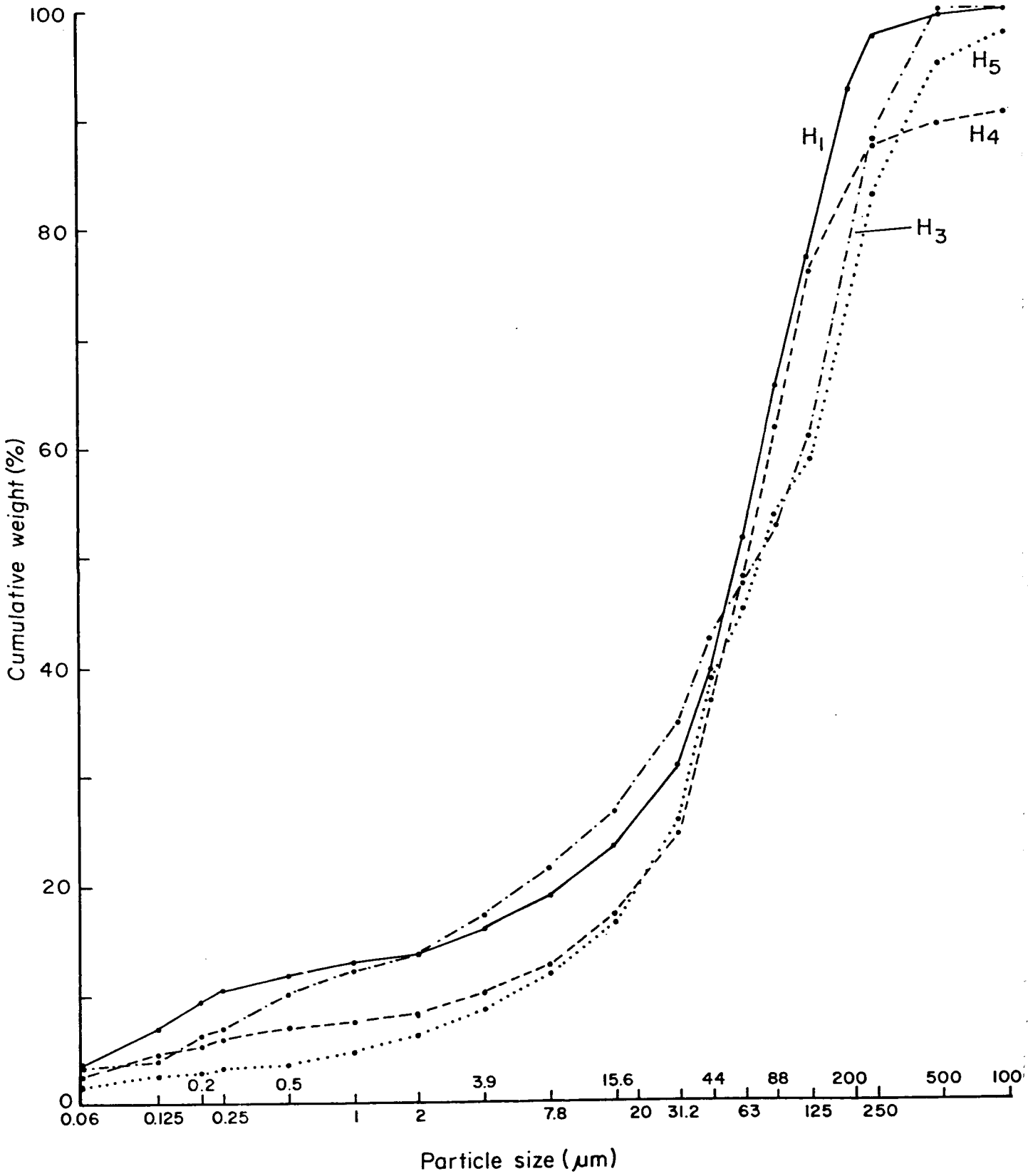

Figure 46.2 Particle-size distributions of B horizons of Hawkesbury sequence

H1 40-58 cm
H3 48-70 cm
H4 43-70 cm

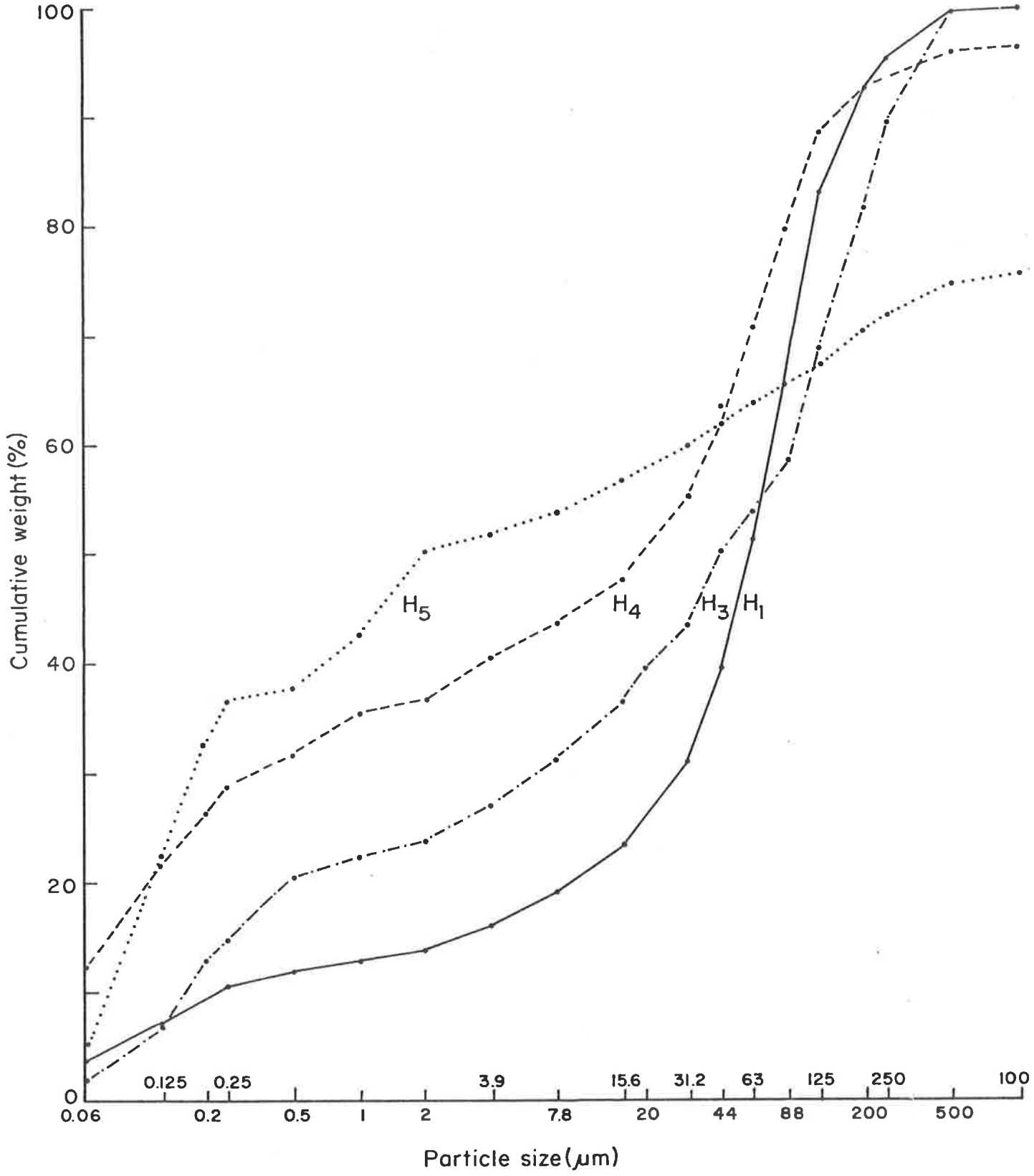

gradient in the silt and clay range indicating the predominance of sand. With time there is a decrease in the gradient in the clay range demonstrating a loss of this fraction.

The log probability plots of B horizons have three segments. This is particularly obvious in the Hawkesbury plot (Figure 46.2) where there is a steep gradient in the fine clay range (0.06 - 0.2 um), a flattening in the coarse clay and silt range (0.2 um - 20 um) and then a steep gradient in the sand range. The fine clay segment steepens significantly with time showing that there is a significant increase in fine and very fine clay at the expense of the coarse silt and fine sand fraction. H5 is distinctly bimodal. The large percentage of fine gravel in H5 is due to the presence of ironstone nodules, probably formed in situ.

4.3.4 Cumulative particle-size distribution index

The CPSD index was calculated from the detailed particle-size data after excluding the gravel and adjusting the accumulative percentages to the range 0-2000 um (Tables 10 (Gooromon Ponds), 11 (Shinglehouse Creek), 12 (Nowra), 13 (Hawkesbury). Langohr and van Vliet (1979) consider that values in excess of 94 indicate extremely high similarity because sampling and analytical errors are of such a magnitude that 94-100 could be considered identical; 85-94 indicates high similarity; 70-85 is considered similar.

Using this criterion, there appears to be good evidence for parent material homogeneity in most profiles. There are several exceptions which can be grouped into two categories. In the first are the surface layers of G3 and H2 (respectively, the 0-12 cm and the 15-30 cm layers). These layers are lithologically very different. In the second category are the older profiles of Gooromon Ponds (G4),

Shinglehouse Creek (S3) and Nowra (N4) where the lowest layers appear to have a different sand size distribution from the upper horizons. These may be lithological discontinuities, but not necessarily.

An assumption is made in the calculation of the CPSD index that the integrity of the sand fraction is maintained following deposition. However, subsequent pedogenesis may alter the particle-size distribution in a number of ways. For example, mobilization of iron and segregation into gravel size nodules and concretions may isolate sand size grains (Chapter 6). In situ physical breakup of sand grains (particularly quartz) fractured during transport and deposition, will cause an increase in the proportion of the finer sand fraction. Whereas a constant ratio is unlikely to have arisen by chance, and is therefore good evidence for textural uniformity of the parent material, lack of agreement may be due to several causes not necessarily related to lithological differences. In these cases, other evidence is required to isolate the cause(s).

Profile	horizons	depth	number	CPSD index				
G1				2	3			
	A1	0-6	1	96.1	84.7			
	IIC	18-32	2		84.5			
	IIIC	42-56	3					
G3				2	3	4	5	
	A11	0-12	1	85.6	67.2	63.2	68.1	
	A12	24-32	2		70.4	70.1	79.8	
	B21	41-55	3			88.7	67.5	
	IIC2	78-88	4				70.7	
	IIC3	102-115	5					
G4				2	3	4	5	
	A11	0-6	1	82.4	65.3	56.4	84.9	
	A22	21-31	2		53.7	47.3	68.2	
	B2	57-69	3			87.0	75.7	
	C	81-96	4				71.5	
	C	96-112	5					
G5				2	3	4	5	6
	A1	0-8	1	93.3	94.2	92.1	82.5	78.7
	A2	8-18	2		98.9	90.4	75.9	72.1
	B21	30-32	3			90.9	76.8	73.0
	B22	42-52	4				84.3	77.7
	B31	65-73	5					92.3
	C2	120-140	6					

Table 10. Cumulative particle-size distribution index of sand fractions for selected horizons of the soils of the Gooromon Ponds sequence.

Profile	horizons	depth	number	CPSD index				
S1				2	3			
	A1	0-6	1	86.7	74.7			
		20-30	2		61.4			
		50-70	3					
S2				2	3	4	5	
	A11	0-8	1	87.1	82.9	75.7	76.3	
	A13	20-30	2		92.6	84.4	83.4	
	B1	42-52	3			92.3	88.9	
	IIC1	70-90	4				95.9	
	IIC2	90-110	5					
S3				2	3	4	5	6
	A1	0-7	1	93.8	89.6	92.4	71.1	59.8
	B21	17-28	2		91.8	89.9	77.4	63.8
	B22	28-38	3			91.1	78.3	67.5
	B3	38-48	4				71.0	62.2
	C1	68-88	5					77.5
	C2	88-108	6					

Table 11. Cumulative particle-size distribution index of sand fractions for selected horizons of the soils of the Shinglehouse Creek sequence.

Profile	horizons	depth	number	CPSD index					
N1				2	3				
	C1	5-18	1	89.7	85.8				
	C2	32-45	2		93.9				
	IIC	45-55	3						
N2				2	3	4			
	A11	0-7	1	93.5	92.1	93.7			
	A12	7-20	2		95.7	90.7			
	B	30-41	3			92.7			
	C	50-60	4						
N3				2	3	4	5		
	A1	0-10	1	92.5	88.7	81.9	85.4		
	B1	10-25	2		95.2	89.4	92.9		
	B21	25-35	3			93.0	94.2		
	B22	35-50	4				94.4		
	B3	50-70	5						
N4				2	3	4	5	6	7
	A1	0-5	1	95.6	96.6	94.1	81.0	64.2	60.6
	A2	5-17	2		95.8	92.5	78.3	61.4	57.8
	B1	17-30	3			91.8	82.5	64.6	61.0
	B2	30-40	4				78.1	61.5	57.9
	B3	40-60	5					81.6	76.1
	C1	80-100	6						91.2
	C1	120-140	7						

Table 12. Cumulative particle-size distribution index of sand franctions for selected horizons of the Nowra Creek sequence.

Profile	horizons	depth	number	CPSD index				
H1				2	3			
	IIC1	40-58	1	93.0	94.2			
	IIC2	58-90	2		93.2			
	IIC3	90-120	3					
H2				2	3	4	5	
	IIA	15-30	1	73.7	74.0	67.2	55.1	
	IIB1	45-67	2		98.6	91.2	81.5	
	IIB21	67-88	3			91.4	81.1	
	IIB31	110-130	4				87.9	
	IIC1	150-170	5					
H3				2	3	4	5	6
	A1	0-18	1	98.9	99.1	92.0	94.5	95.0
	A3	18-32	2		98.7	91.7	95.3	95.1
	B1	32-48	3			92.2	95.1	95.2
	B21	48-70	4				91.7	88.8
	BC	90-120	5					94.5
	C	150-170	6					
H4				2	3	4	5	
	A1	0-11	1	89.7	92.5	80.9	84.4	
	B21	11-23	2		83.3	76.4	77.4	
	B23	43-70	3			83.9	87.4	
	C	100-130	4				96.5	
	C	130-160	5					
H5				2	3	4	5	
	A1	0-10	1	92.1	92.5	86.2	97.6	
	A22	20-35	2		92.9	91.8	91.8	
	B21	35-60	3			88.0	94.4	
	B22	80-100	4				86.4	
	BC	130-160	5					

Table 13. Cumulative particle-size distribution index of sand fractions for selected horizons of the soils of the Hawkesbury River sequence.

4.3.5 Weathering index

It was not practical to calculate the weathering index for any profile because there was little variation in the fine silt:total silt ratio with depth for any profile with the possible exception of N3 (Table 14). On the basis of this criterion there has been an insignificant contribution to the clay fraction by chemical weathering of silt size particles.

Gooromon Ponds

G1		G3		G4		G5	
d	r	d	r	d	r	d	r
0	.42	0	.58	0	.53	0	.43
18	.42	24	.55	21	.52	8	.43
42	.49	41	.54	57	.48	30	.48
		78	.54	81	.42	42	.52
		102	.52	96	.51	65	.54
						120	.49

Shinglehouse Creek

S1		S2		S3	
d	r	d	r	d	r
0	.50	0	.61	0	.41
20	.36	20	.66	17	.45
50	.45	42	.64	28	.45
		70	.64	38	.49
		90	.65	68	.47
				88	.45

Table 14 (continued over page)

Nowra

N1		N2		N3		N4	
d	r	d	r	d	r	d	r
5	.45	0	.40	0	.49	0	.37
32	.44	7	.44	10	.48	5	.37
45	.50	30	.46	25	.42	17	.36
		50	.42	35	.39	30	.34
				50	.34	40	.38
						80	.36
						120	.44

Hawkesbury

H1		H3		H4		H5	
d	r	d	r	d	r	d	r
40	.35	0	.49	0	.31	0	.34
58	.38	18	.51	11	.35	20	.37
90	.38	32	.51	43	.41	35	.44
		48	.52	100	.42	80	.55
		90	.54	130	.43	130	.48
		150	.57				

* d = depth (cm)

† r = ratio fine silt:total silt

Table 14. Ratios of fine silt:total silt (2-5 um:2-20 um) of selected horizons for soils of four terrace sequences.

4.4 Conclusions

The length of time of mechanical disaggregation has a profound effect on the fine clay:coarse clay ratio, subtle changes in which are used to identify whether clay movement has taken place during pedogenesis. It is not possible to choose a particular shaking procedure which is entirely satisfactory; a compromise is necessary.

In all four sequences there is a progressive increase in the fine clay:total clay ratio with time in the B horizons, a result which is consistent with a clay illuviation hypothesis. The CPSD index indicates that most profiles had a texturally uniform parent material; the few exceptions could have a number of causes. There is no evidence for a significant contribution to the clay fraction by in situ chemical weathering of the silt fraction.

Chapter 5

Physical weathering and soil development

5.1 Introduction

While weathering is generally considered to mean physical, chemical and biological weathering, the vast majority of pedogenic studies have been concerned with the nature and extent of chemical and biological weathering mechanisms, particularly chemical. There is a paucity of data for the role of physical breakdown in soil profile development.

In soils on Mt. Kenya, Zeuner (1949) observed variations in particle-size of anorthoclase which he attributed to splitting along cleavage planes. Severe and frequent frosts are common in this area and it therefore appears that cryoclastic breakdown of mineral grains is taking place. Arnaud and Whiteside (1963) observed a redistribution in particle-size of horizons relative to their parent materials from four different Great Soil Groups. They concluded that there had been physical breakdown, by frost action, of the larger rock fragments and minerals. Expansion and contraction of water, rather than of the minerals and rock fragments themselves, was considered the main factor.

In podzols (Typic haplorthods) formed in sandy materials in Denmark, Nornberg (1980) observed that there is a tendency for the proportion of silt and clay size particles to increase with age of profile. He concluded that this has resulted from a two stage process. First, the release of less resistant minerals from rock fragments in sand and gravel fractions,

followed by fragmentation of these minerals into finer particles. Again, cryoclastic breakdown seems the most likely mechanism. It is also the conclusion of Bronger and Kalk (1976) who reported the breakup of micas and feldspars in situ. However, in temperate regions not subject to frosts, or only infrequently so, there will be no freezing and thawing.

Brewer and Walker (1969) noted a decrease in the presence of rock fragments in texture contrast soils with age at Kempsey but did not propose a mechanism. If this decrease was due to in situ disintegration rather than chemical alteration another mechanism, other than freezing and thawing, would have to responsible since the soils are not subject to frosts. One possible mechanism is the action of shrinking and swelling on rock fragments and mineral grains initially weakened during transport and deposition. Evidence for this process comes from several studies. Moss (1973) and Moss and Green (1975) have noted marked weakening of quartz grains, in the form of microfractures, from alluvial deposits and concluded that repeated static loading and collective movement in water weakened the particles considerably. Ritchie *et al.* (1974) observed that volume changes and fabric re-arrangement associated with argillic horizon genesis largely obliterated traces of rock structure presence in the parent glacial till.

It is important to determine the extent of physical breakdown of coarse particles, apart from its contribution to the clay fraction. Parent material uniformity is usually assessed from changes in particle size distributions of minerals of the sand fraction on the assumption that there has been little alteration as a result of pedogenesis. Since the intensity of chemical weathering increases with decrease in particle-size, and will therefore have its greatest effect on the finer particles of silt and clay size, this assumption appears reasonable, from a chemical standpoint.

However, any removal or addition of sand will affect particle-size distributions or ratios of resistant minerals and may lead to the conclusion that the parent material was texturally inhomogeneous whereas it was the result of pedogenesis within an initially uniform material.

Few quantitative studies have taken this process into account. Smeck *et al.* (1981) found that shale disintegration contributed clay to the B2 horizon but that chemical weathering of coarse clay and silt to fine clay was the dominant pedogenic process.

The purpose of this chapter is to determine the extent of physical breakdown of the coarse fraction and the contribution that this may have made to textural differentiation in the terrace soils.

5.2 Methods and materials

5.2.1 Measurement of quartz

Coarse clay (2-0.2 um), fine silt 2-5 um), coarse silt (5-20 um) and fine sand (20-53 um) were separated from a selection of soils representing the A, B and C horizons of the terrace sequences. The coarse fractions, 53-125 um and 125-2000 um, were obtained by wet sieving. Fractions >5 um were hand ground using a mortar and pestle with acetone. Samples were mounted in an end-loading sample holder with a teflon backing (Schultz 1978). The intensities of the quartz line at 3.34A^{o} was determined on an X-ray diffractometer set at 40 kV and 60mA and 4^{o} receiving silts. Each plate was run twice, for a time of 50 seconds each, and a mean count calculated. The quartz content of the fine clay was not measured because early experiments established that there was little quartz in the fraction. The percentage quartz was determined by calculation, knowing the elemental chemistry (Chapter 8) and mass absorption coefficients of each element (Norrish and Taylor 1962).

5.2.2 Measurement of proportion of rock fragments

50-250 um fractions were separated from the same horizons as in 5.2.1 after gentle end-over-end shaking with calgon as a dispersant. Sub-samples were mounted on glass slides and ground and polished to 30 um thickness. Rock fragments and individual grains were counted by traversing the slide with the aid of a point-counting stage. Grains intersecting the horizontal grid line in the eye-piece were counted.

5.3 Results and discussion

5.3.1 Particle-size distribution of gravel

Depth functions of gravel and fine silt + clay indicate little relationship between the two. If there had been a significant contribution to the finer fractions, especially in the B horizons, from disintegration of rock fragments and minerals of gravel size, there should be a general decrease in gravel content in those horizons. Particularly should this be so in the older members of each sequence where clay contents are higher. However, this is not the case. The older soils, G4, G5, N4, H4 and H5 show an increase in gravel over the younger members in their respective sequences (Figures 71, 72, 73, 74). This gravel appears to have a pedogenic origin since the gravels are mostly nodules and concretions of sesquioxide. Evidence for mobilization and segregation of oxides of iron can be seen in thin sections of these soils (Chapter 6).

In spite of the foregoing statement there appears to have been breakdown of gravel. In all sequences, except that Hawkesbury where there is little or no gravel in the first three members of the sequence, there is a marked decrease in the gravel from the youngest to the next member in the sequence i.e. there is a decrease from G1 to G3, S2, to S2, N1 to N2. But the profiles G3, S2 and N2 show no

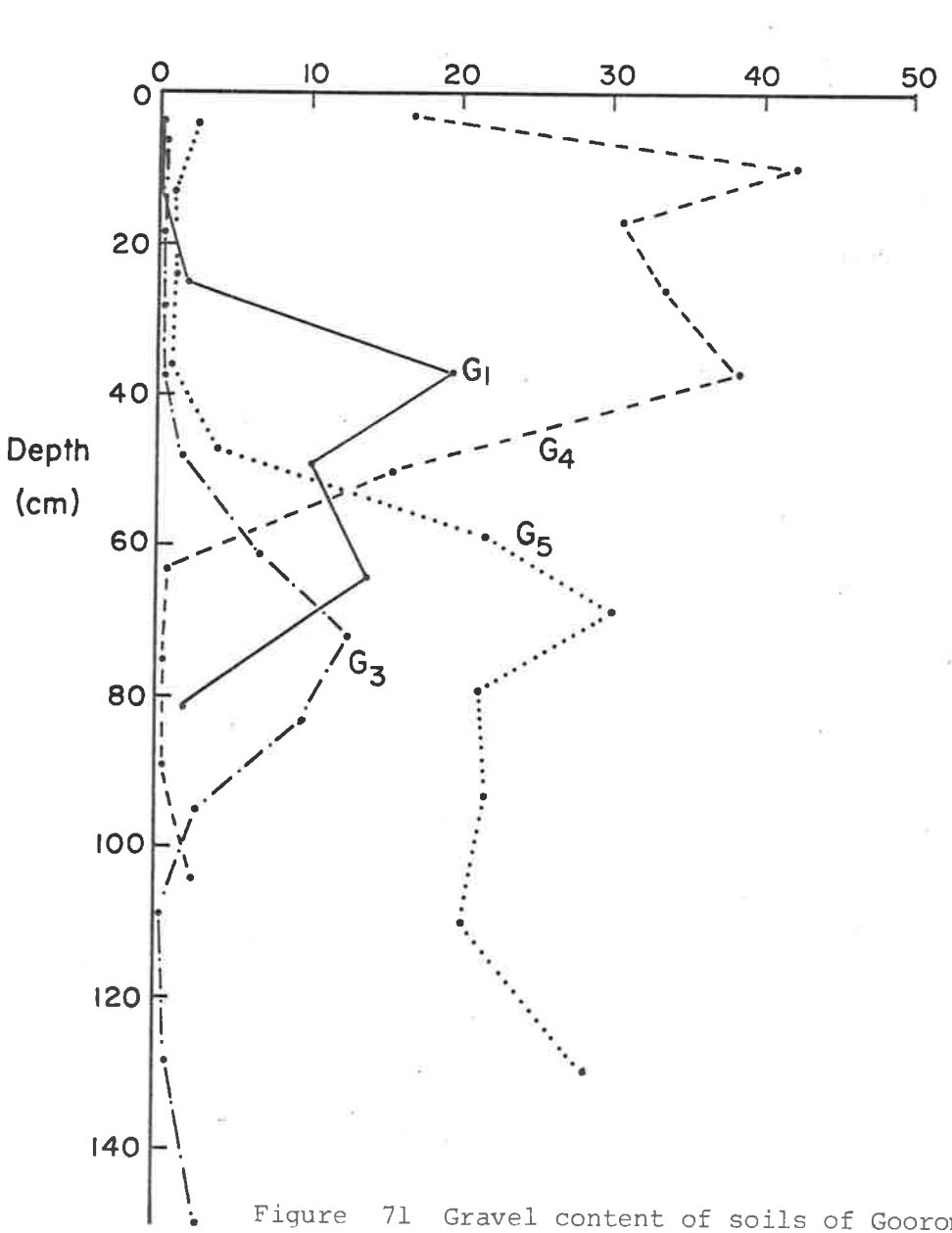

Figure 71 Gravel content of soils of Gooromon Ponds sequence

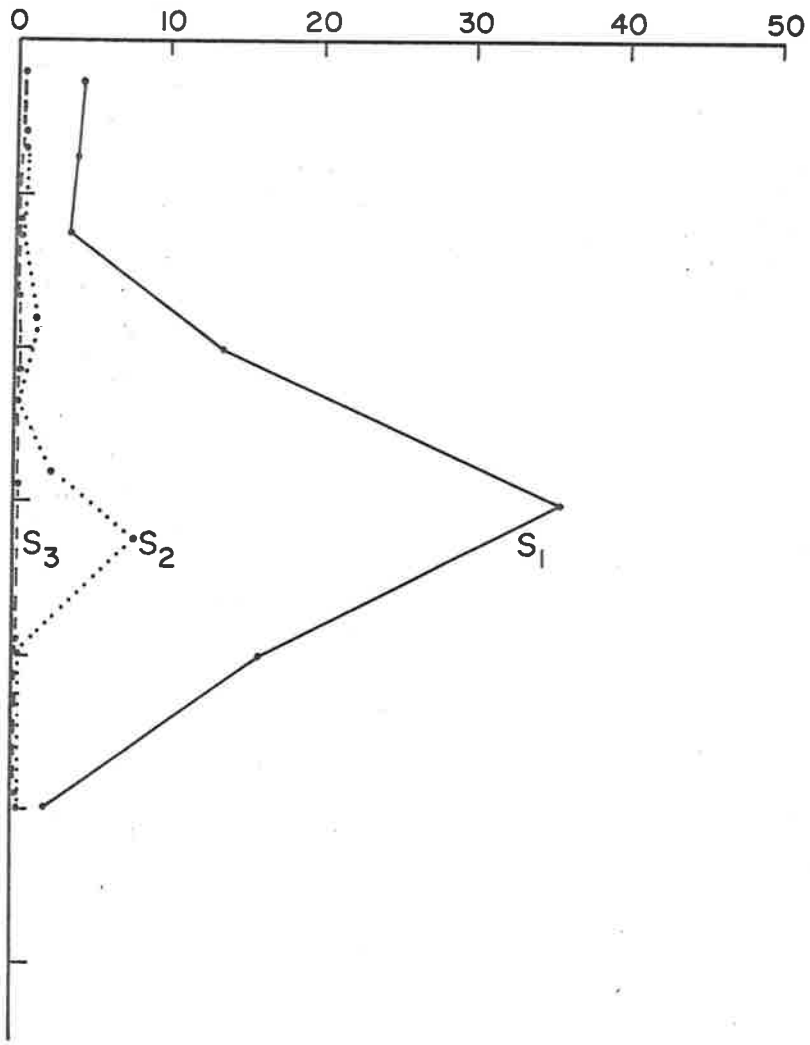

Figure 72 Gravel content of soils of Singlehouse Creek sequence

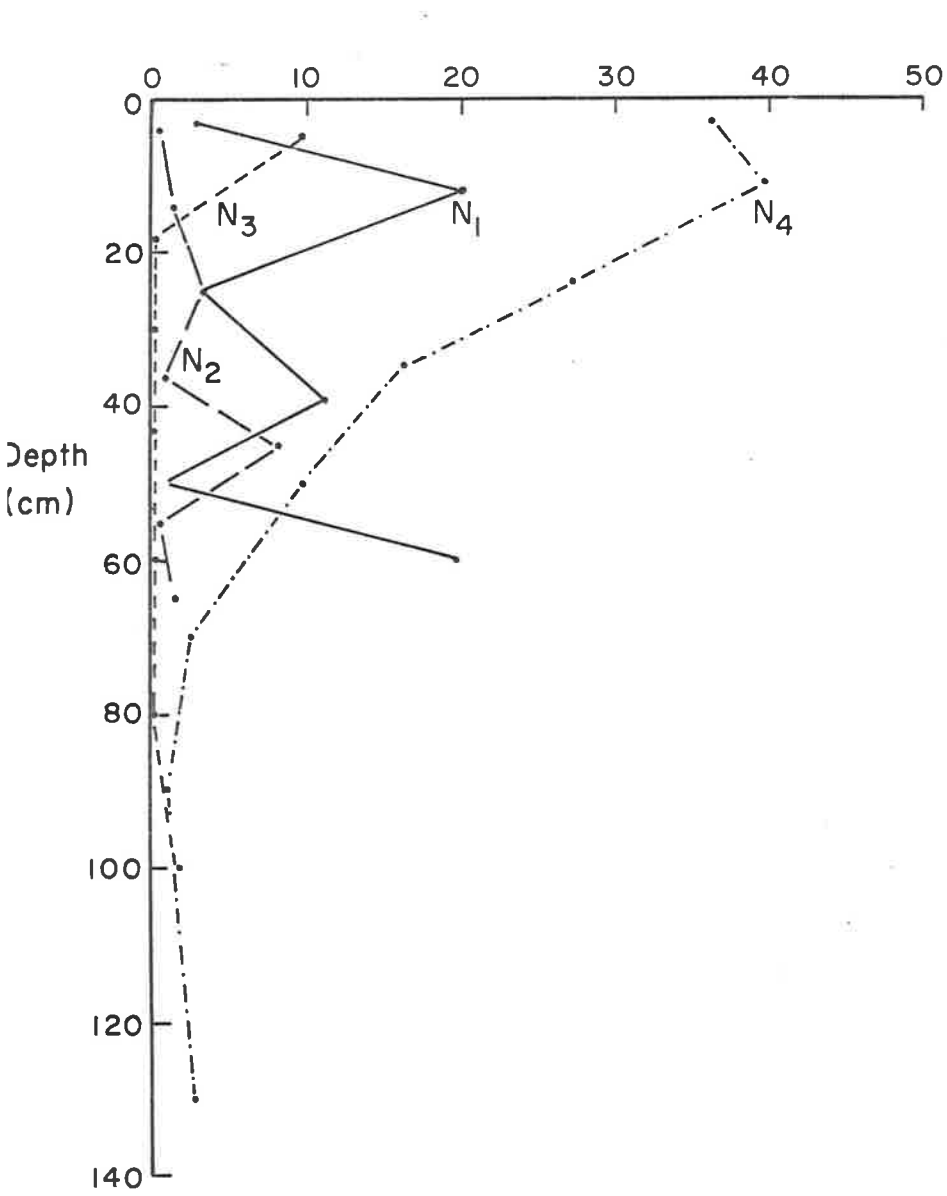

Figure 73 Gravel content of soils of Nowra sequence

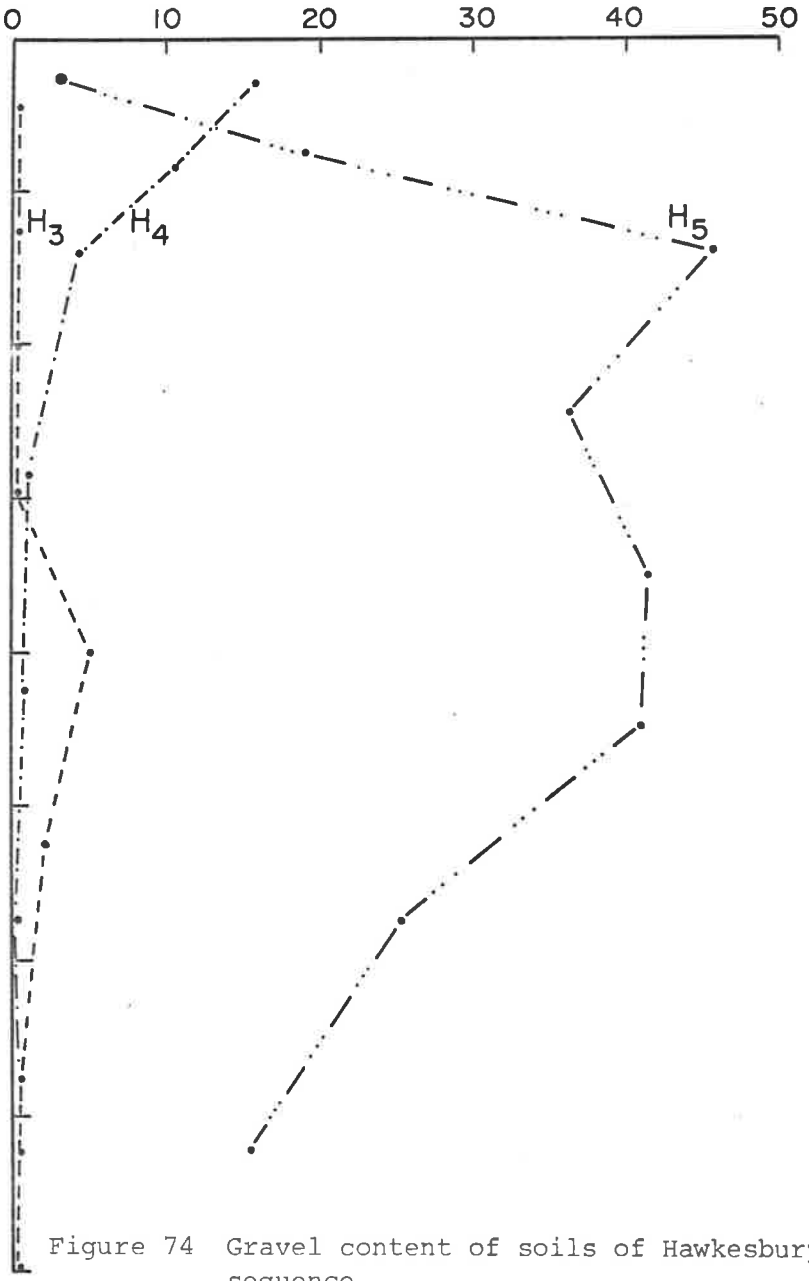

Figure 74 Gravel content of soils of Hawkesbury River sequence

horizon of clay enrichment despite the substantial loss of gravel. Texturally, they are relatively uniform. Comparison of S2 and S3, N2 and N3 shows that there is little change in gravel but the presence of a strong textural B horizon. It appears that gravel may have broken down, in situ, throughout the *whole* profile of the next-youngest soils producing clay which was subsequently translocated to form the textural B horizon of the older soils. Thus, while physical disintegration has occurred, it is not responsible 'per se' for the textural B horizon.

5.3.2 Quartz content of the soil separates

In most of the older profiles of the terrace soils, there is an increase in the quartz content of A and B horizons relative to the parent material (Table 15). Exceptions to this are S2, which shows little change, G4, which shows a decrease, and G5 in which there was an increase in all fractions except fine and coarse sand which showed slight decreases in the B horizon compared to the C.

Profile	horizon	depth (cm)	coarse clay (0.2-2um)	fine silt (2-5um)	coarse silt (5-20um)	fine sand (20-53um)	medium sand (53-125um)	coarse sand (125-2000um)
				Gooromon Ponds				
G1	A1	12	20	53	65	83	73	76
G3	A11	6	18	51	62	78	74	68
	B21	46	20	56	64	81	78	82
G4	A12	9	29	57	64	87	77	67
	B1	47	25	57	72	85	74	64
	C	85	32	66	76	90	82	77
G5	A2	13	53	86	88	92	93	83
	B22	47	33	80	84	86	87	76
	B31	69	21	66	75	98	83	79

Table 15 (continued over page)

				Shinglehouse Creek				
S1	A	25	13	39	70	93	100	98
S2	A12	14	10	23	58	89	92	89
	B1	47	11	27	63	91	93	68
	IIC	80	10	26	64	92	-	72
S3	A2	14	11	39	91	99	100	100
	B3	43	8	20	77	98	92	-
	C1	78	11	25	71	93	95	79
				Nowra Creek				
N1	C1	12	28	50	58	70	81	65
N2	A12	14	27	41	57	74	89	73
	B	36	29	46	60	71	85	79
N3	B1	18	37	46	69	75	88	69
	B22	42	33	63	65	78	88	86
N4	A1	2	45	54	60	84	89	86
	B2	35	39	81	79	90	92	83
	C1	130	-	68	67	83	82	75
				Hawkesbury River				
H1	IIC	49	-	28	53	69	91	98
H2	IIA	23	19	43	62	78	91	88
	IIB21	78	16	43	69	84	91	101
H3	A3	25	34	67	87	96	89	100
	B21	59	34	73	86	99	98	100
	C	160	-	55	73	91	93	89
H4	A1	6	18	52	73	91	100	90
	B22	33	22		71	90	98	94
	C	115	12	35	56	74	81	88
H5	A22	28	-	93	88	100	100	100
	B21	48	-	26	44	74	94	96
	BC	145	26	19	21	62	81	96

Table 15. Quartz content of separates from selected horizons of the soils of the terrace sequences.

These results cannot be explained on the basis of a physical weathering hypothesis. On the basis of such an hypothesis, the increase of quartz in the finer fractions must be matched by a corresponding decrease in the coarse fractions. This is only observed in G5 and even there the decreases in quartz of the fine sand are slight compared to the big increases in the coarse clay and fine silt. The results are best explained by a preferential loss, from all fractions, of minerals other than quartz. This loss could be a combination of chemical breakdown and illuviation of fine colloid (<0.2 um) into the B horizon or from the profile entirely. On the latter hypothesis, the fine fractions, especially the coarse clay and fine silt, should show a greater increase, relative to the C horizon, than the coarser fractions because chemical weathering would be more pronounced in the former. This is so. Moreover, with age, the difference between quartz contents of A and B horizons compared to the C should increase. This was observed (cf H3, H4 and H5, Table 15). The decrease in quartz of G4 may be due to the breakdown of gravel which is higher in minerals other than quartz compared to the fine earth.

However, there may still be breakdown of quartz and quartz-bearing minerals from coarser fractions to provide an increase of fine material in the coarse clay and silt. But the resultant decrease in the quartz content of the coarse fractions may be masked by a simultaneous, but higher, loss of the weatherable minerals. Thus, there could still be a net increase in the quartz content of the sand fractions even though disintegration of quartz bearing minerals was taking place. One way of testing this is to plot the particle-size distribution of quartz. If changes in quartz

Figure 75 Particle-size distribution of quartz within the major horizons of the soils of the Gooromon Ponds sequence

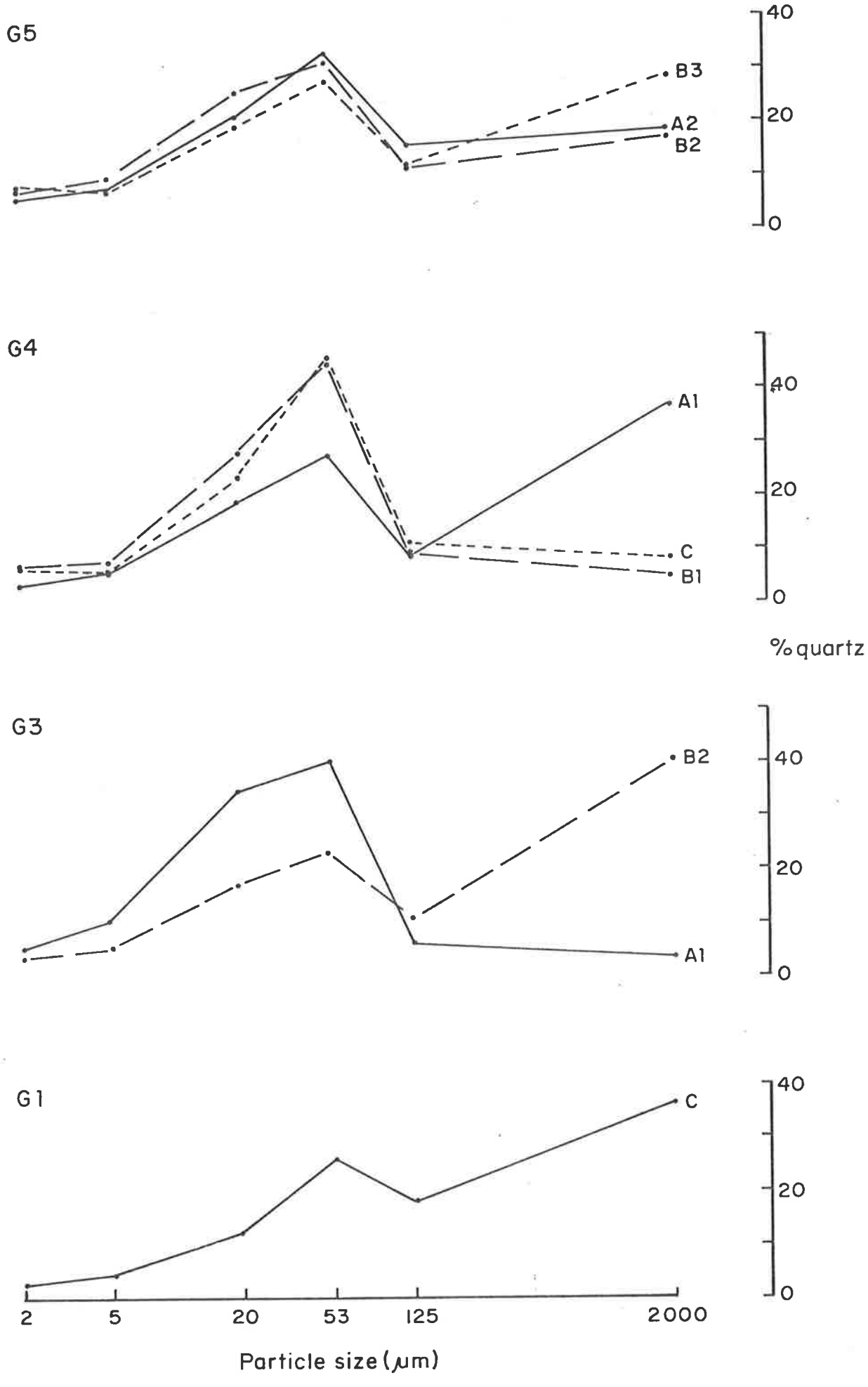

Figure 76 Particle-size distributions of quartz within the major horizons of the Shingle House Creek sequence

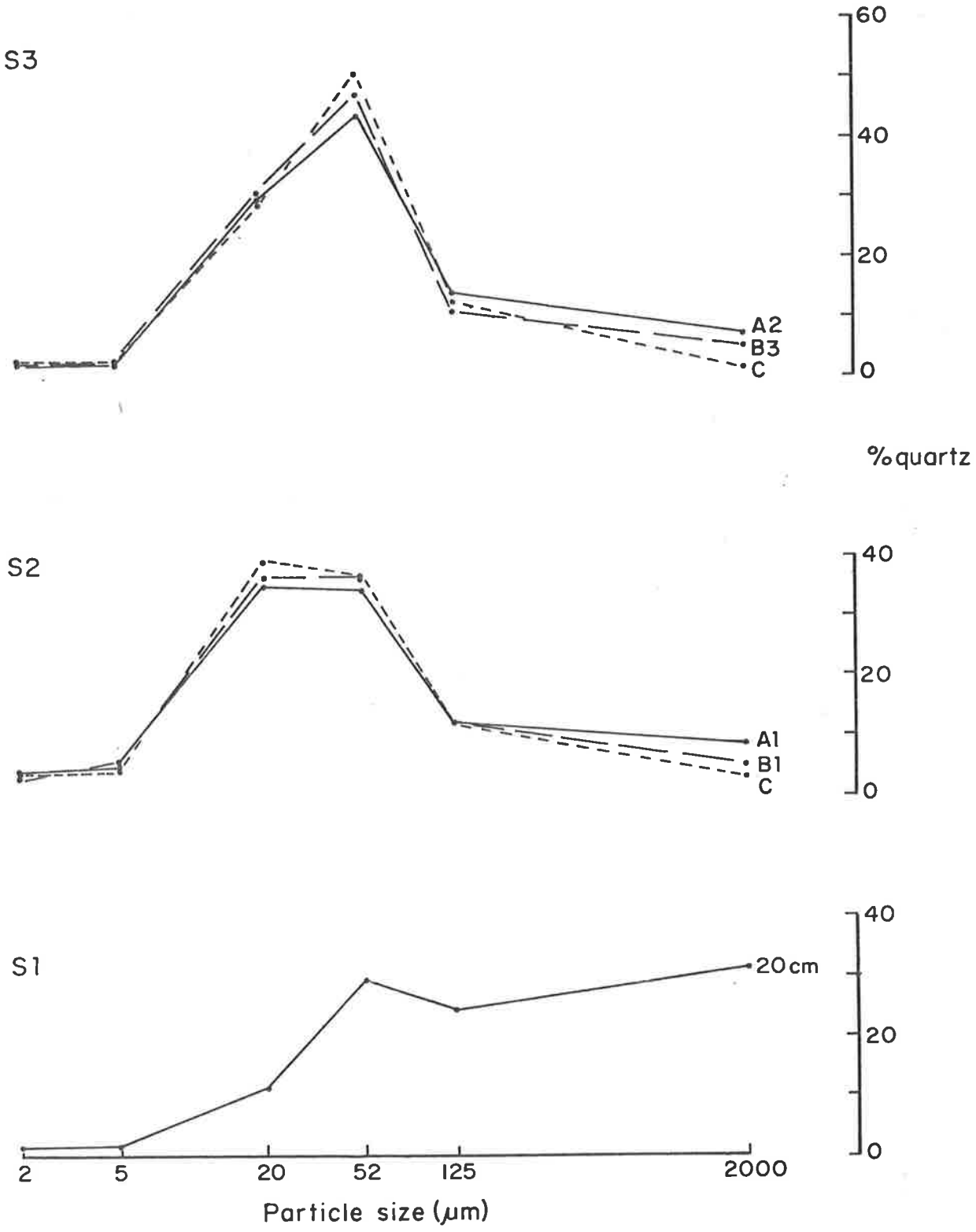

Figure 77 Particle-size distribution of quartz within the major horizons of the Nowra sequence

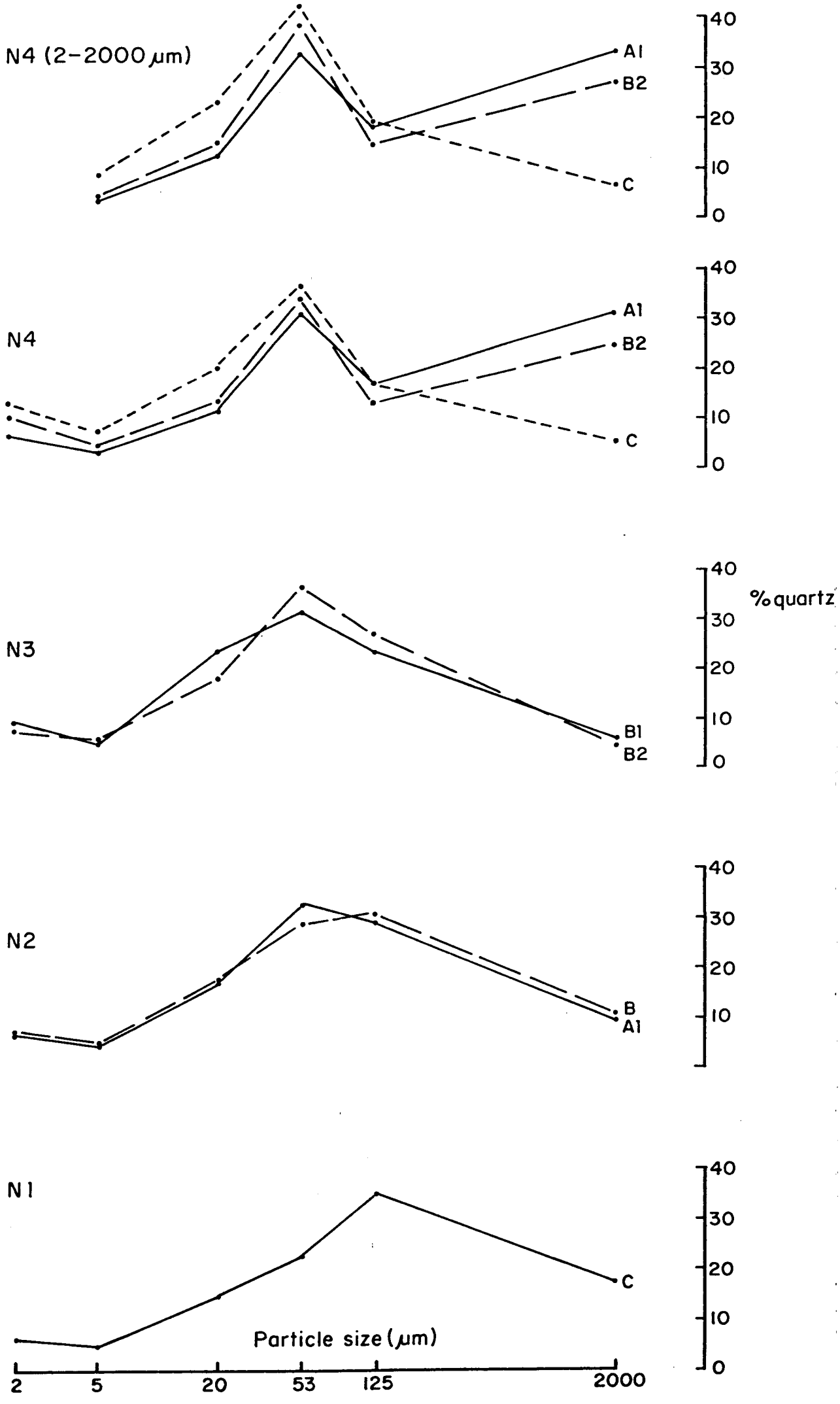

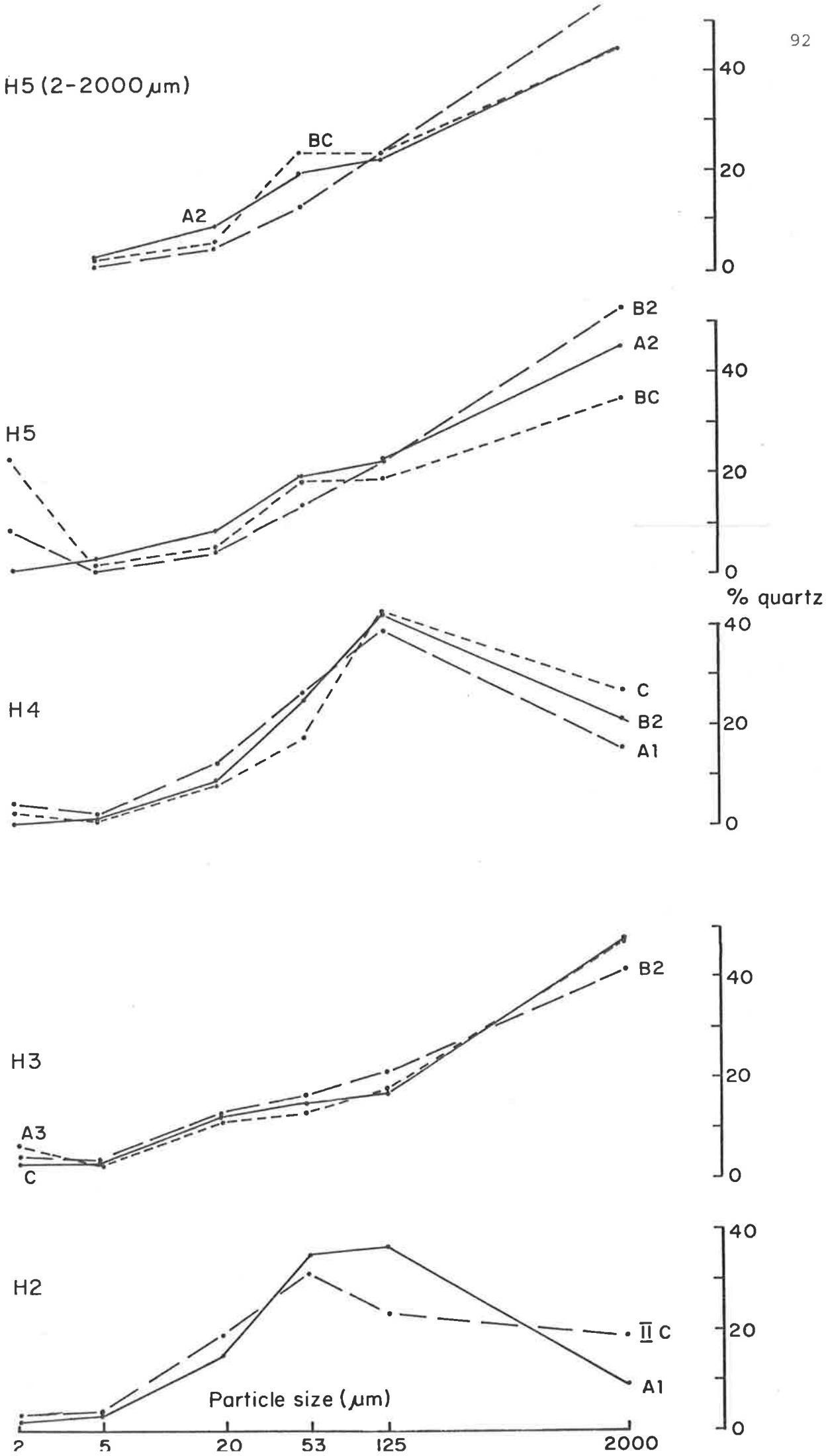

Figure 78 Particle-size distributions of quartz with the major horizons of the would of the Hawkesbury River sequence

percentages as observed in Table 15 were only occurring as the result of changes in the weatherable minerals, there should be no change in the particle-size distribution of quartz throughout the profile.

The particle size distributions of quartz were calculated and are shown in Figures 75, 76, 77 and 78. In the Gooromon Ponds sequence, G4 shows a slight decrease in the coarse fraction of the B horizon. This loss shows up as an increase in the fine sand and silt. There is little contribution to the coarse clay. The effect is more pronounced in the older G5 profile. There is little change in quartz distributions of Shinglehouse Creek soils indicating that physical disintegration of quartz is insignificant. In the Hawkesbury sequence there is a relatively uniform distribution in H3 but in H4 there is a gain in fine sand and silt at the expense of the coarse and medium sand in both A and B horizons. In H5, and also N4, the trend is reversed and there is an increase in the proportion of quartz in the coarse sand and a decrease in the fine and coarse silt and coarse clay. This is probably caused by a breakdown of fine-grained quartz by chemical weathering.

5.3.3 Breakdown of rock fragments

Rock fragments were identified as any grain which appeared to be made up of two or more distinct particles. Some grains were highly fractured and it was difficult to determine whether it was one fractured grain or a number of grains of the same mineralogy. Most were designated rock fragments which means that there may be an over-estimation of the proportion of rock fragments (Table 16).

Profile	horizon	depth (cm)	rock fragments (%)	Profile	horizon	depth (cm)	rock fragments (%)
	Gooromon Ponds				Nowra Creek		
G1	A1	12	76	N1	C1	12	37
G3	A11	6	83	N2	A12	14	66
	B21	46	92		B	36	64
G4	A12	9	75	N3	B1	18	21
	B1	47	73		B22	42	32
	C	85	72				
				N4	A1	2	16
G5	A2	13	49		B2	35	23
	B22	47	65		C1	130	31
	B31	69	65				
	Shinglehouse Creek				Hawkesbury River		
S1	A	25	39	H1	IIC	49	55
S2	A12	14	82	H2	IIA	23	55
	B1	47	66		IIB21	78	44
	IIC	80	-				
				H3	A1	6	27
S3	A2	14	21		A3	25	27
	B3	43	36		B21	59	19
	C1	78	26		C	160	19
				H4	A1	6	8
					B22	33	9
					C	115	22
				H5	A22	28	2
					B21	48	18
					BC	145	25

Table 16. Proportion of rock fragments in sand fractions of soils from four terrace sequences.

In all sequences there is a decrease in the proportion of rock fragments with age, an observation consistent with the changes in gravel percentage in section 5.3.1. Apart from a decrease in the A horizon of G5, each profile has a relatively uniform percentage of rock fragments. In the Shinglehouse Creek sequence the increase in S2 compared to S1 is due to many grains being cemented by iron. This may be an inherited feature but it is more likely to be in situ mobilisation and segregation of iron (Chapter 6). The increase with depth of the rock fragments in the profiles N4, H4 and H5 is also ascribed to this process. The increase from the A horizon to the C horizon is greater in H5 than H4, a result which is consistent with the micromorphology which indicates a greater degree of sesquioxide mobilisation in the oldest Hawkesbury profile.

It appears that breakdown of sand-size rock fragments has occurred but the extent to which it has influenced other fractions, particularly the clay, cannot be ascertained. A very mild procedure was used to isolate the 50-250 mm fraction. If a more vigorous mechanical dispersion had been used, similar to that used for determination of the particle-size distributions (Chapter 3) and heavy mineral ratios (Chapter 7), many weakly aggregated grains and fractured minerals may have been broken down. Nevertheless, except for the oldest profiles, there are no marked changes in proportion within any one profile indicating that breakdown has been relatively uniform within a profile.

5.4 Conclusion

From changes in the depth functions of gravel with time, it is concluded that physical breakdown has occurred but that it has not been responsible for the development of the textural B horizon. The rate of

disintegration is particularly high early in pedogenesis, preceding the development of texture contrast. Breakdown contributes fines to the whole solum and is not generally any more intense in one horizon than another. Grain counts of rock fragments in the medium sand range lend support to this conclusion.

It is concluded from the particle-size distributions of quartz that the contribution to the clay fraction from physical disintegration is only slight and that other mechanisms such as chemical weathering and illuviation are of greater import.

Chapter 6

Micromorphology

6.1 Introduction

Increasingly, micromorphology is being used to provide evidence for soil processes and it is an essential diagnostic tool in several soil classification schemes. In the Soil Taxonomy (Soil Survey Staff 1975) the technique is used as an aid to decide on the presence of an argillic horizon. ~~Clay skins should be present in the B horizon forming at least 1% of the matrix in thin section.~~

In Australia a number of pedogenic studies have involved extensive use of micromorphology (e.g. Stace *et al.* 1968, Churchward 1963) some exclusively (Brewer 1968, Sleeman 1964). Most studies have concluded that, while clay illuviation has occurred, it cannot be considered the main factor in the process of textural differentiation. In a study of four Red-brown earths and four Red podsolic soils, Brewer (1968) measured, by point counting, the proportion of illuviated clay to total clay and concluded that illuviation was relatively insignificant and that weathering in situ was the main factor.

Sleeman (1964) studied the structure variation of two Red-brown earths from the Riverine Plain and concluded that the Hanwood profile consisted of five depositional layers and the Deniboota profile three. Soil formation had occurred between some of the depositional breaks. Based on a micro-morphological study of the nature of the ferruginous and siliceous nodules

in the soils and hardpans as compared with lateritic material from the same area, Brewer, Bettenay and Churchward (1974) decided that both the hardpan and the overlying soil were formed in colluvium derived from older silicified lateritic profiles.

However, some processes may give rise to similar structures. Thus void cutans may form by localised weathering of mineral grains (Koppi 1981) or by translocation. Grain cutans may be a depositional feature i.e. inherited from the parent material, or formed by illuviation (Nettleton et al 1969). Thus, the link between micromorphological observation and process is a tenuous one since there is very little experimental verification linking the two. Appropriate weight can only be given to the micromorphological evidence after due consideration of data derived by other means.

In the following chapter, micromorphological evidence for the processes involved in the development of texture-contrast will be presented and considered in conjunction with data for shrinking and swelling and particle-size.

6.2 Sampling

Undisturbed sections of soil were sampled from the pits as close as practicable to the site at which bulk samples were taken for chemical and mineralogical analysis and where the description was made for the micromorphology.

A column of soil 10 cm x 10 cm and length equal to the depth of the pit was carved by knives and chisels. The column was then cut into 5 cm lengths, prised from the soil mass and packed into tins with cotton wool. In the laboratory, polished thin sections 6 cm x 5 cm and approximately 30 um thick were prepared.

6.3 Method of description and terminology

The terminology used is essentially that of Brewer's (1964) but the descriptions have been abbreviated for clarity and to focus on evidence for sedimentary layering and the kind of reorganisation that has accompanied soil formation. Following the description of each sequence, an interpretation of soil development is given based entirely on the micromorphological evidence.

An attempt has been made to estimate the trends in proportions of pedological features (Stace *et al.* 1968), using the symbols, (F) frequent, (C) common, (O) occasional, (R) rare.

6.4 Micromorphology of the Gooromon Ponds sequence

6.4.1 Description

G1 - Cow Flat Unit

0-8 Argillasepic porphyroskelic fabric. Angular skeleton
8-15 grains mainly quartz but many fine-grained rock fragments. Irregular orthovughs (C). Single branching channels (O). Organic fragments (C).

21-28 As above.

35-42 Intertextic to porphyroskelic fabric, granular patches. Much more void space than above, less organic fragments. Simple packing voids (F) and irregular orthovughs (C). Papules (O). Rock fragments (C), cracked and breaking into smaller fragments (Figures 79.1, 79.2). With depth: increase in gravel and proportion of granular fabric and simple packing voids.

G3 - Bedulluck Unit

0-7 Argillasepic porphyroskelic fabric. Mammillated orthovughs (Figure 79.3) (C), occasional vesicles and fine, irregular channels (C). Welded fecal pellets (C) and iso- and striotubules (C).

14-21 As above but greater void space. Many large vughs up to 2 cm across.

23-29 As above but fabric darker in colour, more coarser skeleton grains. Occasional void ferriargillans, thin and discontinuous. Fabric patchy, consisting of dense, light-coloured material similar to 0-7 cm juxtaposed with darker less dense fabric with greater void space. With depth: more cutans.

48-55 Similar to above. Large skeleton grains with iron staining in fine cracks. Rock fragments and quartz grains cracked and split (C) (Figure 79.8).

56-62 Less organic matter but fabric patchy as in 23-29. Dark red-brown undifferentiated sesquioxidic glaebules, diffuse boundaries (Figure 79.5). Iron staining in rock fragments. (Figure 79.4). With depth: greater proportion of glaebules and less organic matter.

74-81 As above but greater proportion of fine grained rock fragments with intense, red iron staining; and sesquioxidic glaebules. Irregular iron-stained nodules with sesquioxidic halo (O) (Figure 79.6).

85-92 Denser fabric than above. Weak voinsepic porphyroskelic fabric. Ferriargillans in most vughs, occasionally thick and banded (Figure 79.7). Papules (C). Glaebules as above. With depth: Skelvosepic with argillasepic patches (Figure 80.1); abundant cutans.

G4 - Spring Unit

0-6 Argillasepic porphyroskelic fabric. Large proportion of void space. Mammillated orthovughs (C), often interlinked. Channels (O). Meta aggrotubules (C). Many siltstone rock fragments of coarse sand and gravel size but also ironstone and conglomerates of quartz and siltstone, usually rounded and fractured (F).

20-27 As above but more voids.
29-36

35-41 Denser fabric; much greater proportion of plasma; skelvoinsepic fabric. Discrete, irregular orthovughs (F). Irregular channels. Frequent skeleton grains as above. Void ferriargillans (O), 10-50 um thick. Papules (O).

42-49 Similar to above but some masepic fabric in patches (Figure 80.2). Cutans up to 200 um thick, strong continuous orientation (C).

54-60 As above but greater proportion of cutans (Figure 80.3), up
60-66 to 200 um thick, most 10-15 um, less skeleton grains of gravel size. With depth: fewer cutans, less plasma.

80-87 Skelvoinsepic fabric. Few channels; irregular linked
94-101 orthovughs (C). Rounded skeleton grains of varying lithology (quartzite, siltstone, quartz conglomerate. Patches of void argillans 5-50 um thick. Occasional papule clusters, up to 200 um thick (Figure 80.4).

G5 - Tara Unit

0-7 Very porous, open fabric; argillasepic porphyroskelic. Mammillated orthovughs (C), elongate channels up to 3mm across (O). Organic fragments (C), fecal pellets (C), organic aggrotubules (C). Angular quartz and rounded ironstone of coarse sand and gravel size (O). With depth: more porous; sharp break at base (23 cm) to different fabric, described below.

34-41 "Tongues" and pockets of argillasepic fabric similar to surface material in voinsepic porphyroskelic fabric with much greater proportion of plasma; minor skelvoinsepic. Vugh and channel argillans, mostly thin and discontinuous, 5-20 um thick; some continuous, up to 100 um. Skeleton grains of subangular quartz and ironstone nodules. Papules (F), up to 300 m thick. With depth: loss of pockets of argillasepic fabric, increase in proportion of channels and cutans.

44-51 Basic fabric as above but large sesquioxidic nodules up to 5 cm diameter (C). Internal fabric, generally similar to basic fabric but some have high concentrations of glaebules which have argillaceous halos.

54-60 Mavoinsepic fabric. Cutans patchy, less prevalent than above. Papules, higher proportion than above, up to 500 um (F). Metaskew planes (O). Numerous sesquioxidic nodues, as above.

64-70 Similar to above but fabric masepic (Figure 80.5) and more numerous channels aligned to form irregular ortho joint planes.

73-80 Fabric vomasepic porphyroskelic with patches of asepic fabric. Vesicles and orthovughs (C), irregular channels. Greater proportion of void argillans, up to 500 um thick, (Figure 80.6) and papules, up to 1 cm. Ironstone nodules with internal fabric varying from undifferentiated to isotropic (C).

84-90 As above but decreasing proportion of sepic fabric element. Plasma becoming increasingly confined to voids.

6.4.2 Discussion

In G1 there has been little pedogenesis apart from the incorporation of organic matter. Distinct sedimentary layers are

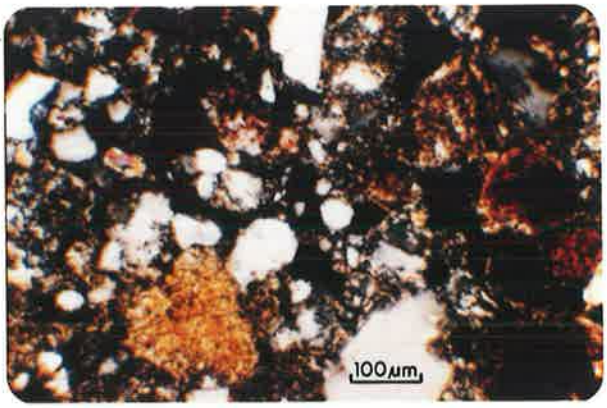

Figure 79.1 Profile G1 Granular fabric with some grains showing evidence of pre-weathering.

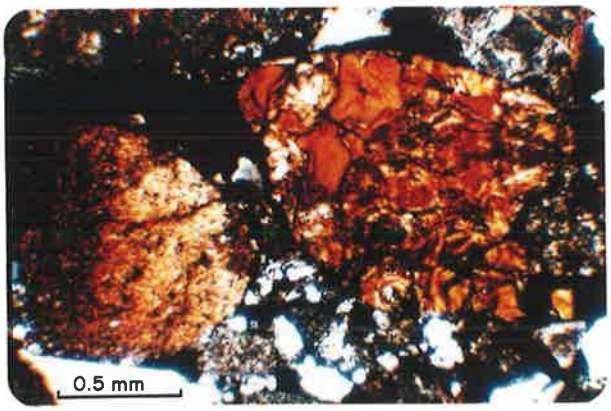

Figure79.2 Profile G1 Rock fragment breaking up.

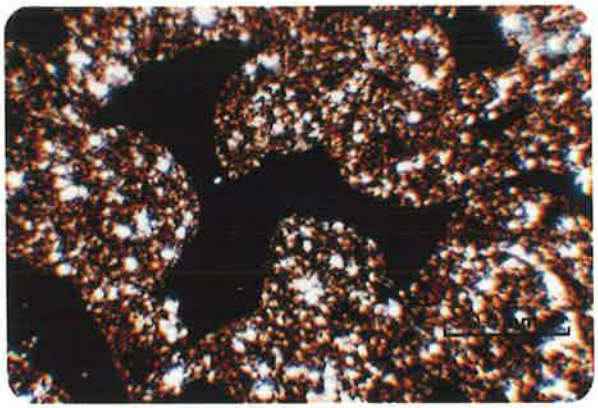

Figure 79.3 Profile G3,14cm Mammillated orthovughs.

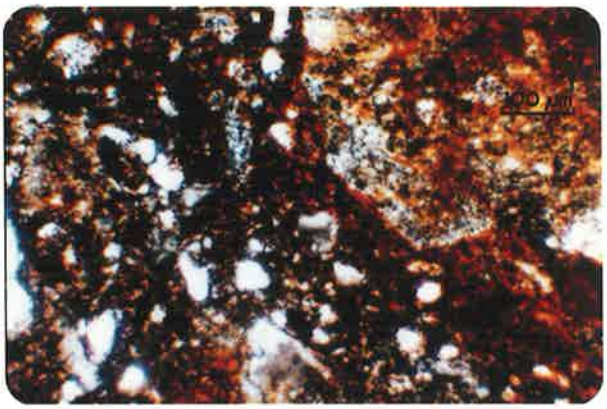

Figure 79.4 Profile G3,48cm Fine grained rock fragment with iron halo.

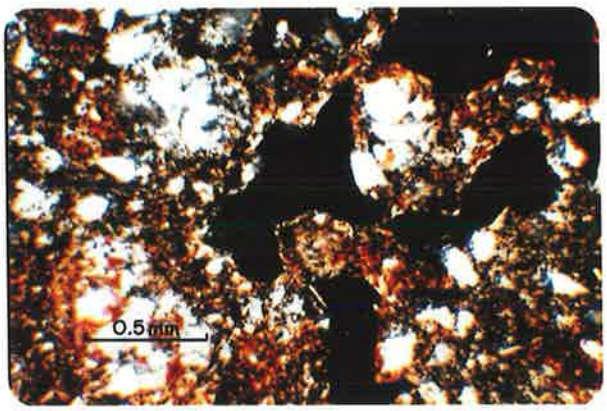

Figure 79.5 Profile G3 Weak vosepic fabric with diffuse sesquioxide glaebule.

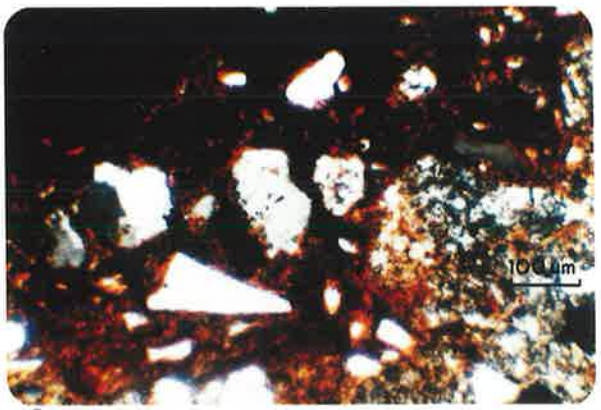

Figure 79.6 Profile G3,74cm. Rock fragment with sesquioxide halo.

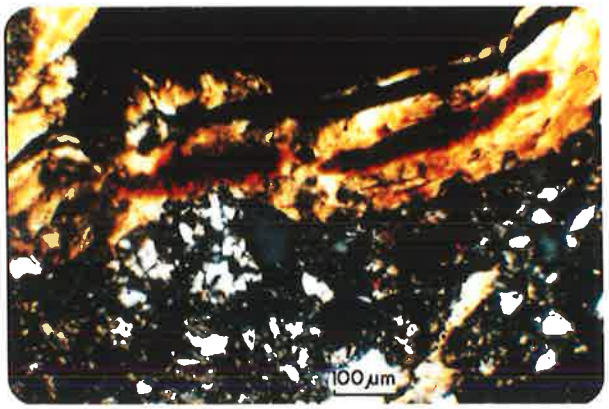

Figure 79.7 Profile G3,85cm. Compound void ferri-argillan.

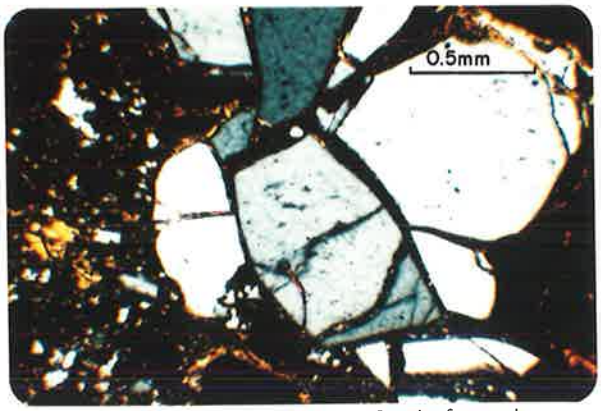

Figure 79.8 Profile G3,98cm. Quartz fragment breaking up along fractures.

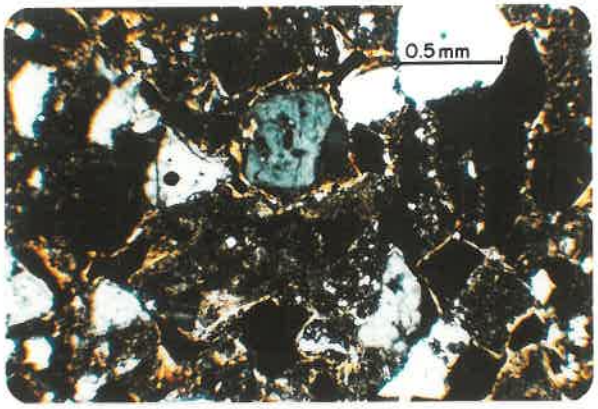

Figure 80.1 Profile G3,98cm. Voskelsepic fabric.

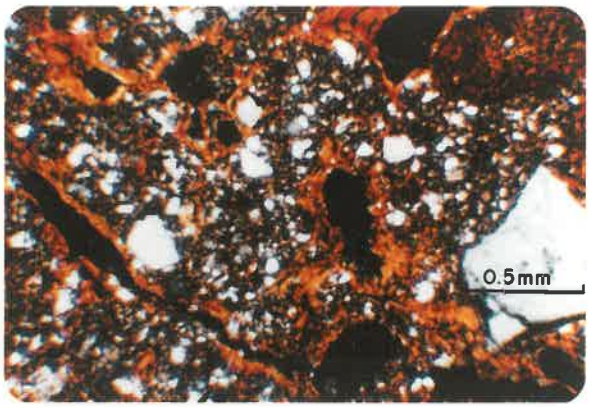

Figure 80.2 Profile G4,42cm. Vosepic fabric.

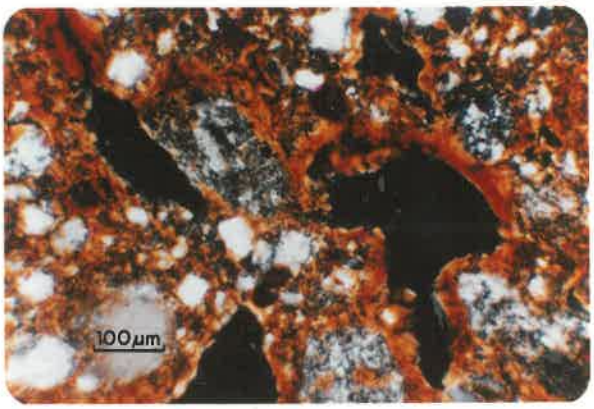

Figure 80.3 Profile G4,60cm. Void ferri-argillans.

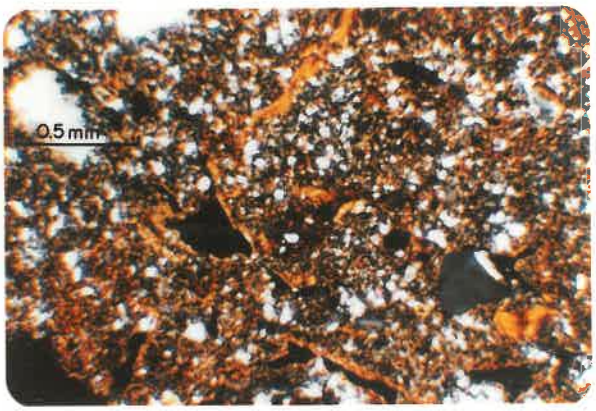

Figure 80.4 Profile G4,80cm. Mavosepic fabric.

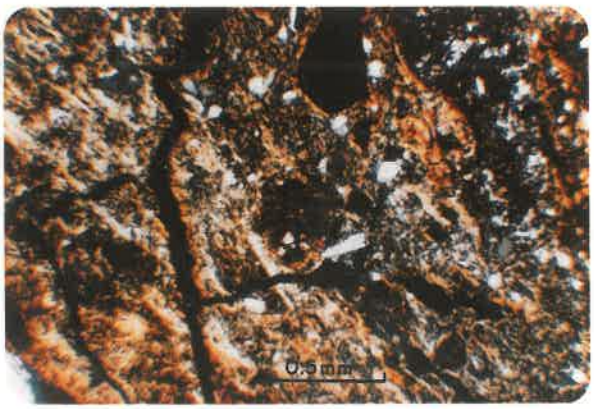

Figure 80.5 Profile G5,64cm. Strong vomasepic fabric

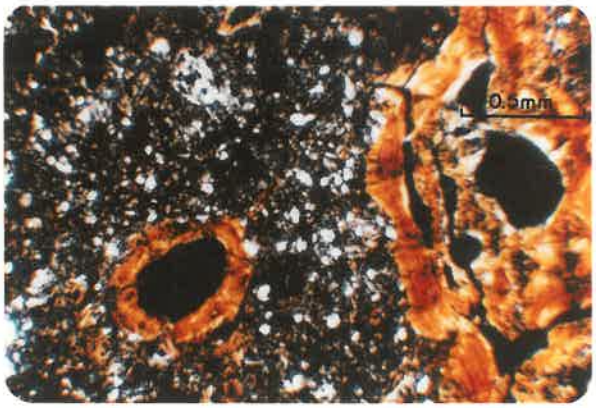

Figure 80.6 Profile G5,73cm. Silasepic fabric with fine laminated void argillans.

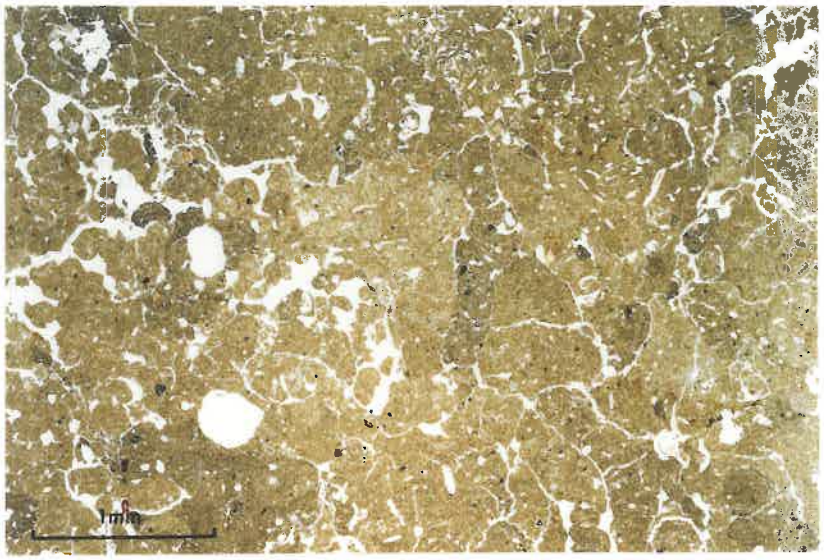

Figure 81.1 Profile G3,7cm. Isotubules.

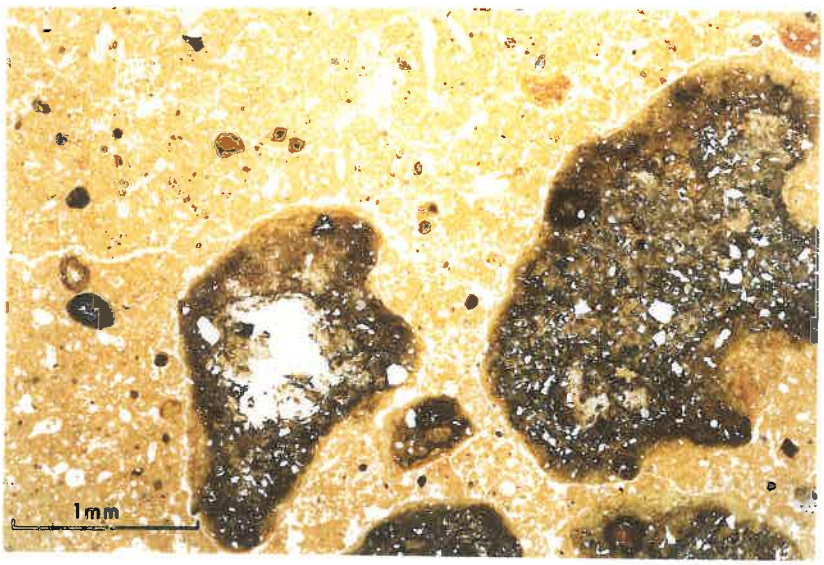

Figure 81.2. Profile G5,44cm. Discrete sesquioxide glaebule with undifferentiated fabric and thin ferri-argillaceous halo.

visible although there has been disruption due to bioturbation as evidenced by the mammillated orthovughs. The fine-grained gravel at the base appears to be breaking into much finer fragments (Figure 79.2). The initial fracturing probably took place during transport.

Profiles G2 (not described here) and G3 are very similar and have much higher levels of organic matter than the younger G1 profile. Numerous fecal pellets, mammillated vughs and various pedotubules (Figure 81.1) indicate considerable churning throughout, but especially in the top 70 cm. The original sedimentary fabric has been obliterated. There is much evidence of iron movement in the form of rock fragments, usually fine grained siltstones, appearing dark red and losing individual grain identity and irregular sesquioxidic concentrations in the basic fabric with diffuse boundaries (Figure 79.4). Some nodules have an iron-rich halo (Figure 79.6). Plasma separations are confined to void cutans and papules at the base of the profile (Figure 80.1). Papules are associated with former voids and, together with their angularity, appear to have originated as void argillans rather than as a product of grain weathering or as inherited features.

In G4 there is a clear boundary at 35 cm separating a surface horizon with low plasma (argillasepic) from a clay-rich subsoil but there is no evidence that this is a sedimentological feature. The mineralogy and conformation of the skeleton grains throughout are similar and there are no obvious sedimentary structures. Reduction in rock fragments by in situ breakdown and clay illuviation appear to be the dominant processes (Figure 80.3).

The textural break between A and B horizons is sharper in G5 than G4. The dominant processes appear to be segregation of iron and manganese oxides and clay illuviation. Argillans increase in

proportion below 70 cm (Figure 80.6). The marked increase in birefringence of plasma in the 60-70 cm zone, the increase in proportion of irregular orthojoint planes and strong planes and strong masepic fabric are indicative of strong shrink/swell forces (Figure 80.5). Papules below 55 cm represent disrupted void argillans. The undifferentiated fabric of the sesquioxidic nodules and the argillaceous halo (Figure 81.2) indicate that they are forming at present and are not inherited features.

6.5 Micromorphology of Shinglehouse Creek sequence

6.5.1 Description

S1 - Trawalla Unit

4-10 Two fabric types (Figure 82.1) separated into three distinct zones of equal thickness. I Argillasepic porphyroskelic. Irregular mammillated orthovughs (C). Skeleton grains of quartz, ironstone, siltstone (highly weathered). Organic fragments (O). II Much more open fabric, granular to intertextic fabric. Orthovughs. Compound and simple packing voids (F). Pedorelicts in form of highly birefringent plasma with sharp boundaries (O). Papules (O) (Figure 82.3). III Similar to I.

10-16 Distinct banding of skeleton grains (Figure 82.4). Granular to inter- textic fabric. Irregular orthovughs (C) and channels (R). Numerous papules and pedorelicts with highly birefringent lattisepic fabric.

34-40 Banded fabric of quartz and feldspar grains with monic fabric (Figure 82.2). Bands have relatively uniform grain size and range from 50-100 um to 15-20 um. Granular bands are intercalated with argillasepic porphyroskelic fabric. Pedorelicts (O), vughs as above.

40-45 Intercalation of a variety of granular and argillasepic porphyroskelic fabrics each of which has a relatively uniform skeleton grain size. Similar to above in mineralogy. Papules (O), of two types: some with continuous yellow birefringence, irregular shape, gradual to diffuse boundaries; others with lamellar fabric, sharp boundaries. Vugh argillans (O).

S2 - Shinglehouse Unit

0-7 Dark, organic rich, argillasepic porphyroskelic fabric. Organic fragments (F). Fecal pellets (F). Numerous iso-aggrotubules (F). Porous, mammillated metavughs (C); elongate irregular channels. Lithorelicts, subangular to subrounded siltstones, most with sesquioxidic coating (C).

16-22 Similar to above but discrete patches of granular and intertextic fabric with coarse mineral grains (mainly quartz).

24-31 As above. Aggrotubules have variety of conformations and sharpness of external boundary viz. diffuse, gradual, clear. Papules (R). Sesquioxidic nodules (C) of two types; dense isotropic; undifferentiated with void ferriargillans.

32-39 Denser fabric, vughs smaller, occasionally mammillated (Figure 82.5). Some vesicles, often with reddish sesquioxidic halo. Basic fabric similar to 24-31. With depth: lighter fabric, less organic fragments, more aggrotubules with diffuse boundaries.

39-45 As above. Remnants of fine grained sedimentary bands (Figure 82.6). Papules (O). With depth: vugh cutans.

45-52 As above. Isotropic sesquioxidic nodules often have argillaceous and ferruginous halos and vugh ferriargillans (O) (Figure 82.7).

61-67 Denser fabric; voinsepic porphyroskelic.

67-72 Less organic matter than above. Vughs (C) and vertical channels (O). Vugh and channel argillans (O) (Figure 82.8). Clusters of papules in weakly developed argillaceous glaebules, diffuse boundaries (C). With depth: texturally and structurally more homogeneous fabric.

79-85 As above but thicker and more continuous channel argillans (plane neostrians) (Figure 83.1).

S3 - Doongalla Unit

0-7 Argillasepic porphyroskelic fabric. Organic fragments (C).
8-14 Irregular orthovughs (C), up to 5 cm x 1 cm, occasionally interconnecting. Fine grained lithorelicts (Figure 83.2) (O).

17-23 Abrupt change to reddish yellow denser fabric; mavoinsepic. Masepic element in discrete patches and as single striations. Vugh and channel argillans. Papules (O). Vesicles and oblate vughs, occasionally interconnected.

23-29 Similar to above but stronger mavoinsepic element. Sharp boundaries between sepic fabric elements and argillasepic fabric which is almost granic. Fine, elongate joint planes, some with plane neostrians, others coated with fine sand-size quartz and feldspar grains of granular fabric, similar to 0-7 cm. With depth: decrease in void cutans.

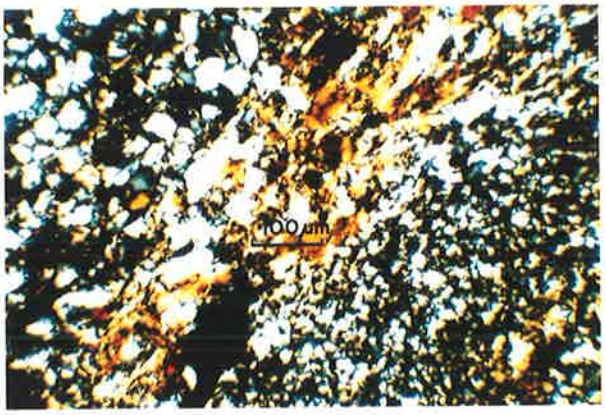

Figure 82.1 Profile S1,4cm. Sedimentary laminae.

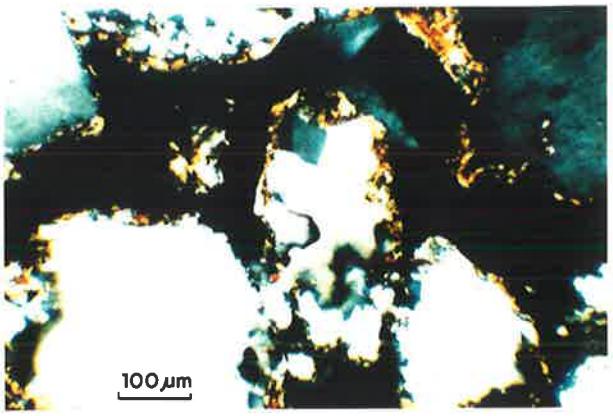

Figure 82.2 Profile S1,34cm. Clay coatings around skeleton grains.

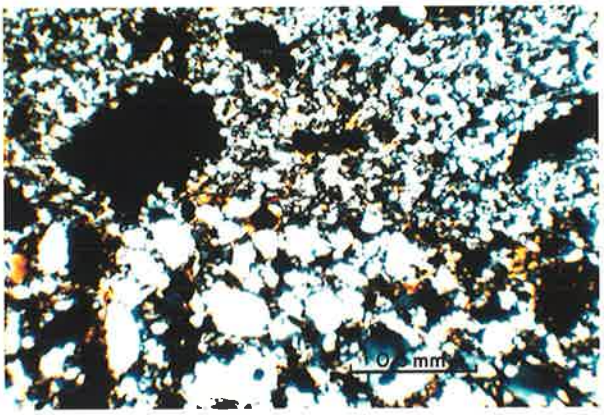

Figure 82.4 Profile S1,40cm. Granular fabric showing inherited papules.

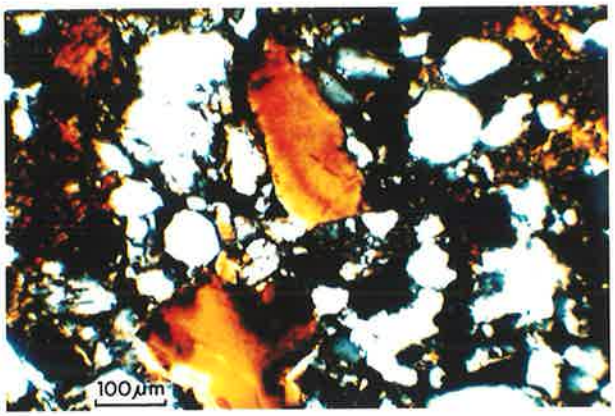

Figure 82.3 Profile S1,40cm. Granular fabric with sedimentary banding.

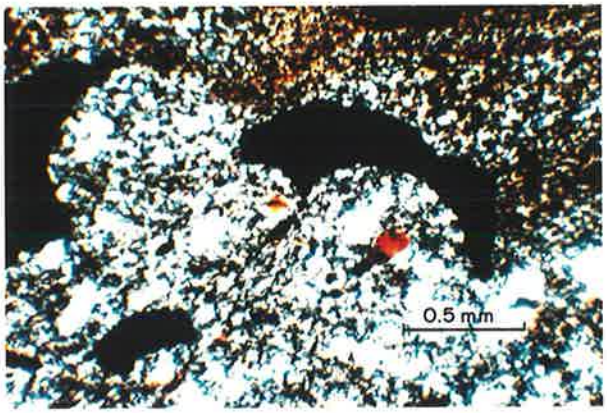

Figure 82.5 Profile S2,39cm. Argillaceous porphyroskelic fabric with mammillated orthovughs.

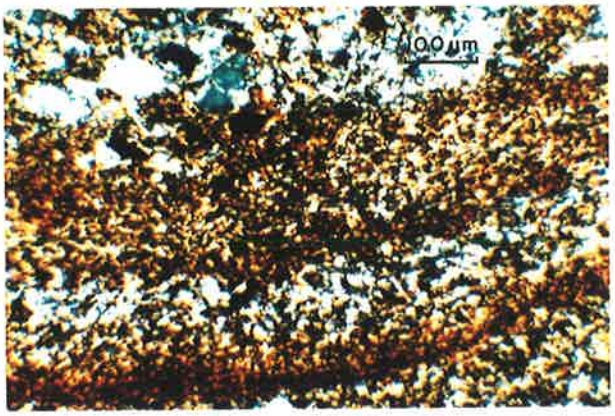

Figure 82.6 Profile S2,39cm. Argillaceous porphyroskelic fabric with fine sedimentary laminae.

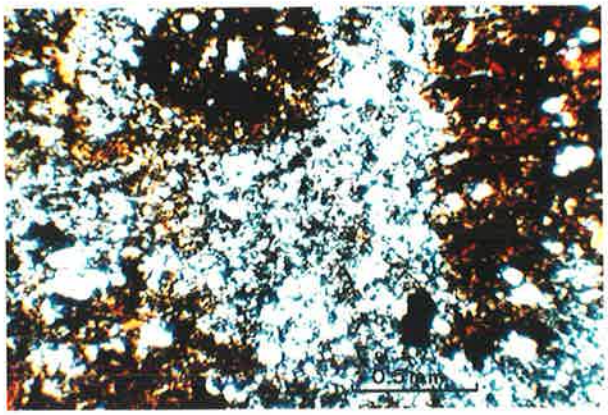

Figure 82.7 Profile S2,54cm. Argillaceous porphyroskelic fabric with irregular sesquioxide nodules.

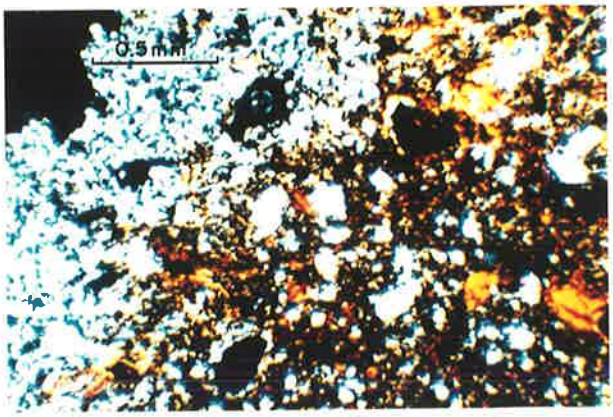

Figure 82.8 Profile S2,61cm. Argillaceous porphyroskelic fabric with granular patches and void cutans.

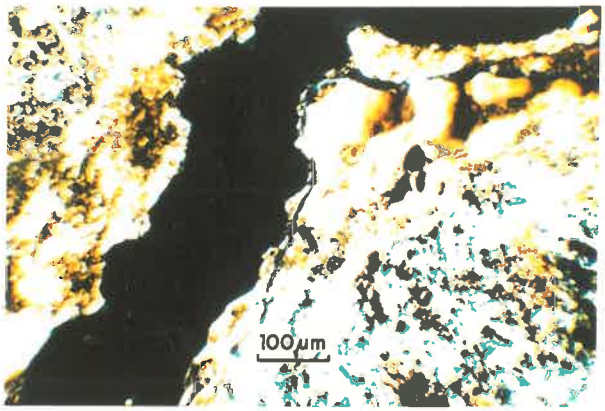

Figure 83.1 Profile S2,79cm. Void argillans.

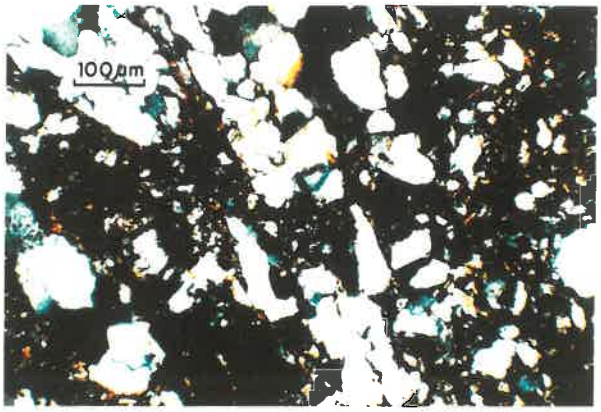

Figure 83.2 Profile S3,0cm. Breakup of rock fragment.

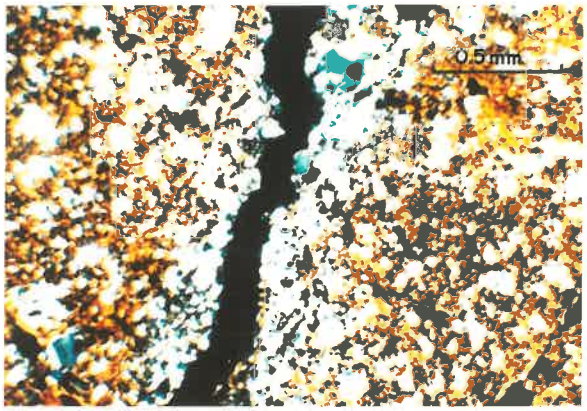

Figure 83.3 Profile S3,23cm. Masepic fabric, with granic fabric along channel.

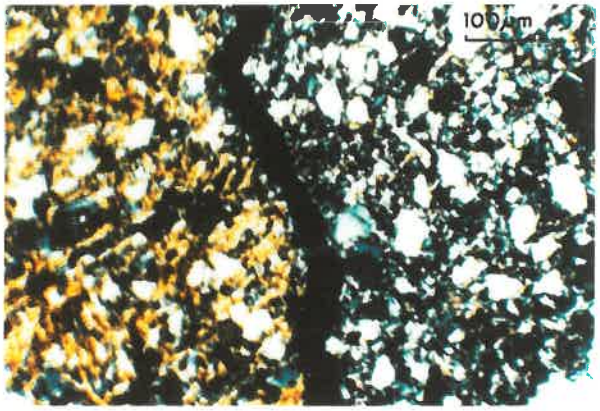

Figure 83.4 Profile S3,23cm. Distinct sepic and granic fabrics.

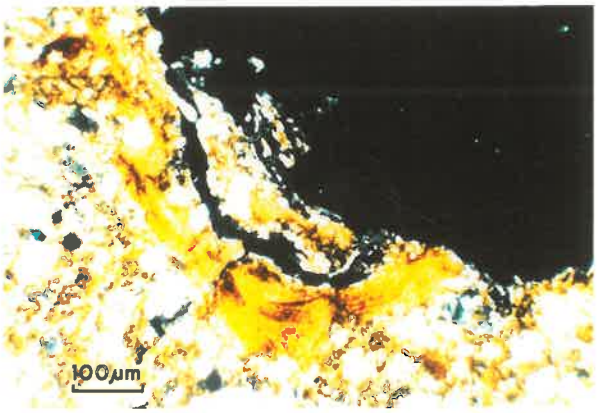

Figure 83.5 Profile S3,32cm. Papule (embedded void argillan).

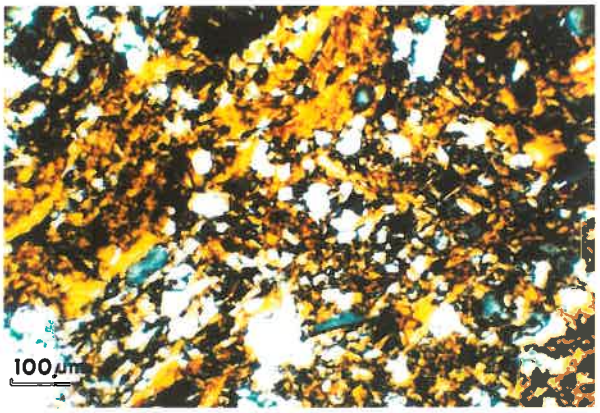

Figure 83.6 Profile S3,32cm. Lattisepic fabric.

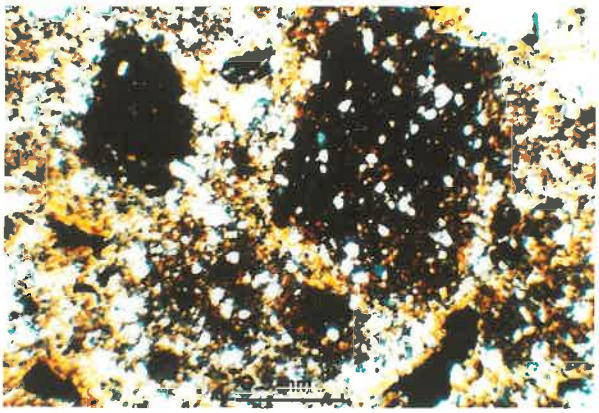

Figure 83.7 Profile S3,63cm. Undifferentiated sesquioxide glaebule.

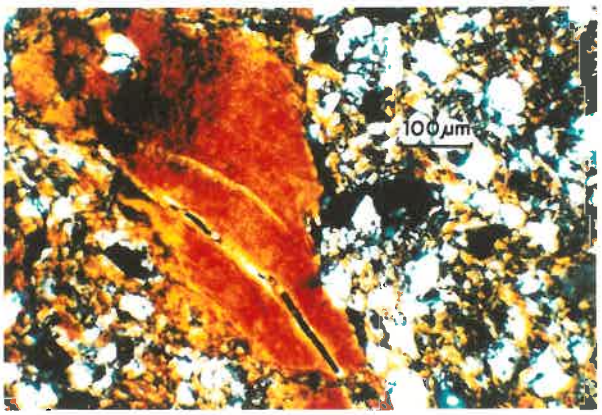

Figure 83.8 Profile S3,74cm. Ferri-argillaceous papule.

32-38 Fabric with high birefringence; masepic with subdominant lattisepic element (Figure 83.6); lower proportion of granular fabric. Ortho and metavughs (C), Joint planes (C), Vesicles (O), Void cutans (O), Papules (C).

54-61 As above but higher proportion of granular fabric as in 23-29 cm, less channels than above and fewer associated plasma separations; thicker void cutans but proportionately less than above.

63-70 As above except some sesquioxidic glaebules with undifferentiated fabric (Figure 83.7), clear to gradual boundaries (O). Fractured lithorelicts of sand-sized quartz and siltstone (O). Void ferriargillans (O).

74-80 Similar to above but lattisepic fabric now dominant; masepic element minor less sesquioxidic glaebules. More, and thicker papules and cutans. Patches of highly vesicular fabric. Channels (O).

6.5.2 Discussion

S1 is clearly a recent alluvial deposit. Sedimentary banding is clearly visible throughout (Figure 82.1) and, although there has been some disruption by faunal activity, there are discrete patches of fine and coarse grained fabric clearly visible (Figure 82.3). Accelerated erosion has taken place in the catchment since man first settled. Evidence of this is visible in the surface layers in the form of highly birefringent pedorelicts, the morphology of which bears a strong resemblance to the masepic fabric of the B horizon of S3. Papules are inherited features, not formed in situ (Figure 82.3).

S2 has a relatively uniform fabric throughout. It is rich in organic matter although this decreases progressively with depth. There is evidence of considerable biological activity in the form of casts pellets and isotubules. This faunal bioturbation is probably the cause of the relatively homogeneous fabric (Figure 82.5). At depth (1 metre) the tubules have been partially incorporated into the matrix and generally have only diffuse boundaries. Clay illuviation is minimal, there being a weak

voinsepic fabric from 61 cm and occasional vugh argillans from 25 cm. Although the dense, isotropic iron nodules are probably inherited, there has been in situ movement of iron as evidenced by diffuse sesquioxidic glaebules (Figure 82.7) and occasional ferriargillans.

The main soil forming process in S3 is clay illuviation. This is more obvious at the base of the profile where there are thick void argillans and clusters of papules. The papules are embedded void argillans (Figure 83.5). Nevertheless, only a small proportion of the total clay is in the form of cutans; most is present as oriented plasma. The presence of joint planes and masepic fabric in the B horizon (Figure 83.3) is evidence of considerable shrinking and swelling. These joint planes are often surrounded by granular asepic fabric 10-50 cm thick resembling material from the A horizon (Figure 83.4). Iron movement has taken place (Figure 83.8).

6.6 Micromorphology of Nowra sequence

6.6.1 Description

N1 - Tapitallee unit

0-5 Argillasepic porphyroskelic fabric with granular and intertextic patches (Figure 84.1). Numerous rock fragments up to 6cm, mostly fine grained iron-rich siltstones and quartz conglomerates with isotropic sesquioxidic matrix (Figure 84.5. Orthovughs (C), Organic fragments (C).

5-10 Basic fabric as above. Some pedorelicts with highly birefringent plasma.

15-21 More plasma, insepic fabric. Thin, discontinuous argillans (O). Increase in size of gravel; mineralogy as in 0-5cm. Irregular orthovughs, often interlinked to give porous fabric.

30-36 Discrete patches of open granular fabric, occasionally banded (Figure 84.2); simple packing voids (C); sand size grains of uniform size. Abrupt boundary to denser fabric with weak skelvosepic fabric. Sesquioxide nodules with isotropic core and diffuse, undifferentiated outer boundary. Gravel size iron stained lithorelicts (F).

41-47 As above

47-53 As above

57-63 As above

N2 - Minnamurra Unit

0-5 Dark, organic rich; argillasepic porphyroskelic fabric. Organic fragments (C). Mammillated orthovughs (C) (Figure 84.6). Numerous isoaggrotubules (F), clear to diffuse boundaries. Vughs (F). Vesicles (C). Porous; approximately 40% fabric is void space.

11-17 As above but with bright red iron staining around small voids (C).

27-33 Basic fabric as above but with some large, lithorelicts with
34-41 iron stained fractures (C) (Figures 84.7, 84.8). Denser fabric than surface. Numerous irregular branching channels.

42-48 As for 34-41 cm but very thin, discontinuous void argillans (Figure 85.1), voinsepic fabric. Increase in proportion of angular gravel.

48-54 As above but lower percentage of gravel, and finer.

56-62 As above but less organic matter; more discrete sesquioxidic
62-68 - organic glaebules with diffuse, irregular boundaries; stronger voinsepic fabric.

N3 - Nowra unit

0-6 Dark, highly organic - rich argillasepic porphyroskelic fabric. Large interconnected metavughs (O). Vesicles (O) Spherical, sesquioxidic nodules (Figure 85.2). Pedotubules (C). Organic fragments (C). Fecal pellets (C).

15-21 As above but less void space, occasional papules.

30-36 Abrupt change to highly birefringent fabric; skelvosepic, minor insepic. Papules, often clustered (C). Numerous sesquioxidic nodules as above. Channel ferriargillans (O) (Figure 85.3).

45-51 As above but skelvosepic fabric not as strongly expressed. Less papules. Less small sesquioxidic nodules. More sesquioxidic glaebules with diffuse boundaries, often associated with voids. Striotubules common.

N4 - Wandandian Unit

0-5 Granular and intertextic fabrics. Packing voids (F). Irregular metavughs (C). Numerous sub-rounded isotropic sesquioxide nodules. Organic fragments (C).

15-21 Top as above. At 18 cm, abrupt change to plasma-rich fabric; skelvomasepic (Figure 85.4). Joint plane argillans. Clusters of ferriargillaceous papules (C) (Figure 85.5). Some major channels with asepic, granular fabric similar to 0.5 cm. Ironstone nodules. With depth: stronger masepic fabric.

28-34 As above but undifferentiated ferri- argillaceous glaebules
42-48 (C), clear to diffuse boundaries, masepic fabric elements often transgress (Figure 85.6). Argillans, up to 100 um (Figure 85.7).

58-64 As above but papule clusters more frequent.

72-78 As above but increase in ferriargillaceous nodules, less ironstone nodules.

85-91 Skelvomasepic fabric but masepic element not as strongly
122-128 expressed and patches of insepic. With depth: decrease in masepic element (Figure 85.8), thicker papules and argillans.

6.6.2 Discussion

N1 is an immature profile showing little evidence of profile development apart from some slight clay movement to form weak discontinuous argillans at 30-36 cm and some iron movement to form thin coatings around voids in the matrix(Figures 84.3 and 84.4). The clay and iron may have originated by lateral movement from upslope. The profile is colluvial because of the juxtaposition of different fabric types with distinct boundaries. There is little evidence of bioturbation.

The main soil-forming process in N2 has been bioturbation which has produced a relatively homogeneous texture and structure throughout the profile. Clay illuviation has been minimal. There is some segregation of sesquioxides as mottling (irregular nodules) in the lower horizons.

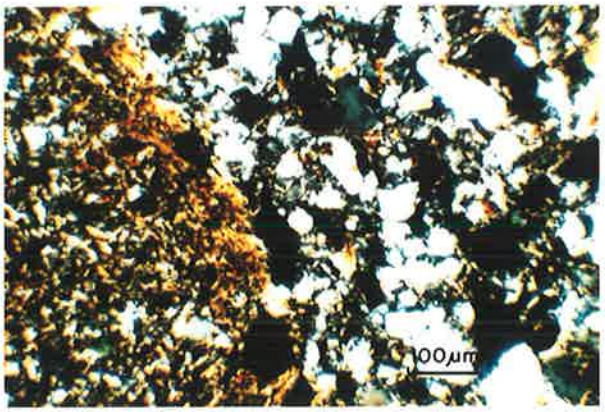

Figure 84.1 Profile N1. Distinct granular and argillasepic fabrics.

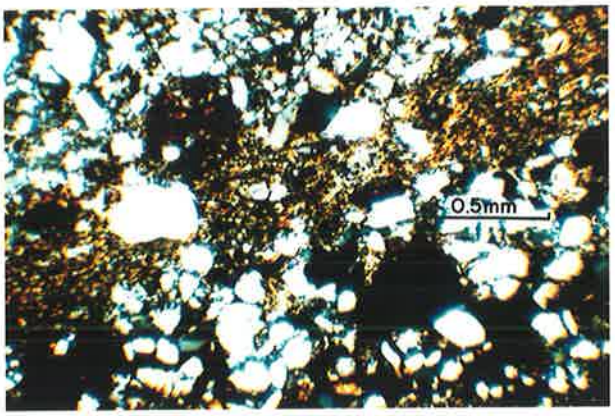

Figure 84.2 Profile N1. Sedimentary banding.

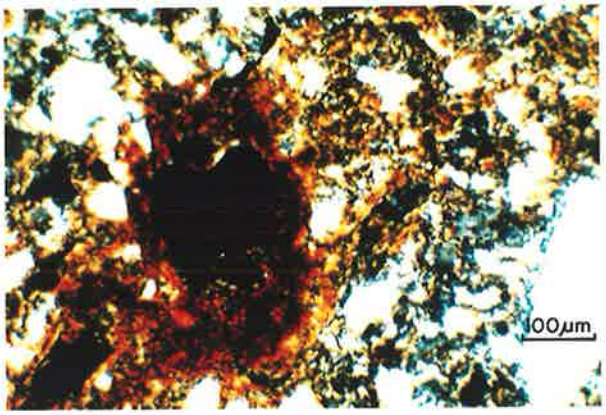

Figure 84.3 Profile N1. Sesquioxide concentration around void(sesqan).

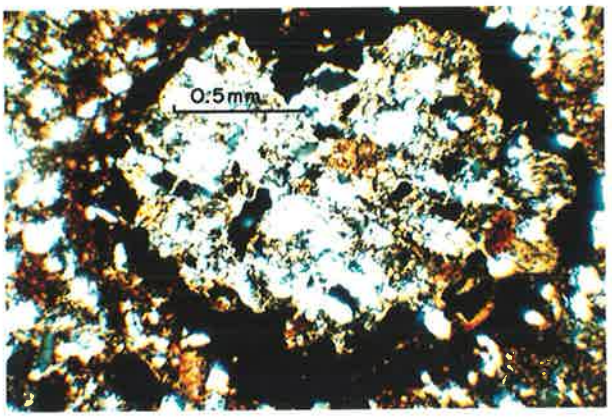

Figure 84.4 Profile N1. Argillasepic porphyroskelic fabric with sesquioxide concentration enclosing part of matrix.

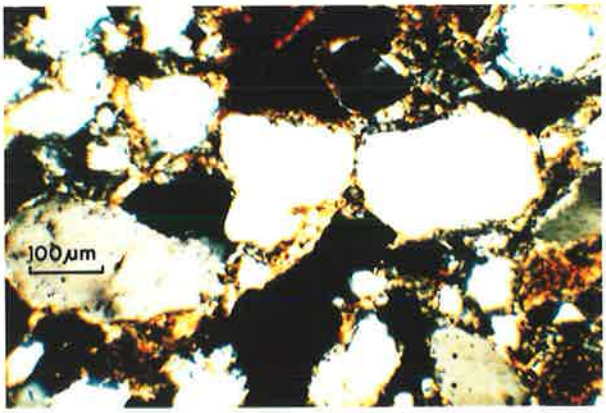

Figure 84.5 Profile N1. Chitonic fabric.

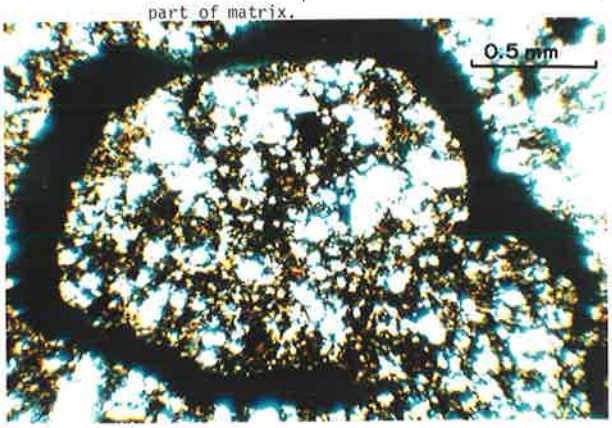

Figure 84.6 Profile N2,11cm. Mammillated vugh.

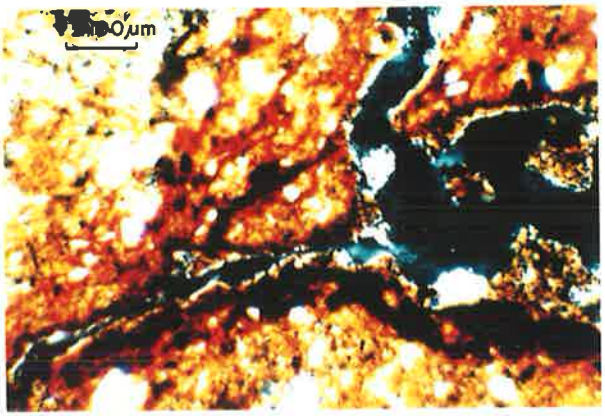

Figure 84./ Profile N2, 27cm. Fractured fine grained rock fragment(siltstone) with sesquioxide concentrations along fractures.

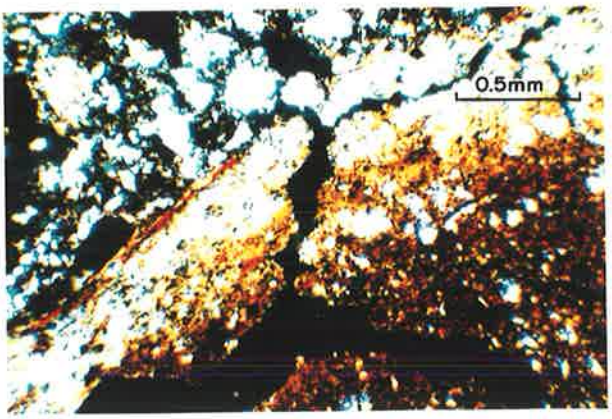

Figure 84.8 Profile N2,42cm. Fractured rock fragment.

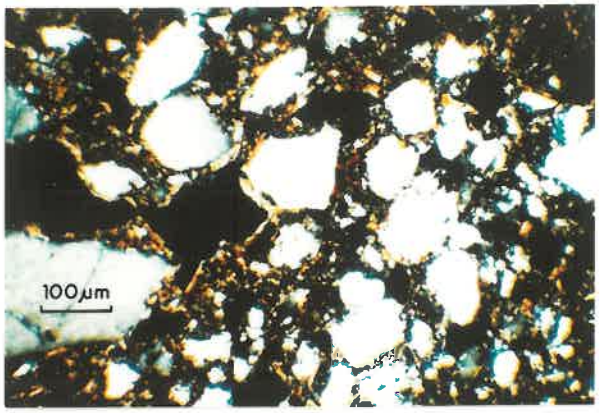

Figure 85.1 Profile N2,48cm. Argillasepic porphyroskelic fabric with intertextic patches.

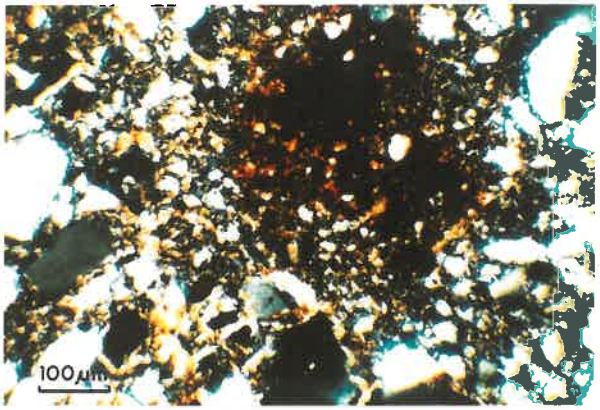

Figure 85.2 Profile N3,15cm. Undifferentiated sesquioxide nodule.

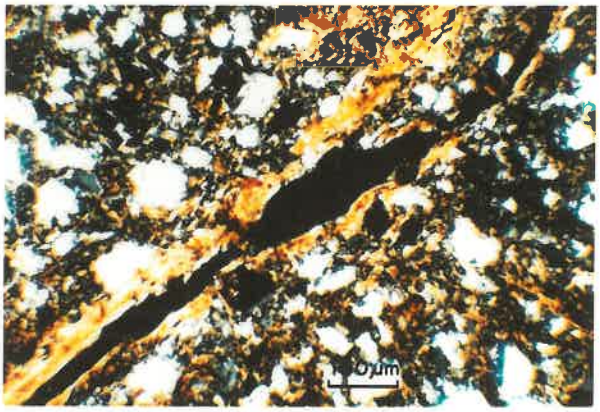

Figure 85.3 Profile N3,30cm. Mavosepic fabric.

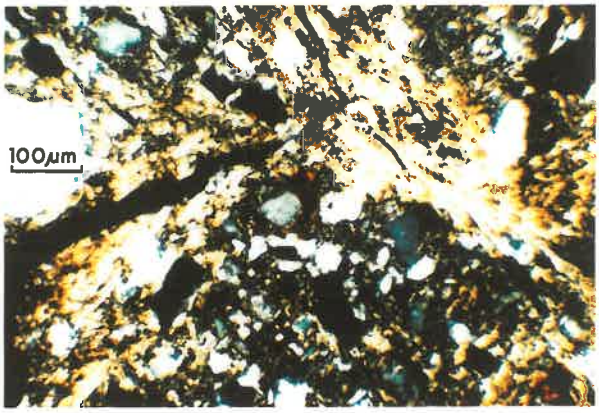

Figure 85.4 Profile N2,15cm. Skelvomasepic fabric.

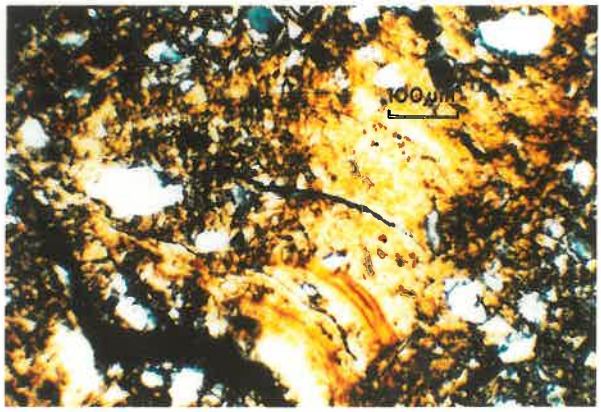

Figure 85.5 Profile N4,15cm. Thick papule with iron banding.

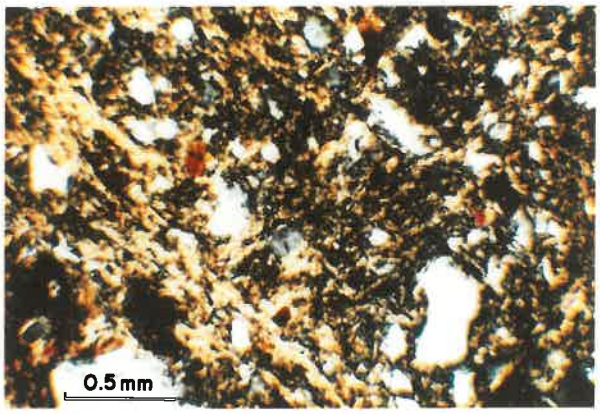

Figure 85.6 Profile N4,28cm. Masepic fabric.

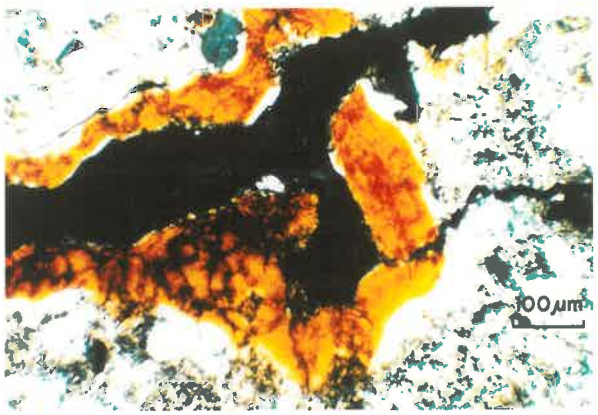

Figure 85.7 Profile N4,58cm. Void argillan

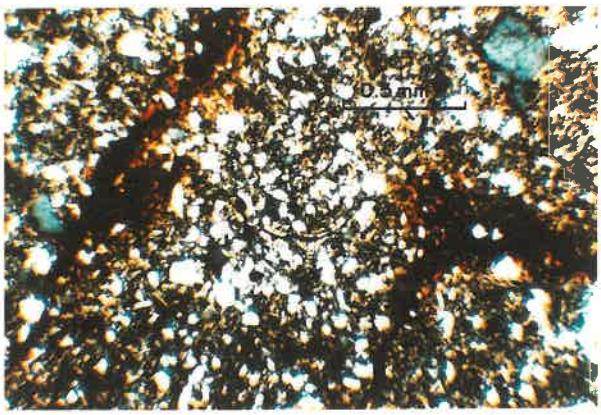

Figure 85.8 Profile N4,122cm. Skelvosepic fabric with sesquans.

N3 and N4 are texture contrast profiles. In both, the dominant process appears to be clay illuviation because of the numerous void argillans throughout the profile (Figures 85.3, 85.7). Papules are also common and are interpreted to be embedded void cutans rather than the product of weathering of mineral grains (Figure 85.5). Shrinking and swelling has modified the texture in the upper B horizon, more strongly so in N4 than N3. This is indicated by joint planes with linings of A horizon material. Lower in the profile, the masepic element is not as strong but the papules and void argillans are thicker. Possibly shrink-swell forces have not disrupted and incorporated them into the matrix.

6.7 Micromorphology of Hawkesbury sequence

6.7.1 Description

H1 - Lowlands unit

22-26 Granular fabric (Figures 86.1, 86.2), patches of porphyroskelic argillasepic. Skeleton grains, subangular. Organic fragments (C). Packing voids (F).

44-48 As above but darker, more organic fragments, less porous. Diffuse pedotubules (O). Rare ferriargillans.

64-70 As above
92-98
110-116

H2 - Unnamed

16-32 Inhomogeneous fabric; argillasepic porphyroskelic with granular patches. Isotubules (O). Occasional void ferriargillans. Organic fragments (O). Disturbed by ploughing.

33-39 Weak voinsepic fabric; birefringence of plasma low. Ferriargillans, strong continuous orientation, up to 50 um thick (Figure 86.3). Vesicles and irregular orthovughs (F). Organic fragments (O).

53-62 As above but with occasional thick ferriargillanceous papules, up to 50 um.

72-29 As above. Patches of two mineralogically distinct cutans as judged by colour; ferriargillans (red, O) and argillans (yellow, O).

86-92 As above but less organic matter, lighter in colour and
105-111 greater proportion of coarser skeleton grains (mainly quartz) > 50 um. With depth: increasing coarse grains > 250 um.

120-126 Similar to above but thin grain cutans; skelvoinsepic
132-138 fabric (Figure 86.4). Proportion of cutans same as above.

H3 - Late Clarendon - Cranebrook unit

0-6 Argillasepic porphyroskelic fabric (Figure 86.5), granular patches. Porous with irregular metavughs (F) and simple packing voids (C). Skeleton grains, angular, > 200 um (C). Organic fragments (C). Aggrotubules (C).

21-27 As for 0.6 cm but with isolated clusters of ferriargillans (O), up to 100 um thick. With depth: proportion of plasma increases.

35-41 Higher proportion of plasma (Figure 86.6); weak skelvoinsepic fabric. Ferriargillans (C) (Figure 86.7). Metavughs (C). Packing voids (C).

51-57 Skelvosepic fabric, weak masepic (O); patches in fabric which are almost asepic and have sharp boundaries with birefringent fabric. Granotubules (O). Sesquioxide concretions (O) with diffuse to prominent boundaries.

73-79 As above but greater number of glaebules; internal fabric of which is undifferentiated (i.e. B horizon - like) or differentiated (A horizon - like); outer rim can be isotropic (F) or ferriargillaceous. Granotubules (O).

95-101 As above
125-131

H4 - Early Clarendon - Cranebrook Unit

4-10 *Granular with simple and compound packing voids (F) and irregular channels (O). Isotropic ironstone nodules (F).*

18-24 *Abrupt change to highly birefringent plasma; skelvomasepic; discrete granular linings in coarse channels (Figure 86.8). Undifferentiated sesquioxide glaebules, irregular sharp, diffuse boundaries (F). Isotropic ironstone nodules (O). Aggro and striotubules (O). Metavughs (C) and channels (O). Papules (C). Void argillans (O).*

30-36 *As above*
53-54

73-79 *As above but skelvomasepic not as strongly expressed.*
84-100 *Papule clusters up to 1 cm (Figure 87.4).*

106-112 *Less plasma, skelvosepic. More open fabric with metavughs (C), packing voids (C) but absence of channels. Sesquioxide glaebules (O). Void argillans (F), up to 1 cm (Figures 87.1,87.2). Papules (F) (Figure 87.3).*

116-122 *As above but with joint planes (O) with associated masepic fabric element. With depth: decrease in masepic element.*

146-152 *As above*

H5 - Londonderry Unit

8-14 *Granular, with simple and compound packing voids (F) and interlinked metavughs (O). Subangular skeleton grains. Isotropic ironstone nodules (F).*

19-25 *As above but less porous*
36-40

42-48 *To 44 cm, as above. Below, sharp break to skelmavosepic fabric with void argillans having strong continuous orientation (F). Plasma in S-matrix is dark red, ferriargillaceous. Ironstone nodules (C) with sesquioxidic halos. Papules (F), up to 100 um (Figure 87.5). Irregular channels (O). Vughs (C).*

46-52 *Skelvomasepic (Figures 87.4, 87.8). Distinct blotchiness in fabric; dark red-brown patches with high sesquioxide content with voinsepic fabric transgressed by plane neostrians (F) (Figure 87.7) and very pale yellow "grainy" patches with mavosepic fabric. Channels (F) Vughs (C). Isotropic ironstone nodules (C). Sesquans (F) and argillans (F) (Figure 87.6).*

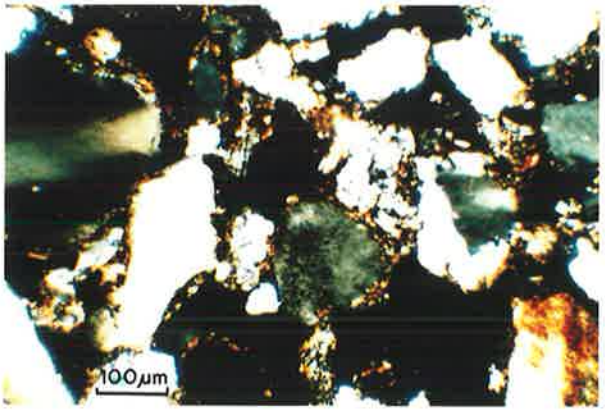

Figure 86.1 Profile H1,44cm. Granular fabric.

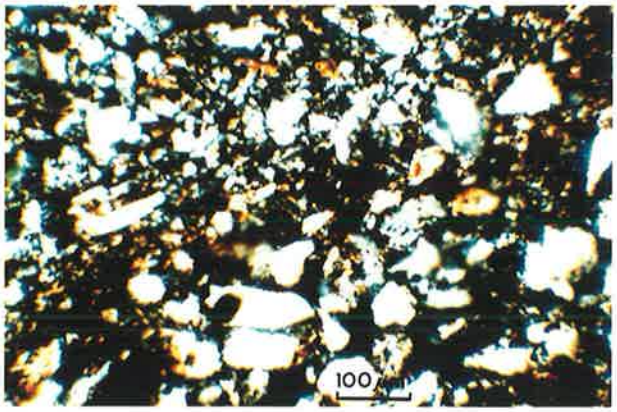

Figure 86.2 Profile H2,16cm. Sedimentary banding.

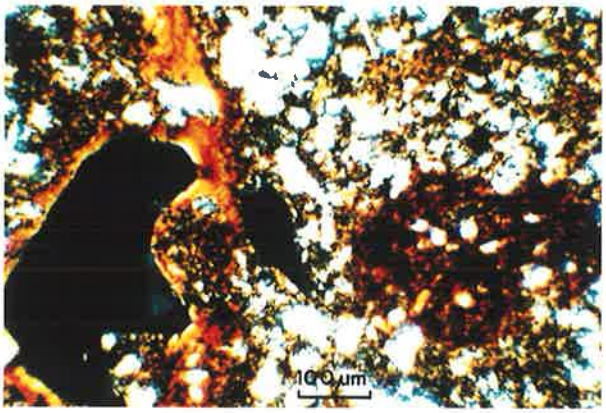

Figure 86.3 Profile H2,33cm. Void ferri-argillans and undifferentiated sesquioxide nodule.

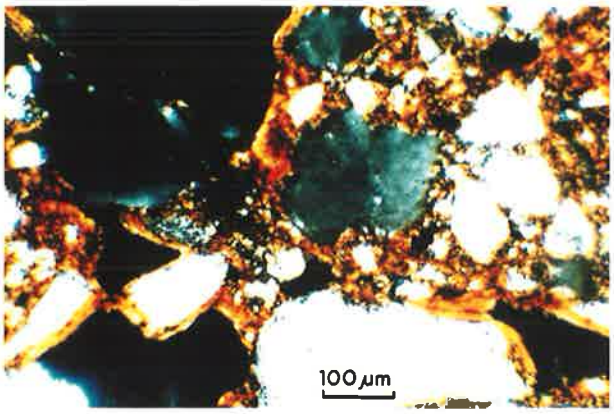

Figure 86.4 Profile H2,120cm. Voskelsepic fabric.

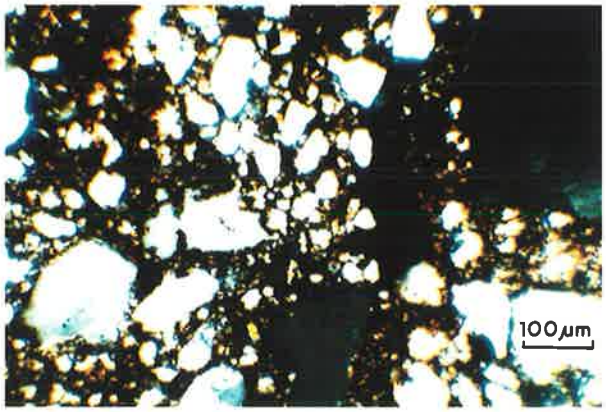

Figure 86.5 Profile H3,2cm. Argillasepic porphyroskelic fabric.

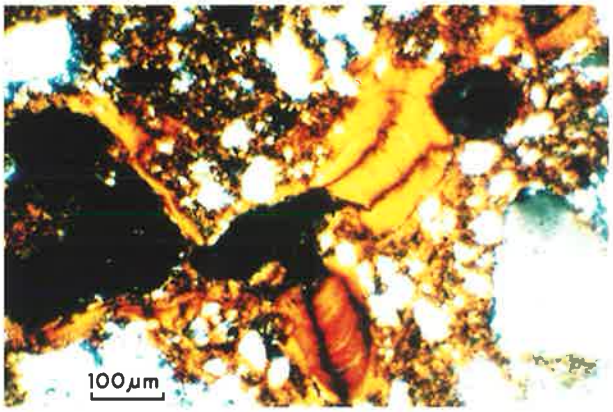

Figure 86.6 ProfileH3,51cm. Thick papules with strong continuous orientation.

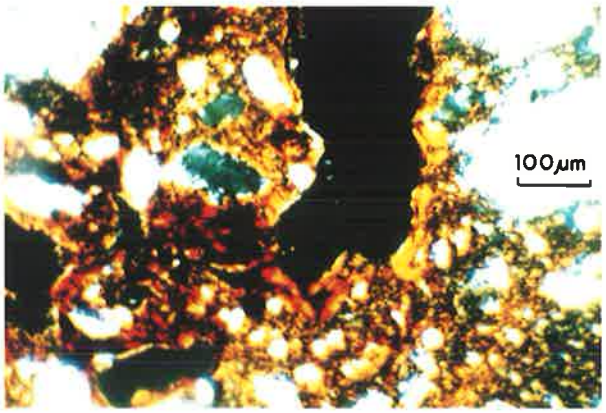

Figure 86.7 Profile H3, 43cm. Void ferri-argillans and diffuse,irregular sesquioxide glaebules.

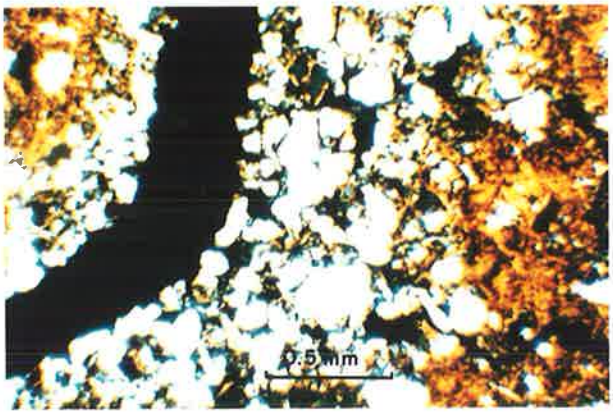

Figure 86.8 Profile H4,73cm. Granular fabric lining channel.

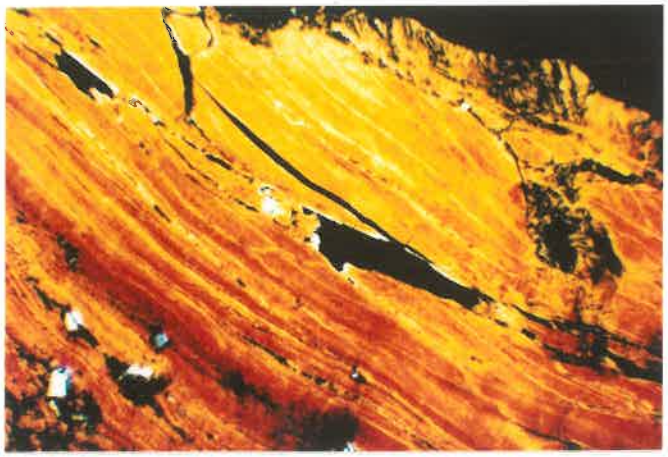

Figure 87.1 Profile H4,73cm. Thick finely laminated void ferri-argillan.

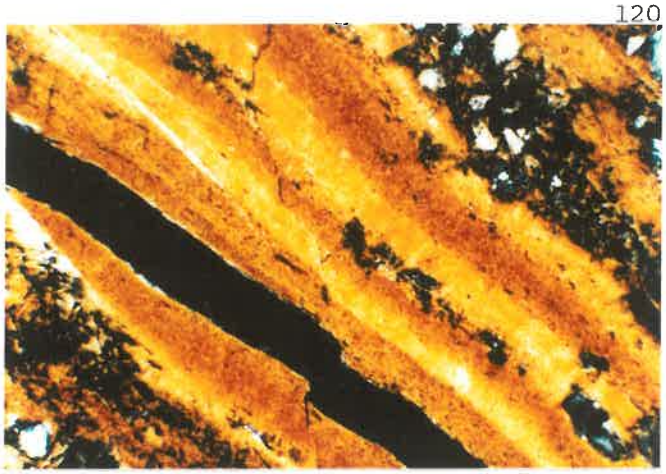

Figure 87.2 Profile H4,84cm. Coarsely laminated void ferri-argillan with silt-size particles.

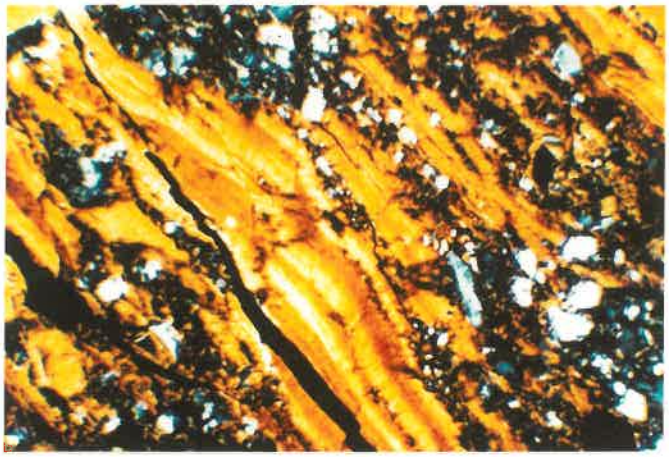

Figure 87.3 Profile H4,84cm. Void ferri-argillans and papules (embedded void ferri-argillans).

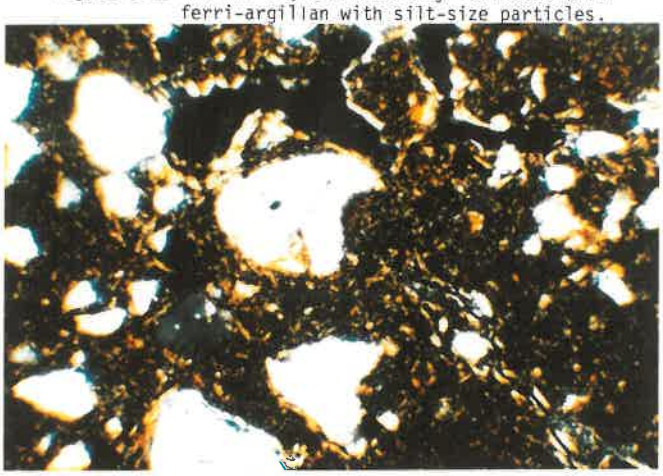

Figure 87.4 Profile H5,61cm. Mavosepic fabric.

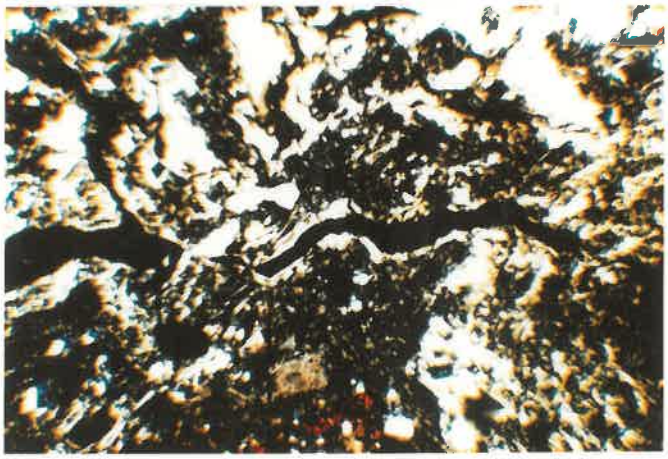

Figure87.5 Profile H5,61cm. Thick papules composed of kaolinite.

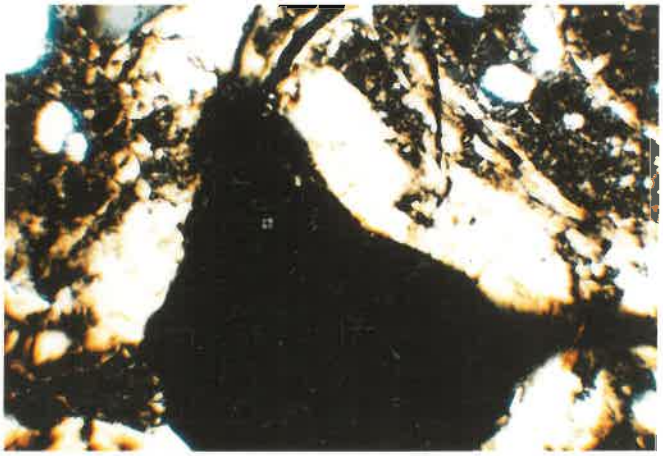

Figure 87.6 Profile H5,61cm. Void argillan with fine transverse fractures.

Figure 87.7 Profile H5,61cm. Fabric of sesquioxide nodule.

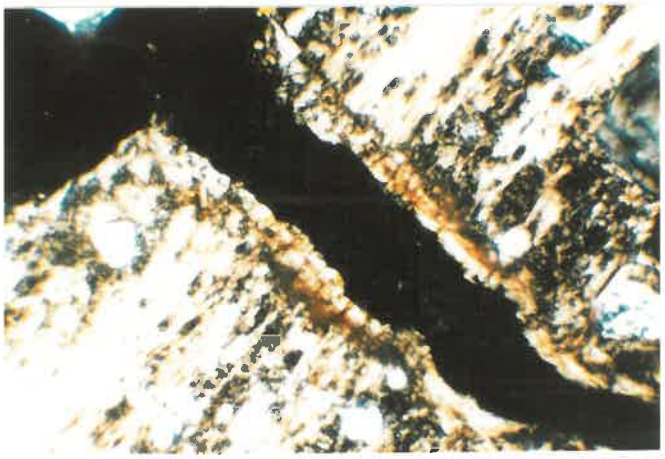

Figure 87.8 Profile H5,116cm. Strong masepic fabric.

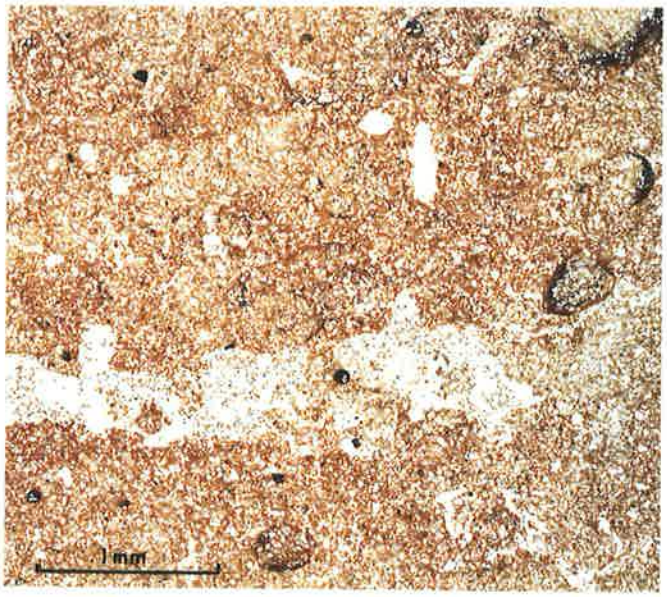

Figure 88.1 Profile H3,73cm. Sesquioxide glaebules with undifferentiated fabric.

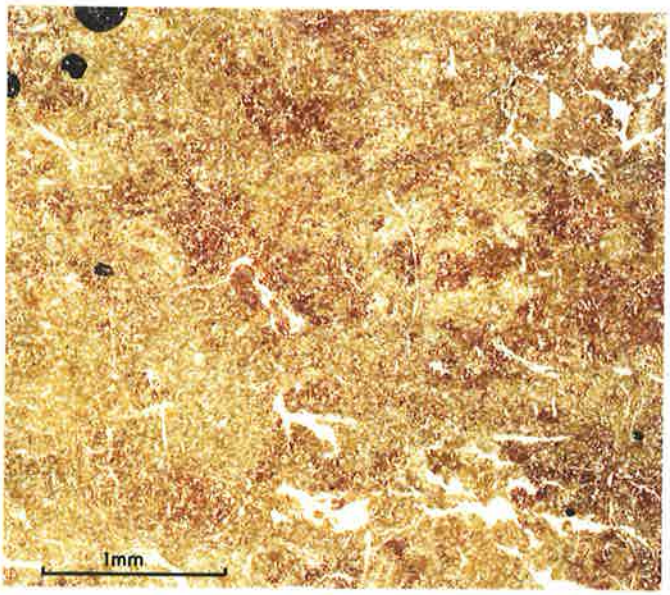

Figure 88.2 Profile H4,30cm. Diffuse irregular sesquioxide nodules,strongly adhesive.

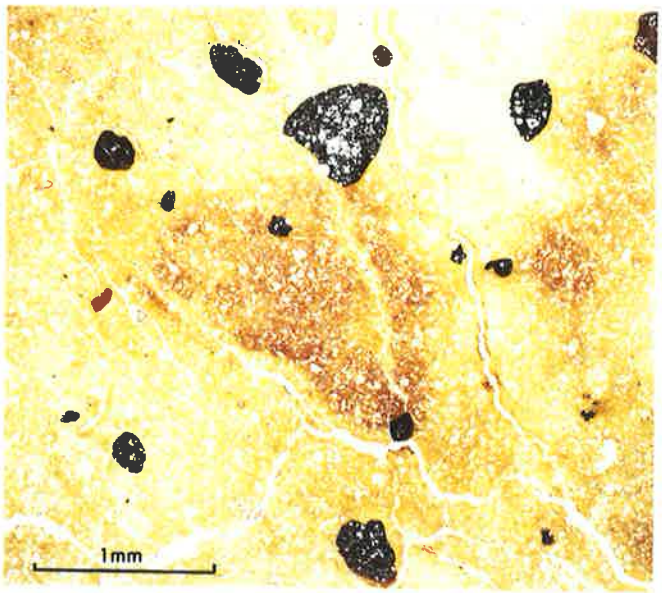

Figure 88.3 Profile H5,51cm. Two forms sesquioxide nodules 1.normal;equant,rounded,sharp external boundary 2.irregular;diffuse external boundary,strongly adhesive. Iron staining along channels.

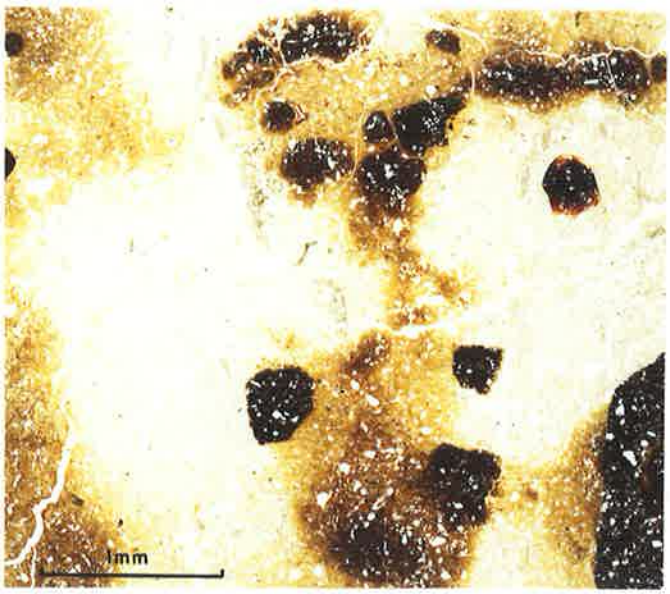

Figure 88.4 Profile H5,120cm. As for figure 88.3 except sesquioxide segregation more discrete.

61-67 As above but blotchiness more prominent and boundaries
76-82 between two become more distinct.
90-96
104-110
116-122

126-132 As above but with greater proportion of void and skel-cutans. Thick composite cutans of sesquans and argillans.

6.7.2 Discussion

H1 is a relatively uniform alluvial deposit. Layering of skeleton grains of different size but similar mineralogy is visible. There is considerable evidence for the alluvial origin of the parent material in H2 as expressed by the zones of skeleton grains of different size and banding within zones, especially in surface horizon (Figure 86.2). Pedogenesis has been minimal apart from some minor clay illuviation. Clay and sesquioxide movement have occurred in concert because many of the cutans are ferriargillaceous. There has been no deposition of clay around skeleton grains; it is found only in voids.

The gradual increase in plasma from 10 to 57 cm and the similarity of mineral and gravel assemblage throughout the whole profile of H3 suggest that soil development has taken place in a relatively uniform sedimentary deposit. The main processes have been clay illuviation and segregation of iron. There is evidence for considerable faunal activity throughout the profile in the form of aggro- and granotubles. This bioturbation may account for the different forms of sesquioxidic glaebules in the B horizon. Some are spherical, with an outer organo-sesquioxide rim with an internal fabric similar to the A horizon; others have B horizon - like internal fabric (Figure 88.1). The former may have been emplaced by soil animals or they may be older glaebules which formed prior to

segregation of plasma and development of B the horizon. The latter are more recent.

There is a strong texture contrast between A and B horizons of H4 but it is not possible to be sure that the two were formed in situ from one deposit or whether they had a different geological origin. Clay illuviation (Figure 87.2) and iron segregation (Figure 88.2) are the dominant processes but the former may not necessarily account for the textural B. Only a small proportion of the clay in the upper B can be attributed directly to clay concentrations (void and grain argillans); the dominant amount is present as clay separations; hence the strong masepic fabric. The maximum amount of cutans occurs at the base of the profile i.e. it does not coincide with the total clay maximum (Figures 87.1, 87.2).

There has been considerable shrinking and swelling, as indicated by the linings of A horizon - like material in joint planes (Figure 86.8). This extends throughout the profile. The presence of discrete ironstone nodules in the matrix of the lower B horizon may be accounted for by this process.

In H5 there is evidence for considerable chemical weathering in situ, clay translocation and segregation of sesquioxides (Figures 88.3, 88.4). Iron and manganese have weathered from the clays to form discrete bright red sesquioxide glaebules leaving patches of pale yellow, almost white, 'grainy' plasma (Figures 87.4). The plasma concentrations and highly convoluted and contorted indicating extreme pedoturbation.

6.8 General discussion

All four sequences show remarkably similar micromorphological trends as a function of time and four distinct stages of soil profile development are proposed.

In stage one sedimentary features are prominent in all the youngest profiles adjacent to the stream channel (G1, S1, N1, H1) and there is little pedogenesis, apart from some minor clay illuviation in N1 which may be lateral movement from upslope.

During the second stage there is considerable faunal pedoturbation (G2 and G3, S2, N2, H2). It is particularly obvious in the surface but has also occurred at depth (> 1 metre) because of the numerous isotubules. These structures exhibit various forms; the youngest having distinct external boundaries and appear dark compared with the rest of the matrix; the oldest ones are fragmented and have diffuse outlines. There is incipient iron movement.

In stage three (G4, N3, H3) clay illuviation and segregation of sesquioxides are the dominant processes. Significant bioturbution is confined to the A horizon. Because cutans and papules (embedded void argillans) are common throughout the profile, a relatively large amount of the plasma can be described to clay movement. However, as the clay builds up in the B horizon, (G4, S3, N4 and H4 are examples) the sepic fabric becomes more highly birefringent and ubiquitous, especially in the upper B horizon. A much smaller proportion of the clay is present in cutans and papules i.e. much less of the plasma can be confidently ascribed to clay illuvation. The maximum in illuviated clay shifts towards the lower B horizon and therefore there is a progressive displacement of the illuviated clay and total clay maxima with time. Total clay maxima occur in the B1 and B2, illuviated clay maxima in the B3.

Some workers have interpreted this phenomena as weathering in situ i.e. chemical breakdown of silt and sand. However, the skeleton grains show little evidence of weathering. It would be expected that, for such a large amount of clay to be formed in situ, that many grains would show weathering features such as diffuse edges and an increase in, and variable, birefringence. This was not observed.

An alternative hypothesis is that the clay buildup represents a further stage in the clay illuviation process. As more clay is deposited in the B, one would expect the potential for shrinking and swelling, in response to seasonal moisture fluctuations, to increase. This effect would be more pronounced at the top of the B and should be reflected in the microfabric of the soil. In all four sequences this appears to be the case. The B1/B2 horizons of G4, S3, N4 and H4 show thick and continuous plasma separations in the form of a strong vomasepic fabric. This fabric type is considered by many workers (Rode 1964, Nettleton *et al* 1969) as indicative of shrinking and swelling. The presence of granular, asepic A horizon material in the joint planes is further evidence that pedoturbation has been taking place.

Profile	Horizon	Cole	Profile	Horizon	Cole
G4	A11	0.007	N4	A1	0.006
	A22	0.004		A2	0.023
	B1	0.016		B1	0.048
	B2	0.015		B2	0.069
	C	0.023		C1	0.057
S3	A1	0.003	H4	A1	0.003
	A2	0.008		B21	0.045
	B2	0.019		B23	0.055
	B3	0.015		B3	0.027
	C1	0.024		C	0.025

Table 17. COLE values for various horizons of four terrace soils.

(Brasher et al 1966)

In Table 17 the $COLE_A$ is high in the upper B horizon of all four profiles. Thus the absence of void cutans, clusters of papules and grain cutans would be expected. As clay illuviation progresses, the shrink-swell potential increases, and further clay moving into the B horizon is rapidly incorporated into the fabric. Cutans do not form, or if they do, are quickly destroyed. Cutans are definite evidence that movement has occurred; however *absence* does not necessarily mean that illuviation has not taken place. The results presented here are consistent with the data of Holzey *et al.* (1974) who found that the degree of stress-oriented soil fabric is inversely related to the occurrence of illuviation argillans.

In stage 4, chemical weathering becomes the dominant soil forming process. This is particularly evident in profiles H4 and H5 of the Hawkesbury sequence where clays in the B horizon lose iron and aluminium to form glaebules rich in sesquioxides. The presence of highly contorted and convoluted sesquans and argillans indicates that localized clay movement and pedoturbation are continuing. Darkening on the ped faces at the top of the B indicates a second phase of clay illuviation (probably as a clay-organic complex) has begun.

It is hypothesized that the development of lateritic profiles does not necessarily need a change in climate to very warm, moist tropical or subtropical. The onset of mineral breakdown in stage four can be explained simply as a feedback response to intrinsic processes occurring within the profile. Buildup in clay in the B horizon, and loss from the A, creates an horizon of relatively low permeability which remains moist for much longer periods. Reducing conditions, conducive to chemical weathering, increase in intensity and duration.

The micromorphology of these sequences throws doubt on the separate sedimentary layering hypothesis as an explanation for the textural contrast between A and B horizon. While distinct sedimentary (alluvial or

colluvial) layers can be observed in the youngest profiles, these textural bands are destroyed in stage 2. The bioturbation in stage 2 homogenises the profile and subsequent pedogenesis (stages 3 and 4) takes place in a relatively uniform (texturally, structurally, mineralogically) parent material i.e. subsequent textural differentiation is not the result of inheritance but in situ soil forming processes.

6.9 Conclusions

The pedogenic history of the four chronosequences was similar. Following deposition of the parent material there was extensive, and intensive homogenisation by soil fauna producing a relatively uniform textural profile. Clay illuviation and iron segregation gradually became the dominant soil forming processes.

As the clay concentration increased, pedoturbation by seasonal shrinking and swelling, disrupted (or prevented the formation of) cutans and produced a pedal B horizon with prominant plasma separations. In the final stages, chemical weathering in situ became progressively more significant.

Chapter 7

Elemental Chemistry

7.1 Introduction

Elemental chemistry has been used extensively in pedogeneic studies to provide evidence for the provenance of the parent material, as an indicator of weathering and as a basis for calculating the losses and gains of mobile constituents.

Establishment of the uniformity of the parent material is a pre-requisite for any pedogenetic study in order to enable changes to be ascribed to soil forming processes and not to lithological discontinuities (Chapter 1). However, even in a deposit which was originally uniform texturally, variations in the resistant mineral assemblage, and hence its chemistry, are to be expected since some degree of sorting has been observed in most recent sedimentary deposits (Mitchell 1975). The significant point therefore, is that variations in the properties of the parent material should be minor compared to those produced during soil development (Brewer 1964).

In view of the difficulties in selecting a suitable resistant mineral (see Chapter 1 for discussion), it is surprising to note the number of studies which use only one. It would seem prudent to use, not only a number of different minerals, but also a number of size fractions. However, in most soils, resistant minerals are present in very low concentrations. Statistically sound deductions can only be made if these minerals can be isolated in sufficient quantity for identification and counting. An alternative is to use concentrations of elements specific for these minerals as a measure of the abundance. Zirconium and titanium, as indices of zircon and rutile, have been most widely used (e.g. Chapman and Horn 1968, Smith and Wilding 1972, Sudom and Arnaud 1971). Recently Murad (1978) has suggested yttrium, which occurs predominantly in xenotime.

Another which has been used in sedimentological studies but not, to the author's knowledge, in pedogenetic studies, is monazite. In the 20-100 um fraction of density 2.96 gm cm^{-3}, phosphorus can be used as a chemical index (Mitchell 1975).

Assessment of the degree of chemical weathering can be made using ratios of the concentrations of weatherable to resistant minerals in the silt fraction. Beavers *et al.* (1963) used CaO : ZrO_2 molar ratios as an index of weathering in six loessial soils comprising a chronosequence and were able to show that the degree of weathering was closely related to the pattern of loess thickness. Foss and Rust (1968) used CaO : ZrO_2 and Fe_2O_3 : ZrO_2 ratios to indicate a period of soil development between the deposition of two sediments. Most studies have shown that the intensity of weathering is greatest in the A horizon although the majority appear to have been on podzol profiles. These have shown a relatively rapid rate of chemical decomposition of less resistant minerals e.g. ferromagnesium minerals. Krebs and Tedrow (1957) studied three different soils of the same age and found that the amount of weathering decreased in the order Podzol, Grey-brown podzolic intergrade, Brown podzolic. Weathering intensity has also been studied as a function of time (Ruhe 1956, Bhattacherya 1963). Ruhe (1956) observed little weathering in soils < 6,800 years old but that thereafter, up to 100,000 years old, there was a progressive increase.

Losses and gains of constituents as a result of soil development have been calculated on the basis of a resistant mineral but such calculations are critically dependent on two factors, the choice of parent material and the choice of the stable, immobile constituent (Chapter 1, Brewer 1964). Assessments are made in relation to this unaltered component. Most studies have used only one stable constituent, often zirconium but occasionally

quartz (Bourne and Whiteside 1962) and titanium (Wilding *et al.* 1972). Few workers have assessed the internal standards despite the marked influence these variations have on the results. Sudom and Arnaud (1971) evaluated quartz, zirconium and titanium and showed that the weathering and mobilisation of titanium in all fractions limited its usefulness. From soils derived from mudstones in a typical catenary sequence in Wales, Evans and Adams (1975) assessed the usefulness of zirconium, titanium, quartz and the residue from tri-acid treatment (Akhtyrstev 1968). They also found titanium had been mobilised. Linear regressions showed that there was good agreement between the other indices.

Calculations of losses and gains have shown a marked redistribution of elements and minerals within the soil and losses from the profile (e.g. Wilding *et al.* 1972, Evans 1978). A few studies have reported the redistribution of clay. Barshad (1965) concluded that clay migration is the most important process in the occurrence of an horizon of clay accumulation and the large changes in chemical composition of the whole soil. Smeck *et al.* (1980) showed that some clay is contributed by carbonate leaching and shale disintegration but that comminution of coarse clay and silt to fine clay is the dominant process.

In this chapter, data on the elemental chemistry will be used to provide evidence for the relative importance of three hypotheses proposed to account for the textural differentiation of the soils of the terrace sequences.

7.2 Methods

7.2.1 Bulk density

Bulk density was measured by a technique similar to that of Brasher *et al.* (1966). Clods of soil 7-10 cm diameter were prized

from the pit face immediately adjacent to the section where samples were taken for chemical analysis. Three or four clods were taken for each horizon. The bulk density of each clod was measured at 1/3 bar and oven dried. It was found necessary to modify the procedure of Brasher *et al.* (1966). In order to ensure even and complete wetting up after coating with Saran resin, each clod was ground flat on one surface by carefully rubbing on a coarse glass paper. The smooth surface so obtained obviated the necessity for packing of the clod with glass beads to ensure enough contact with the plate. From the bulk density values, the coefficient of linear extensibility (COLE) was calculated.

7.2.2 Acid residue

Duplicate 1g samples of fine earth from each horizon of every terrace soil were digested for 1 hour with a tri-acid mixture of HCl, HNO_3 and H_2SO_4 (Hardy and Follet-Smith 1931). Each sample was heated to 80°C. This was continued until all brown fumes had disappeared, after which heating was continued for one hour. The residue was washed several times with distilled water using a centrifuge, dried and weighed. Any duplicates which varied by more than 2% were repeated.

7.2.3 Heavy minerals

From each horizon, fractions of size 10-125 um were isolated by sedimentation to remove < 10 um and by wet sieving to remove > 125 um. Heavy minerals of density > 2.96 gm cm^{-3} were separated centrifugally in tetrabromoethane from 100 g sub-samples of the 10-125 um fraction. Since earlier studies had shown that heavy minerals constituted <2% by weight of the fine sand and coarse silt

fractions, very large quantities of soil were necessary from those horizons high in clay in order to ensure an adequate amount of mineral for analysis.

7.2.4 Clay separations

25 g soil was mixed with 25 ml of 2M sodium chloride in a 75 ml plastic vial and shaken on a Spex Mixer Mill for 30s. Up to 200g were fractionated for horizons low in clay, 50g for those B horizons with high clay contents. The samples were dialysed against distilled water until all salt was removed. The dialysis procedure was adopted to reduce the loss of fine clay which inevitably occurs when salts are removed from suspension during washing and centrifugation. Clay was removed after gravity sedimentation of larger particles.

Fine clay (<0.2 um) was separated from coarse clay (2-0.2 um) by two methods.

In the preliminary study on the Urrbrae loam (Chapter 1) clay was separated in an MSE High Speed 18 centrifuge or a Sorvall RC-2B centrifuge fitted with a continuous action rotor. Dispersed clay (<0.5% suspension) was pumped at 109 cm^3 min^{-1} through a flow cell surrounding the stephorn of an ultrasonic probe immediately prior to entering the rotor. Centrifugation was carried out at 9,000 rpm. The coarse clay inside the rotor basket was resuspended and recentrifuged three times. Both coarse and fine clay fractions were concentrated to 2 litres in a cyclone evaporator at 40°C, further concentrated in a rotary evaporator and finally freeze dried, weighed and stored at 0°C prior to analysis. This technique is ideal when large quantities of clay are required or where the concentration of fine clay is so low that large volumes of

suspension must be centrifuged. Where these conditions did not apply, clay was fractionated in a centrifuge with swing-out buckets at 5000 rpm. Five or six centrifugations were required to remove the clay. Concentration and drying was performed in identical fashion.

7.2.5 Chemical analysis

Fractions of size >5 um i.e. 5-10, 10-20 and >20 um were ground in a tungsten carbide mill to a fine powder. After ignition in a furnace at 1000°C, 0.28 g of each sample was mixed with 1.52g of lithium borate and lanthanum oxide and a glass disc made. Elemental analysis was carried out by X-ray fluorescent spectroscopy according to the method of Norrish and Hutton (1969). Yttrium and zirconium were measured with the scintillation counter. Matrix corrections were made for each element.

7.2.6 Calculation of losses and gains of constituents

Reconstruction of elemental and clay gains and losses accompanying soil development were calculated on the basis of the stable constituent method of Brewer (1964). Changes in volume, thickness and weight were also computed by this method.

If Vp = volume of parent material from which the present day horizon was derived then

$$Vp = Vs \frac{Ds\ Rs}{Dp\ Rp}$$

where Ds = bulk density (at 1/3 bar) of weathered soil horizon ($g\ cm^{-3}$)

Rs = % of stable constituent in a certain size fraction x % of this size fraction in the whole soil (g per 100 g)

Dp = bulk density (at 1/3 bar) of parent material ($g\ cm^{-3}$)%

Rp = % of stable constitutent in a particle size fraction x % of this size fraction in the parent material (g per 100 g)

Change in volume (ΔV) on soil development is given by

$$\Delta V = Vs - Vp$$

and the relative change in volume

$$= \frac{\Delta V}{Vp} \times 100$$

If Wp is the weight of parent material from which weight of present day horizon (Ws) was derived, then

$$Wp = Vs\ Ds\ \frac{Rs}{Rp}$$

and the change in weight (ΔW) is given by the relationship

$$\Delta W = Vs\ Ds\ (1 - \frac{Rs}{Rp})$$

The weight of elemental constituent or clay (X) lost from, or gained by, an horizon is given by the formula

$$X = Ds\ (Px - Rs\ Px')$$

where Px = % by weight of constituent x in the present day horizon

Px' = % by weight of constituent x in the parent material

Net changes of constituents can be compared on a volume basis in terms of gain or loss in g per 100 cm^3. In order to compute the total loss or gain from a whole profile or group of horizons, the thickness of the horizons must be taken into account by

multiplying the net change in an horizon by its thickness and summing the products.

Loss or gain of clay by migration Calculations outlined above give only the net change in a constituent during soil development. There is no indication of the relative importance of a particular process. An attempt was made to assess the relative importance of clay illuviation and clay formation by apportioning the losses and gains to each process. The method is based on the loss of elemental oxides from the non clay fraction (2-2000 um) relative to the parent material (Barshad 1965).

If f is the amount of clay formed in the A horizon from 100 g of non clay parent material then

$$f = \frac{a_1 - \frac{a_1 b_1}{b_2}}{a^1 - \frac{a_2 b^1}{b_2}}$$

where

b_1, a_1 = % oxide (e.g. Fe_2O_3 and SiO_2) in the non clay of the parent material

b_2, a_2 = % oxide (e.g. Fe_2O_3 and SiO_2) in the non clay of the soil horizon

b^1, a^1 = % oxide (e.g. Fe_2O_3 and SiO_2) in the clay fraction of the soil horizon.

The amount of clay formed in the A horizon which resulted in the present amount of non clay in 100 g of soil (F) is calculated as follows

$$F = \frac{f \ (100-d)}{(100-f)\ k}$$

Where

d = % clay in A horizon

k is the proportionality factor affecting the oxide content (e.g. Fe_2O_3, SiO_2) of the non clay of the A horizon due to losses or gains other than to clay formation and is given by

$$k = \frac{100\ a_1 - fa^1}{a_2\ (100 - f)}$$

k was calculated for a number of oxides viz K_2O, Fe_2O_3, SiO_2 and $Al_2\ O_3$ and the value chosen was the mean of the two oxides which agreed most closely.

The original amount of non clay (O) in the parent material before clay formation began in the horizon is given by

$$O = \frac{100F}{f}$$

and the amount of clay originally present in the horizon (N) is calculated as follows.

$$N = \frac{c}{(100-c)} \frac{100\ F}{f}$$

where c = % clay in parent material

F+N = total clay present prior to migration

If LGC = loss or gain of clay by migration (g per 100 g soil) then LGC = weight of clay now present in the horizon - (F+N).

If RLGC = relative loss or gain of clay by migration (g per 100 g parent material) in the horizon.

then

$$RLGC = LGC \frac{Ws}{Wp}$$

where

Ws = weight soil (g)

Wp = weight parent material (g)

total oxides (g per 100 g parent material) in the present soil (To) is given by

$$To = \frac{Ws}{Wp} \cdot 100$$

total loss due to soil formation (Sf) in g per 100 g parent material is given by

$$Sf = To - 100$$

gain or loss due to clay formation (g per 100 g parent material)

$$= Sf - RCLG$$

7.3 Results and discussion

7.3.1 Parent material uniformity

Three criteria, falling into two general categories, were applied.

1. Particle-size distribution (PSD) of resistant minerals of the non clay fractions
   (i) ratio of concentrations of TiO_2 in coarse silt and sand fractions.
2. Ratio of two resistant minerals in any one fraction.
   (i) Y_2O_3 : ZrO_2, ZrO_2 : TiO_2, P_2O_5 : TiO_2 of the 10-125 um fraction of density > 2.96 gcm^{-3}, where Y_2O_3 is assumed to represent the concentration of xenotime, ZrO_2 of zircon, TiO_2 of rutile + ilmenite, P_2O_5 of monazite.
   (ii) ratio of TiO_2 : ZrO_2 in the coarse silt fraction.

Results are presented in Tables 18, 19, 20 and 21 for Gooromon Ponds, Shinglehouse Creek, Nowra Creek and Hawkesbury River sequences respectively.

Profile	depth (cm)	ratios of oxides Y_2O_3 / ZrO_2 x 10^{-1} (1)	ZrO_2 / TiO_2 (1)	P_2O_5 / TiO_2 x 10^{-1} (1)	ZrO_2 cs / TiO_2 cs (2)	TiO_2 s / TiO cs (3)
G1	0	0.43	0.28	0.20	0.31	0.58
	6	0.42	0.38	0.23	0.29	0.60
	18	0.43	0.36	0.23	0.30	0.62
	42	0.44	0.43	0.24	0.33	0.50
	56	0.44	0.35	0.22	0.32	0.51
	71	0.42	0.35	0.22	0.33	0.54
G2	0	0.44	0.20	0.15	0.33	0.65
	20	0.45	0.22	0.18	0.29	0.66
	40	0.47	0.18	0.14	0.30	0.73
	50	0.49	0.19	0.15	0.30	0.67
G3	0	0.50	0.15	0.14	0.32	0.79
	12	0.47	0.19	0.14	-	-
	24	0.46	0.23	0.15	0.31	0.73
	32	0.47	0.25	0.17	0.31	0.64
	41	0.44	0.31	0.17	0.33	0.59
	55	0.47	0.26	0.16	0.30	0.53
	66	0.46	0.27	0.18	0.28	0.47
	78	0.45	0.22	0.16	0.28	0.40
	88	0.47	0.22	0.17	0.29	0.45
	102	0.45	0.24	0.17	0.35	0.48
	115	0.45	0.29	0.20	0.32	0.45
	140	0.47	0.24	0.22	0.29	0.43
G4	0	0.47	0.23	0.18	0.30	0.64
	6	0.47	0.23	0.19	0.30	0.60
	13	0.47	0.24	0.19	0.28	0.59
	21	0.48	0.22	0.17	0.31	0.59
	31	0.48	0.20	0.17	0.30	0.61
	42	0.50	0.20	0.16	0.27	0.66
	57	0.50	0.20	0.14	0.29	0.72
	69	0.40	0.20	0.15	0.33	0.73
	81	0.48	0.20	0.16	0.24	0.68
	96	0.47	0.23	0.17	0.29	0.59

G5	0	0.45	0.25	0.16	0.31	0.63
	8	0.48	0.24	0.16	0.40	0.63
	18	0.48	0.23	0.14	0.38	0.62
	30	0.47	0.25	0.15	0.36	0.62
	42	0.45	0.24	0.15	0.31	0.61
	52	0.51	0.23	0.17	0.32	0.59
	65	0.45	0.25	0.16	0.31	0.59
	73	0.47	0.24	0.15	0.37	0.48
	85	0.47	0.23	0.14	0.39	0.54
	100	0.49	0.22	0.12	0.40	0.55
	120	0.47	0.21	0.13	0.35	0.56

Table 18 Ratios of oxides from various size and density fractions of soils from Gooromon Ponds.

(1) ratios from the 10-125 um, > 2.96 g cm^{-3} fraction

(2) ratio from coarse silt (5-20 um) fraction

(3) ratio from sand(s) and coarse silt (cs) fractions

Profile	depth (cm)	ratios of oxides Y_2O_3/ZrO_2 (1)	ZrO_2/TiO_2 (1)	P_2O_5/TiO_2 x 10^{-1} (1)	ZrO_2 cs / TiO_2 cs (2)	TiO_2 s / TiO_2 cs (3)
S1	0	1.45	0.23	0.31	0.47	0.56
	10	0.53	0.35	0.27	0.44	0.50
	20	0.50	0.35	0.26	0.48	0.52
	30	0.47	0.35	0.33	0.47	0.50
	50	-	-	-	0.43	0.41
	70	0.67	0.26	0.82	0.39	0.43
	90	0.62	0.25	0.73	0.38	0.43
S2	0	0.54	0.28	0.49	0.31	0.55
	8	0.48	0.27	0.50	0.37	0.47
	20	0.63	0.21	0.39	0.35	0.57
	30	0.86	0.17	0.27	0.40	0.55
	42	0.50	0.29	0.73	0.38	0.62
	52	0.53	0.29	0.22	0.40	0.62
	60	0.52	0.31	0.19	0.38	0.61
	70	0.56	0.30	0.24	0.41	0.58
	90	0.51	0.29	0.15	0.42	0.62
S3	0	0.50	0.30	0.21	0.54	0.57
	7	0.48	0.30	0.21	0.59	0.55
	17	0.51	0.29	0.18	0.60	0.54
	28	0.50	0.24	0.16	0.48	0.56
	38	0.54	0.23	0.20	0.44	0.56
	48	0.54	0.25	0.17	0.37	0.63
	68	0.54	0.25	0.15	0.43	0.58
	88	-	-	-	0.44	0.58

Table 19 Ratios of oxides from various size and density fractions of soils from Shinglehouse Creek.

(1) ratios from the 10-125 um, > 2.96 g cm^{-3} fraction

(2) ratio from coarse silt (5-20 um) fraction.

(3) ratio from sand (s) and coarse silt (cs) fraction.

Profile	depth (cm)	ratios of oxides $\frac{Y_2O_3}{ZrO_2}$ (1)	$\frac{ZrO_2}{TiO_2}$ (1)	$\frac{P_2O_5}{TiO_2}$ x 10^{-1} (1)	$\frac{ZrO_2 \text{ cs}}{TiO_2 \text{ cs}}$ (2)	$\frac{TiO_2 \text{ s}}{TiO_2 \text{ cs}}$ (3)
N1	0	0.25	0.46	0.72	0.40	0.61
	5	0.23	0.48	0.74	0.53	0.63
	18	0.26	0.30	0.92	0.40	0.61
	32	0.24	0.41	0.81	0.41	0.59
	45	0.24	0.30	0.86	0.33	0.52
	55	-	-	-	-	-
N2	0	0.25	0.28	0.97	0.39	0.56
	7	0.24	0.28	0.92	0.37	0.60
	20	0.23	0.33	0.82	0.36	0.59
	30	0.24	0.29	0.84	0.39	0.58
	41	0.22	0.30	0.92	0.41	0.63
	50	0.23	0.30	0.78	-	-
	60	0.23	0.29	0.83	0.41	0.51
N3	0	0.21	0.31	0.72	0.40	0.58
	10	0.24	0.27	0.75	0.45	0.58
	25	0.26	0.24	0.78	0.41	0.57
	35	0.27	0.24	0.80	0.39	0.57
	50	0.23	0.31	0.67	0.43	0.51
	70	0.22	0.32	0.61	-	-
	90	0.22	0.35	0.72	0.42	0.44
N4	0	0.20	0.37	0.54	0.35	0.43
	5	0.21	0.34	0.58	0.47	0.40
	17	0.22	0.30	0.67	0.49	0.44
	30	0.21	0.30	0.75	0.47	0.45
	40	0.24	0.28	0.86	0.26	0.41
	60	0.23	0.26	0.85	0.43	0.47
	80	0.24	0.25	0.75	-	-
	120	0.24	0.24	0.78	0.39	0.54

Table 20 Ratios of oxides from various size and density fractions of soils from Nowra Creek.

(1) ratios from the 10-125 um, > 2.96 g cm^{-3} fraction

(2) ratio from coarse silt (5-20 um) fraction.

(3) ratio from sand (s) and coarse silt (cs) fraction.

Profile	depth (cm)	ratios of oxides $\frac{Y_2O_3}{ZrO_2}$ (1)	$\frac{ZrO_2}{TiO_2}$ (1)	$\frac{P_2O_5}{TiO_2} \times 10^{-1}$ (1)	$\frac{ZrO_2 \text{ cs}}{TiO_2 \text{ cs}}$ (2)	$\frac{TiO_2 \text{ s}}{TiO_2 \text{ cs}}$ (3)
H1	15	0.29	0.25	0.63	0.03	0.50
	40	–	–	–	0.03	0.52
	58	0.24	0.23	0.64	–	–
	90	0.37	0.25	0.73	0.02	0.47
H2	0	0.23	0.24	0.63	0.03	0.42
	15	0.24	0.28	0.59	0.03	0.53
	30	0.29	0.23	0.32	0.03	0.54
	67	0.25	0.24	0.28	0.03	0.44
	88	0.21	0.29	0.17	–	–
	110	0.27	0.24	0.28	0.03	0.35
	150	0.23	0.26	0.34	0.03	0.29
H3	0	0.18	0.34	0.18	0.04	0.34
	18	0.19	0.33	0.15	0.04	0.33
	32	0.19	0.32	0.15	0.04	0.34
	48	0.19	0.35	0.20	0.04	0.35
	90	–	–	–	0.04	0.39
	120	0.20	0.30	0.22	–	–
	150	–	–	–	0.03	0.41
H4	0	0.20	0.39	0.18	0.03	0.44
	11	0.19	0.32	0.16	0.03	0.43
	23	–	–	–	0.03	0.40
	70	0.23	0.23	0.23	0.03	0.39
	130	0.25	0.25	0.24	0.04	0.41
H5	0	0.15	0.48	0.14	0.04	0.24
	25	0.16	0.48	0.14	0.05	0.20
	35	0.14	0.47	0.17	0.03	0.23
	80	0.16	0.40	0.21	0.02	0.36
	130	0.16	0.31	0.38	0.02	0.31

Table 21 Ratios of oxides from various size and density fractions of soils from Hawkesbury River.

(1) ratios from the 10-125 um, > 2.96 g cm $^{-3}$ fraction

(2) ratio from coarse silt (5-20 um) fraction.

(3) ratio from sand (s) and coarse silt (cs) fraction.

Results for Gooromon Ponds indicate that the parent material for each soil was initially homogeneous. All ratios show a very high degree of similarity with depth. There is no evidence that the textural differentiation in the older profiles G4 and G5 is the result of sedimentary layering.

Furthermore, the parent material for all five profiles can be considered identical since the ratios are the same throughout. Drees and Wilding (1978) stated that percentage deviations of over 22% were required to detect lithologic discountinuities while Chapman and Horn (1968) considered differences of 100% or more were required. If the ratios for all soils are considered to be normally distributed and part of the same population, relative standard deviations (rsd) are < 24% for all ratios and < 5% for the yttrium oxide : zirconium oxide ratio (Table 22). This result has important implications if these soils are to be considered part of a chronosequence. It means that the independent soil forming factor, parent material, can be considered constant.

Similar conclusions can be drawn from the data for Shinglehouse Creek (Table 19). Only the surface layer of S1 can be considered to be different. The P_2O_5 : TiO_2 ratio shows a good deal of variation in profiles S1 and S2 (rsd > 50%). In view of the relative constancy of other ratios, the results are probably due to sampling and analytical error : there is < 0.05% phosphorus in many heavy mineral samples compared to > 30% for titanium, > 5% for zirconium and > 2% for yttrium. Apart from the ZrO_2 : TiO_2 ratio all ratios show a decrease in rsd with age. The somewhat higher ZrO_2 : TiO_2 ratios in the silt fraction may be caused by some weathering and mobilisation of titanium in the A horizon. Because the elemental ratios derived from the heavy mineral fraction

are constant, the higher ZrO_2 : TiO_2 ratios may be caused by a breakdown of weatherable minerals of silt size in the light fraction (< 2.96 g cm^{-3}). These minerals may contain titanium either as part of its mineralogical structure or as micro inclusions of rutile and anatase which are released on breakdown.

The ratios for the Nowra sequence show only minor variations, similar to those for Gooromon Ponds (Table 20). Rsd's both within and between profiles, for all ratios, are < 20% with the exception of only the ZrO_2 : TiO_2 ratio of N1. Profiles can be considered as having been formed from a mineralogically similar parent material.

Variations in the Hawkesbury sequence are somewhat greater than those of the other three sequences but, with the exception of the P_2O_5 : TiO_2 ratio for H2 and H4, rsd's are < 25%. The variations in the P_2O_5 : TiO_2 ratio are probably due to sampling and analytical error (because of the extremely low phosphorus values) in H2 and a combination of analytical error and weathering in H4. Between profile rsd's (with the exception of P_2O_5 : TiO_2), indicate that lithological variations in the parent material were not great and the five soils can be considered part of a chronosequence.

In general there is less variability in the Y_2O_3 : ZrO_2 ratios derived from the > 2.96 g cm^{-3} fraction than other ratios. This is an indication that the minerals xenotime and zircon are more resistant and immobile, and therefore more reliable indicators of parent material variations than rutile or monazite. The problem of monazite may also be due to difficulties in analysis as explained earlier. Some breakdown and release of titanium may account for the

slightly higher rsd's in the ZrO_2 : TiO_2 ratios of the silt fraction and TiO_2 sand : TiO_2 silt ratios.

Studies by Khangarot *et al* (1971) and Drees and Wilding (1978) of the distribution of elements in the light (< 2.89 g cm^{-3}) and heavy mineral fractions, as discussed in Chapter 1, have thrown doubt on the validity of assigning elemental percentages to specific minerals as has been done in this section. Not all the heavy mineral may be in the denser fraction (in this case the fraction > 2.96 g cm^{-3}). Both light and heavy fractions were assayed for zirconium, titanium, yttrium and phosphorus to check if there had been a 'clean' separation. Results presented in Figures 89 (Gooromon Ponds), 90 (Shinglehouse Creek), 91 (Nowra Creek) and 92 (Hawkesbury River) show that there is little, if any heavy mineral present in the light fraction. What little there is may be part of the crystal structure of other minerals but in no way effects the conclusions.

In the following sections of this chapter it will be assumed that all profiles were form in an initially uniform parent material.

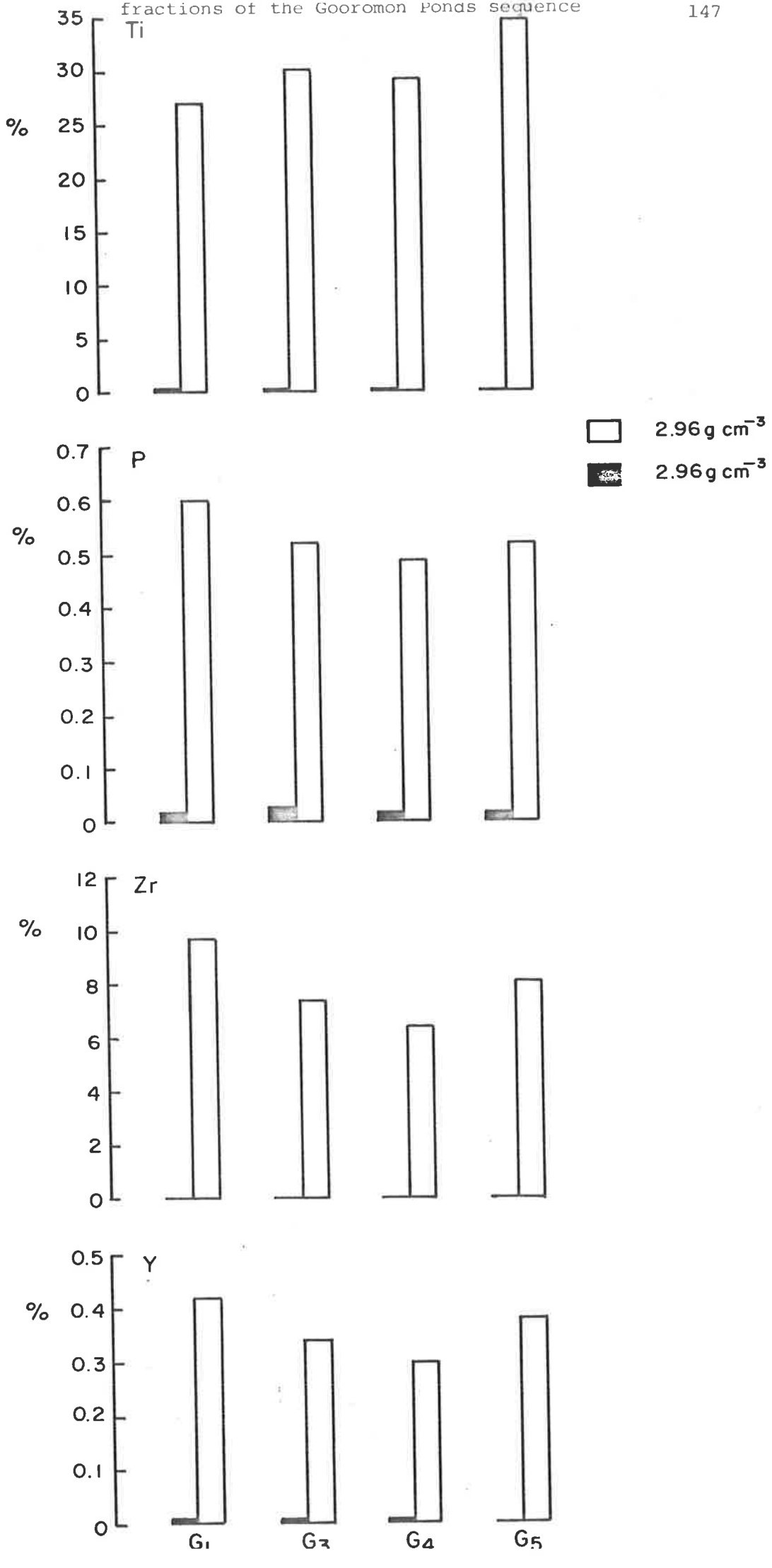
Ti
%
35
30
25
20
15
10
5
0
2.96 g cm⁻³
2.96 g cm⁻³
P
%
0.7
0.6
0.5
0.4
0.3
0.2
0.1
0
Zr
%
12
10
8
6
4
2
0
Y
%
0.5
0.4
0.3
0.2
0.1
0
G1
G3
G4
G5

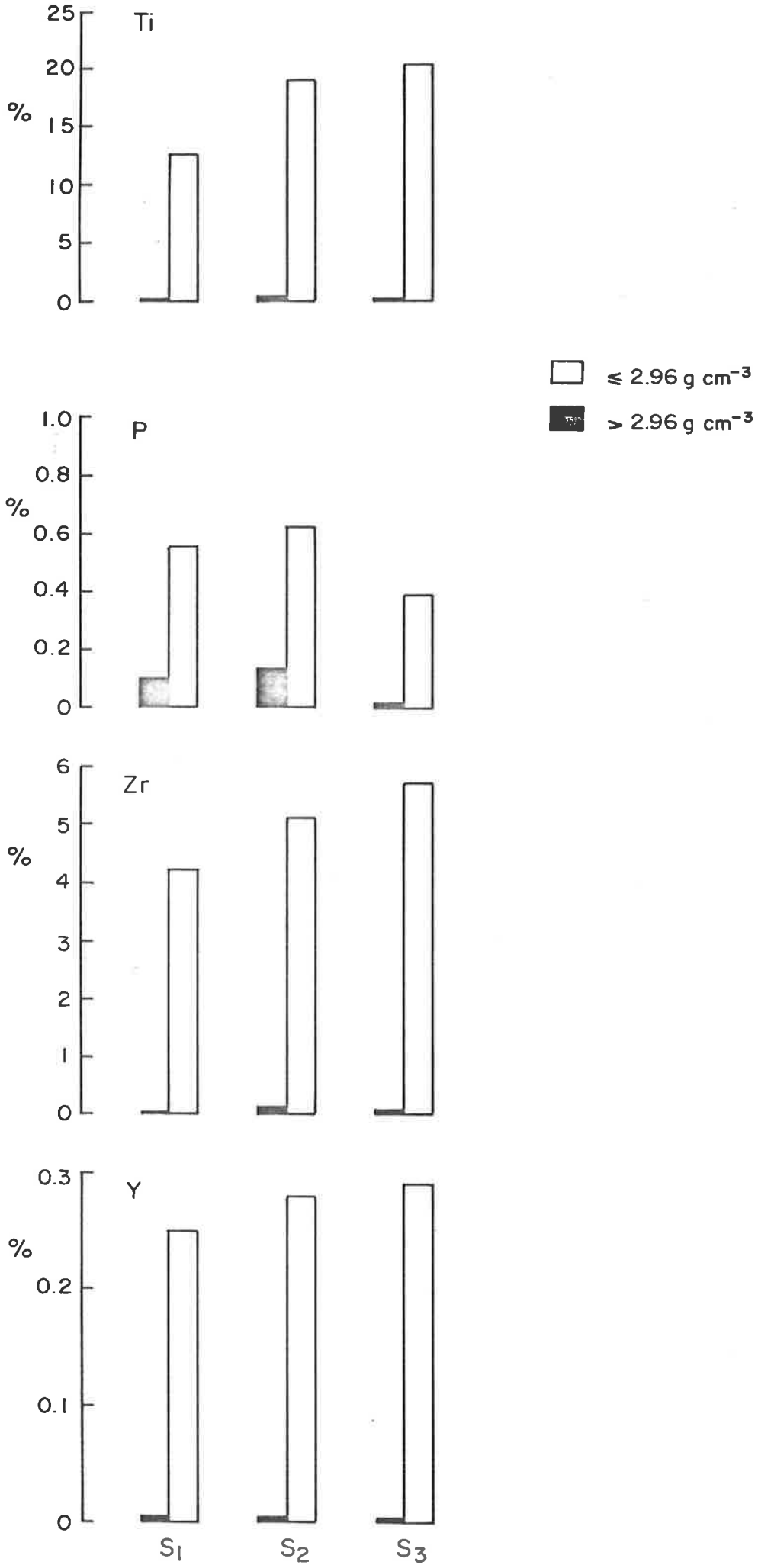

Figure 90 Proportion of elements in light and heavy mineral fractions of the Shinglehouse Creek sequence

Fig. 91 Proportion of elements in light and heavy mineral fractions of the Nowra Creek sequence

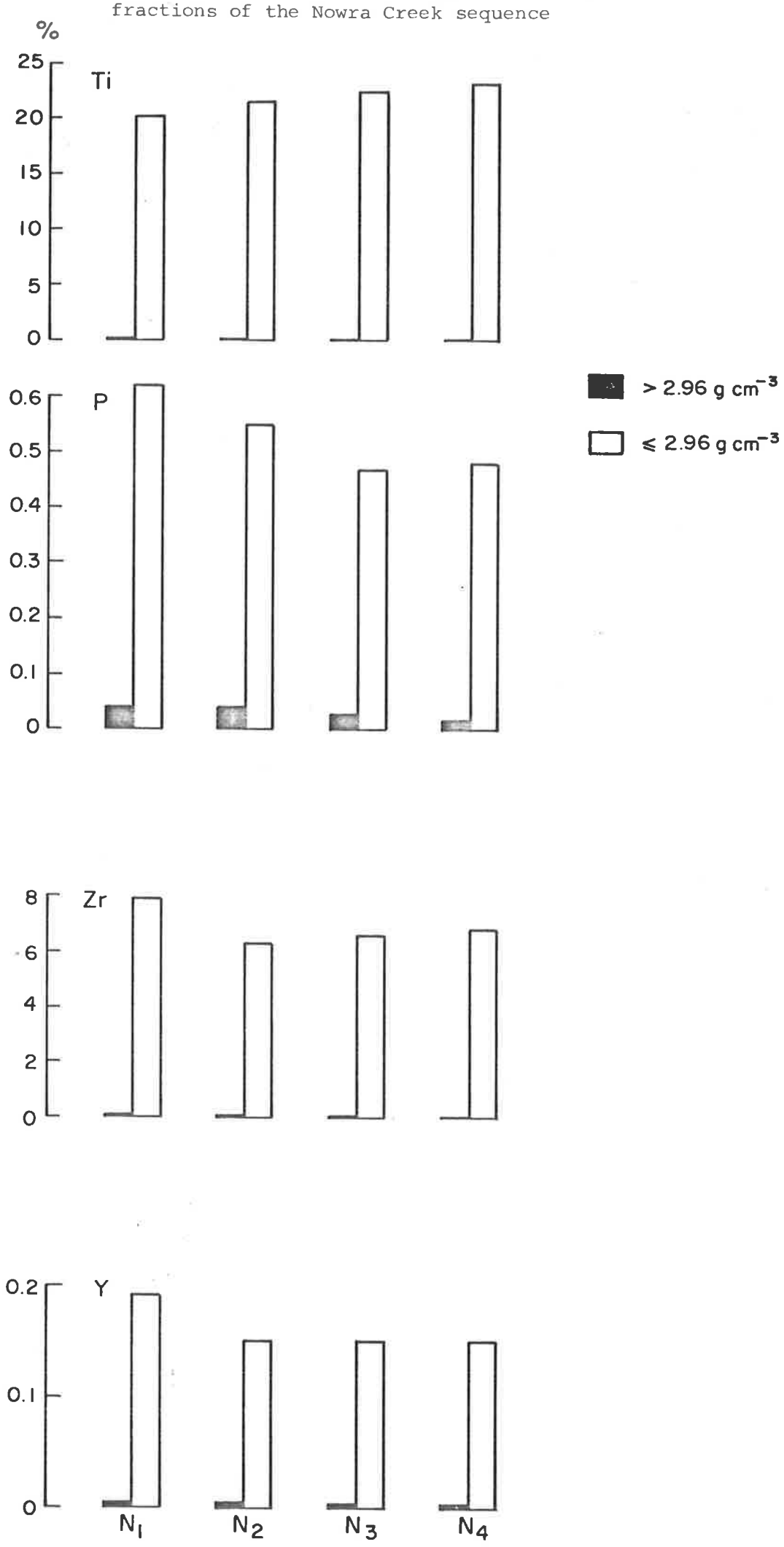

Figure 92 Proportion of elements in light and heavy mineral fractions of the Hawkesbury River sequence

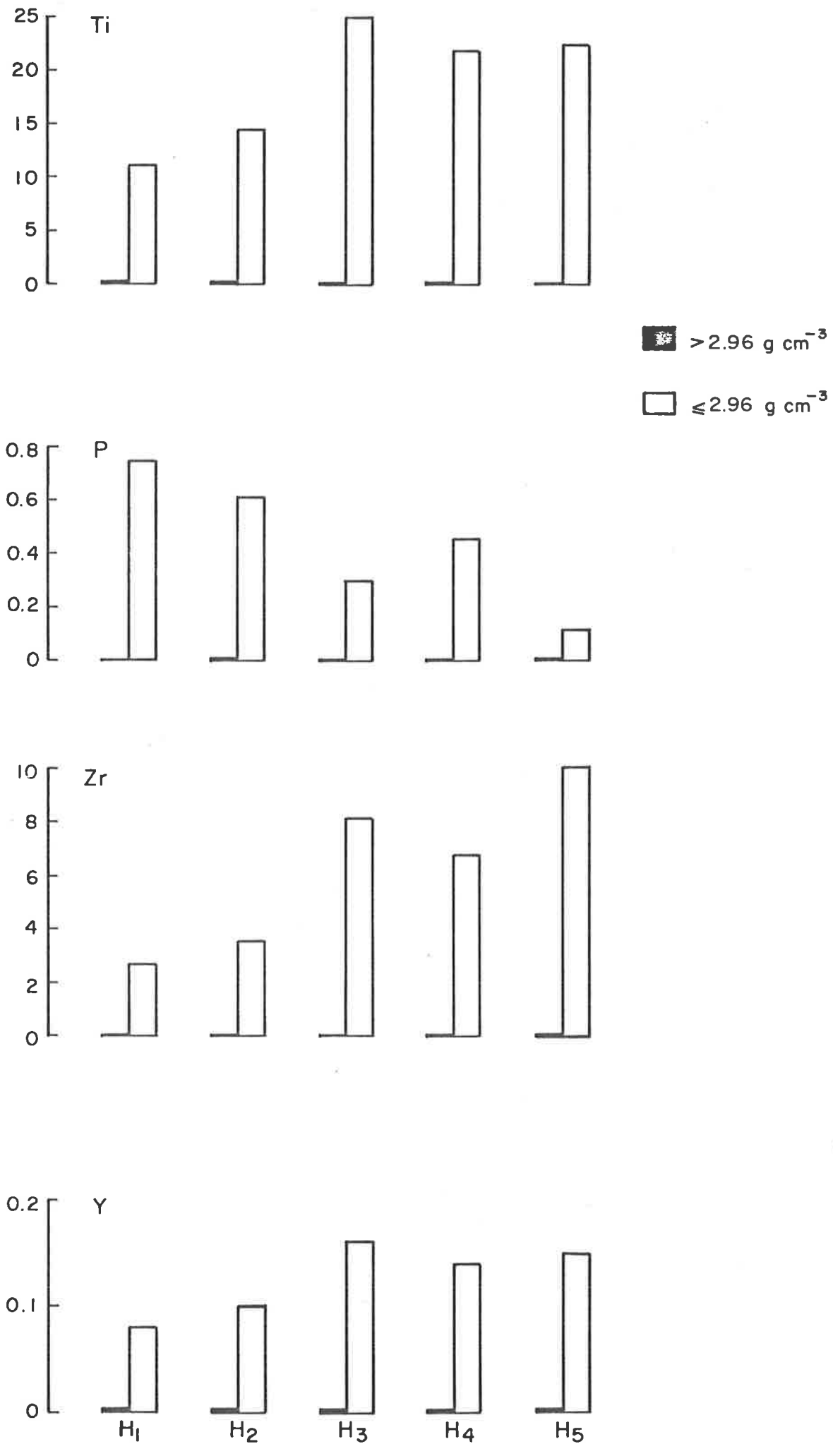

profile	Y_2O_3 / ZrO_2		ZrO_2 / TiO_2		P_2O_5 / TiO_2		ZrO_2 cs / TiO_2 cs		TiO_2 s / TiO_2 cs	
	m (x 10^{-1})	r	m	r	m (x 10^{-1})	r	m	r	m	r
Gooromon Ponds										
G1	0.43	2.3	0.36	13.9	0.22	4.6	0.31	5.2	0.56	8.8
G2	0.46	4.4	0.20	10.0	0.16	12.5	0.31	5.6	0.68	5.3
G3	0.46	4.3	0.24	16.7	0.17	11.8	0.31	7.1	0.54	24.4
G4	0.47	6.4	0.22	9.1	0.17	11.8	0.29	8.4	0.64	8.5
G5	0.47	4.3	0.24	4.2	0.15	6.7	0.35	10.5	0.58	8.1
All profiles	0.46	4.4	0.25	24.0	0.17	17.7	0.32	10.9	0.59	15.0
Shinglehouse Creek										
S1	0.56	15.0	0.31	16.8	0.48	56.4	0.44	9.1	0.48	11.6
S2	0.57	20.5	0.27	17.3	0.35	54.3	0.38	8.9	0.58	8.5
S3	0.52	4.7	0.27	11.1	0.18	13.5	0.49	16.8	0.57	4.8
All profiles	0.55	15.9	0.28	16.3	0.33	62.7	0.43	16.4	0.55	11.3
Nowra Creek										
N1	0.24	4.8	0.39	22.0	0.31	12.3	0.41	17.6	0.59	7.2
N2	0.23	4.2	0.30	5.7	0.26	5.3	0.39	5.2	0.58	7.0
N3	0.24	9.3	0.29	14.6	0.21	11.1	0.42	5.1	0.54	10.4
N4	0.22	7.3	0.29	15.5	0.21	9.8	0.41	20.0	0.45	10.4
All profiles	0.23	7.2	0.31	19.4	0.24	19.2	0.41	12.2	0.53	13.9
Hawkesbury River										
H1	0.30	21.9	0.24	4.8	0.67	8.2	0.24	4.8	0.50	5.0
H2	0.25	10.8	0.25	9.2	0.47	59.7	0.25	9.2	0.43	22.9
H3	0.19	3.7	0.33	5.8	0.18	17.1	0.33	5.8	0.36	9.0
H4	0.21	12.0	0.29	22.1	0.21	16.4	0.29	22.1	0.41	5.1
H5	0.15	6.0	0.43	17.2	0.21	47.8	0.43	17.2	0.27	24.2
All profiles	0.22	23.8	0.31	25.6	0.30	62.0	0.31	25.6	0.39	23.3

Table 22 Means and relative standard deviations of the oxide ratios of various fractions from the soils of terrace sequences. m = mean ; rsd = relative standard deviation (%).

7.3.2 Weathering

Changes in the ratios in the coarse silt fraction (5-20 um) of iron, calcium and sodium to zirconium were used as indexes of the degree of chemical weathering. Depth functions of the three ratios for each soil are presented in the form of plots.

In the Gooromon Ponds sequence (Figure 93) there is little difference between the depth functions of the G1, G2, G3 and G4 profiles in spite of the development of a texture contrast profile in G4 (8% clay in the A horizon, 22% in the B). In G5 the ratios are less throughout the profile in comparison to the younger soils. The decrease is most marked in the A horizon indicating that weathering and mobilisation of iron, sodium and calcium are more intense in this part of the profile. The development of a bleached A2 horizon has accompanied this weathering.

Ratios for the Shinglehouse Creek (Figure 94) and Nowra Creek (Figure 95) sequences show similar trends with age of profile as Gooromon Ponds, although the difference in ratios between S3 and N4 and the younger member of their respective sequences are not as marked even though S3 and N4 have a stronger textural differentiation than G5 (for S3 % clay in A is 9, B 37%, N4 % clay in A is 8, B 43%). Weathering in situ appears to have been less intense. The increase in iron at the base of S1 may be due to lateral movement of iron and deposition around silt and sand grains. Iron concretions of silt and sand size were observed in this section.

In the Hawkesbury sequence there is a difference in the depth functions between ratios with time (Figure 96.1, 96.2, 96.3). The $Na_2O:ZrO_2$ ratio is relatively constant with depth in all profiles except H5 where there is a sharp drop in the A1 and A2

horizons. The same holds for the Fe_2O_3 : ZrO_2 ratios except for a very high value in the B3 horizon of H4. This is due to the formation of sesquioxide concretions in situ, an explanation which accounts for similarly high values in the B horizon of H5. Within profiles the ratios show more variability than the other sequences. Analytical error may account for this. ZrO_2 concentrations are one tenth the values in other sequences (mean ZrO_2 is 0.04% compared to 0.4% for Nowra Creek). CaO_2 : ZrO_2 ratios could not be calculated because the calcium concentrations were so low.

If weathering in situ is to account for the clay enrichment in the B horizon then there should be a decrease in ratios in the B horizon compared to the A and C horizon. This would indicate the loss of weatherable minerals in that horizon and the formation of clay from the weathering products.

Furthermore, this decrease should be more pronounced the older the profile. The results show no such trend. In the older profiles (G4, S3, N4) there is a decrease in the A horizon showing more intense weathering. If this process has produced some of the clay of the B horizon, then a combination of the processes of weathering and illuviation is necessary to account for the clay enrichment. On the basis of these criteria this mechanism can only be of relatively minor significance since strong texture contrast has already developed in younger profiles (e.g. G3, N3) prior to any obvious change in the ratios. The weathering indices provide no evidence that weathering in situ makes a significant contribution to the development of texture contrast.

7.3.3 Loss and gain of constituents

All calculations of changes in volume and weight of the present

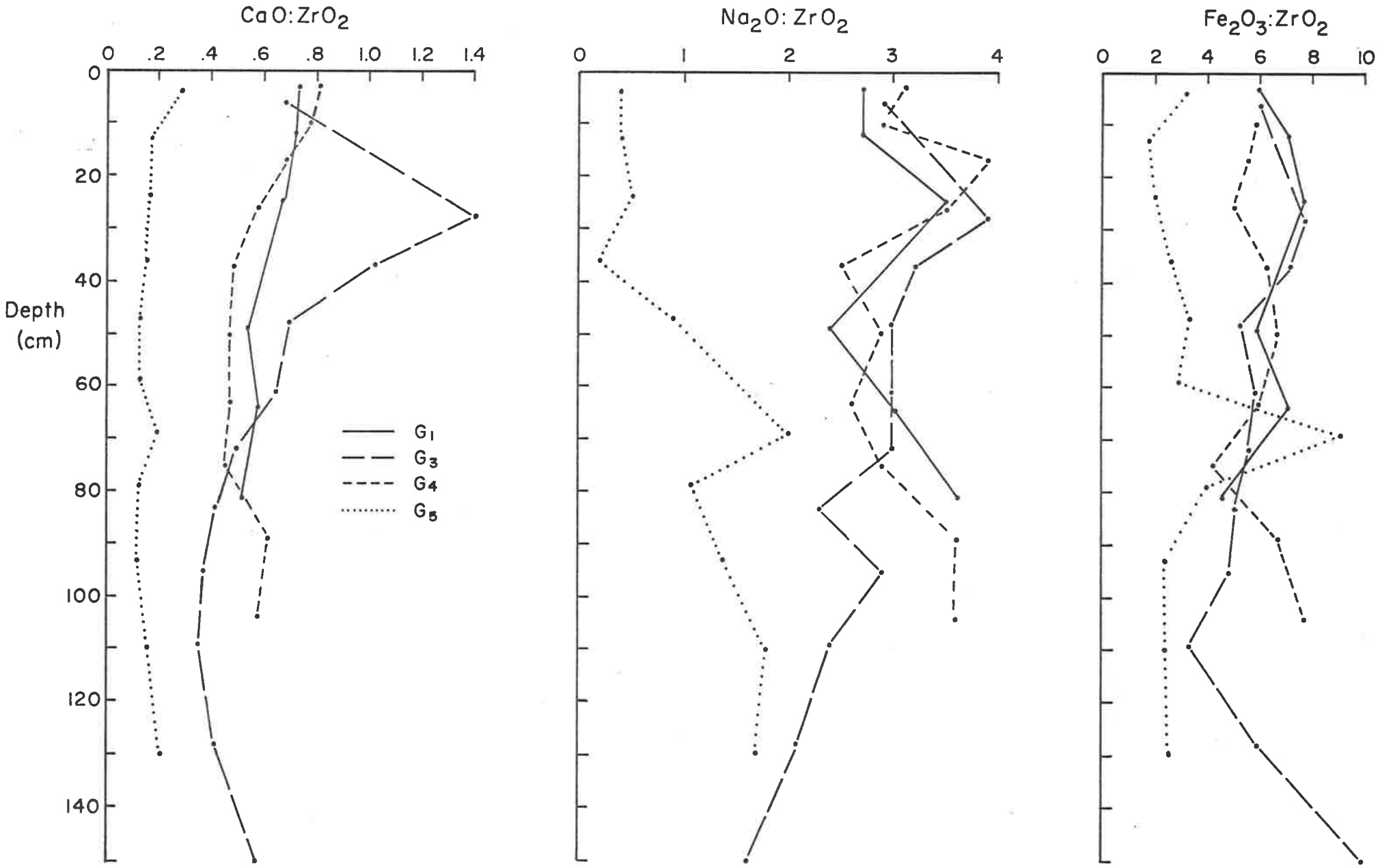

Figure 93 Depth functions of the ratios, $CaO:ZrO_2$, $Na_2O:ZrO_2$, $Fe_2O_3:ZrO_2$ for soils of the Gooromon Ponds sequence

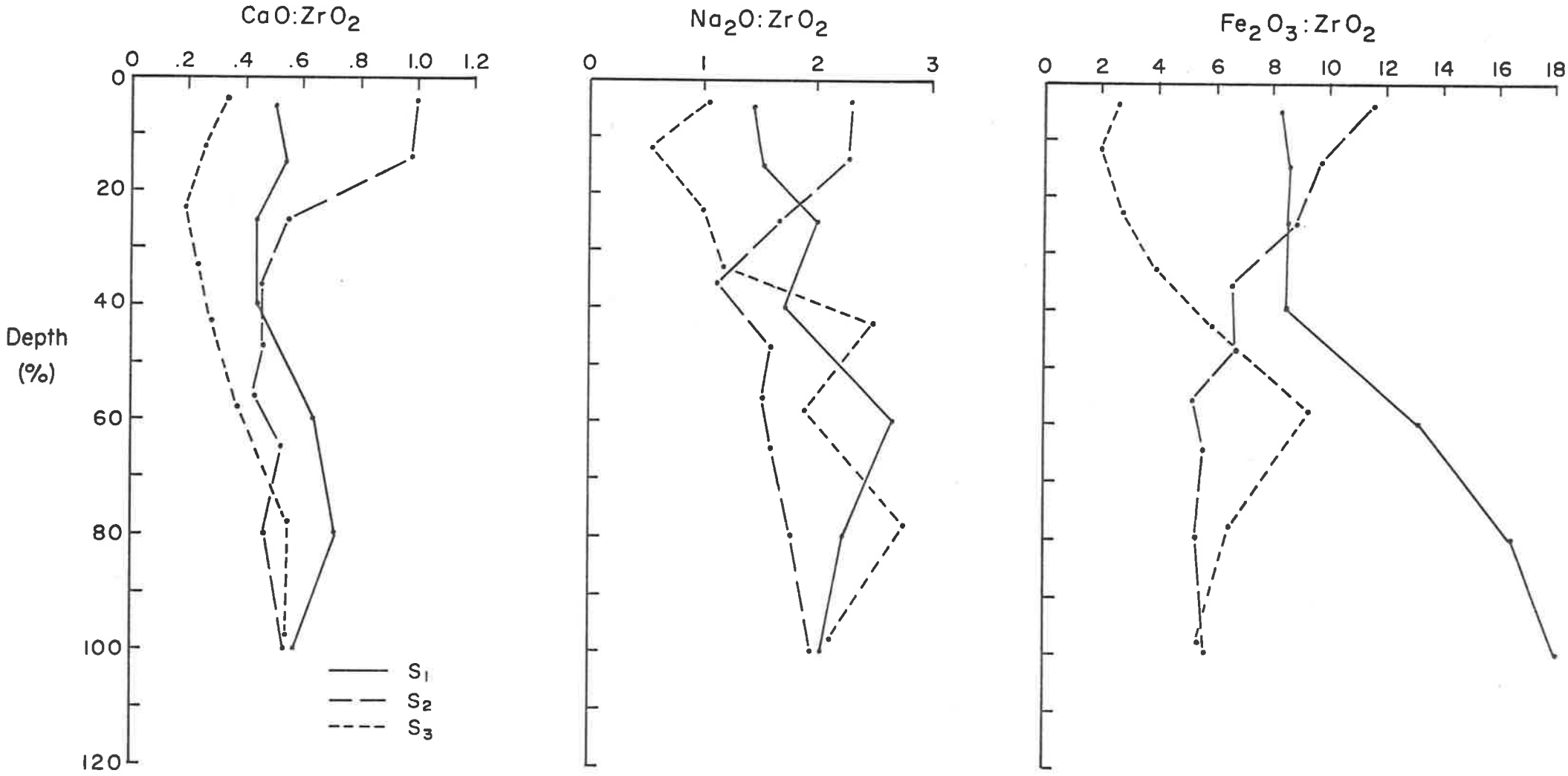

Figure 94 Depth functions of the ratios $CaO:ZrO_2$, $Na_2O:ZrO_2$, $Fe_2O_3:ZrO_2$ for soils of the Shinglehouse Creek sequence

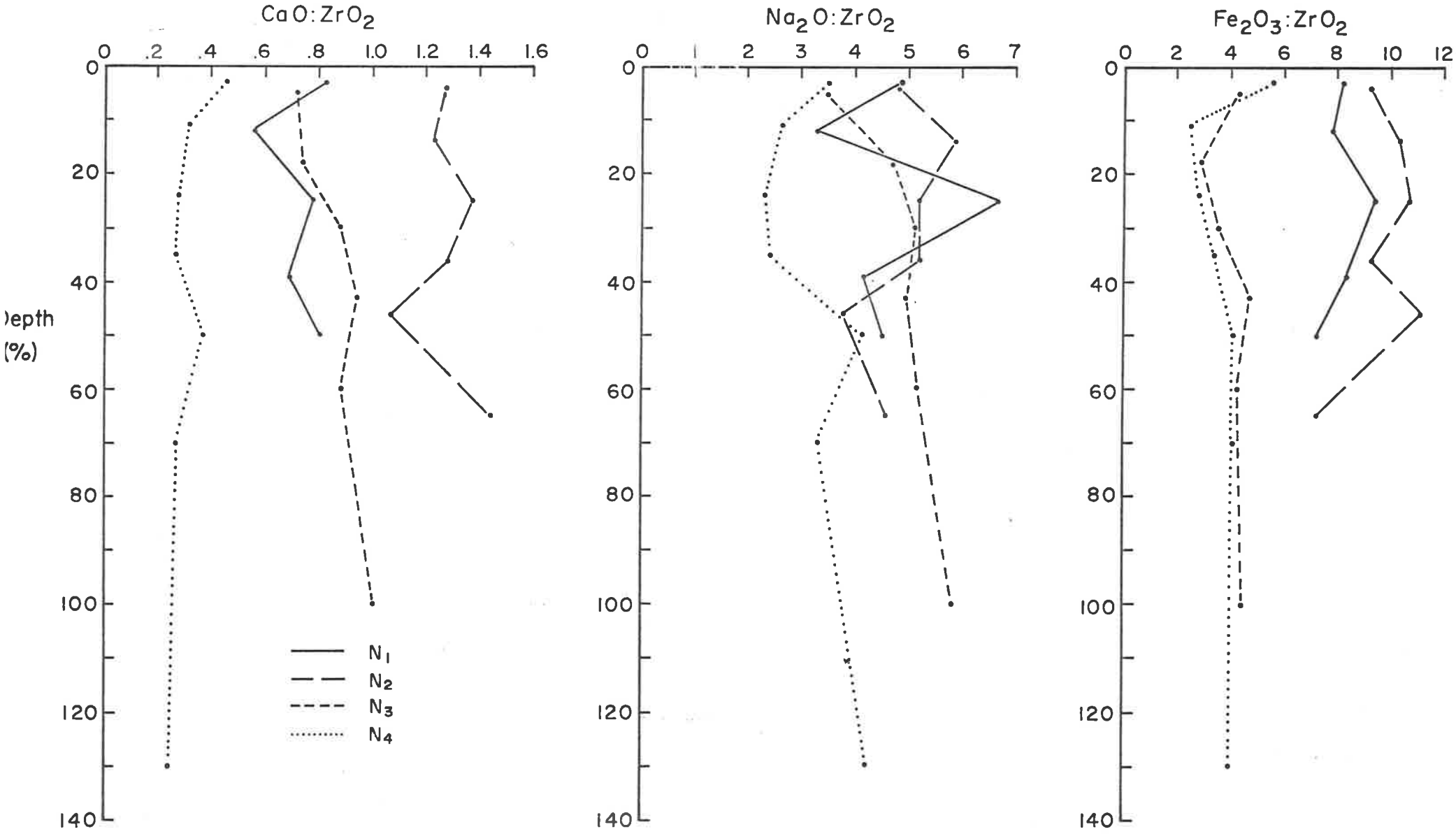

Figure 95 Depth functions of the ratios, $CaO:ZrO_2$, $Na_2O:ZrO_2$ and $Fe_2O_3:ZrO_2$ for soils of the Nowra Creek sequence

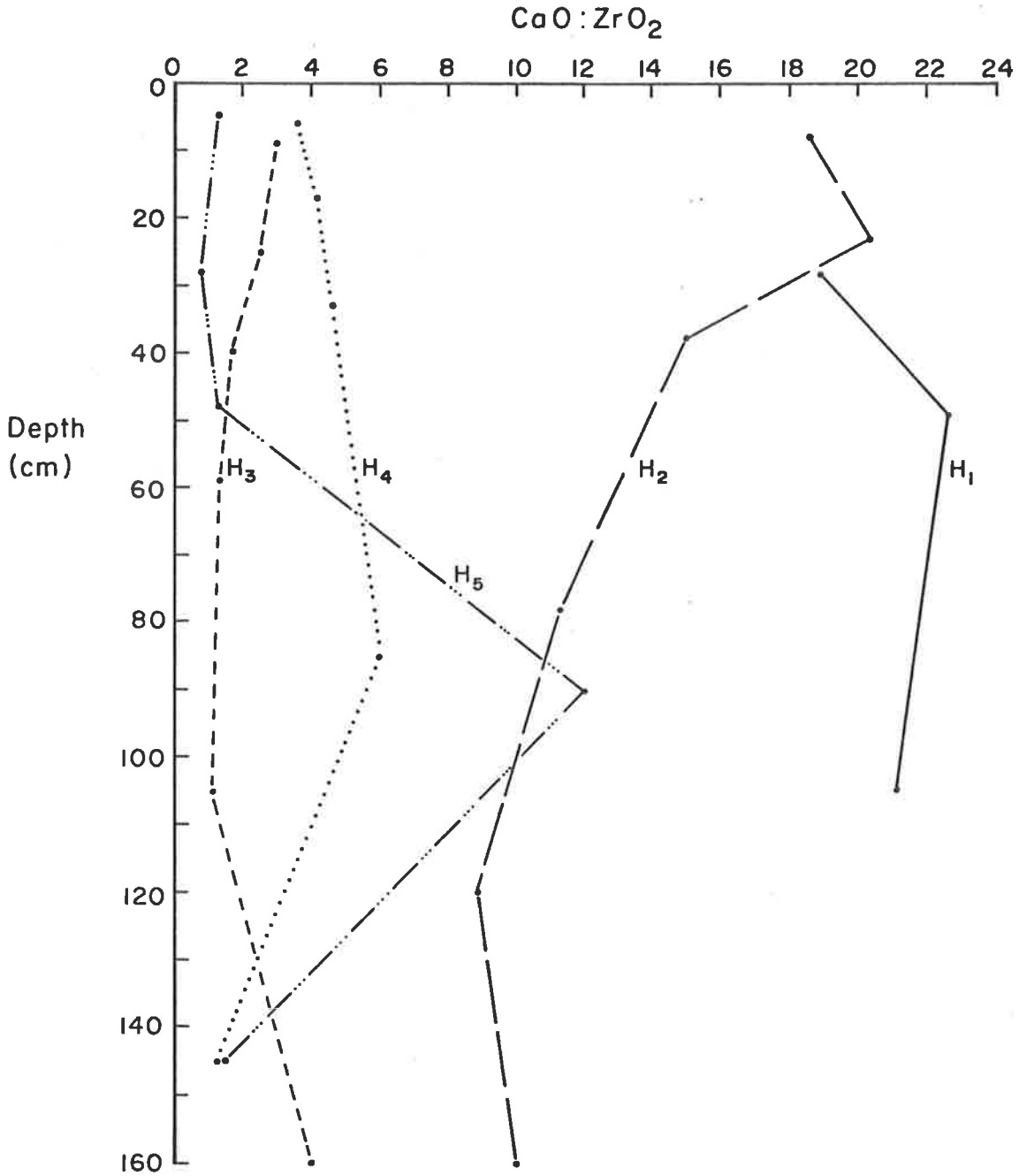

Figure 96.1 Depth functions of the ratio $CaO:ZrO_2$ for soils of the Hawkesbury River sequence

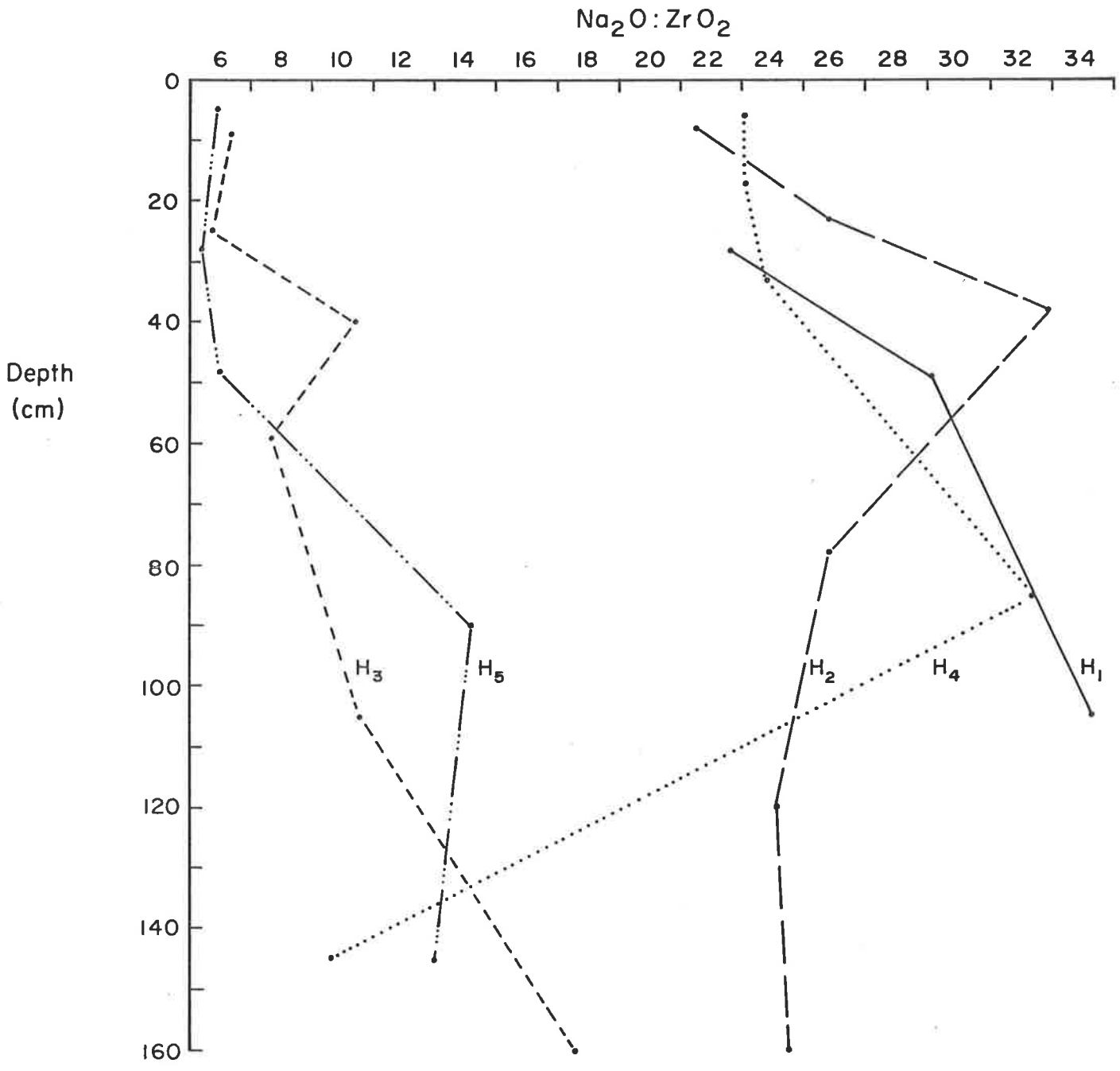

Figure 96.2 Depth functions of the ratio $Na_2O:ZrO_2$ for soils of the Hawkesbury River sequence

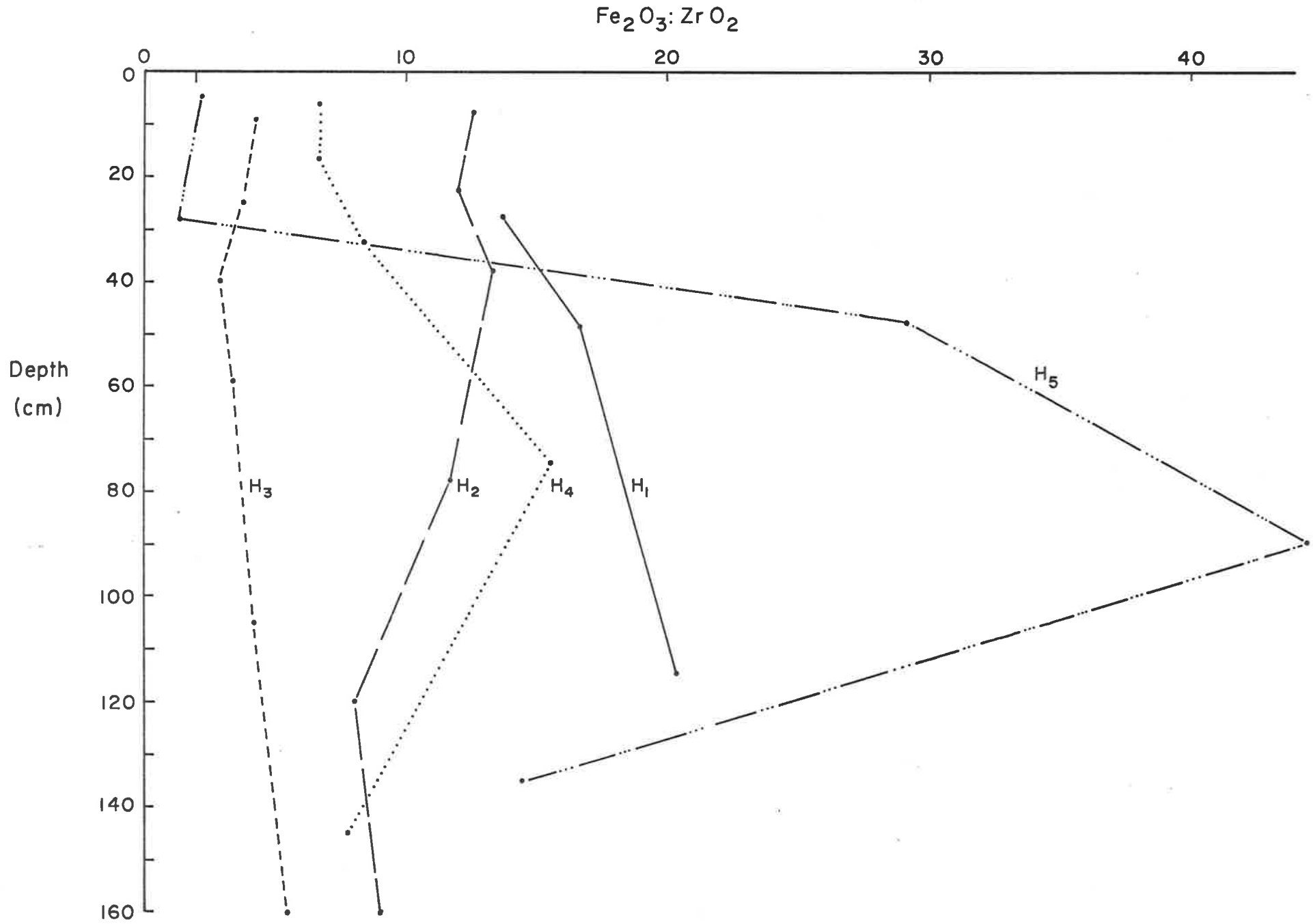

Figure 96.3 Depth functions of the ratio Fe_2O_3:ZrO_2 for soils of the Hawkesbury River sequence

soil compared to the parent material were made for a column of soil having dimensions equal to an area of 1 cm^2 and length equal to the thickness of the particular horizon. All calculations were based on bulk density measurements at 1/3 atmospheric suction.

Values of losses and gains are critically dependent on the choice of the stable constituent. Of the five considered, the acid resistant fraction was chosen because it constituted a relatively large proportion of the whole soil. There was good agreement between replicates of each horizon. Slight errors in analysis can have a pronounced affect on the losses and gains when calculated on the basis of constituents occurring in very small quantity. The concentrations of zirconium and yttrium in the heavy mineral fraction of the 10-125 um fraction, expressed as a proportion of the whole soil, was < 0.03% whereas the acid resistant fraction was in the range 50-70%. Titanium in the sand fraction and/or the heavy mineral fraction was ruled out because of the likelihood of weathering in some of the older profiles.

Changes in weight, volume, clay content and elemental constituents were calculated for G3, G4 and G5 profiles of the Gooromon Ponds sequence (Table 23). The increase in volume and weight in the 0-55 cm layer of G3 was offset by a decrease in the 55-140 cm layer such that there was a statistically insignificant loss in weight and an overall increase in volume of 9%. Results for G4 are somewhat surprising in view of the fact that it is a moderately duplex profile. There is a loss in weight in all horizons except the top of the B2 horizon and a small decrease in volume throughout. It was expected that the lower B horizon would also show an increase in weight in order to account for the increase in clay. There appears to have been a loss of constituents from the

whole profile, particularly the A horizon. In G5 the A horizons show a loss in weight and the B horizons an increase. The net effect is a negligible weight change indicating that soil development primarily involves a redistribution of components inherited from the parent material. The increase in weight of the B horizon has also been accompanied by a marked volume increase.

Shinglehouse Creek (Table 24), Nowra Creek (Table 25) and Hawkesbury (Table 26) sequences have similar trends with age of development as Gooromon Ponds viz an initial increase in volume for the highly organic texturally uniform and weakly gradational profiles (S2, N2, H2). The strongly duplex profiles (S3, N4, H4, H5) have marked decreases in volume and weight accompanying the loss of clay and A horizon formation and vice versa for the B horizon but net profile weight and volume changes are not great (< 10%).

Changes in clay, iron and silica parallel those for weight and show that formation of the texture profile involves a net loss of elemental constituents from the A horizon and a net increase in the B. Two mechanisms may account for this viz.

1. Loss of weathering products from the A by lateral movement and retention in the B ; the clay formation hypothesis, or
2. Movement of clay from surface to subsurface : the eluviation - illuvation hypothesis.

profile	horizon	volume change ($cm^3/h/cm^2$)*	relative volume change (%)	weight change ($g/h/cm^2$)	relative weight change (%)
G3	A11	4.1	51.4	2.0	16.2
	A12	4.0	49.4	2.6	20.3
	B21	3.1	53.0	1.0	10.7
	IIC1	0.4	4.0	- 0.2	- 1.2
	IIC2	0.1	1.5	- 0.2	- 1.1
	IIC3	- 1.1	8.0	- 1.8	- 8.0
	summation	12.1	9.4	- 2.2	- 1.1
G4	A11	- 1.0	-14.2	- 1.9	-17.5
	A12	- 0.3	- 3.9	- 0.9	- 7.5
	A21	- 1.1	-12.4	- 1.6	-11.3
	A22	- 2.1	-17.2	- 2.5	-13.0
	B1	- 0.1	- 0.7	1.0	4.3
	B2	- 1.0	- 7.3	- 0.4	- 2.0
	summation	- 9.3	- 8.8	-10.7	- 6.4
G5	A1	0.8	11.2	- 1.8	-13.7
	A2	- 0.1	- 0.7	- 2.4	-13.2
	B21	1.7	16.3	0.3	1.7
	B22	2.1	25.7	1.7	12.0
	B31	2.0	18.2	0.8	4.0
	summation	15.1	14.4	2.9	1.5

Table 23 Losses and gains in volume and weight for selected horizons of three soils of the Gooromon Ponds sequence. *h - horizon.

profile	horizon	volume change ($cm^3/h/cm^2$)*	relative volume change (%)	weight change ($g/h/cm^2$)	relative weight change (%)
S2	A11	0.7	9.7	- 0.9	- 9.1
	A12	1.5	13.9	- 0.5	- 3.2
	A13	0.9	9.8	- 0.7	- 5.1
	A3	- 0.1	- 0.6	- 1.4	- 8.4
	B1	- 0.2	- 2.4	- 0.3	- 2.4
	summation	2.8	5.7	- 3.8	- 5.5
S3	A1	0.2	2.6	- 2.3	-20.2
	A2	- 1.6	-13.8	- 3.4	-17.5
	B22	1.4	15.9	2.2	15.2
	B3	2.2	27.6	3.5	26.8
	B3C	0.1	0.5	1.6	4.8
	summation	3.7	4.4	4.6	3.3

Table 24 Losses and gains in volume and weight for selected horizons of two soils of the Shinglehouse Creek sequence. *h = horizon.

profile	horizon	volume change ($cm^3/h/cm^2$)*	relative volume change (%)	weight change ($g/h/cm^2$)	relative weight change (%)
N2	A11	0.4	5.5	- 0.4	- 4.4
	A12	0.4	3.0	- 0.1	- 0.5
	B(20)	0.4	4.3	0.5	3.6
	B941)	1.2	1.8	1.5	10.3
	summation	1.6	2.7	0.2	- 0.2
N3	A1	2.8	38.2	0.8	7.0
	B1	2.3	19.2	1.7	9.1
	B21	1.1	11.9	1.5	10.5
	B22	1.4	10.2	2.3	10.2
	B3	0.5	2.4	0.8	2.4
	C(70)	- 0.1	0.4	- 0.1	- 0.4
	summation	8.0	9.9	7.0	5.3
N4	A1	- 1.2	-19.2	- 1.7	-17.1
	A2	- 3.7	-23.4	- 4.5	-18.1
	B1	- 2.1	-13.8	- 3.3	-13.8
	B2	- 0.4	- 3.5	- 1.6	- 9.6
	B3	- 0.6	- 2.7	- 3.3	-10.1
	C1	1.4	7.3	0.6	1.9
	summation	- 5.3	- 5.0	-13.1	- 7.8

Table 25 Losses and gains in volume and weight for selected horizons of three soils of the Nowra Creek sequence. *h = horizon.

profile	horizon	volume change ($cm^3/h/cm^2$)*	relative volume change (%)	weight change ($g/h/cm^2$)	relative weight change (%)
H2	IIA	2.8	22.7	2.9	13.1
	IIB1	4.5	26.0	4.8	15.5
	IIB21	4.7	29.1	5.3	18.3
	IIB31	2.9	10.6	4.0	8.2
	summation	24.2	20.3	28.9	13.4
H3	A1	- 2.4	-11.9	- 4.2	-11.9
	A3	- 1.5	- 9.6	- 2.6	- 9.6
	B1	- 1.6	- 9.0	- 2.9	- 9.5
	B21	- 1.6	- 6.9	- 2.0	- 4.8
	B23	0.5	2.4	0	0
	summation	- 6.6	- 6.8	-11.7	- 7.0
H4	A1	- 2.0	-15.7	- 4.1	-19.3
	B21	2.1	21.5	3.1	19.3
	B22	2.8	16.2	4.8	16.9
	B23	1.7	6.7	3.3	8.0
	B3	1.0	3.3	1.9	3.9
	summation	5.8	4.7	10.6	5.2
H5*	A1	- 2.6	20.8	- 5.3	-25.6
	A21	- 4.7	-32.0	- 6.3	-26.2
	B21	10.4	71.4	16.1	67.2
	B22	7.3	57.3	13.7	65.9
	BC	4.9	98.5	23.2	93.6

Table 26 Losses and gains in volume and weight for selected horizons of four soils of the Hawkesbury River sequence. *Changes in H5 were calculated from the parent material of H4 because parent material of H5 was not sampled. *h = horizon.

Clay migration and clay formation Weight changes due to clay migration and clay formation were calculated for the older members of each sequence. In the case of N4, particle-size and micro-morphological evidence indicated that there was input of fine clay into the upper C horizon. The value for the clay percentage which was chosen for calculation was the value for the parent material of N2. This was deemed justifiable on the grounds that resistant mineral studies had shown that the profiles had formed from similar parent materials (7.3.1). Losses and gains could not be calculated for H5 because the lower B and C horizons were not sampled.

Results of all sequences show that the major cause of the loss of weight in the A and the gain in the B is due to clay migration. However, the contribution of clay from chemical weathering of minerals increases with age, initially in the A horizon (cf G4, G5) and then throughout the whole profile. In the case of N4, approximately 30% of the gain of clay in the B2 is the result of clay formation.

Losses and gains of elements iron, silicon, and potassium follow the trends observed with changes in weight (Table 27). Changes are predominantly the outcome of migration. Since weathering is not a significant factor until the profiles have become mature, much of the elemental redistribution must have been as clay movement i.e. lessivage (Rode 1964). In a number of the older profiles (G5, N4, H3, H4) clay formation has led to a loss of potassium.

Following deposition, the clay moves downward. Some is also lost from the profile entirely probably by lateral movement (see W of S2 in Table 24). However, the quantities translocated are

relatively minor probably because of the homogenisation by soil fauna. There is a marked increase in the amount of illuviation and the profile is on a terrace which is only infrequently flooded, or not at all. As the textural contrast between A and B horizons becomes more marked, the internal hydrology of the profile is altered in such a way that water percolates more freely through the A horizon than the B. This means that the top of the B and bottom of the A are subject to water logging for progressively longer periods of time during the winter and spring. The reducing conditions which are a consequence of this cause a pH drop and lead to an increase in weathering. Hence the reason why the contribution to the profile texture by the process of clay formation is manifest initially in the A2 horizon. The texture contrast becomes more pronounced as a result of the combined effects of migration and weathering leading to a further increase in the length of the period of saturation, more prolonged reducing conditions and thus further mineral breakdown. This is a feedback process (Torrent and Nettleton 1978) produced entirely by intrinsic morphological changes.

Profile	horizon	Fe_2O_3		SiO_2		K_2O	
		M	F	M	F	M	F
				Gooromon Ponds			
G4	A11	-1.1	-0.4	-5.8	1.7	-0.4	0.2
	A21	-1.1	-0.3	-6.0	1.1	-0.4	0.2
	A32	-1.0	-0.4	-5.4	-0.6	-0.3	0.2
	B1	0.5	-0.6	2.4	-2.5	0.1	0.2
	B2	0.7	-0.9	3.5	2.6	0.2	-0.1
G5	A1	-0.7	0.1	-6.6	6.9	-0.7	-0.2
	A2	-0.5	-0.1	-4.7	13.1	-0.5	-0.2
	B21	1.6	1.2	14.6	3.4	1.6	-1.4
	B22	1.2	1.2	10.9	1.8	1.2	-1.2
	B31	0.8	0.9	7.8	2.8	0.8	-0.9

Table 27 - Continued over page

Profile	horizon	Fe_2O_3 M	Fe_2O_3 F	SiO_2 M	SiO_2 F	K_2O M	K_2O F
			Shinglehouse Creek				
S1	A12	-0.1	0.7	-0.9	-1.7	-0.1	0
	A13	-0.1	0.5	-0.9	-2.8	-0.1	0
	B1	-0.1	0.9	-0.9	2.3	-0.1	2.4
S2	A1	-2.4	-0.7	-8.8	0.6	-0.4	-0.4
	A2	-1.8	-1.1	-6.7	0.4	-0.3	-0.3
	B21	0.1	-1.2	0.3	0.4	0	0.1
	B22	2.3	-0.3	8.4	-0.3	0.4	0.4
	B3	2.7	1.0	9.8	-0.1	0.4	0.5
			Nowra Creek				
N3	A1	-0.2	-0.2	-1.1	-2.0	0	0.1
	B1	0	0.2	0.2	-0.4	0	0
	B22	0.3	-0.2	1.3	-2.2	0.1	0.1
N4	A1	-0.4	1.4	-2.5	13.8	-0.1	-0.1
	A2	0.1	2.9	0.7	31.9	0	-0.1
	B1	-3.4	9.8	21.5	38.5	0.6	-0.3
	B2	5.9	2.7	37.3	35.4	1.0	-0.1
	B3	5.3	2.9	33.8	37.4	0.9	-0.1
			Hawkesbury River				
H3	A1	-1.7	0.3	-9.5	36.1	-0.5	0.4
	A3	4.4	-4.3	24.7	45.6	1.3	-0.6
	B1	5.4	-4.6	30.7	36.9	1.6	-0.8
	B21	0.9	-0.9	4.8	4.6	0.3	-0.2
H4	A1	-1.8	4.0	-9.1	16.0	-0.6	-0.2
	B21	3.9	3.1	19.1	13.0	1.2	-0.7
	B22	5.3	1.6	26.3	11.0	1.6	-0.6
	B3	0.8	0.5	3.8	-3.5	0.2	-0.2

Table 27 Losses and gains of oxides due to clay formation (F) and clay migration (M) as a result of soil formation (g/100g parent material).

The process described here is similar to a phenomenon described by Brinkman (1969/70) occurring in seasonally wet soils in East Pakistan. He uses the term ferrolysis to describe a process which has two phases. In the anaerobic phase free iron is reduced and displaces exchangeable cations which are leached. During the aerobic phase ferrous iron is oxidised to produce ferric hydroxide mottles by the hydrogen ions and more ferrous ion is released. The process is distinct from podsolization which is not dependent on seasonal reduction and illuviation (more specifically lessivage) which does not involve any clay destruction.

7.4 Conclusions

From three separate lines of evidence; heavy mineral ratios, weathering indices and calculations of losses and gains of weight, volume and constituents, it is concluded that the major cause of the development of texture contrast is clay illuviation. Clay formation from chemical breakdown makes a significant contribution only in the very mature profiles of each sequence. There is no evidence that textural variations in the parent sediment have caused the observed textural contrast.

References

Akhtyrstev, B.P. (1968). Removal and accumulation of oxides in soils of broadleaf forests in the central Russia Forest Steppe. Soviet Soil Sci. 1968, 1423-34.

Arnaud, St. R.J. and Whitesi de E.P. (1963). Physical breakdown in relation to soil development J. Soil Sci. 14, 267-81.

Barshad, I. (1965). Chemistry of Soil Development. In 'Chemistry of the Soil' (Ed. F.E. Bear) (Reinhold, N.V.).

Beavers, A.H., Fehrenbacher, J.B., Johnson, P.R. and Jones, R.L. (1963). CaO-ZrO_2 molar ratios as in index of weathering. Soil Sci. Soc. Am. Proc. 27, 408-12.

Bhattacherya, N. (1963). Weathering of glacial tills in Indiana. II Heavy Minerals. J. Sed. Pet. 33, 789-94.

Bourne, W.C. and Whiteside, E.P. (1962). A study of the morphology and pedogenesis of a medial chernozem developed in loess. Soil Sci. Soc. Am. Proc. 26, 484-90.

Brasher, B.R., Franzmeier, D.P., Valassis, V. and Davidson, S.E. (1966) Use of Saran nesin to coat natural soil clods for bulk density and water retention measurements. Soil Sci. 101, 108.

Brewer, R. (1964). 'Fabric and mineral analysis of soils' Krieger, N.Y.

Brewer, R. (1968). Clay illuviation as a factor in the particle-size differentiation in soil profiles. Trans. 9th Int. Congr. Soil Sci. 4, 489-99.

Brewer, R., Bettenay, E. and Churchward, H.M. (1974). Some aspects of the origin and development of the red and brown hardpan soils of Western Australia. Tech. Pap. Div. Soils CSIRO Aust., 13.

Brewer, R. and Walker, P.H. (1969). Weathering and soil development on a sequence of river terraces. Aust. J. Soil Res. 7, 295-305.

Bronger, von A. and Kalk, E. (1976). Zur feldspatverwitterung und ihrer bedeutung fur die Tonmineralbildung. Z. Pflanzenern Bodenk., 1, 37-55.

Brinkman, R. (1969/70). Ferrolysis, a hydromorphic soil forming process. Geoderma, 3, 199-206.

Butler, B.E. (1959). Periodic phenomena in landscapes as a basis for soil studies. CSIRO Aust. Soil Publ. No. 14.

Butler, B.E. (1967). Soil periodicity in relation to landform development in south-eastern Australia. In 'Landform studies in Australia and New Guinea'. (Eds. J.N. Jennings and J.A. Mabbutt). (Aust. Nat. Univ. Press: Canberra).

Byers, H.G., Kellogg, C.E., Anderson, M.S. and Thorp, J. (1938) Formation of soil. In 'Soils and Men'. USDA Yearbook.

Chapman, S.L. and Horn, M.E. (1968). Parent material uniformity and origin of silty soils in North West Arkansas based on zirconium-titanium contents. Soil Sci. Soc. Am. Proc. 32, 265-71.

Chittleborough, D.J. and Oades, J.M. (1979). The development of a red-brown earth. I. A reinterpretation of published data. Aust. J. Soil Res. 17, 371-81.

Chittleborough, D.J. and Oades, J.M. (1980). The development of a red-brown earth. II. Uniformity of the parent material. Aust. J. Soil Res. 18, 375-82.

Chittleborough, D.J. and Oades, J.M. (1980). The development of a red-brown earth. III. The degree of weathering and translocation of clay. Aust. J. Soil Res. 18, 383-93.

Churchward, H.M. (1963). Soil studies at Swan Hill, Victoria, Australia. Aust. J. Soil Res. 1, 117-28.

Coventry, R.J. (1967). The geology of Shinglehouse Creek Valley with particular reference to its Cenozoic history. Unpubl. B.Sc.(Hons.) thesis, Aust. Nat. Univ.

Day, P.R. (1965). Particle fractionation and particle-size analysis. In 'Methods of Soil Analysis', Part I. (Eds. C.A. Black et al.) (Am. Soc. Agron).

Dixit, S.P. (1978). Measurement of the mobility of soil colloids. J. Soil Sci. 29, 557-66.

Drees, L.R. and Wilding, L.P. (1978). Elemental distribution in the light mineral isolate of soil separates. Soil Sci. Soc. Am. J. 42, 976-8.

Evans, L.J. (1978). The quantification of pedological processes. Abstracts 11th Int. Congr. Soil Sci. 1, 315.

Evans, L.J. and Adams, W.A. (1975). Quantitative pedological studies on soils derived from Silurian mudstones. IV Uniformity of parent material and evaluation of internal standards. J. Soil Sci. 26, 319-26.

Foss, J.E. and Rust, R.H. (1968). Soil genesis study of a lithologic discontinuity in glacial drift in Western Wisconsin. Soil Sci. Soc. Am. Proc. 32, 393-8.

Geological Survey of New South Wales (1971). 1:250,000 geological series: Canberra sheet.

Greenland, D.J., Oades, J.M. and Sherwin, J.W. (1968). Electron-microscope observations of iron oxides in some red soils. J. Soil Sci. 19, 123-6.

Greenland, D.J. and Wilkinson, G.K. (1969). Use of electron microscopy of carbon replicas and selective dissolution analysis in the study of the surface morphology of clay particles from soils. Proc. Int. Clay Conf., Tokyo 1, 861-70.

Hardy, F. and Follet-Smith, R.R. (1931). Studies in tropical soils. II. Some characteristics igneous rock soil profiles in British Guiana, South America. J. Agric. Sci. 21, 739-61.

Holzey, C.S., Yeck, R.D. and Nettleton, W.D. (1974). Microfabric of some argillic horizons in udic, xeric and torric soil environments of the United States. In 'Soil Microscopy' (Ed. G.K. Rutherford) (Limestone Press, Ontario).

Hutton, J.T. (1955). A method of particle-size analysis of soils. CSIRO Aust. Div. Soils, divl. Rep. No. 11/55.

Khangarot, A.S., Wilding, L.P. and Hall, G.F. (1971). Composition and weathering of loess-mantled Wisconsin and Illinoan-age terraces in Central Ohio. Soil Sci. Soc. Am. Proc. 35, 621-6.

Koppi, A.J. (1981). Microanalytical evidence for short range clay coatings in weathered granodiorite. Aust. J. Soil Res. 19, 251-4.

Krebs, R.D. and Tedrow, J.C.F. (1957). Genesis of three soils derived from Wisconsin till in New Jersey. Soil Sci. 83, 207-18.

Langohr, R. and Van Vliet, R. (1975). Clay migration in well to moderately well drained acid brown soils of the Belgian Ardennes: morphology and clay content determination. Pedologie, 29, 367-85.

Loveday, J. ed. (1974). 'Methods for analysis of irrigated soils'. Comm. Agric. Bureaux. Tech. Comm. No. 54.

McIntyre, D.S. (1976). Subplasticity in Australian Soils. I. Description, occurrence and some properties. Aust. J. Soil Res. 14, 227-36.

Mitchell, W.A. (1975). Heavy Minerals. In 'Soil Components Vol. 2 Inorganic constituents' (Ed. J.E. Gieseking) (Springer-Verlag, N.Y.).

Moss, A.J. (1973). Fatigue effects in quartz sand grains. Sedim. Geol. 10, 239-47.

Moss, A.J. and Green, P. (1975). Sand and silt grains: predetermination of their formation and properties by microfractures in quartz. J. Geol. Soc. Aust. 22, 485-95.

Mulcahy, M.J. and Churchward, H.M. (1973). Quaternary environments and soils in Australia. Soil Sci. 116, 156-69.

Murad, E. (1978). Yttrium and zirconium as geochemical guide elements in soil and stream sediment sequences. J. Soil Sci. 29, 219-23.

Nettleton, W.D., Flach, F.W. and Brasher, B.R. (1969). Argillic horizons without clay skins. Soil Sci. Soc. Am. Proc. 33, 121-5.

Nikiforoff, C.C. and Drosdoff, M. (1943). Genesis of a claypan soil. Soil Sci. 55, 459-82.

Nornberg, P. (1980). Minerology of a podzol formed in sandy materials in northern Denmark. Geoderma 24, 25-43.

Norrish, K. and Hutton J.T. (1969). An accurate X-ray spectrographic method for the analysis of a wide range of geological samples. Geochim. Cosmochim. Acta 33, 431-53.

Norrish, K. and Taylor, R.M. (1962). Quantitative analysis by X-ray diffraction. Clay Min. Bull. 5, 98-109,

Norrish, K. and Tiller, K.G. (1976). Subplasticity in Australian Soils. V. Factors involved and technique of dispersion. Aust. J. Soil Res. 14, 273-89

Northcote, K.H. (1968). 'A factual key for the recognition of Australian soils'. 1st Edition (Rellim: Glenside, Sth. Aust.).

Northcote, K.H. (1979). 'A factual key for the recognition of Australian soils'. 4th Edition. (Rellim: Glenside, Sth. Aust.).

Oertel, A.C. and Giles, J.B. (1966). Development of a red-brown earth profile. Aust. J. Soil Res. 5, 133-47.

Raad, A.T. and Protz, R. (1971). A new method for the identification of sediment stratification in soils of the Blue Springs Basin, Ontario. Geoderma, 6, 23-41.

Reynders, J.J. (1972). A study of argillic horizons in some soils in Morocco. Geoderma 8, 267-79.

Ritchie, A., Wilding, L.P., Hall, G.F. and Stahnke, C.R. (1974). Genetic implications of B horizons in Aqualfs of North-eastern Ohio. Soil Sci. Soc. Am. Proc. 38, 351-8.

Rode, A.A. (1964). Podsolization and lessivage. Soviet Soil Sci., 660-71.

Ruhe, R.V. (1956). Geomorphic studies and the nature of soils. Soil Sci. 82, 441-55.

Schultz, L.G. (1978). Sample packer for randomly oriented powders in X-ray diffraction analysis. J. Sed. Pet. 48, 627.

Sleeman, J.R. (1964). Structure variation within two red-brown earth profiles. Aust. J. Soil Res. 2, 146-61.

Smeck, N.E. and Wilding, L.P. (1980). Quantitative evaluation of pedon formation in calcareous glacial deposits in Ohio, U.S.A. Geoderma 24, 1-16.

Smeck, N.E., Ritchie, A., Wilding, L.P. and Drees, L.R. (1981). Clay accumulation in sola of poorly drained soils of western Ohio. Soil Sci. Soc. Am. J. 45, 95-102.

Smith, B.R. and Buol, S.W. (1968). Genesis and relative weathering intensity studies in three semi-arid soils. Soil Sci. Soc. Am. Proc. 32, 261-5.

Smith, H. and Wilding, L.P. (1972). Genesis of argillic horizons in ochraqualfs derived from fine textured till deposits of north-western Ohio and south-eastern Michigan. Soil Sci. Soc. Am. Proc. 36, 808-15.

Soil Conservation Service (1975). 'Soil Taxonomy', U.S. Dept. Agric.

Soil Survey Staff (1951). 'Soil Survey Manual'. U.S. Dept. Agric. Handbook No. 13.

Stace, H.C.T., Hubble, G.D., Brewer, R., Northcote, K.H., Sleeman, J.R., Mulcahy, M.J. and Hallsworth, E.G. (1968). 'A Handbook of Australian Soils'. (Rellim: Glenside, Sth. Aust.).

Steele, J.G. and Bradfield, R. (1934). The significance of size distribution in the clay fraction. Bull. Am. Soil Surv. Ass. 15, 88-93.

Sudom, M.D. and Arnaud, R.J. St. (1971). Use of quartz, zirconium and titanium as indices in pedological studies. Can. J. Soil Sci. 51, 385-96.

Tamura, T. (1958). Identification of clay minerals from acid soils. J. Soil Sci. 9, 141-7.

Tinsley, J. (1950). The determination of organic carbon in soils by dichromate mixtures. Trans. IV. Int. Congr. Soil Sci., Amsterdam 1, 161-4.

Torrent, J. and Nettleton, W.D. (1978). Feedback processes in soil genesis. Geoderma 20, 281-7.

Torrent, J. and Nettleton, W.D. (1979). A simple textural index for assessing chemical weathering in soils. Soil Sci. Soc. Am. J. 43, 373-7.

Van Dijk, D.C. (1959). Soil features in relation to erosional history in the vicinity of Canberra. CSIRO Aust. Soil Publ. No. 13.

Van Dijk, D.C. and Woodyer, K.D. (1961). Soils of the Yass River Valley. Regional research and extension study, Southern Tablelands, N.S.W. Rept. No. 6.

Vreeken, W.J. (1975). Principal kinds of chronosequences and their significance in soil history. J. Soil Sci. 26, 378-94.

Walker, P.H. (1962a). Terrace chronology and soil formation on the south coast of N.S.W. J. Soil Sci. 13, 167-77.

Walker, P.H. (1962b). Soil layers on hillslopes: a study at Nowra, New South Wales, Australia. J. Soil Sci. 13, 167-77.

Walker, P.H. and Coventry, R.J. (1976). Soil profile development in some alluvial deposits of eastern New South Wales. Aust. J. Soil Res. 14, 305-17.

Walker, P.H. and Green, P. (1976). Soil trends in two valley till sequences. Aust. J. Soil Res. 14, 291-303.

Walker, P.H. and Hutka, J. (1977). Particle-size properties of selected soils and sediments with special reference to fine clay. CSIRO Aust. Div. Soils Div. Rep. No. 22.

Walker, P.H. and Hutka, J. (1979). Size characteristics of soils and sediments with special reference to clay fractions. Aust. J. Soil Res. 17, 383-404.

Whitby, K.T. (1955). A rapid general purpose centrifuge sedimentation method for measurement of size distribution of small particles - apparatus and method. J. Air Poll. Con. Ass. 5, 120-6.

Wilding, L.P., Drees, L.R., Smeck, N.E. and Hall, G.F. (1971). Mineral and elemental composition of Wisconsin-age till deposits in west-central Ohio. In 'Till - A symposium'. (Ed. R.P. Goldthwaite) (Ohio State Univ. Press, Columbus, Ohio).

Zeuner, F.E. (1949). Frost soils on Mount Kenya and the relation of frost soils of aeolian deposits. J. Soil Sci. 1, 20-30.